The University Of Sheffield.

Delineating the signals in anterior-posterior patterning of hPSC derived Neural Crest cells.

By:

Thomas James Roy Frith

Submitted in partial fulfilment of the requirements for the degree of Doctor of Philosophy

The University of Sheffield
Faculty of Science
Department of Biomedical Science

October 2017

Acknowledgements

This has been a long process that no one can ever tell you how bad some of it will be, but throughout I have been lucky to have the support from people who have kept me going through it all. First, I'd like to thank my supervisor, Peter Andrews. Thanks for taking a punt on me when I got flat out rejected from the general round of applications. Throughout my time in the lab, you have shown non-stop faith in me, even during my crisis of confidence and never stopped thinking of new routes to go down and encouraged me to keep thinking bigger You have changed the way I see everything, and I think that may be the most valuable lesson I may ever learn.

To Jim Hackland, my neural crest buddy throughout this. Couldn't have done half of this without working with you and thoroughly enjoyed all the conferences and the beers together. We made the neural crest crew great, and long may it continue. Also can't forget Ana Marin Navarro- honorary Spanish member of the neural crest team. Bro, are you for real?

Huge thanks to the E floor beer pong playas Tom Allison, Dylan Stavish, Ollie Thompson, Jason Halliwell and Chris Price. Also big thanks to Nick Childs, many hours sat talking NFL and general nonsense have got me through writing/PhD life in general.

I must also thank all the past members of the lab too- you made my time there very enjoyable and I've made a lot of good friends throughout this process.

Also, thanks to Gareth, Aleks, Joe and Dan- the best all day drinking pals you could ever need.

I'd also like to thank my collaborators down in London, Conor McCann, Julie Cooper, Dipa Natarajan, Ben Jevans, Nikhil Thapar and Alan Burns. Really enjoyed working with you guys and it has been a long but interesting process in trying to cure Hirschsprung's disease.

Also, Thanks to Lesley Forrester for ZIPs cell line. Thanks to Gabsang Lee and Yohan Oh for sending the Phox2b:GFP reporter line. Thanks to Lorenz Studer and Mark Tomashima for the Sox10 reporter line.

To Laura, for keeping me grounded, for being listening to my endless rants about everything and anything, for eating a lot with me. You kept me on track for the last year and a bit of this, thank you.

Finally, thanks to my family through all of this. You've been there every step of the way and I couldn't have done it without your support.

Abstract

The neural crest is a multipotent, embryonic cell type that gives rise to a range of derivatives including the neurons and glia of the peripheral nervous system, bones and cartilage of the craniofacial skeleton and pigment cells. Whilst much of the biology has been focussed on developmental organisms such as *xenopus* and the chicken embryo, there have only been two reports of neural crest in the human, due to the scarcity of tissue. Recent progress has been made in characterising the signals to derive neural crest cells from hPSCs, but these have not established the signals and genes that are crucial to neural crest patterning. In this work, we show a short, fully defined differentiation protocol to derive neural crest cells from hPSCs and characterise their differentiation into derivatives. Subsequently, we also show that retinoic acid signalling can pattern the neural crest in a dose dependent manner down to the cervical spinal cord. These cells are indicative of putative vagal neural crest cells that give rise to the enteric nervous system. We characterise early differentiation steps of vagal neural crest cells to enteric neural progenitors and show preliminary data of *in vivo* transplantations of these cells for potential regenerative medicine approach for a cell replacement therapy for Hirschsprung's disease.

Furthermore, we also propose a novel ontogeny of trunk neural crest cells through a distinct gene regulatory network and posterior progenitor cell population called Neuromesodermal progenitors. We show that hPSC derived Neuromesodermal progenitors show gene expression similarities with neural crest cells and by exposing them to signals permissible for neural crest differentiation, we show that trunk neural crest cells can be derived from these *in vitro*.

Abbreviations

DNA	Deoxyribonucleic Acid
RNA	Ribonucleic Acid
GRN	Gene regulatory network
NMP	Neuromesodermal Progenitor
FCS	Foetal Calf Serum
KOSR	Knockout Serum Replacement
FACS	Fluorescence Activated Cell Sorting
HH	Hamburger Hamilton stages of Chick development
FGF	Fibroblast Growth Factor
BMP	Bone Morphogenic Protein
TGFβ	Transforming Growth Factor Beta
ENS	Enteric Nervous system
SAP	Sympathoadrenal Progenitor
qPCR	Quantitative Polymerase Chain Reaction
CT value	Cycle threshold value
RAR	Retinoid A Receptor
RXR	Retinoid X Receptor
RARE	Retinoic acid response element
M	Molar (concentration)

Table of Contents

Table of Figures

Chapter 1: Introduction

1.1 The Neural Crest

The Neural Crest is a transient population of embryonic precursor cells that begins to arise at Carnegie stage 12 in the human (O Rahilly and Müller, 2007). These cells are present across all vertebrates and the acquisition of the neural crest has been proposed as the one of the defining characteristics in the origin of vertebrates (Gans and Northcutt, 1983). The neural crest forms in the early ectoderm between the presumptive epidermis and neural ectoderm at the neural plate border. It was described as 'the cord in between' by Wilhelm His who first described the neural crest in Chick embryos (His, 1868). These cells subsequently undergo Epithelial to Mesenchymal Transition (EMT), delaminate from and migrate out from the neural tube. They undergo further differentiate to form many derivatives including the neurons and glia of the PNS, bone and cartilage of the craniofacial skeleton (termed ectomesenchyme), pigment cells and structural elements of the heart (Le Lièvre and Le Douarin, 1975). Due to the diversity of neural crest derivatives, including cells that are typically seen as both ectodermal (neurons and glia) and mesodermal (bone and cartilage) in origin, it has been termed the 'Fourth Germ Layer' (Hall, 2000).

The induction of the neural crest begins early in development, during gastrulation and involves the same signals and genes that are key to other aspects of ectodermal development, such as NOTCH, BMP, WNT and FGF signalling (Simões-Costa and Bronner, 2015). These signals act in a stepwise process to induce different stages in neural crest formation. Signals are maintained along the Anterior-Posterior axis of the body in formation of the neural crest to form many axial populations. These different axial populations, although being very similar in terms of gene expression, show different fates *in vivo.* In particular, the ability to form ectomesenchyme is restricted to the cranial neural crest population, even if trunk neural crest cells are transplanted to the correct region of the embryo (Le Lièvre and Le Douarin, 1975). Despite this fate restriction being well characterised *in vivo,* NCCs have been demonstrated to be multipotent both *in vitro* (Baroffio,

Dupin and Le Douarin, 1991) and *in vivo* (Baggiolini et al., 2015). Migratory pathways also inform specification into derivative fates by altering signals they are exposed to after delamination from the neural tube (Bhatt, Diaz and Trainor, 2013).

1.2 Signals Involved in Neural Crest Specification

1.2.1 Bone Morphogenic Protein Signalling

Bone Morphogenic Protein (BMP) signals are widely expressed around the embryo during gastrulation and subsequently neurulation. BMP signalling was identified as a key pathway through the identification of its inhibitors being released from the organiser (Lamb et al., 1993; Piccolo, Sasai, Lu and De Robertis, 1996). Thus, high and low BMP signalling specified the formation of non-neural and neural tissues respectively. The axial mesoderm, that lies medially in the embryo, secretes Noggin, whilst the paraxial mesoderm (that is at the lateral edges of the embryo) secretes BMP. The combination of BMP inhibitors from the axial mesoderm and BMP ligands from the lateral mesoderm create a gradient of BMP activity across the medio-lateral axis of the embryo. This has been demonstrated *in vivo* by phospho-SMAD1/5/8 being highest at the lateral edges and absent in the medial aspect of the embryo (Faure, de Santa Barbara, Roberts and Whitman, 2002). This BMP gradient signals for the subsequent induction of ectodermal tissues overlying the mesoderm. Overlying the paraxial mesoderm at the lateral edges, the non-neural ectoderm is formed, and is marked by expression of *Gata2/3* (Sheng and Stern, 1999). In the medial aspect, the absence of BMP signalling results in the formation of the neural plate (Faure et al., 2002). Between these two tissues, intermediate levels of BMP signalling is results in neural crest formation (Bonstein, Elias and Frank, 1998). The effect of these tissues on BMP signalling has been When the activity of BMP signalling is higher, in the lateral non-neural ectoderm, expression of the non-neural markers. This combination of agonists and antagonists resulting in different cell fates is a notable example ‘French Flag Model’ proposed by Lewis Wolpert (Wolpert, 1969).

Early BMP signalling patterns the medio lateral axis of the embryo but as the neural tube folds, it patterns the dorso-ventral axis (Timmer, Wang and Niswander, 2002). At HH stage 10, as the neural tube folds, there is a high level of expression of both BMP4 and BMP7 in the epidermal ectoderm (Liem, Tremml, Roelink and Jessell, 1995). In addition, BMP inhibitors from the organiser bind to and inhibit BMP4 at the ventral side of the neural tube (Piccolo et al., 1996) This localisation of BMP signals to the dorsal neural tube coincides with the expression of neural crest specifiers *Slug*, *Msx* and HNK-1. Following addition of the ventralising signal Shh and inhibition of the dorsalising BMP signal to chick neural tube, expression of neural crest markers *Slug*, *Msx* and HNK-1 is lost (Liem, Jessell and Briscoe, 2000; Liem et al., 1995). In recent years, the development of protocols for directed differentiation of human pluripotent stem cells have also demonstrated the conservation of these signals to the human system by 'Dual-SMAD inhibition' (Chambers et al., 2009). Meanwhile, altering the levels of BMP signalling in pluripotent stem cell differentiation has been shown to induce a full range of ectodermal fates including placodal, non-neural and also neural crest (Leung, Kent Morest and Li, 2013; Leung et al., 2016; Tchieu et al., 2017).

In recent years, the development of protocols for directed differentiation have also instructed the conservation of these signals to the human system- a robust and widespread method for neural induction is 'Dual-SMAD inhibition' (Chambers et al., 2009) and altering the levels BMP signalling in pluripotent stem cell differentiation protocols can induce a variety ectodermal fates including placodal, non-neural and also neural crest (Leung, Kent Morest and Li, 2013; Leung et al., 2016; Tchieu et al., 2017).

1.2.2 WNT signalling

Early investigations into neural crest specification had shown that perturbations of BMP signalling, whilst able to change expression domains of both neural and non-neural ectoderm, were insufficient to induce the neural crest in *Xenopus* (LaBonne and Bronner-Fraser, 1998). In the chick, *Wnt6* is expressed in the

developing neural folds, and required for neural crest induction (García-Castro, Marcelle and Bronner-Fraser, 2002), whilst Wnt1 is expressed by mouse neural crest cells and a Wnt1 driven CRE recombinase marks neural crest cells (Lewis et al., 2013).

The proximity of intermediate mesoderm to the neural crest in *Xenopus* embryos implicated it as the source of neural crest inducing signals. Both *Wnt8* and *Chordin*, that are required for neural crest induction, are expressed in the intermediate mesoderm and explanting the mesoderm with the overlying ectoderm is sufficient to induce neural crest formation (Steventon et al., 2009). Steventon et al also demonstrated the requirement of Wnt signalling by demonstrating loss of neural crest tissue following injection of *GSK3* mRNA and pharmacologically by incubating embryos with *DKK1* (Steventon et al., 2009). In addition, Wnt has been shown to play a role upstream of BMP signalling in the formation of the medio-lateral and dorso-ventral patterns required for neural crest formation (Fuentealba et al., 2007). It was subsequently shown that injecting *XWnt8* and *Xβ-catenin* mRNA into 2 cell *Xenopus* embryos expanded the formation of neural crest whilst negative regulation of Wnt inhibited neural crest formation (LaBonne and Bronner-Fraser, 1998). Furthermore, modulating the canonical Wnt pathway alone signalling alone is sufficient to induce neural crest in hPSCs and zebrafish (Leung et al., 2016) (Lewis et al., 2004). Following activation of the canonical Wnt signalling pathway, β-catenin is translocated from the cytoplasm to nucleus and binds to DNA in conjunction with TCF binding proteins (MacDonald, Tamai and He, 2009). The mechanism by which Wnt signalling induces neural crest is still an active area of research. Firstly, direct activation of enhancers of early neural plate border specifiers *zic3* and *pax3a,* where Wnt works in conjunction with Bmp and Fgf signalling (Garnett, Square and Medeiros, 2012). This has also been demonstrated for the neural crest specifier Slug (Sakai et al., 2005). A recently identified Wnt target in neural crest formation is *Axud1,* which has a binding site in the *FoxD3 N1* enhancer. In addition, morpholino mediated knock out of *Axud1* results in a loss of *FoxD3* expression and loss of neural crest specification (Simões-Costa, Stone and Bronner, 2015).

ChIP-sequencing for β-catenin in hPSCs subjected to WNT activation has shown direct binding to upstream promoters of neural crest specifiers such as *TFAP2α*, *MSX1* and *PAX3* (Funa et al., 2015).

It has been suggested that Wnt acts as an inductive signal of the neural crest gene regulatory network, BMP (Steventon et al., 2009) and FGF (LaBonne and Bronner-Fraser, 1998) work to maintain neural crest character in a two-step inductive model. These signalling pathways co-opt with a cell autonomous mechanism of neural crest formation that is discussed below.

1.3 Neural Crest Gene Regulatory network

1.3.1 Neural plate specifiers

The signals required for early neural crest specification go on to induce expression of genes known as neural plate border specifiers (Khudyakov and Bronner-Fraser, 2009). Neural plate border specifiers provide the key spatial information in the ectoderm and are used by cells to induce neural crest specifiers (Sauka-Spengler, Meulemans, Jones and Bronner-Fraser, 2007). The *paired box* genes *Pax3* and *Pax7* are two of the earliest genes expressed in the developing ectoderm. In particular, *Pax7* has been shown to be amongst the first genes induced by BMP and Wnt signalling in the prospective neural plate border in the stage 4 chicken embryos (Basch, Bronner-Fraser and García-Castro, 2006). As the neural tube folds, the neural plate border develops and *Pax7* expression is retained and required for neural crest specification (Basch, Bronner-Fraser and García-Castro, 2006; Murdoch, DelConte and García-Castro, 2012) (Betters et al., 2010b). *Pax3* is also expressed early in development, with similar expression patterns to *Pax7* demonstrated in the chick neural folds at stage 7 (Basch, Bronner-Fraser and García-Castro, 2006). Both FGF and Wnt signals have been shown to induce *pax3a* expression in *Xenous* (Monsoro-Burq, Wang and Harland, 2005; Garnett, Square and Medeiros, 2012), whilst high levels of BMP signallung repress it (Garnett, Square and Medeiros, 2012). These signalling inputs reflect on the expression domain of *Pax3* extending from the neural plate border domain into the neural

plate where *Pax3* is also a pro-neural factor (Maczkowiak et al., 2010). *Pax3* shows a retained expression throughout neural crest development all along the anterior posterior axis and is subsequently expressed in migratory neural crest cells. *Pax3* also shows key roles in the formation of neural crest derivatives including pigment cells and the enteric nervous (Bondurand et al., 2000) (Lang and Epstein, 2003).

TFAP2α is another key neural plate border specifier required for neural crest formation and is expressed early in development with expression spanning the neural plate border and non-neural ectoderm (Nikitina, Sauka-Spengler and Bronner-Fraser, 2008; Roellig, Tan-Cabugao, Esaian and Bronner, 2017; Khudyakov and Bronner-Fraser, 2009). It is widely expressed in the ectoderm from HH stage 4, at HH stage 10, expression is restricted to the dorsal neural folds (Khudyakov and Bronner-Fraser, 2009). Signalling from both the BMP and WNT signalling pathways have a key role in *TFAP2*α, as both are required for its induction (Luo, Lee, Saint-Jeannet and Sargent, 2003; Funa et al., 2015; Tchieu et al., 2017), and upon knockdown, the BMP expression domain expands, whilst WNT signalling from the axial mesendoderm is reduced (Wang et al., 2011). Its expression at the early stages of ectodermal development shown to induce neural crest formation when ectopically expressed in *xenopus* neural plate (Luo et al., 2003). This may be due to *TFAP2*α acting as a pioneer factor in the induction of the neural crest gene regulatory network as it binds to enhancers in key neural crest genes such as *PAX7*, *SOX9* and *SNAI1* (Rada-Iglesias et al., 2012). Loss of function in *TFAP2*α induces phenotypes consistent with a loss of neural crest, most notably craniofacial defects (Knight et al., 2003) (Schorle et al., 1996) and it is mutated in some cases of branchio-oculo-facial syndrome (Milunsky et al., 2008). In hPSC models of ectodermal differentiation, deletion of *TFAP2*α results in the reduced capacity to form neural crest and the loss of non-neural ectoderm differentiation entirely (Tchieu et al., 2017).

Gene expression in neural plate border cells have been shown to be dynamic and not committed to a specific ectodermal fate in the early chicken development (Roellig et al., 2017). *Pax7*, *Tfap2*α and *Sox2* have been found to be co-expressed

in the neural plate border (Roellig et al., 2017). Cell fate tracking in the chicken demonstrates that these cells can interconvert between different ectodermal fates. In particular, neural (Sox2+) cells can subsequently end up differentiating into non-neural ectoderm and modulation of gene expression levels indicates a gene dosage requirement for commitment to one ectodermal fate (Roellig et al., 2017).

1.3.2 Neural crest specifiers

Following induction by the neural plate border specifiers, neural crest specifiers reinforce the neural crest identity by stabilising neural plate border identity and induce the expression of epithelial to mesenchymal (EMT) genes which work to change cell shape, remodel cell-cell contacts and allow migration to occur (Sauka-Spengler and Bronner-Fraser, 2008). The SoxE group of genes (*Sox8*, *Sox9* and *Sox10*) (Bowles, Schepers and Koopman, 2000) are key neural crest specifiers, meanwhile, *Slug* and *Snail,* function in EMT. Homologues of neural crest specifiers are present and required in many models of neural crest development from *Xenopus* (LaBonne and Bronner-Fraser, 1998) to human pluripotent stem cell models models (Betters et al., 2010b; Hackland et al., 2017). The SoxE genes have been demonstrated to play a main role in neural crest identity by ectopic expression inducing neural crest identity *in vivo* (McKeown et al., 2005b) and *in vitro* (Motohashi et al., 2016; Kim et al., 2014).

The first SoxE gene to be expressed is Sox9, which is shown in the dorsal neural tube (Cheung and Briscoe, 2003a) (Spokony et al., 2002). *Sox9* knockdown in *xenopus* do show deficiencies in the formation of the craniofacial skeleton (Spokony et al., 2002), which is consistent with its role in chondrogenesis (Mori-Akiyama, Akiyama, Rowitch and de Crombrugghe, 2003; Umeda et al., 2015). Both *Sox8* and *Sox10* are expressed shortly after, but in a more restricted domain than *Sox9* (Cheung and Briscoe, 2003b). *Sox8* is expressed in the premigratory cranial neural crest in the chick (Simões-Costa and Bronner, 2016), whilst it does not show an axial restriction in xenopus (O'Donnell et al., 2006). *Sox10* is expressed in the neural crest at dorsal neural folds and overlaps with expression of *Slug*

(Cheung and Briscoe, 2003b). In all of these genes, disruption leads to malformation of neural crest derived structures, particularly the *Sox10* null mouse- *Dominant megacolon*, that is a model of Hirschsprung's disease (Southard-Smith EM, 1998). Sox9 mutations result in failure of neural crest to form derivatives, instead undergoing apoptosis (Cheung et al., 2005). Mutations in *Sox9* do not affect neural crest specification in the chick, which suggests that these *SoxE* genes do display functional redundancy in neural crest specification. In addition, substituting *Sox8* into the *Sox10* locus shows that these genes function similarly in neural crest development (Kellerer, 2006), but show functional differences later in development (Stolt, Lommes, Friedrich and Wegner, 2004a). Sox10 in particular plays a key role in retaining the multipotency, potentially by interfering with co-factor binding that is required for further differentiation (McKeown et al., 2005a) (Kim, Lo, Dormand and Anderson, 2003). Examles of co-factors for further differentiation include Mitf which pairs with Sox10 for melanocyte development (Bondurand et al., 2000), and the enteric nervous system, c-RET (Lang and Epstein, 2003).

FoxD3 is another neural crest specifier that is expressed in the anterior epiblast and neural plate (Khudyakov and Bronner-Fraser, 2009). As development continues, *FoxD3* becomes restricted to the neural folds, with the highest expression in the neural crest region from HH stage 8 through to 10 (Khudyakov and Bronner-Fraser, 2009). *FoxD3* is expressed very early in development and has roles in the transition from mouse embryonic stem cells into epiblast stem cells (Respuela et al., 2016; Krishnakumar et al., 2016) and loss of function in hPSCs results in mesoderm differentiation (Arduini and Brivanlou, 2012). During neural crest differentiation, input from FGF8 from the paraxial mesoderm (Monsoro-Burq, Fletcher and Harland, 2003) and Wnt (Simões-Costa, Stone and Bronner, 2015) is required for *FoxD3* expression. In addition to signalling inputs, neural plate border specifiers also affect *FoxD3* expression with *Pax3* and *Zic1* required (Monsoro-Burq, Wang and Harland, 2005; Sato, Sasai and Sasai, 2005). Identification of the *FoxD3* NC1 and NC2 enhancers indicates additional axial specific inputs during neural crest formation (NC1 cranial neural crest only and

NC2 vagal and trunk neural crest) (Simões-Costa et al., 2012). Input from *Pax3* and *Zic1*, *Pax7* and *Msx1* are required for both enhancers (Simões-Costa et al., 2012). Whilst the cranial specific gene *Ets1* (Barembaum and Bronner, 2013) is required for NC1 (Simões-Costa et al., 2012). *FoxD3* overexpression results in the formation of HNK1+/SOX10+ neural crest cells in the chicken and is upstream of events inducing EMT (Cheung et al., 2005). *FoxD3* has recently been found to play two roles during neural crest specification in the zebrafish (Gavriouchkina et al., 2017), it first acts as a pioneer factor to induce and maintain the early neural crest GRN and subsequently acts as a repressor of further differentiation by preventing H3K27 acetylation (Gavriouchkina et al., 2017).

1.3.2 Epithelial to Mesenchymal transition (EMT)

The final stage in neural crest formation is the induction of EMT and delamination from the neural tube. This involves both a change in gene expression and a change in cell adhesion and cytoskeleton remodelling (Sauka-Spengler and Bronner-Fraser, 2008). The two most prominent genes in the cascade are *Slug* and *Snail* that are in the Snail family of genes that were first identified in *Drosophila* (Alberga et al., 1991) where it was described in mesoderm formation. Studies have found vertebrate homologues of this gene found in zebrafish (Hammerschmidt and Nusslein-Volhard, 1993), mouse (Nieto, Bennett, Sargent and Wilkinson, 1992) and human (Paznekas et al., 1999; Cohen et al., 1998). Comparison of these genes in the mouse led to the hypothesis that a gene duplication arose somewhere in vertebrates and as a result, these genes are now termed Snai1 (Snail) or Snai2 (Slug) (Sefton, Sanchez and Nieto, 1998).

Slug was first described in the chick with expression noted in the primitive streak and neural crest. Morpholino mediated knockdown of *Slug* showed impaired migration of cells from the neural tube at HH stage 9 implicating its role in neural crest development (Nieto, Sargent, Wilkinson and Cooke, 1994). These data were also found in *xenopus* whereby overexpression of *XSlug* increased the domain of

neural crest induction as well as gain of neural crest derivatives (LaBonne and Bronner-Fraser, 1998), whilst knockout showed a reduction in neural crest migration (LaBonne and Bronner-Fraser, 2000). It was purported that *XSlug* acted to repress transcription during neural crest development, and thus its role in expansion of neural crest domains indirect through repression of alternate fates (LaBonne and Bronner-Fraser, 2000).

Snail has also been well characterised in neural crest development and has been shown to be expressed before Slug in *xenopus* neural crest development (Linker, Bronner-Fraser and Mayor, 2000; Aybar, Nieto and Mayor, 2003) which has been shown in mouse (del Barrio and Nieto, 2002). Thus, whilst *Slug* plays a key role in the EMT of neural crest, Snail may play a key role in the onset of neural crest differentiation by induction of other neural crest specifiers such as *Ets1* and *FoxD3* (Aybar, Nieto and Mayor, 2003).

Potential *Slug* targets include cell adhesion molecules such as Cadherin6B (Taneyhill, Coles and Bronner-Fraser, 2007) and N-Cadherin (Cheung et al., 2005), whilst *Snail* has been shown to be involved in the breakdown of tight junctions (Ikenouchi, Matsuda, Furuse and Tsukita, 2003). Following the breakdown of molecules tying neural crest cells to the neural tube, neural crest cells change cell-cell adhesion to looser adhesions such as β1-Integrin (Cheung et al., 2005) and Cadherin-7 (Nakagawa and Takeichi, 1995). It was also apparent that there was greater delamination cells from the neural tube and a model by which Slug acts with Sox9, which is anti-apoptotic, and FoxD3, that induces cell-cell contacts, for full delamination to occur (Cheung et al., 2005). In addition to the change of cell-cell contacts, neural crest cells also begin to express matrix remodelling proteins for successful migration in the embryo. The matrix metalloproteinases have been shown to have critical roles in neural crest migration and subsequent differentiation (Cai et al., 2000; Cai and Brauer, 2002) as well as ADAM family of proteins that is involved in the cleavage of membrane bound proteins in neural crest cells and required for migration (McCusker, Cousin, Neuner and Alfandari, 2009; Neuner et al., 2008).

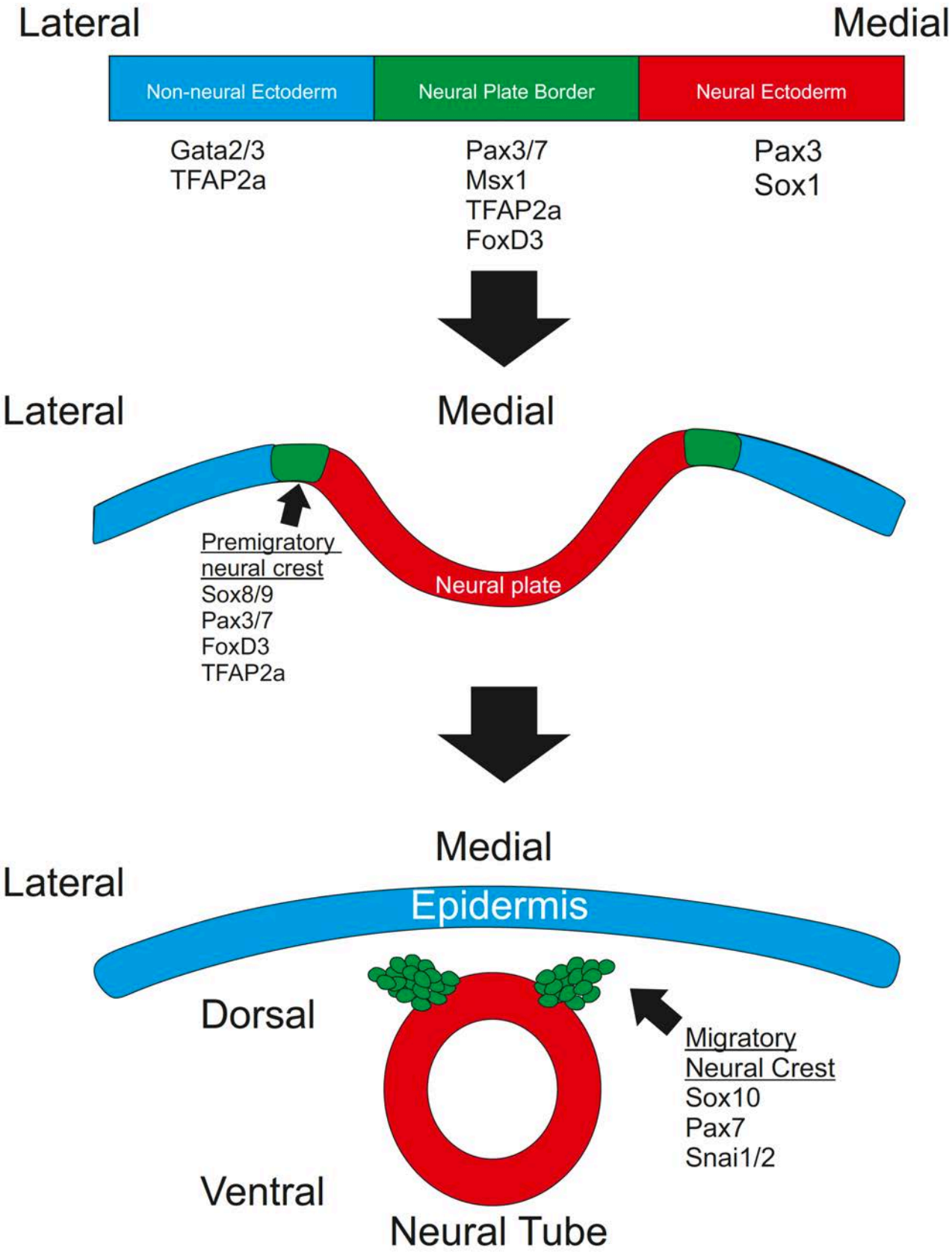

Caption next page

Box 1: Schematic of neural crest differentiation. In the developing ectodermal plate, the neural crest derives from the neural plate border, between the neural and non-neural ectoderm. External signals such as BMP, WNT and FGF from the underlying mesoderm induce neural plate border genes. In addition, Tfap2a and FoxD3 are pioneer genes that work to allow for the induction of neural crest specifiers.

As the neural tube starts to fold, the neural plate border cells are further specified to pre-migratory neural crest as the outer edges of the neural folds. Genes expressed in the pre-migratory neural crest function to induce genes that are involved in EMT such as Snai1/Snai2. In addition, other early neural crest genes such as Sox8 and Sox9 are expressed and work to induce later neural crest specifiers such as Sox10. In the last stages of neural crest differentiation, EMT genes work to remodel neural crest cells for delamination from the dorsal neural tube. Targets of EMT genes include breaking down cell adhesion molecules and inducing matrix remodelling genes to assist migration. In addition, later neural crest specifiers, such as Sox10, work to retain the multipotency of migratory neural crest cells which ensures that there are enough progeny to migrate and differentiate to form all the derivatives that are required.

1.4 Neural Crest derivatives

1.4.1 The Fourth Germ layer

The range of neural crest derivatives was determined mainly by quail chick grafting experiments pioneered by Nicole Le Douarin (Le-Douarin, 1973). By grafting neural crest from the quail to the chicken embryo and by tracing the destination of the quail cells, the wide array of derivatives that neural crest cells contribute to were discovered. The neural crest contribution to the peripheral nervous system has been shown by this method, with the enteric nervous system, autonomic nervous system, pigment cells and the craniofacial mesenchyme (Reviewed in Le Douarin and Dupin, 2003; Baggiolini et al., 2015). This wide array of neural crest derivatives has led to the hypothesis of a new evolutionary split, whereby vertebrates with the vast contribution of the neural crest to higher vertebrates equating it to its own germ layer (Hall, 2000).

1.4.2 Enteric nervous system

The enteric nervous system contains 400 to 600 million neurons (equivalent to the number of neurons in the spinal cord) and includes many subtypes of neurons. It plays roles in gut motility, fluid and nutrient absorption as well as integration with the gut immune and endocrine systems (Reviewed in Furness, 2012). Neural crest origin of the enteric nervous system was first identified in the chicken by ablation of the vagal neural crest (Yntema and Hammond, 1954). Heterotopic grafts of quail neural crest into the chicken showed that the sacral neural crest were the source of enteric neurons in the most caudal part of the colon (Le Douarin and Teillet, 1973; Burns and Douarin, 1998). In the mouse, neural crest cells leave the neural tube at embryonic day 8 (E8) and express markers of multipotent neural crest such as P75 (Wilson et al., 2004), Endothelin receptor B (*Ednrb*) (Nataf, Amemiya, Yanagisawa and Le Douarin, 1998) and *Sox10* (Southard-Smith EM, 1998) undertaking a ventral migration from the neural tube to the gut. During this ventral migration, they undergo initial specification into

enteric neural crest cells and have gained expression of Ret (Heanue and Pachnis, 2008) and Phox2b as they enter the gut (Elworthy et al., 2005; Anderson, Stewart and Young, 2006). These cells then migrate in a rostral-caudal fashion balancing proliferation, migration and differentiation as they go as well as a subset of enteric neural crest cells migrating toward the gut lumen and forming ganglia in the submucosa (Sasselli, Pachnis and Burns, 2012). The two main signals in the gut are glial-cell derived neurotrophic factor (GDNF) and endothelin-3 (ET-3) (Heanue and Pachnis, 2007) that act to balance the migration, proliferation and differentiation of enteric neural crest cells. GDNF is secreted by the gut mesoderm and forms a gradient of increasing concentration from the foregut down to the caecum (Natarajan, Marcos-Gutierrez, Pachnis and de Graaff, 2002) that enteric neural crest cells migrate along. The concentration of GDNF is far lower in the hindgut than the caecum and so the mechanism of migration here is not clear, although recent studies showing a subset of enteric neural crest cells that cross the mesentery and contribute to most the innervation of the hindgut (Nishiyama et al., 2012). Although GDNF is required for the initial migration across the mesentery, they found Cxcr4 and signals from the vasculature are also required in some part for this (Nishiyama et al., 2012) and may be indicative of the signals required for migration in the hindgut. GDNF is also a key signal for proliferation and differentiation of enteric neural crest cells in the gut (Chalazonitis, Rothman, Chen and Gershon, 1998). Endothelin-3 is secreted by the gut mesenchyme, whilst enteric neural crest cells express endothelin receptor b (Ednrb) (Barlow, de Graaff and Pachnis, 2003). Endothelin-3 signalling retains multipotency of enteric neural crest cells (Bondurand et al., 2006) and premature differentiation is seen when Endothelin 3 loss (Bondurand, 2003). Thus, balancing differentiation and multipotency is key in proper formation of the enteric nervous system. Enteric neural crest cells subsequently undergo differentiation into a wide array of neural subtypes that are described as intrinsic- they are involved in their own closed loop, or extrinsic and create connections with the central nervous system. Enteric neural subtypes involve secretion of a wide range of neurotransmitters such as acetylcholine (excitatory enteric motor neuron) and nitric oxide synthase

(inhibitory motor neuron) (McCann et al., 2017); (Furness, 2012; Hirst et al., 2015).

1.4.2 Sympathoadrenal precursors

Whist sympathetic ganglia are derived from the neural crest all along the anterior-posterior axis, in the trunk (between somites 18-24), a population of neural crest cells in this pathway also form neuroendocrine cells that are present in the adrenal gland (Le Douarin and Teillet, 1974) (Reviewed in Le Douarin, 2004). Following delamination of the neural crest cells from the neural tube migrate ventrally receiving Sonic Hedgehog and BMP signals from the floorplate and dorsal aorta respectively (Morikawa, Maska, Brody and Cserjesi, 2009; Unsicker, Finotto and Krieglstein, 1997) (Huber et al., 2008). Following exposure to Sonic Hedgehog and BMP, neural crest cells begin to upregulate early markers of the sympathoadrenal lineage including *Phox2b* (Pattyn et al., 1999), *Phox2a* (Hirsch et al., 1998) , *Mash1* (*Ascl1*) (Guillemot et al., 1993) and *Hand2* (Howard, 2005). Following induction of the aforementioned genes, neural crest cells are subsequently committed to forming either sympathetic neurons that will reside in suprarenal ganglia or celiac ganglia (Lumb and Schwarz, 2015), or chromaffin cells in the adrenal medulla (Huber, 2006). The signals that mediate the fate decision between sympathetic neural and chromaffin cell differentiation have not been fully elucidated, as mutations in candidate genes often result in a loss in both cell types. Glucocorticoids had been postulated to be the key signal in determining the difference between the two lineages due to its role in inducing phenylethanolamine N-methyltransferase (PNMT), which is in the catecholamine biosynthesis pathway (Wurtman and Axelrod, 1966), although this was not the case when glucocorticoid receptors were deleted in mice (Finotto et al., 1999). The function of these cells is to produce and release catecholamines in homeostasis (Huber, Kalcheim and Unsicker, 2009) in order to regulate haematopoiesis (Fitch et al., 2012) and cardiomyocyte function (Oh et al., 2016).

1.5 Patterning and Plasticity in neural crest

The fate of the neural crest *in vivo* has been shown to be dependent on its position along the anterior posterior axis. In particular, the key example of this is the inability of trunk neural crest cells to form ectomesenchymal derivatives when transplanted into the cranial region (Le Lièvre and Le Douarin, 1975). This has subsequently raised the question of when neural crest cells commit to fate decisions, how are they patterned, and what determines their anterior posterior identity. In the cranial neural crest, cells migrate in three characteristic pathways going into the first three branchial arches (Reviewed in Trainor and Krumlauf, 2000b). The branchial arches are populated by neural crest cells from rhombomeres 1-8, with each one being populated by distinct rhombomeres without any mixing of streams between rhombomeres (Kulesa and Fraser, 1998). Transplanting neural crest cells from one branchial arch stream to another resulted in neural crest cells forming structures characteristic of their point of origin and led to the hypothesis of neural crest fate being determined before they delaminated from the neural tube (Noden, 1983). This contrasted with experiments where tissue was taken from regions of the embryo caudal to the otic vesicle and transplanted to the rhombomeres regions (rostral to the otic vesicle). The area caudal to the otic vesicle expressed Hoxb4 and following transplant, their Hox profile was altered to that of the area it was grafted to. Thus the role of surrounding mesoderm tissue in patterning argued for plasticity in neural crest cells themselves (Itasaki, Sharpe, Morrison and Krumlauf, 1996). Subsequent experiments in the mouse involving transplants between rhombomeres three, four and five showed cells typically retained their axial identity, as per Noden et al 1983. Only when cells broke away from the graft clumps and were single cells did they reprogram their identity to their new location (Trainor and Krumlauf, 2000a). These data all showed the key role of the neighbouring mesoderm in conveying patterning signals to the neural crest, whilst plasticity and axial identity were informed by the community effect (Gurdon, 1988). Furthermore, recent work has shown the presence of 'poised' enhancers in neural crest cells destined to migrate to the three different branchial

arches and only when these cells are subjected to region specific signals, do they sense the appropriate patterning cues. This gives rise to the underlying epigenetic regulation behind the plasticity and fate of neural crest cells from different parts of the neural tube (Minoux et al., 2017).

1.6 Neurocristopathies

1.6.1 An umbrella term for a range of conditions

Neurocristopathy is a term that is used to describe conditions caused by malformation of the neural crest and their derivatives (Bolande, 1974). They encompass defects in many aspect of neural crest formation, such as Waardenburg syndrome, that presents with pigmentation defects (notably a patch of white hair on the head), characteristic facial structure and very pale or very blue eyes (Waardenburg, 1951). Treacher-Collins syndrome is another neurocristopathy showing severe craniofacial defects. This is caused by a mutation in *TCOF1,* a gene involved in ribosome assembly and results in fewer cranial neural crest cells differentiating into ectomesenchyme (Reviewed in Trainor, 2010) In addition, many cancers such neuroblastoma and melanoma originate from the neural crest. Melanoma cells in particular has been shown to recapitulate characteristics of early developing neural crest cells, and epigenetic remodelling consistent with early neural crest cell (Kaufman et al., 2016). Kaufman et al used a zebrafish model of melanoma to demonstrate the reacquisition the embryonic neural crest cell gene expression and the interaction of super enhancers as the mechanism (Kaufman et al., 2016). In addition, peripheral neuropathies can also be classified as neurocristopathies. In particular, familial dysautonomia presents with sufferers having difficulty suckling (a common symptom of cleft palate) and reduced pain sensitivity has been well modelled *in vitro* using iPSC models which showed reduced ability of neural crest cells to differentiate to autonomic neurons *in vitro* (Zeltner et al., 2016; Lee et al., 2009).

1.6.2 Hirschsprung's disease

Hirschsprung's disease is a congenital disorder present in 1 in 5000 live births and occurs when parts of the gut are aganglionic (Heanue and Pachnis, 2007). Patients are born with a constricted distal colon, through which the stool cannot pass, and resulting in a distended bowel. It is diagnosed shortly after birth if the fetal stool has not passed and confirmed with a biopsy. The only currently treatment is removal of the constricted distal colon by a 'gut pull through' procedure where the aganglionic section of gut is removed (Amiel et al., 2008; McKeown, Stamp, Hao and Young, 2013; Bolande, 1975). This procedure often results in morbidity and results in significant burden to the healthcare system (Tsuji et al., 1999). The most common mutations in Hirschsprung's disease are in the GDNF-RET pathway and the Endothelin pathways. In addition, there are several modifier genes described in Hirschsprung's disease that give rise to the varied length of aganglionosis that is seen in different patients (Amiel et al., 2008). Hirschsprung's disease is also seen alongside another neurocristopathy, such as Waardenburg Shah(Hofstra et al., 1996), and patients with Down syndrome having a greater incidence of Hirschsprung's disease (Goldberg, 1984). Mutations in the receptor tyrosine kinase RET (Sancandi et al., 2000; Edery et al., 1994) and the endothelin pathway (Hosoda et al., 1994) are frequently found and confirm their role in the formation of the ENS. Mutations in genes crucial to the formation of neural crest derivatives explain the coincidence of Hirschsprung's disease with other neurocristopathies, such as endothelin (Baynash et al., 1994) and Sox10 (Southard-Smith EM, 1998). Due to the varied nature of the disease and overlapping function of the key genes, the exact mechanism by which these mutations cause Hirschsprung's disease are not fully elucidated.

Hirschsprung's disease has been a good target for developing cell replacement therapy. The premise of a cell replacement therapy with Hirschsprung's disease is by transplanting cells into the aganglionic region of gut to regain some motility. Studies on this have so far involved transplantation of endogenous ENS adult stem cells expanding and transplanting them into the gut. These cells have been isolated from both human and mice and transplanted into the bowel (Lindley et

al., 2008; Li et al., 2016; Findlay et al., 2014). These have often shown some signs of rescue, and in one study demonstrated no ectopic migration of transplanted cells or tumorigenicity after 24 month follow up (Cooper et al., 2016). Despite these cells having advantages and being readily available, they have not shown the ability to migrate far along the gut and innervate the length of gut that is required for a full rescue of the disease phenotype. Furthermore, despite the advantage of these cells being allogenic, they would require gene correction and validation before being useful to treat Hirschsprung's disease or any other genetically driven enteric neuropathy. Recent advances utilising hPSCs have demonstrated the greatest potential, with their ability to integrate into the gut and migrate along the entire rostro-caudal axis being demonstrated (Fattahi et al., 2016). This study by Fattahi et al, has gone the furthest in terms of showing the ability to rescue Hirschsprung's disease with the greatest level of integration, migration and survival of a Hirschsprung's mouse model showing the promise of developing this approach (Fattahi et al., 2016).

1.7 Hox Genes

The Hox genes are the vertebrate homologues of the HOM-C genes described in *Drosophila melanogaster*. These genes show distinct spatial expression in the embryo that go on to form distinct structures in the embryo (Reviewed in Krumlauf, 1994). The HOM-C genes form a cluster on chromosome 3 in *Drosophila* and are activated sequentially with the first gene (3' end) in the cluster, *labial,* activated at the anterior and final gene in the cluster (5' end) *Abdominal-B,* expressed at the very posterior. In between the anterior (3' of the cluster) and posterior, the HOM-C genes in the middle of the cluster are expressed this pattern was described as co-linearity (Lewis, 1978). In the mouse, the induction of Hox genes in a co-linear fashion over time was seen and called temporal collinearity (Izpisua Belmonte et al., 1991) and 4 distinct clusters of HOX genes(A, B, C and D) have been identified in vertebrates that arose through two duplication events (Kappen, Schughart and Ruddle, 1989). Due to the complex expression domains

of HOX genes across the embryo, mutations in *HOX* genes give rise to a variety of phenotypes in many different tissues (Gaunt, Krumlauf and Duboule, 1989).

Hox genes position was originally assessed by their induction by differing concentrations of retinoic acid, with the 3' genes being most sensitive, and the 5' less sensitive, with the most 5' genes being insensitive retinoic acid. Subsequent analyses has shown that The 3' Hox genes (Hox1-5) respond to retinoic acid, whilst Hox6-13 respond to FGF, through a *Cdx* gene dependent mechanism (Bel-Vialar, Itasaki and Krumlauf, 2002). Both retinoic acid and FGF have been shown to be the signals upstream in chromatin remodelling events that will allow for HOX gene induction. These events occur in a saltatory fashion, i.e retinoic acid signalling de-represses all of the retinoic acid responsive HOX genes as a first layer of control of gene expression (Mazzoni et al., 2013). Box 3 below shows a cartoon of Hox gene expression domains and their responsiveness to signals.

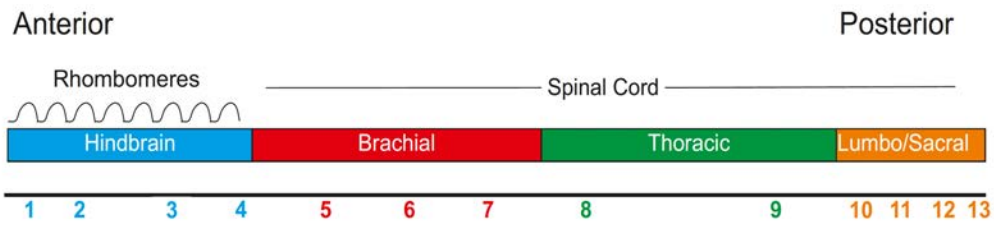

Box 3: Schematic of HOX gene anterior limits of expression throughout the spinal cord. 3' HOX genes (with lower numbers) are expressed at the anterior aspect of the embryo at the rhombomeres and are induced by retinoic acid. 5' HOX genes show anterior limits at the posterior end of the embryo and are responsive to WNT/FGF signalling induction of the CDX family of genes.

1.8 Retinoic Acid patterning of the embryo

1.8.1 Retinoic Acid Metabolism

Retinoic Acid is a naturally occurring metabolite that has long been associated with anterior posterior patterning from *in vivo* systems through to its key role now in many *in vitro* models of development. Retinoic Acid is synthesis occurs following the intake of retinol, usually from dietary source and is transported

round the body bound to RBP4 (Retinol-binding protein 4) and transthyretin (Noy, Slosberg and Scarlata, 1992) (Reviewed in Rhinn and Dollé, 2012). Once inside the target cell, retinol is then bound to cellular retinol binding proteins (CRBP) or undergoes oxidation to retinoic acid. The first step in this process involves oxidation of retinol to retinaldehyde by alcohol dehydrogenase enzymes (ADHs), which is oxidised to retinoic acid by retinaldehyde dehydrogenases (RALDHs) (Reviewed in Das et al., 2014; Rhinn and Dollé, 2012). Retinoic acid is then either stored in the cell, by binding to cellular retinoic acid binding proteins (CRABP) or it is further oxidised into further metabolites by cytochrome P450 26 (CYP26) enzyme subfamily into metabolites such as 4-OH-all-*trans*-retinoic acid (Chithalen, Luu, Petkovich and Jones, 2002).

1.8.2 Retinoic acid induction of gene expression

Following its biosynthesis, retinoic acid works to induce gene expression by crossing the cell membrane and binding one of two nuclear receptor families RARs and RXRs. There are three RARs (RARα, RARβ, RARγ) and RXRs (RXRα, RXRβ, RXRγ) that form differing combinations of homodimers and heterodimers with different affinities for different isomers of retinoic acid (Reijntjes, Gale and Maden, 2004). 9-cis retinoic acid is able to activate both RARs and RXRs, whilst all-trans retinoic acid can only bind to RARs (Mangelsdorf, Ong, Dyck and Evans, 1990; Levin et al., 1992). Following activation of the RA nuclear receptors, RARs/RXRs bind to a retinoic acid response elements (RAREs) that are conserved DNA motifs with the sequence 5 -(A/G)G(G/T)TCA-3 (Shimozono et al., 2013; Rhinn and Dollé, 2012). Retinoic acid binding to these receptors then results in a recruitment of activator complexes to induce target gene expression (Rhinn and Dollé, 2012; Balmer and Blomhoff, 2005). Genes that have been shown to have RAREs in their promoter regions include HOX genes, a family of genes that give spatial identity along the anterior posterior axis (Mallo and Alonso, 2013), consistent with the evidence showing the role of retinoic acid in patterning the embryo. In addition, genes encoding proteins involved in retinoic acid synthesis, such as retinoic acid receptors, have RAREs implying a feedback loop to control

retinoic acid signalling (Rhinn and Dollé, 2012). In addition, retinoic acid has recently been implicated in epigenetic regulation of gene expression by regulating TET enzyme activity and methylation of promoters (Hore et al., 2016).

1.8.3 Retinoic acid as a morphogen

Retinoic Acid was postulated to be a patterning factor after exposing *Xenopus* embryos to exogenous retinoic acid led to a loss of anterior structures (Papalopulu et al., 1991). Papalopulu and colleagues found that the loss of anterior structures depended on the concentration of retinoic acid that the embryo was exposed to, with the highest concentrations resulting in the complete lack of head structure (Papalopulu et al., 1991). They later determined the molecular changes in this with marker *Xotx2,* that is present in the forebrain, and a rostral expansion of *Xhoxb3,* that is present mid-hindbrain, indicating that much of the nervous system had gained a more posterior identity (Papalopulu and Kintner, 1996). The dose dependent change in anterior phenotype recapitulated the findings from retinoic acid human embryonal carcincoma differentiation models that showed a concentration effect in the induction of genes in the HOX2 cluster (Simeone et al., 1990). These data indicated the presence of a retinoic acid gradient in Hox gene patterning the head structures and indicated that is worked as a morphogen. The first paper describing retinoic acid as a morphogen was in the chicken limb bud, whereby application of retinoic acid mimicked the activity of the 'Zone of Polarising Activity' (Tickle, Alberts, Wolpert and Lee, 1982). It was subsequently shown that retinoic acid induced Sonic Hedgehog, which was the morphogen in the Zone of Polarising activity (Riddle, Johnson, Laufer and Tabin, 1993). Further analysis of components of the retinoic acid pathway showed enzymes involved in synthesis and degradation showed very distinct expression domains. The CYP26A1 enzyme, involved in the oxidation of Retinoic Acid, shows expression at the anterior domains of the chick embryo, along the developing brain as well as in the tailbud at HH stage 6 to 8 in the chick embryo (Shimozono et al., 2013). Furthermore, *raldh2* shows highest expression in the mid trunk region of the mouse embryo (Niederreither et al., 1997) These expression profiles control the activity of retinoic acid along the

embryo and have been postulated in the creation of a gradient along which the embryo is patterned. It has not been until recently, that gradient of retinoic acid in the visualised in the chick embryo. Utilising Fluorescence Resonance of Transfer (FRET) reporters bound to retinoic acid, Shimozono and colleagues were able to observe levels of retinoic acid *in vivo* in live early Zebrafish embryos (Shimozono et al., 2013). They showed the formation of a two-tailed source-sink pattern, where by the highest concentration of physiological retinoic acid was at the mid trunk region of the embryo that decreased as you look at the anterior and posterior edges of the embryo **(See Box 2).**

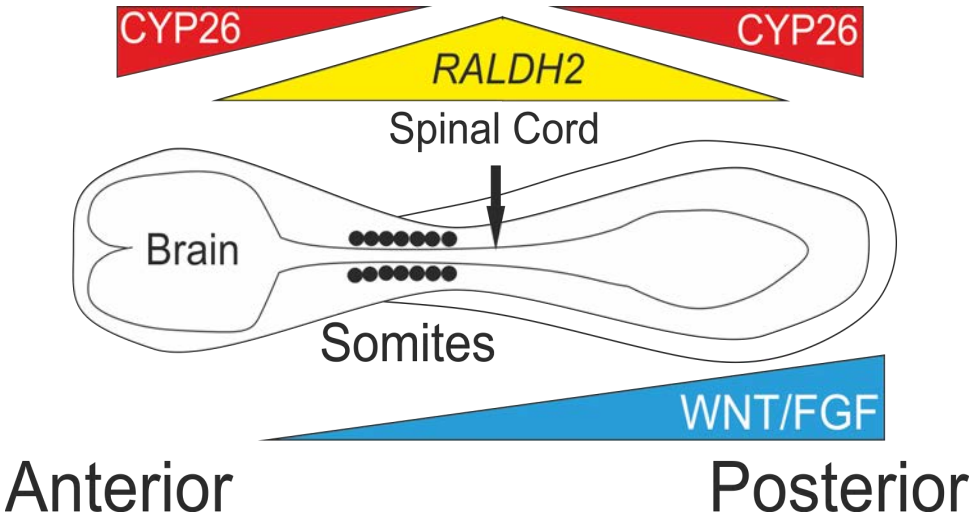

Box 2: Cartoon of a HH stage 10 embryo with anterior-posterior axis of the embryo labelled. Expression patterns of RALDH2 enzyme in biosynthesis, this is a proxy for high RA concentration in the embryo. This is highest at the mid trunk and decreases towards the anterior and posterior limits of the embryo. CYP26 enzyme expression is highest at the two poles of the embryo and works to oxidise Retinoic Acid. This thus creates the gradient of Retinoic Acid in the embryo that works to pattern the Anterior-Posterior Axis. FGF and WNT are highly expressed in the trunk and create a gradient from posterior to anterior.

1.9 Axial stem cells and the making of the trunk

1.9.1 Early formation of the anterior-posterior axis

Anterior or posterior identity is determined early during development. In the mouse, before gastrulation, the distal visceral endoderm begins to secrete inhibitors of nodal and Wnt signalling by secreting *Cer1* and *Dkk* into the embryo (Arnold and Robertson, 2009; Stern et al., 2006) and shows the asymmetry that is created during gastrulation. The future anterior portion showing high expression of these inhibitors and the future posterior showing high expression of Wnt. The high level of Wnt, in combination with the node, that is formed at the point of highest Nodal expression, induces expression of primitive streak genes such as *Brachyury* (Kispert and Herrmann, 1994) and *Mixl1* (Pearce and Evans, 1999). Prospective primitive streak cells undergo EMT and ingress and form a range of derivatives depending on their site of ingression in the primitive streak (Reviewed in Arnold and Robertson, 2009). The anterior primitive streak can give rise to the axial mesoderm and definitive endoderm under the influence of BMP signalling (Winnier, Blessing, Labosky and Hogan, 1995; Loh et al., 2016). Meanwhile the posterior primitive streak appears later and gives rise to somitic mesoderm, through CDX2 mediated signalling, and cardiac mesoderm through a NANOG dependent mechanism. (Mendjan et al., 2014). In the primitive streak, there is evidence for an axial stem cell that contributes to the notochord, somites and posterior Neurectoderm in chicken (Selleck and Stern, 1991) and mouse (Cambray and Wilson, 2002). The presence of the axial stem cells *in vivo* was finally demonstrated by retrospective clonal analysis in the mouse embryo (Tzouanacou et al., 2009a). Using the spontaneous recombination of an inactive LaacZ to LacZ, Tzouanacou and colleagues showed that clones where recombination occurred late (after gastrulation) contributed to neural and mesodermal tissues in the posterior of the embryo. Thus, this data demonstrated that from one cell originating cell, daughter cells were found to contribute to spinal cord and somatic mesoderm. In addition, these cells showed a posterior restriction and was the first *in vivo* evidence to demonstrate a population of axial

progenitors that give rise to neural and mesodermal tissues (Tzouanacou et al., 2009a). Recent work in the mouse has shown that these axial progenitors reside in the caudal lateral epiblast, but that their position within the caudal lateral epiblast dictates their fate and gene expression (Wymeersch et al., 2016).

Wnt and FGF signalling are crucial to the formation of the posterior of the embryo, *Fgf8* mRNA has been shown to be very highly expressed in the tailbud and decay of mRNA creates a gradient towards the tailbud (Dubrulle and Pourquie, 2004). In addition, *Wnt3a* (Aulehla et al., 2003) and β-*catenin* (Aulehla et al., 2008) are expressed in a gradient with highest expression in tailbud and is required for correct formation of the trunk. Mutations in Wnt signalling result in improper formation of somites which is seen when both β-*catenin* (Aulehla et al., 2008) and *Wnt3a* are knocked out (Ikeya and Takada, 2001). It has also been shown that reiterated *Fgf8* expression is dependent on *Wnt3a* (Aulehla et al., 2003) and thus the high expression of these two signals forms a positive feedback to retain the *Wnt*/*Fgf* gradient in the tailbud. The formation of a gradient in these two signals suggests a mechanism by which the reduction of their expression results in the formation of a segment of the embryo. Recent work has identified Wnt and FGF signals in the retention of a stem cell phenotype in the axial stem cells of the tail bud. FGF signalling downstream of Wnt has been shown to retain the expression of *Sox2*, a gene involved in the pluripotency associated network and expressed in axial stem cells in the mouse (Cunningham, Kumar, Yamaguchi and Duester, 2015b). Thus, the combination of Wnt and FGF are required for axis elongation.

Furthermore, retinoic acid is also shown to play a role in axial elongation, that is contrary to its role as a patterning morphogen in the anterior neural plate. Retinoic acid is synthesised the most in the mid-trunk of the embryo (Shimozono et al., 2013), with a sink at the tail-bud where the highest levels of Wnt and FGF are. In the elongating posterior, Retinoic acid has been shown to repress Wnt and FGF signalling in order to terminate elongation (Olivera-Martínez, Harada, Halley and Storey, 2012) and thus result in the differentiation of axial stem cells (Kumar and Duester, 2014) and proper somitogeneis (Cunningham et al., 2015a).

Meanwhile studies utilising techniques to knockout retinoic acid metabolism enzymes led to truncation of the embryo and loss of trunk structures (Niederreither, Subbarayan, Dolle and Chambon, 1999).

1.9.2 The gene regulatory network of axial elongation

Wnt, FGF and Retinoic acid signalling that plays a role in the elongation and correct segmentation of the embryo induce expression of genes that control the process of axis elongation. The axial stem cells that had been shown *in vivo* (Selleck and Stern, 1991; Cambray and Wilson, 2002; Tzouanacou et al., 2009a) have been shown to express the primitive streak gene *Brachyury* and the pluripotency/neural associated gene *Sox2* (Martin and Kimelman, 2012; Tsakiridis et al., 2015). The functions of both *Sox2* and *Brachyury* have been studied regarding their role in the retention of mechanism of induction; stem cell characteristics and subsequent differentiation have been investigated. *Sox2* is expressed in embryonic stem cells and is well characterised with this respect (Takahashi and Yamanaka, 2006) and its expression in embryonic stem cells is required for the retention of self-renewal. In addition, it is also seen as a key determinant of neural fate in Neuromesodermal progenitors (Axial stem cells) following interaction with the mesodermal gene *Tbx6* (Takemoto et al., 2011) indicating the threshold and cross repression of these genes in either neural or mesodermal fate. Furthermore, analysis of the cis-regulatory units of the Sox2 gene implicate the formation of the trunk nervous system, part of secondary neurulation, as part of a distinct mechanism (Uchikawa et al., 2003). This process has been shown to segregate early in development, with the anterior neural plate forming through an *Otx2* mediated process and activation of the *Sox2* N2 enhancer (Iwafuchi-Doi et al., 2012), whilst the posterior neural plate is from the N1 enhancer, which is Wnt responsive (Takemoto, Uchikawa, Kamachi and Kondoh, 2006). Furthermore, Brachyury is another key gene in the formation and differentiation of neuromesdoermal progenitors. *Brachyury* is induced by Wnt

signalling (Funa et al., 2015; Garriock et al., 2015) and knockouts in Brachyury often show defects in full axial elongation, with mutants showing a reduction in tail size (most notably, no tail is the name of the Zebrafish homologue for *Brachyury*) (Schulte-Merker et al., 1994; Beddington, Rashbass and Wilson, 1992; Yamada, 1994; Kispert and Herrmann, 1994). Further to this, interaction of *Brachyury* and *Tbx6*, with Sox2 has been shown to induce mesodermal fates over neural in Neuromesodermal progenitors through inducing chromatin remodelling permissive for mesoderm induction (Koch et al., 2017).

As previously discussed induction of Hox genes by Retinoic acid during hindbrain patterning (Section 1.7.3). Further to the role of these signals in the induction of the posterior end of the embryo, posterior Hox genes have been shown to be responsive to FGF and not Retinoic acid (Bel-Vialar, Itasaki and Krumlauf, 2002). Whilst a thorough analysis of the signals involved in patterning motor neurons showed that Fgf and Gdf signalling were required for thoracic and lumbosacral Hox genes respectively *in vivo* (Liu, Laufer and Jessell, 2001) and *in vitro* (Lippmann et al., 2015). These data are consistent with the secondary axis being crucial for the formation of the very posterior of the embryo. Bel-Vialar and colleagues showed that *Hoxb9* was expressed near the tail bud and in the trunk region of the chicken embryo and addition of Retinoic acid, the expression domain for *Hoxb9* decreased. Whilst addition of Fgf and transfection of a constitutively active version of *Cdx2*, the expression domain of *Hoxb9* was more rostral and encroaching the hindbrain (Bel-Vialar, Itasaki and Krumlauf, 2002). Thus they proposed that FGF signalling and *Cdx2* expression were required for the induction of trunk *Hox* genes in the chicken embryo.

Caudal related homeobox (*CDX*) genes, particularly *Cdx2* also show high expression in the tail bud and in cases where its expression it lost, there are defects in the correct formation of the tail (Chawengsaksophak et al., 1997). Furthermore, mouse embryos lacking both *Cdx2* and *Brachyury* show even more severe loss of the trunk and ChIP-Seq analysis demonstrated that they both bind to regulatory regions in *Fgf* and *Wnt* genes to retain the high expression required for elongation (Amin et al., 2016). Furthermore, Amin and colleagues also

demonstrated that *Cdx2* binds to the promoters of *Hox1*-9 in each of the four paralogous groups, as a functional determination of *Wnt* mediated *Cdx2* expression inducing *Hox* genes along with Fgf (Amin et al., 2016).

The transition from trunk to tail is the first step in the termination of axis elongation. Continued expression of *Oct4* under control of the *Cdx2* promoter can induce mice with elongated trunks (Aires et al., 2016). In addition to the elongated tail in these mice, Aires at al found that this ectopic expression of Oct4 prevented the activation of Hox groups 10 to 13, that are active in the tail bud (Aires et al., 2016). In contrast, expression of the posterior Hox groups (9 to 13) have been shown to slow the elongation of the axis by repression of Wnt signalling and its target Brachyury (Denans, Iimura and Pourquie, 2015). *Hox* gene mediated repression of Wnt signalling coincides with the increase of Retinoic acid in the tail that negatively regulates Fgf signalling (Olivera-Martínez et al., 2012). Furthermore, GDF signalling has also been implicated in the transition from tail to trunk with its expression required for the induction of sacral Hox clusters in motor neurons (Liu, Laufer and Jessell, 2001). *Gdf11* knockout mutants show a posterior transformation of the sacral Hox genes and result in an extension of the trunks, These data combined elucidate a model by which *Gdf* signalling induces the *Hox 10-13* genes to terminate axial elongation (McPherron, Lawler and Lee, 1999).

1.9.3 A potential origin of trunk neural crest cells

The posterior neurectoderm is formed during secondary neurulation, which is originally from the tailbud and induced by the node (Catala et al 1995; Beddington 1994). Axial stem cells have been identidied and mapped *in vivo* that contribute to the posterior neural tube and paraxial mesoderm (Tzouanacou et al., 2009b; Tsakiridis and Wilson, 2015; Gouti et al., 2014). Meanwhile, there has not been significant research to assess whether the neural crest, that arises from adjacent to the neural plate and delaminates from the dorsal aspect of the neural tube is formed during secondary neurulation or an extension of primary neurulation.

Neural crest cells show different fates dependent on their axial identity and has been discussed previously during this introduction, but the question of what determines the difference in fate has not been answered and there is evidence suggesting that fate is governed cell autonomously (Le Lièvre and Le Douarin, 1975), or by the environment (Trainor and Krumlauf, 2000a).

Analysis of the chicken tail bud region, formed during secondary neurulation, has shown that neural crest cells can emanate from the neural tube of this region (Schoenwolf, Chandler and Smith, 1985a). In addition, transplantation of quail neural crest cells into this region gave rise to neurons and glia, particularly in the spinal ganglia which has been well characterised as a destination for neural crest derivatives (Schoenwolf, Chandler and Smith, 1985b). Furthermore, molecular analysis of marker expression showed a retention of many of the classical neural crest genes between anterior and posterior, such as Pax7, Pax3 and FoxD3 (Osorio, Teillet, Palmeirim and Catala, 2009). Osorio et al showed the expression of these neural crest specifiers in the dorsal neural tube following its formation. In addition, they also report Pax3 expression rostral to the tail bud in the primitive streak mesoderm (Osorio et al., 2009). Conversely, they also demonstrate some differences in the migration, whilst neural crest cells from primary and secondary neurulation delaminate from the neural tube upon closure, the neural crest from the secondary neurulation seems to do so in a BMP dependent manner (Osorio et al., 2009), whilst cranial neural crest requires Ets-1 to do so (Barembaum and Bronner, 2013). Furthermore, it has also been shown that *Cdx2*, key for axial elongation of NMPs, also has direct inputs into the core neural crest genes, *Pax3* and *Msx1* (Sanchez-Ferras et al., 2016). Whilst knockdown of the *Cdx2* mediated *Pax3* expression results in pigmentation defects towards the trunk of the embryo, but not the anterior (Sanchez-Ferras et al., 2016). This is consistent with divergent gene regulatory networks and potentially different origins of the rostral and caudal neural crest populations.

Chapter 2: Characterisation of hPSC derived Neural Crest Cells

2.1 Introduction

Human pluripotent stem cells are a unique tool that allow insight into human development by directed differentiation to somatic cell types. The first set of protocols published to generate neural crest cells from hPSCs utilised a co-culture system with either PA6 (Jiang et al., 2009) or MS5 (Lee et al., 2007) cells. Although these protocols produced neural crest cells expressing many of the markers, Fluorescence Activated Cell sorting (FACs) for the neural crest markers P75 and HNK1 was essential for any downstream applications (Lee et al., 2007). These were followed by protocols utilising neurosphere differentiation of hPS cells, and upon plating of the spheres, allowing the neural crest cells to migrate away from the sphere (Bajpai et al., 2010). Whilst these protocols all allowed for the formation of neural crest cells *in vitro*, it gave little information on the signals and genes that informed formation of human neural crest from hPS cells and any downstream applications required purification to remove unwanted stromal layers or Neurectoderm spheres. The first protocol to derive neural crest cells directly from hPSCs in a monolayer differentiation utilised inhibition of GSK3β to stimulate WNT signalling, and inhibition of TGFβ/NODAL pathway, that will promote ectodermal specification from hPSCs, to form neural crest cells directly from hPS cells (Menendez, Yatskievych, Antin and Dalton, 2011). In addition to the requirement of WNT signalling and inhibition of TGFβ/NODAL, it was also demonstrated that modulation of BMP signalling by its inhibitor NOGGIN or even the application of recombinant BMP4 disrupted neural crest specification. This is in agreement with the findings that the inhibition of both BMP and TGFβ/NODAL pathways by dual-SMAD inhibition gives rise to neural cells from hPS cells (Chambers et al., 2009). In addition, it was subsequently found that the addition of the GSK3β inhibitor CHIR99021 to dual SMAD gave rise to neural crest cells efficiently (Mica et al., 2013) further showing the requirement of WNT signalling to neural crest induction from hPS cells. These protocols differed in their findings

with respect to BMP signalling, where the Menendez protocol found that inhibition of BMP signalling perturbed neural crest differentiation. Both the Chambers (Chambers et al., 2009) and Mica (Mica et al., 2013) protocols both utilised a BMP inhibitor in combination with either serum (Knockout serum replacement) (Chambers et al., 2009; Mica et al., 2013), whereas the Menende protocol required passaging steps (Menendez et al., 2011) and so also had drawbacks with finding the precise signals and genes that induced neural crest signalling. WNT signalling has long been known as the key signal in neural crest specification in chicks (García-Castro, Marcelle and Bronner-Fraser, 2002). This finding was subsequently shown in hPSC induction to neural crest where it was shown recently that exposure to CHIR99021 alone was needed and confirmed by knockdown of β-catenin by shRNA (Leung et al., 2016). In the meantime, our group had been developing the first xeno-free differentiation media to generate neural crest cells utilising GSK3β inhibition (CHIR99021) and TGFβ/NODAL inhibition (SB431542) to form neural crest cells (Hackland et al., 2017). In addition, we had found that whilst this protocol worked, it was not robust. There was variation in neural crest formation within the same cell line and previous protocols had shown both activation and inhibition of BMP signalling perturbed neural crest specification.(Menendez et al., 2011). This reflects what is known *in vivo*, where intermediate BMP signalling is required for neural crest formation (Tribulo et al., 2003). Thus, the difference and unpredictability of BMP signalling within the starting hPSC population had an impact on the ability to form neural crest and demonstrated that neural crest formation required a specific low level of BMP signalling in conjunction with WNT signalling. We combined a BMP inhibitor (DMH1) with recombinant BMP4 to produce a robust system that can control BMP4 activity in neural crest differentiation for robust efficiency. We found that these cells expressed transcription factors and antigens indicative of neural crest fate such as *SOX10*, *PAX3*, *SOX9* and the antigens P75 and HNK1 (data not shown). The true test of these putative neural crest cells is their functional ability to differentiate into the correct derivatives in vitro. Specifically, neural crest cells have the unique ability for form both derivatives that are characteristic of both ectoderm (neurons and glia) and mesoderm (bone and cartilage). In

addition, the ability of neural crest cells to form specific derivatives has been linked to their anterior-posterior identity and this factor has so far been overlooked in hPSC neural crest differentiation protocols and the ability to pattern these cells may reflect the ability of these cells to make certain derivatives.

2.2 Aims

To address the issues regarding the early fate decisions and anterior posterior identity in Neural Crest cells derived from hPSCs, we have performed experiments to address these first specific aims.

1. Characterise the stages of neural crest differentiation from hPSCs

2. Characterise the ability of putative hPSC derived neural crest cells to form derivatives

3. Determine the anterior-posterior identity of putative hPSC derived neural crest cells.

2.3 Results

2.3.1 Characterisation of Optimised Xeno-Free Differentiation Protocol

The current method used in our lab to generate neural crest cells takes 8 days and requires a plating step in a basal E6 media at 10 000 cells/cm^2 before changing to the differentiation media **(Figure 2.1A)** (Hackland et al., 2017). However, another recently published method involves plating hPSCs down in differentiation media at a higher density, and only takes 5 days while still generating robust amounts of neural crest cells (Leung et al., 2016). To test if we could utilise the media from the Hackland protocol (termed TDI for Top Down Inhibition) which contains the GSK3β inhibitor CHIR99021 (1μM); TGFβ/NODAL inhibitor SB431542 (2μM); BMP4 (20ng/ml) and the ALK2 inhibitor DMH1 (1μM) (Hao et al., 2010) We plated down 30 000 cells/cm^2 in TDI media supplemented with 10μM of the ROCK inhibitor Y-27632 hydrochloride to prevent cell death as shown in the schematic labelled 'Revised Hackland Protocol' **(Figure 2.1A)**. Media was changed at day 2

to remove the ROCK inhibitor and day 4 to replenish growth factors and analysed on day 5 for SOX10::GFP and the $P75^{NTR}$ antigen by flow cytometry **(Figure 2.1B)**. We found that this shortened protocol to 5 days from the original 7 day protocol in Hackland et al was able to derive high levels of SOX10::GFP+/$P75^{++}$ cells in H9:SOX10::GFP transgenic cells and unmodified Mastershef7 cells after 5 days **(Figure 2.1B)**. As reported in both the Menendez and Hackland protocols, $P75^{++}$ expressing cells were shown to be SOX10+ putative neural crest cells. FACs analysis in SOX10::GFP reporter showed the same results with GFP expression restricted to cells with P75 expression intensity measured above 10^2 by flow cytometry. Thus, we also used this high P75 gate to assess the formation of neural crest cells in MasterShef7 cells and found a similar level of induction of 63% $P75^{++}$ cells. To further test the formation of putative neural crest cells, we took whole cell RNA from day 0 (starting hPSC population), day 3 and day 6 differentiated H9:SOX10::GFP cells and carried out qRT-PCR for neural crest associated transcription factors. There was significant increase in transcripts indicative neural plate border cells including *SOX9, PAX7, TFAP2*α and *MSX1* after three days of differentiation. *PAX7, FOXD3, MSX1 and SOX9* show their highest expression at day 3 of differentiation and then show a decrease in expression as the differentiation continues through to day 6. This contrasts to what is seen for genes such as *SOX10, SLUG* and *PAX3* where expression increases at day 3, but peaks on day 6 differentiated cells reflecting a further change to putative migratory neural crest cells where these genes are expressed at higher levels. There is also a level of expression of many neural crest associated genes in the starting hPSC population such as FOXD3, SLUG and SNAI1. The mean delta CT values after normalising genes to *GAPDH* for these genes from 3 independent experiments in the starting hPSCs cells *FOXD3*=8.3, *SLUG*=11.9, *SNAI1*=10.9 and *SOX9*=9.7, compared to 6.1, 4.5, 8.5 and 6.5 in day 6 neural crest cells respectively. Overall, these data are consistent with the upregulation of genes involved in neural crest differentiation from hPSCs (Menendez et al., 2011; Mica et al., 2013) and by looking at the change of gene expression throughout the differentiation, we also see that this transition in cell fate is consistent with the this differentiation occurring through a neural plate border intermediate.

2.3.2 Tracking differentiation by Flow Cytometry Analysis

We have shown changes of gene expression consistent of neural crest differentiation from hPSCs. To continue from this, we wanted to assess the antigen expression of these cells throughout the differentiation to determine how the profile changes to assess yields of cells and to sort out populations. There are two commonly used neural crest associated markers for flow cytometry P75 and CD49d that recognises an epitope on Integrin α4 (Fattahi et al., 2016). We utilised the H9:SOX10::GFP reporter line and undertook FACS analysis of cell from days 3 to 5 of differentiation. On each day, we set the baseline using the antibody P3X (an antibody that is secreted from the P3X63AG8 myeloma cell line) and GFP negative cells **(Figure 2.2A)** and then assessed the expression of the immunoreactivity of the CD49d antibody and ME20.4 that recognises an epitope on P75 (Ross et al., 1984a). On day 3, we observed homogenous low P75 expression close to negative **(Figure 2.2B i)**. The fluorescence intensity (Arbitrary units) was between 10^1 and 10^2, classified as $P75^+$ (Menendez et al., 2011) this coincided with no SOX10::GFP expression which is consistent with the transcript data from **Figure 2.1C** where expression is at a low level. At day 4, there is an increase of P75 expression towards 10^2 and even some reaching 10^3 fluorescence intensity **(Figure 2.2B ii)**. This higher level of P75 expression (In the upper half of the 10^2 decade: termed $P75^{++}$) coincides with all the SOX10::GFP positive cells, reflecting our previous data (Hackland et al., 2017) and the Menendez protocol. This trend of increased P75 fluorescence intensity and the association of this with the expression of the SOX10::GFP reporter is also seen at day 5 **(Figure 2.2B iii)** showing the transition of differentiation from $P75^+$ to $P75^{++}$ and the expression of SOX10::GFP. This indicates that P75 is expressed by the putative neural plate border cells found at day 3. These findings are the same as those from the 7 day Hackland and Menendez protocols and provide further evidence that this modified Hackland protocol produces putative neural crest cells faster than previously. We did not see CD49d immunoreactivity at day 3 coinciding with no GFP expression. On day 4, there are two additional populations that emerge, a SOX10::GFP+/CD49d- (11%) and SOX10::GFP+/CD49d+ (14%) which then at day 5

go on to be 7% and 71% respectively. The transition of expression in these cells contrasts that of P75, where P75 expression increases and then SOX10::GFP expression is seen. In the case of CD49d, SOX10::GFP appears first and then subsequently there seems to be immunoreactivity of CD49d. Thus, from this we can conclude that there is no significant difference in the use of $P75^{++}$ and CD49d+ populations in marking hPSC derived putative neural crest cells. Where they both coincide with SOX10::GFP expression. The key difference is in the timing of this, where P75 appears early and at low levels and subsequently increases expression throughout differentiation transiting from a $P75^{+}$ to$P75^{++}$/SOX10::GFP- to $P75^{++}$/SOX10::GFP+ populations. Thus, we can conclude P75 can be used to track the onset of differentiation. CD49d on the other hand appears only in cells that are SOX10::GFP+ with the transition being SOX10::GFP negative/CD49d- to Sox10::GFP+/CD49d negative to SOX10::GFP positive/CD49d negative. This may be due to CD49d binding to integrin $\alpha 4$ which may be marking neural crest cells that have undergone EMT and so being the *in vitro* equivalent to cells that have undergone delamination from the neural tube.

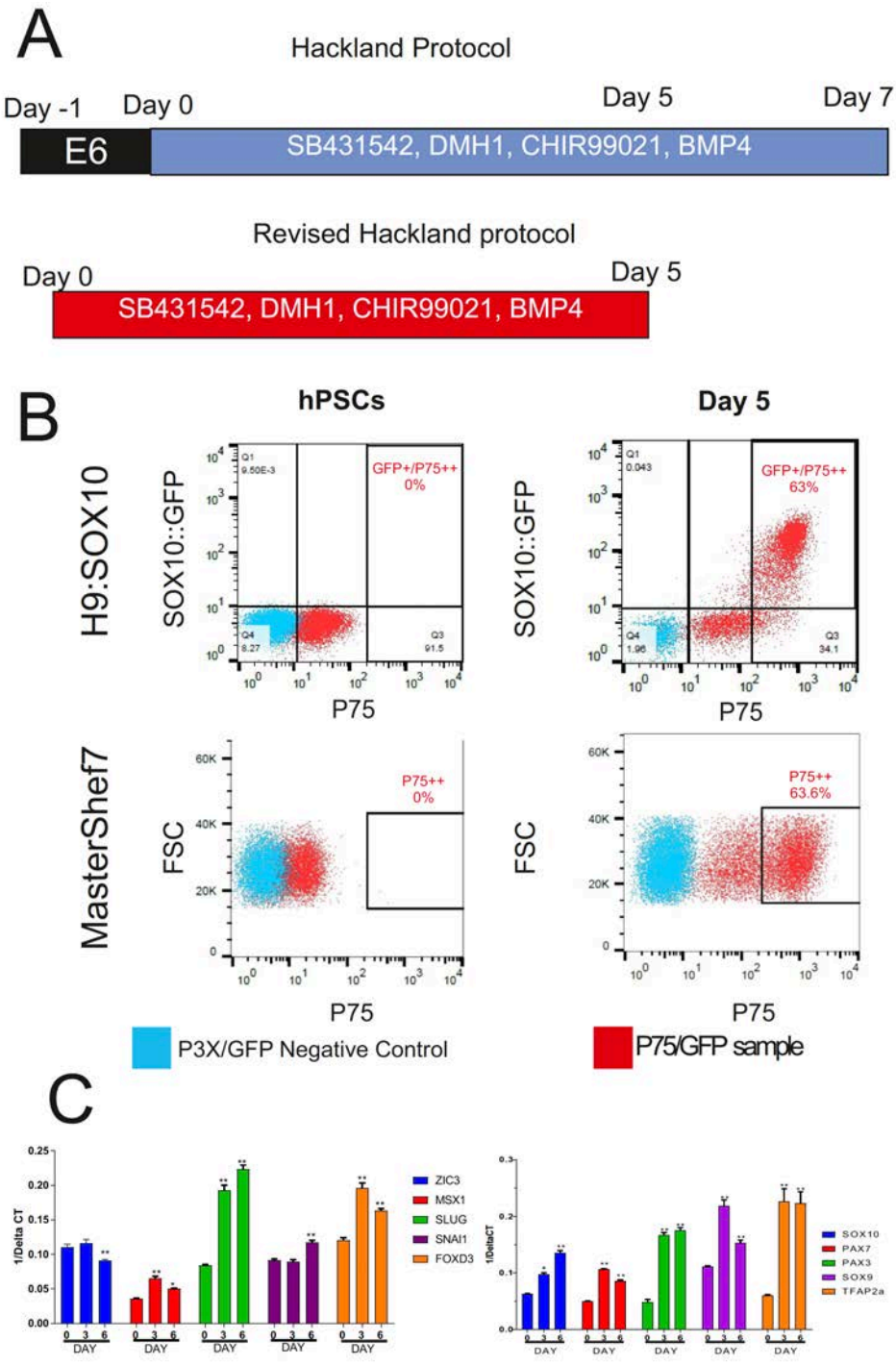

Figure 2.1. Characterisation of faster Neural Crest differentiation protocol. (A) Schematic showing the timings and components of neural crest differentiation media as outlined in Hackland et al 2017 and the new faster protocol. **(B)** Representative FACS plots showing expression of SOX10::GFP and P75 in hPSCs and cells after 5 days of differentiation. Co-expression of the antigen P75 and SOX10::GFP reporter is only seen after 5 days of differentiation. Differentiated cells show a high level of P75 expression (termed P75++) compared to hPSCs that only show a low level of P75 expression. This same profile is also seen in MasterShef7 cells that have been subjected to the same differentiation. **(C)** qPCR profiles of total RNA from cells taken at day 0 (hPSCs), day 3 and day 6 of differentiation show induction of neural crest associated genes SOX10, PAX7, SOX9,

MSX1, SNAI1 and SLUG. Data is presented as 1/Delta CT relative to GAPDH and significance calculated relative to hPSCs using a two-way ANOVA (Dunnett's multiple comparison test *=P<0.05; **=P<0.01).

2.3.3 Neural Crest cells are specified early in differentiation

Having used P75 to track the onset of differentiation from day 3 to day 5, we wanted to test if the immunoreactivity of the SSEA3 antibody which is commonly used to mark undifferentiated hPSCs, throughout this period to determine the loss of stem cell associated markers. We performed FACS analysis on hPSCs and cells being differentiated from day 3 to day 5 of the differentiation protocol **(Figure 2.3A)**. We found that hPSCs show homogeneous expression level of SSEA3 (94%) which was to be expected from a uniform starting population of hPSCs **(Figure 2.3a i)**. At day 3 **(Figure 2.3A ii)**, we found that there was still a high proportion (71%) of cells that were still positive for SSEA3, but rather than one homogenous population, there was a trend toward the downregulation of SSEA3. By day 4 **(Figure 2.3A iii)**, SSEA3 had largely turned off (in 65% of the cells now being negative for SSEA3), but there was a population of low expressing cells (26%). SOX10::GFP had appeared in a subset of these cells and on the whole, these two markers appear to be mutually exclusive, aside from a small population (approximately 5%) that co-express both GFP and SSEA3 by flow cytometry. By day 5 **(Figure 2.3A iv)**, the trend of SSEA3 turning off and SOX10::GFP turning on had continued with the 75% of cells being SSEA3-/GFP+, whilst a further 15% of cells were SSEA3-/GFP-. There were still 3% of cells found to be SSEA3+/GFP- and the 5% population of SSEA3+/GFP+ cells had also remained at day 5. Cells at day 3 of the protocol have already upregulated transcription factors associated with neural crest specification, such as *PAX7*, *SOX9*, and *TFAP2*α **(Figure 2.1C)**, but they also still show expression of pluripotency associated markers such as SSEA3, we next wanted to test if these cells at day 3 were expressing other pluripotency associated markers such as the transcription factors *POU5F1 (OCT4), NANOG* and *SOX2* by qPCR **(Figure 2.3B)**. *OCT4* and *SOX2* are expressed ay very high levels in hPSCs, whilst NANOG is expressed, but has a very low transcript level. These genes all show reduced levels of expression after three days of differentiation,

with *OCT4* showing the greatest reduction in expression between day 0 hPSCs and day 3 differentiated cells and *NANOG* also shows reduced transcript expression from day 0 (hPSCs) to day 3. SOX2 is reduced in day 3 differentiated cells, but the level of reduction between these two stages of differentiation is lesser than the downregulation of *OCT4*. Between day 3 and 6, both *OCT4* and *SOX2* levels are reduced, but in the case of *OCT4* this downregulation is far less than the reduction between day 0 hPSCs and day 3 cells. *SOX2* is still expressed at a high level which can be indicative of either *SOX2* being active in Neural Crest differentiation; the presence of neural plate contamination, or a retention of *SOX2* in its association with hPSCs. To test if there was contamination of neural plate cells, we assessed the levels of the early pro neural gene *SOX1* **(Figure 2.3C)** and found that there was similar low level of SOX1 throughout all days of the differentiation and no significant increase from day 0 hPSCs to day 3 differentiated cells indicating that there was no significant contamination of neural plate contaminants. The retained expression of SSEA3 to day 3 of differentiation **(Figure 2.3A)** combined with transcript data showing acquisition of neural plate border transcripts **(Figure 2.1C)** and no significant increase in SOX1 expression from day 0 to 3 **(Figure 2.3C)** offer further weight to the notion that neural crest cells may be specified early on *in vitro*. To test this, we subjected cells to neural crest differentiation, but wanted to see how early they were specified by only keeping the cells in the differentiation media for different periods of time early (days 0-1 or days 0-2) or late (days 2-5) and the rest of the time being kept in the N2 basal media. If the neural crest was determined early, then we would expect to see similar levels of neural crest induction measured by SOX10+ cells after 5 days. Control cultures subjected to the growth factors for all 5 days gave rise to 65% SOX10+ cells at the end of the differentiation which is like the yields usually found from this differentiation **(Figure 2.1)**. Exposure to growth factors between days 0 and 1 resulted in approximately 23% SOX10+ cells, indicating some cells being determined early. In addition, two days' exposure resulted in 51% SOX10+ cells showing, which is lower than the control, but is higher than the yield from one day exposure. On the other hand, late exposure to growth factors (days 2-5) perturbed the ability of hPSCs to form neural crest with only 4% of cells expressing

SOX10. Thus, the ability of cells to form neural crest cells with only two days of signalling may offer additional evidence that neural crest cells are determined early in *vitro* and they are specified directly from hPSCs.

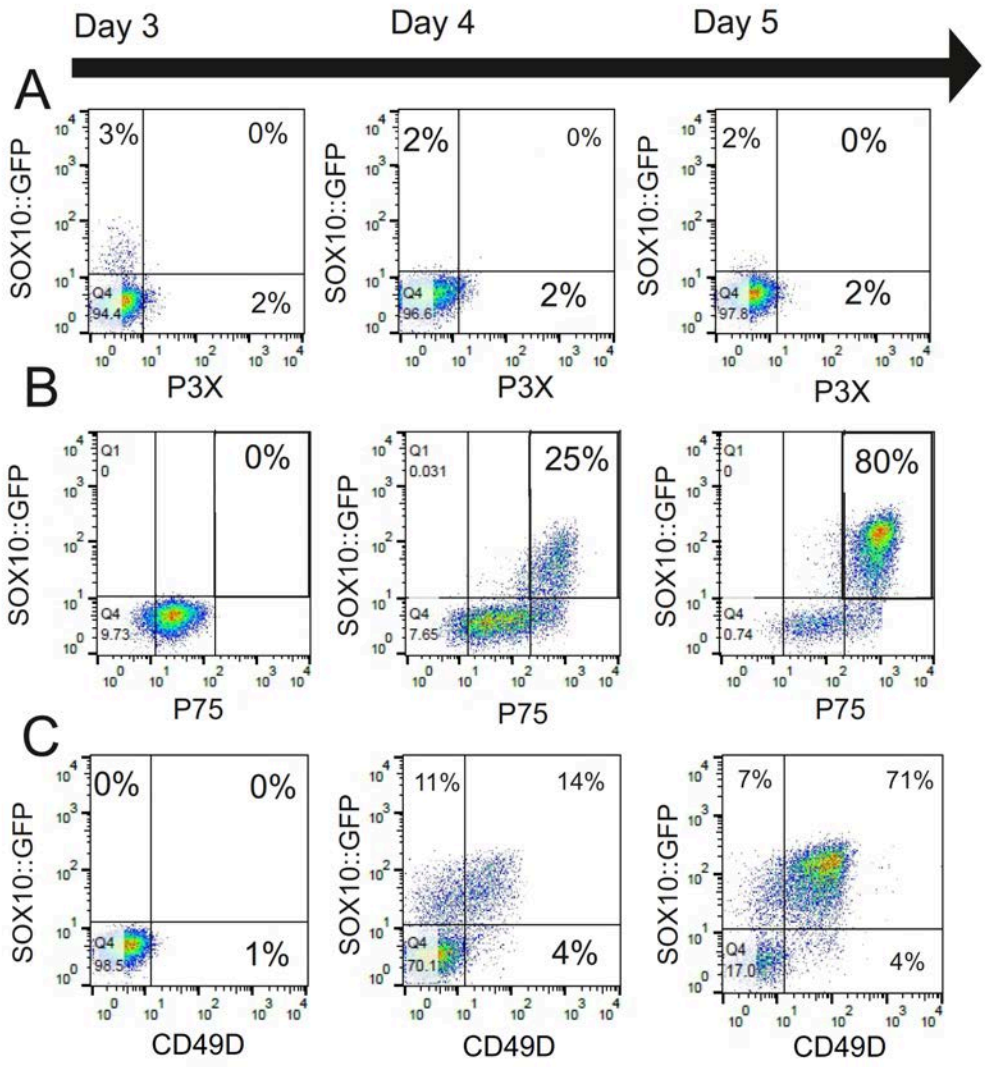

Figure 2.2 Figure 2.2 P75 and CD49d comparison for analysis of Neural Crest differentiation. (**A)** Time course FACs analysis from day 3 to 5 of neural crest differentiation. baseline negative control for both GFP and antibody staining is shown in the top row for all days. **(B)** P75 shows a homogenous low expression (between 10^1 and 10^2) in all cells on day 3 which increases to show some cells with greater than 102 expression on day 4 and 5. This increase in P75 expression correlates with the SOX10::GFP reporter construct with P75++/SOX10::GFP+ population comprising 25% of cells on day 4 and 80% on day 5. **(C**) On day 3, there is no expression of SOX10::GFP or CD49d expression in any of the cells. Although on day 4, two populations emerge a SOX10::GFP+/CD49d-(11%) and SOX10::GFP/CD49d+ (14%). The double positive population increases to 71% on day 5 with 7% being SOX10::GFP+/CCD49d-. On both of these days there are only 4% of cells that are SOX10::GFP-/CD49D+

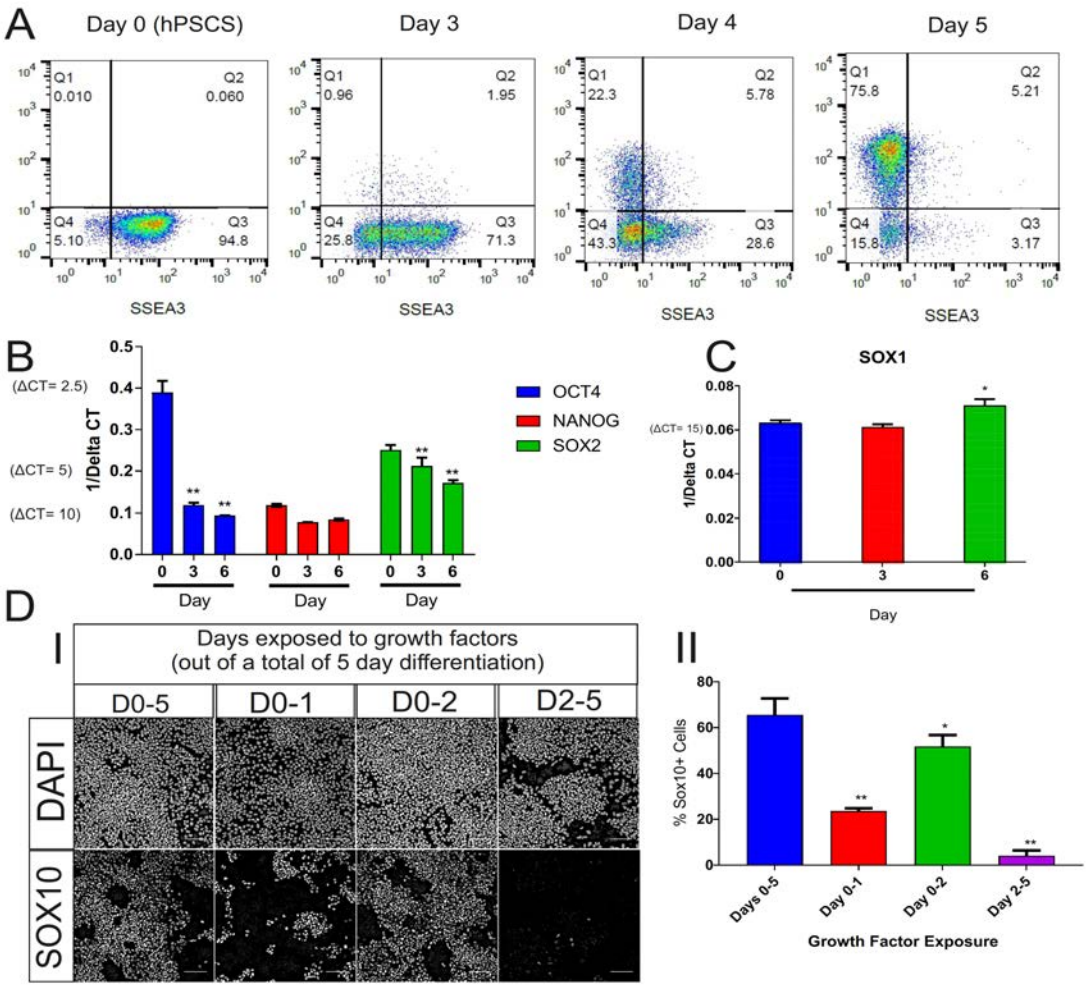

Figure 2.3. Early determination of neural crest cells from hPSCs. (A) FACs plots showing SOX10::GFP expression and SSEA3 immunoreactivity throughout neural crest differentiation. hPSCs express SSEA3 homogenously and lack SOX10::GFP expression. At day 3, there is still SSEA3 immunoreactivity, but this is decreasing and a negative population emerges. By day 4, the SSEA3 negative population increases and begins to show expression of SOX10::GFP. This trend continues to day 5 where SSEA3 immunoreactivity is only 3% whilst SOX10::GFP is at 75%. **(B)** Pluripotency associated genes OCT4, NANOG and SOX2 show downregulation throughout differentiation, but still show some expression throughout the differentiation, (N=3 independent experiments; two way ANOVA **P<0.01 whilst the pro neural marker SOX1 shows low level expression throughout **(C)** N=3 independent experiments one way ANOVA (*P<0.05) **(D)** Timed exposure of growth factors shows that the exposure to growth factors for the first two days alone can result in high yields of neural crest cells in vitro **(I)** and quantification of images of 7 random fields **(II)** (n=3 technical repeats) (One-Way Anova *P<0.01, **P<0.0001).

2.3.4 Neural Crest cells can form Neural and non-neural derivatives *in vitro*

To fully characterise the formation of neural crest cells from hPSCs *in vitro*, we wanted to test whether the putative neural crest cells produced by this protocol could be further specified to derivatives **(Figure 2.4a)** The Neural Crest has been shown to form a wide variety of derivatives *in vivo* and so we wanted to test to see if our *in vitro* counterparts could recapitulate this. This has been reported with other hPSC derived neural crest protocols (Lee et al., 2007; Menendez et al., 2011; Leung et al., 2016) . First, we tested if how ectomesenchyme was specified from neural crest, previous reports have cultured hPSC derived neural crest cells in serum containing media and seen acquisition of stromal cell assosciated antigens CD73, CD90 and CD105 (Menendez et al., 2011; Lee et al., 2007). Due to serum being undefined, we tested a proprietary defined medium from Stem Cell Technologies Mesencult –Animal Component Free (ACF) culture media (Stem Cell Technologies Catalogue #05449). We grew sorted SOX10::GFP hPSC derived neural crest cells in this media for 10 days **(Figure 2.4B)** and used FACs analysis to test the immunoreactivity of CD73, CD90 and CD105 of the resulting cells. **(Figure 2.4C)**. The day 5 hPSC derived neural crest cells show little to no reactivity to CD73 and CD90 (red histograms), with any positive expression being a tail of expression, whilst the bulk culture was in the negative. These cells did show immunoreactivity to CD90, which recognises THY-1, with 96.7% positive cells being found. After 10 days of growth in Mesencult-ACF, we saw that the FACs profile changed with respect to immunoreactivity to CD73 and CD105 with 97 % and 93% of the cells being positive following this induction. We next wanted to test if these cells could further differentiate into later derivatives such as bone (Figure 2.4D) and cartilage (Figure 2.4E). We further differentiated these in the Mesencult osteogenic stimulatory kit (Stem Cell Technologies Catalogue #05404). We took putative neural crest derived ectomesenchyme and cultured them in this media for 3 weeks and assessed for calcium deposits by Alizarin Red staining. Cells cultured in the differentiation media showed more Alizarin Red reactivity than those cultured in the basal media without the supplements added. A pellet based chondrocyte

assay to determine the formation of cartilage *in vitro*. We pelleted ectomesenchyme cells and grew then in either basal media of chondrocyte differentiation media (Stem Cell Technologies Catalogue #05455) and assessed for glycosaminoglycan deposition by Toluidine Blue staining. The chondrocyte differentiation was greatly enhanced in the differentiation conditions and saw more Toluidine blue staining from this condition than the basal condition. Overall, these data show that hPSC derived neural crest cells and be further differentiated to mesodermal derivatives and subsequent downstream derivatives.

In addition to forming mesodermal derivatives, we wanted to test the ability of these cells to form peripheral neurons *in vitro*. We cultured SOX10::GFP+ sorted hPSC derived neural crest cells in neurogenic media containing CHIR99021, SU5402 and DAPT for 10 days (Chambers et al., 2012). We then replaced this media for neurotrophin media (containing BDNF, GDNF and NGF) and allowed cells to differentiate for 7 days. Over the course of this 10-day further culture, we saw a morphology change from the stellate morphology of neural crest cells to an elongated neuronal morphology. We performed immunostaining on these cells for the pan-neuronal class III beta tubulin (assessed by TUJ1 staining) and PERIPHERIN, an intermediate filament found in the peripheral nervous system (Portier, de Nechaud and Gros, 1983). We found that this differentiation gave rise to neurons that expressed TUJ1+ **(Figure 2.5C)** PERIPHERIN+ **(Figure 2.5B)** neurons *in vitro*. The expression of these two markers gives further weight to the conclusion that these neurons are neural crest derived and not from any contaminating CNS precursors. In addition, the inhibitor cocktail used to accelerate neuronal differentiation had been shown to produce high yields of sensory neurons (Chambers et al., 2012) and so we assessed the expression of the two sensory neuron markers BRAIN3A (BRN3A) **(Figure 2.5C)** and Islet 1 (ISL1) **(Figure 2.5B)** by immunostaining in conjunction with Tuj1 and Peripherin respectively. We saw that most these cells showed co-expression of these two markers indicating that these peripheral neurons were specifically sensory neurons.

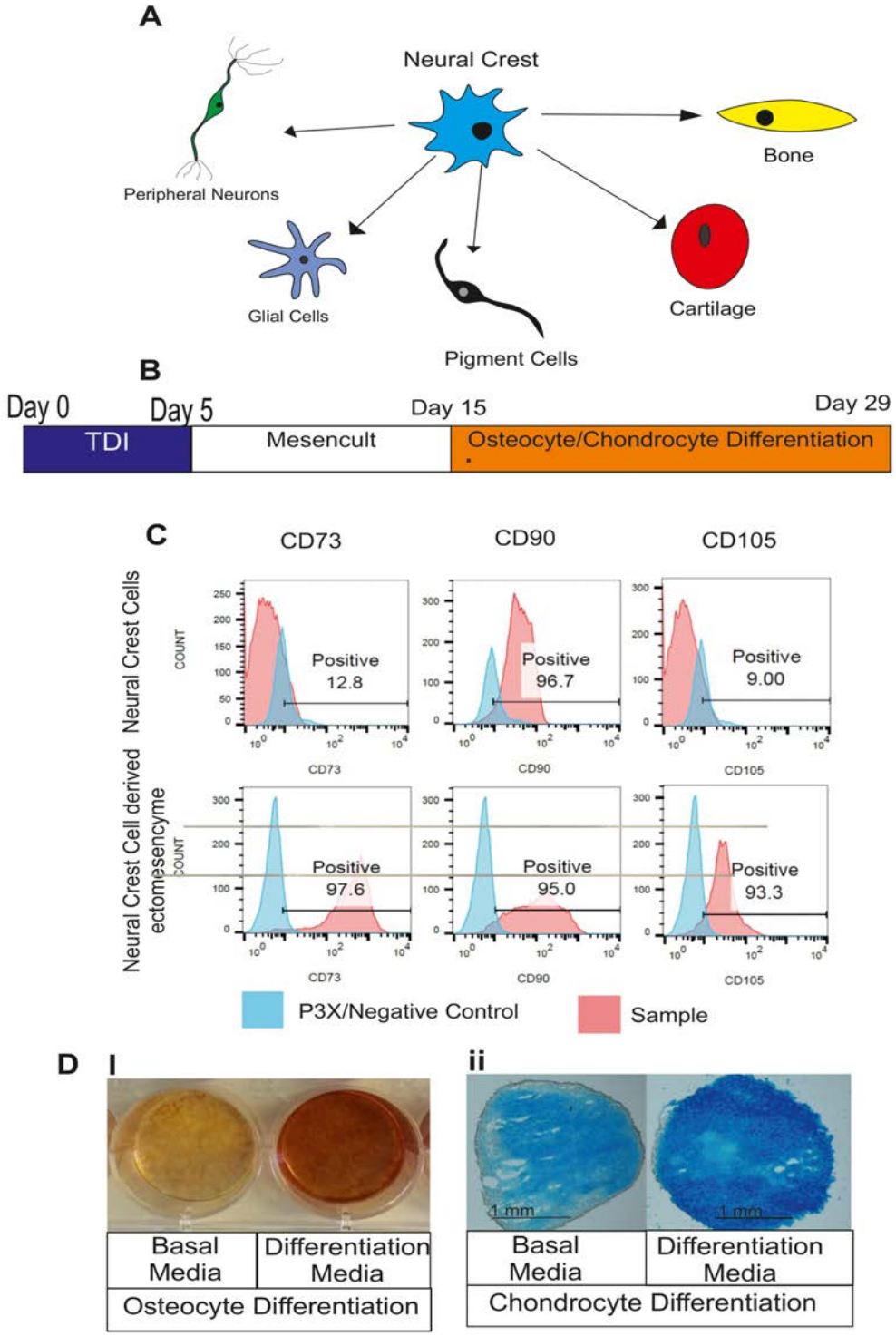

Figure 2.4 **Further Differentiation of hPSC derived neural crest cells. (A)** Schematic showing the derivatives of neural crest cells *in vivo.* **(B)** Schematic of differentiation time line to make ectomesenchyme from hPSC derived neural crest cells *in vitro*. **(C)** FACS plots showing hPSC derived neural crest cells do not express the antigens CD73 or CD105, but do express CD90 (THY1). After 10 days differentiation to ectomesenchyme, expression of stromal cell markers CD73, CD90 and CD105 is seen as well as Alizarin Red positive putative osteocytes and Toluidine Blue positive chondrocytes after three weeks further differentiation (D). Images also in Hackland et al 2017

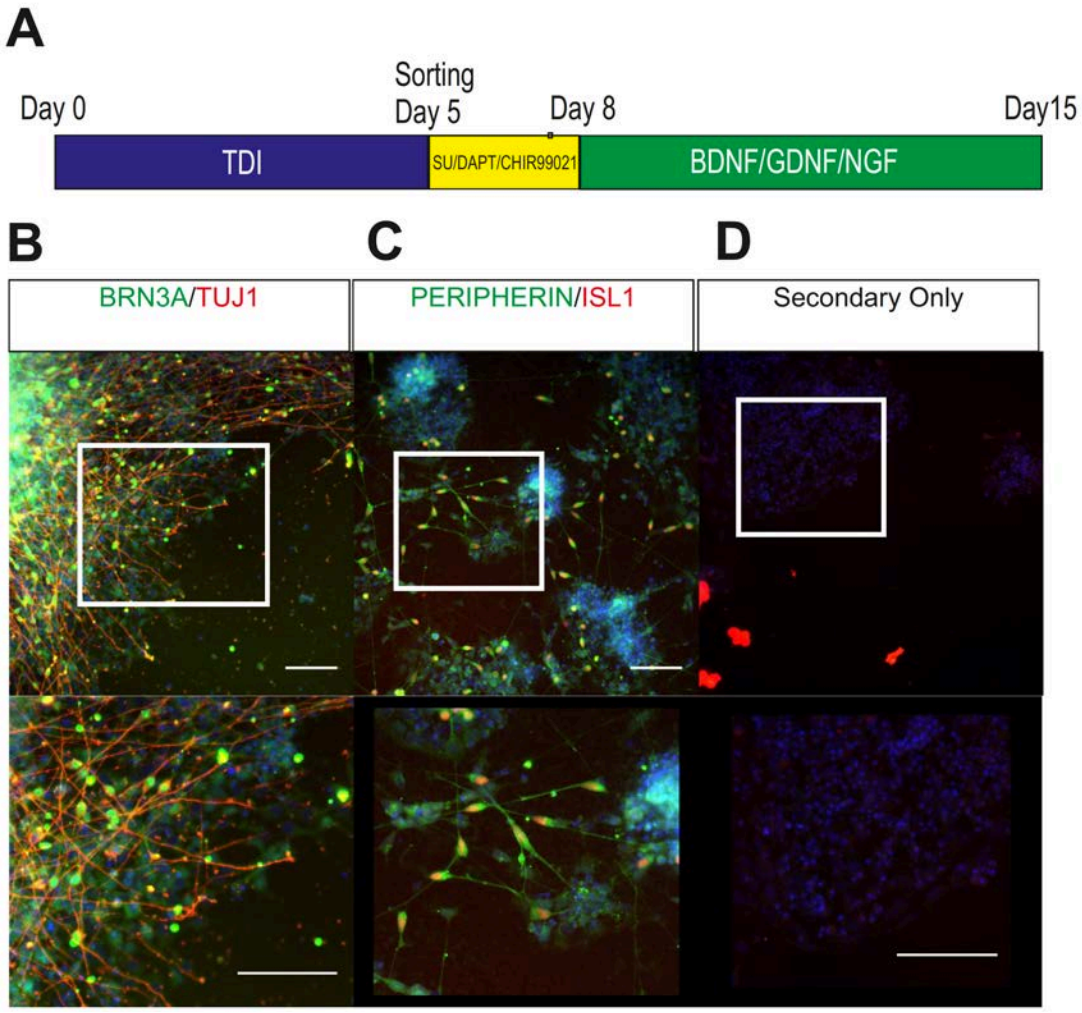

Figure 2.5 **hPSC derived neural crest cells form peripheral sensory neurons in vitro. (A)** Schematic showing differentiation of sorted neural crest cells into peripheral neurons. **(B)** After 10 days of differentiation, neurons showed neural morphology including processes and ganglia forming. These show positive expression of the sensory neuron markers Brn3a **(B)** and Islet1 **(C)** being coexpressed with neural markers Peripherin **(C)** and TUJ1 **(B).** Peripherin expression confirms the identity of these cells as being neural crest derived peripheral neurons (Scale bar =100µm). Bottom row is zoomed in section of the boxed areas of images above. Pictures also in Hackland et al 2017 (Figure 2D)

2.3.5 Neural Crest cells from this protocol are cranial.

The spatial identity of neural crest cells with respect to the anterior posterior axis of the embryo has been shown to impact the ability of neural crest cells to form derivatives *in vivo*, particularly with respect to the formation of mesectoderm (Le Lièvre and Le Douarin, 1975). Cranial neural crest and not trunk neural crest has been shown to form the bone and cartilage of the craniofacial skeleton in *vivo* (Le Lièvre and Le Douarin, 1975) and thus, the ability of these cells to form ectomesenchyme *in vitro* led to us questioning the anterior-posterior identity of these cells. A comparative analysis of cranial and trunk neural crest by RNA-seq in the chick has found 6 genes upregulated in cranial neural crest over trunk neural crest. Of these 6 genes, *Dmbx1, Brn3C*, *Lhx5* between HH stage 4-10 in the neural plate border and *Tfap2β, Sox8, Ets1* were expressed later from HH stage 7-11 in the premigratory and migratory neural crest (Simoes-Costa and Bronner 2017). In addition, *OTX2* has been implicated in the induction of the anterior neural tube (Iwafuchi-Doi et al., 2012). Thus, we took RNA from day 0 (hPSCs), day 3 and day 6 and assessed the expression of these genes by qPCR. We observed amplification at all three time points for all 6 genes **(Figure 2.6A)**. *DMBX1* and *LHX5* show a peak of expression at day 3 of differentiation at the neural plate border stage, which is consistent with *in vivo* data (Simões-Costa and Bronner, 2016). They then show a subsequent reduction in expression with delta CT values changing from 8.14 to 13.2 for *DMBX1* and 7.67 to 12.85 for *LHX5*, although these values all show that these genes are expressed in these cell populations. *TFAP2*β is another gene that shows a high upregulation from day 0 hPSCs to day 3 differentiated cells, but unlike *DMBX1* and *LHX5*, continues to increase in expression through to day 6 neural crest cells. We also see genes retained from hPSCs through to the end of differentiation, which is consistent with anterior being the default identity and induction of a posterior identity being required (Gouti et al., 2014; Lippmann et al., 2015). *OTX2* and *ETS1* show a retention of their expression throughout the time course which is consistent with this notion. To confirm the hypothesis that there is a retention of these genes through to day 6, rather than a downregulation and switching off transcription, we wanted to

confirm expression of both *LHX5* and *ETS1* by protein level to corroborate transcript data **(Figure 2.6B)**. We differentiated MIFF1 iPSCs to neural crest cells performed immunostaining for these genes, we found that both LHX5 expressed at day 3 and ETS1 at day 5, confirming the presence of the protein level expression. HOX genes are the classical genes used to identify anterior posterior position. We performed qPCR analyses on neural crest cells throughout the differentiation to assess HOX gene expression **(Figure 2.6C)**. There was low expression of *HOXB1* and *HOXB2* in all the differentiation samples, but this was significantly lower than the positive control (Two Way ANOVA $P<0.001$). In addition, the delta CT values relative to *GAPDH* across 3 independent experiments for HOXB1 were 14.62 at day 0, 16.25 at day 3 and 15.1 at day 6 and 23.37, 23.5 and 21.9 at the same time points for *HOXB2*. The positive control RNA showed delta CT values of 5.2 for HOXB1 and 6.1 for *HOXB2* and the high levels of expression here indicate that the levels of *HOXB1* and *HOXB2* found in the differentiation samples are very low. We did not see any amplification for more posterior HOX genes such as *HOXB4*, *HOXB5* (hindbrain) and *HOXB8* and *HOXC9* (Thoracic) in our neural crest differentiation samples which is consistent with anterior identity. To confirm the technical success of the qPCR and to validate that the lack of amplification we assessed the delta CT of another housekeeping gene *TATA binding protein* (*TBP*) **(Figure 2.6D)** and found no significant difference in the 1/Delta CT values between any of the samples for this gene (One Way ANOVA).

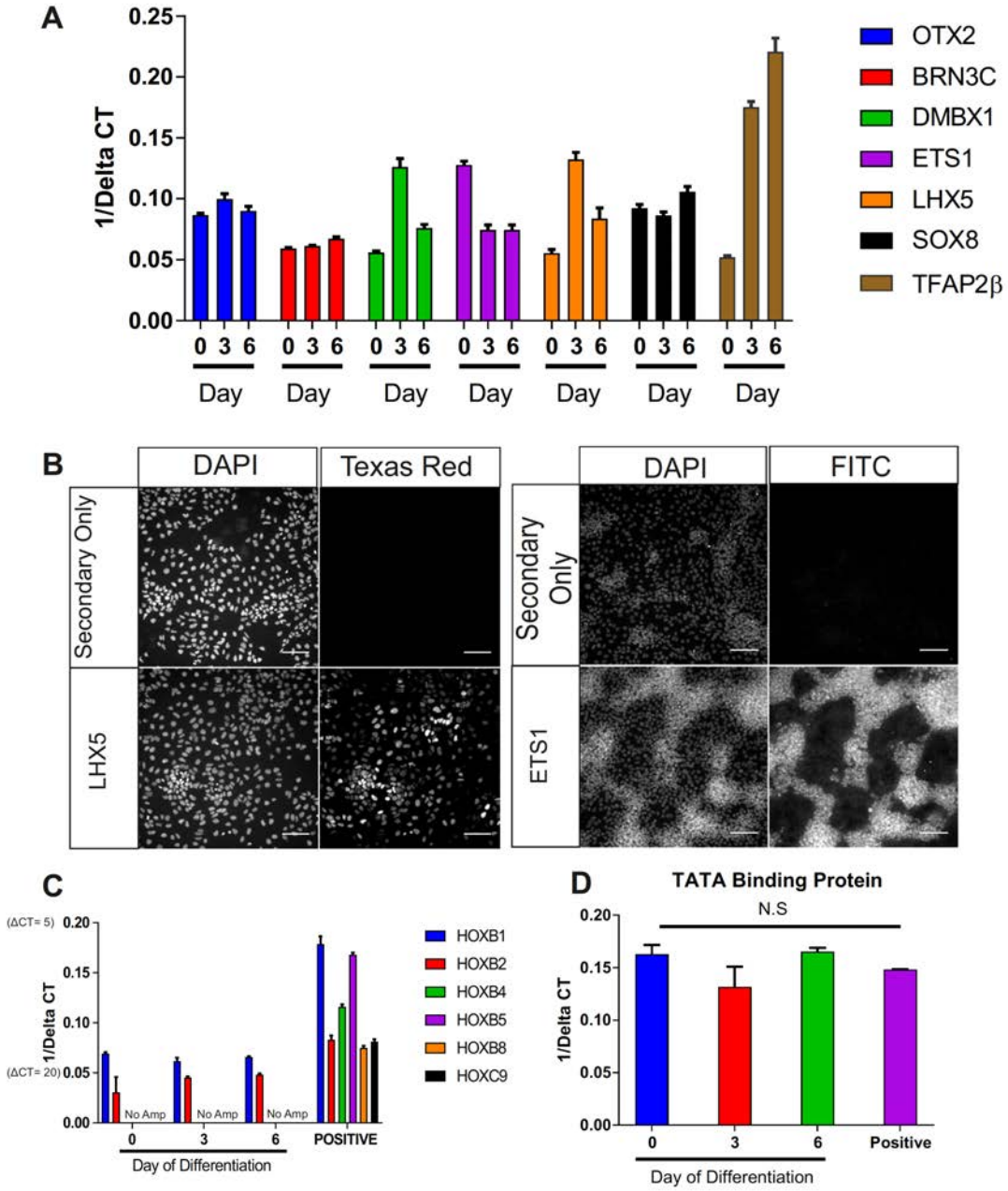

Figure 2.6 Neural Crest Cells have a HOX negative identity indicative of Cranial Neural Crest. (A). qPCR analyses showing the expression of transcription factors identified as markers of cranial neural crest (Mean+SEM). **(B)** MIFF1 iPSCs differentiated to neural crest cells show protein expression of LHX5 after three days and ETS1 after 5 days of differentiation (scale bar 100µm) with secondary only control in top row. **(C)** qPCR analysis (normalised to GAPDH) shows the lower amplification (Mean+SEM) of HOXB1 and HOXB2 and no amplification of HOXB4, B5, B8 and C9) of expression of HOX genes throughout neural crest differentiation that are significantly lower (Two Way Anova P<0.001) than positive control **(D)**
TATA binding protein expression does not significantly vary between these samples (n=3 independent experiments for differentiation samples, 3 technical repeats for positive control) Mean+SEM; One-way ANOVA).

2.4 Discussion

2.4.1 A faster 5 day Xeno-free protocol for derivation of neural crest cells from hPSCs.

The aim of this work was to build on the protocol previously developed in our lab utilising a xeno-free differentiation medium and characterise the neural crest cells that arise from this protocol with regards to further fate specification and their axial identity. Developing a xeno-free protocol is beneficial in the ability for more control and judgement over the activity of small molecules and recombinant proteins that are added into the media. Other protocols developed to generate neural crest have serum supplements (such as Knockout serum replacement) or BSA or utilise different small molecule combinations or concentrations (Mica et al., 2013) (Chambers et al., 2012) (Leung et al., 2016). In addition, protocols that generate neural crest cells through neurosphere differentiation do not inform us fully as to the fate decisions and mechanisms of differentiation of these cells, or can give different outcomes- for example, the neural crest may be specified from a neural intermediate from a neurosphere based differentiation.

The protocol derived here combines the faster method as outlined in (Leung et al., 2016) whereby cells are plated at higher density than outlined in the Hackland protocol (Hackland et al., 2017), but are plated directly into differentiation media, but it retains the advantages of a fully defined xeno-free protocol that allows for full control of the system. A xeno-free protocol also reduces the risk for future clinical output, with no risk of adventitious agents from media components if this model is taken forward for a clinical output.

2.4.2 Signals and switches in neural crest differentiation.

Developing a system to understand the neural crest in humans requires us to understand the activity of the molecules added to the system. By not using any serum based additives to the differentiation cocktail, we can establish the fate decisions made *in vitro* during differentiation. Recent work has shown a link between developing mesendoderm and neural crest from hPSCs through both SMAD2 and β-catenin signalling (Funa et al., 2015). Combining SB431542 (a TGFβ/Nodal inhibitor) in conjunction with low CHIR99021 in our protocol matches these findings. Higher concentrations and reiterated exposure to higher CHIR99021 led to the formation of mesendoderm over neural crest without TGFβ/Nodal signalling inhibition. These findings can be linked to the finding that cells in early neural crest differentiation protocol by Leung et al show low, transient BRACHYURY expression. This may be due to the higher concentration of CHIR99021 used in this protocol (3μM) in conjunction with additional BSA compared to the lower CHIR concentration without BSA in our protocol. The requirement for this higher concentration of CHIR99021 in the presence of BSA may be due to sequestration of molecules supplemented to the media. Thus the presence of BRACHYURY in the Leung protocol may be due to the uneven exposure of some cells to higher levels of CHIR that induce early mesendoderm (Leung et al., 2016).

In addition, many protocols to derive mesodermal tissues from hPSCs utilise higher concentrations of WNT activators (such as GSK3β inhibition) such as the generation of anterior primitive streak using 4μm CHIR99021 and mid primitive streak using 6μm CHIR99021 (Loh et al., 2016). We have previously demonstrated that endogenous signalling of BMP has a dramatic impact on the formation of neural crest specification *in vitro* and it has also been shown that endogenous WNT signalling can also influence the fate of hPSCs. Utilising a TCF:LEF fluorescent reporter to read out WNT signalling, it was demonstrated that sorted WNT^{HIGH} cells were formed less PAX6 positive cells in Neurectoderm differentiation than WNT^{LOW} cells.

2.4.3 A five-day protocol- Assessing the dynamics and cell fate decisions of cells undergoing neural crest differentiation *in vitro.*

Through FACs and transcript analyses **(Figure 2.1)**, we have been able to identify time points that correspond to stages of neural crest development *in vitro.* Days 3 and 6 of differentiation show key differences in their marker expression that are consistent with reports from *in vivo* models showing the formation of a neural crest intermediate cell type before these cells form migratory neural crest cells. Neural crest specifier genes such as *Pax7* (Basch, Bronner-Fraser and García-Castro, 2006), *Msx1* (Khudyakov and Bronner-Fraser, 2009), TFAP2α (Rada-Iglesias et al., 2012) are also found to be induced to a high level after three days' differentiation indicative of a phase of differentiation where the Neural Crest GRN is overlapping with the GRN of the starting pluripotent population. In addition, these data corroborate the findings from the two studies utilising human embryos for validation of neural crest markers. *PAX7*, *PAX3*, *TFAP2*α and *SOX9* are all robustly seen in Carnegie stage 12 human embryos at the dorsal neural tube (Betters et al., 2010b).

Antigen expression of cells is a useful tool to characterise cells without sacrificing a whole culture, as is needed for immunofluorescence or transcriptomic approaches. In addition, it also allows the heterogeneity of a whole culture to be easily assessed and sub populations to be picked out. We have utilised the P75, a long used marker of neural crest cells *in vivo* and *in vitro* (Stemple and Anderson, 1992) to follow the differentiation of cells in this protocol. We have compared the expression of P75 and a CD49d **(Figure 2.2)** as to what cells the mark in this protocol. CD49d has seen a recent uptake in its use to mark neural crest cells with recent papers favouring it over P75 to purify populations (Fattahi et al., 2016). CD49d recognises an epitope on INTEGRINα4 (Lobb and Hemler, 1994) and P75/CD49d co-expressing cells in the Rat Sciatic nerve have been touted as neural crest stem cells *in vivo* (Bixby et al., 2002). Whilst this publication shows co-expression, it is in E14.5 rat embryos with cells taken from areas where neural crest derivatives are found, such as the gut, sciatic nerve and dorsal root ganglion,

whilst we are assessing *in vitro* cells that are purported to be the equivalent of recently delaminated neural crest cells. Our data is consistent with the overall notion that CD49+/P75+ cells are neural crest stem cells (as seen by expression of both of these antigens with SOX10::GFP at day 5 *in vitro*) **(Figure 2.2C)** To confirm this, a strategy using a non-green line and assessing co-expression of these antigens or a tri colour flow cytometric analyses would further confirm co-expression simultaneously. Whilst functional assessment, such as clonogenic assays or *in vivo* grafting to assess cell potency and fate would ascertain the 'stemness' of these cell populations. From the expression patterns at day 5, the use of both $P75^{++}$ and CD49d expression coinciding with SOX10::GFP is consistent with the hypothesis that they both mark neural crest stem cells *in vitro* and they may both be used at this time point in isolation to purify neural crest cells for downstream applications. They main difference between the immunoreactivity to antibodies for P75 and CD49d is the time of expression. We see P75 expression throughout the differentiation, consistent with the notion that $P75^{+}$ cells are neural crest and Neurectoderm precursors, and transition to $P75^{++}$ as we have previously reported (Hackland et al., 2017). In particular, we see $P75^{++}$ cells that are SOX10::GFP negative, so it may be possible that P75 upregulation is the first step towards the development of these neural crest cells from being pre-migratory to migratory (marked by SOX10::GFP). On the other hand, we do not see CD49d immunoreactivity in cells that are not SOX10::GFP positive, which indicates that SOX10::GFP is expressed first followed by the expression of INTEGRINα4. This may be due to CD49d binding to cells that are migratory neural crest cells and so have undergone EMT and delaminated from the neural tube, to test this, staining embryos (human, mouse or chick) and determining the location of CD49d+ cells with relation to the dorsal neural tube may give this answer. In addition, a potential *in vitro* assay to assess this would be to determine the motility of CD49d+ and negative cells with the hypothesis that cells having undergone delamination are migratory and so will show more motility.

In addition to $P75^{++}$ marking neural crest cells and subsequent emergence of two populations of P75 expressing cells, we only see one population of $P75^{+}$ cells at in

pluripotent cells and at day 3 of differentiation, yet within this, lies cells with the capacity to form neural crest and neural ectoderm (as we see *PAX6* expression within neural crest cultures (data not shown). This raises the question of the whether there are two populations intermixed in here, or one multipotent progenitor population. This question is further raised by the expression of antigens and genes associated with pluripotent stem cells such as SSEA3 immunoreactivity **(Figure 2.3A)**. OCT4 and SOX2 expression is also seen in day 3 differentiated cells that express these neural plate border markers. One key question is the function of these genes during differentiation and how their regulatory architecture will influence the role of these genes through the differentiation. For example, SOX2 is a key gene in both pluripotency, as demonstrated by its requirement for reprogramming (Takahashi and Yamanaka, 2006) and also in neural and placodal development (Uchikawa et al., 2003). By assessing the active enhancers in these cells, we could determine SOX2 interactions during the differentiation neural crest to determine if plays a role in early neural crest differentiation, or whether it is residual expression its role in hPSCs. Recent work in the chick has also showed similar data wherein neural plate border can co-express markers of different ectodermal fate (Roellig et al., 2017). This may relate to the $P75^{+}$ population at day 3 of differentiation marking one multipotent neural plate progenitor that is further specified over time. In Roellig et al, they demonstrate co-expression of *Sox2* with *Msx1/2*, *Pax7* and Tfap2α in HH stages 6-10. In addition, they further showed that some cells retained co-expression of *Pax7* and Sox2 through to HH stage 10-11, which later than when the neural plate border and neural crest have split which occurred at stages 5-6 in most cells. Expression of *Pax7* over *Sox2* led to acquisition of neural crest fate, whilst neural fate was acquired if *Sox2* overcame *Pax7* expression and an imbalance of expression was achieved by mutual repression. It may be possible that *Sox2* retention from the epiblast and the transition to neural crest may be the slow switch off of the pluripotency network. This hypothesis would be consistent with findings from hPSC derived neural crest differentiation, there was *OCT4* and *PAX7* co-expressing cells as assessed by immunostaining (Leung et al., 2016). *OCT4* expression in the Leung protocol is consistent with our transcript

data from day 3 differentiated cells, whilst we also see high expression of *SOX2*. To test if the function of *SOX2* is due to overlap of neural crest and pluripotency GRNs as suggested by Leung et al, or whether *SOX2* is a pro neural gene, taking single *SOX2* positive cells and assessing their ability to form derivatives is the best way. If these cells formed only neural/neural crest cells, we could determine that Sox2 is a pro neural/neural crest factor and these cells correspond to true neural plate border cells. On the other hand, the formation of any mesendoderm cell types would indicate that SOX2 here is working similarly to its role in pluripotent stem cells. In addition, by taking single SOX2 positive cells, this could take the hypothesis suggested by Roellig et al that these neural plate border cells are multipotent progenitors and confirm it to determine if they form derivatives indicative of neural, neural crest or placodal fate.

To further confirm this hypothesis, and to separate this population, single cell transcriptomics of cells from days hPSCs, day 0, 1,2 and 3 of our differentiation protocol would allow the early dynamics of differentiation to be revealed specifically to see if SOX2 high and PAX7 high cells segregate- indicating two separate progenitor populations, or whether the differences are more finely tuned with cells that are $PAX7^{HIGH}/SOX2^{HIGH}$; $PAX7^{LOW}/SOX2^{HIGH}$; $PAX7^{HIGH}/SOX2^{LOW}$ with and subsequent creation of a dual reporter to undertake functional tests as outlined above to determine prospective potency and prospective fate of these cells.

Moreover, our data from day 6 differentiated cells are consistent with these cells being migratory neural crest cells. SOX10 expression is seen in cells that have delaminated from the neural tube of Carnegie stage 12 human embryos (Betters et al., 2010b). In addition, we also see increased expression of SLUG, which is only expressed in migratory neural crest in the chick (del Barrio and Nieto, 2002). To functionally test this hypothesis, a combination of live time-lapse migratory assays- such as a scratch assay or migration toward a bead soaked in chemoattractant and comparing speed and directionality of any motile cells would confirm this. A true test of migration (and potential cell fate) would be grafting of these cells into chicken embryos. This would be the gold standard to

determine the migratory routes of these cells and the range of fates they may acquire- such as the craniofacial skeleton or peripheral neurons and has already been utilised for many hPSC derived neural crest cells (Menendez et al., 2011; Lee et al., 2007) (Denham et al., 2015).

Our findings that two days of growth factor exposure is sufficient to determine neural crest differentiation is like the findings from Mica et al where they test the times where WNT signalling is required (Mica et al., 2013). They show that WNT is required as neural crest doesn't form in cells subjected to dual-SMAD inhibiton. CHIR treatment between days 2-3 of their 11 day protocol (CHIR treatment begins at day 2 in their protocol) gives rise to SOX10::GFP expression, whilst one day of CHIR99021 exposure followed by culture with the tankyrase inhibitor XAV939 (a WNT inhibitor) also results in some SOX10::GFP positive cells being found (Mica et al., 2013). This indicates that WNT signalling early in the differentiation protocol is a critical period and is similar that CHIR exposure early (from seeding until day one or day two) results in neural crest specification. In addition, we found that later application of growth factors did not result in efficient differentiation. Whilst our data are provisional, they do match the findings that this early period is crucial, the findings from Mica et al give rise to further notion that even a transient activation of the WNT signalling pathway is sufficient to drive neural crest differentiation and that continued WNT signalling may not be necessary. This also reiterates the findings from Funa et al whereby early low levels of WNT can induce β-catenin binding to neural crest promoters.

2.4.4 Putative hPSC derived Neural Crest cells form correct derivatives *in vitro*

Further to the marker expression of day 5/6 differentiated neural crest cells, our data shows that neural crest cells from our protocol function to form the correct derivatives *in vitro.* Our data demonstrates that these cells can form both neural and non-neural derivatives consistent with cell types that are formed *in vivo* **(Figure 2.4a)**.

A unique facet of neural crest biology is the ability of these cells, from the ectoderm to form downstream derivatives that are both ectodermal and mesenchymal **(Figure 2.4).** We have also demonstrated this value *in vitro*. We demonstrate that hPSC derived neural crest cells can be sorted and further differentiated to ectomesenchyme cells that express the same markers as mesenchymal stromal-cells (CD73, CD90 and CD105). These are then able to form osteocytes and chondrocytes *in vitro*. Whilst these final derivatives are also formed by the neural crest in vitro, it is not clear how the ectomesenchymal cell population formed *in vitro* corresponds to those cells found *in vivo.* Whilst the approach we have taken is also demonstrated elsewhere (Menendez et al., 2011), the signals and switches that are necessary for this differentiation are not well characterised. These protocols cultured cells in the presence of serum, which does not allow the understanding for how neural crest cells *in vitro* form mesenchymal derivatives. To our knowledge, only on other group has claimed to make ectomesenchyme from this approach in a serum free media (Fukuta et al., 2014) whose data also shows the acquisition of both CD73 and CD105 by flow cytometry and further differentiation to osteocytes by alizarin red.

In contract to these approaches, there has also been the report of a different method without serum to derive ectomesenchyme using SOX9 as a marker of these cells (Umeda et al., 2015). Culturing of neural crest cells sorted for $P75^{++}$ and subsequent exposure to FGF2 and the TGFβ/NODAL inhibitor SB431542 shows the induction of SOX9, an early specifier of chondrogenic differentiation from cranial neural crest (Mori-Akiyama et al., 2003; Bhatt, Diaz and Trainor, 2013). In addition, these SOX9 positive ectomesenchymal precursors could form cartilage in pellet culture, whilst osteocytic differentiation was not presented. This is consistent with findings from mouse neural crest cells exposed to Fgf8 inducing Sox9 *in vitro* (John, Cinelli, Wegner and Sommer, 2011). These data show that FGF signalling is the early signal for chondrogenic differentiation from neural crest cells, which has also been shown in the mouse. Our data and other work show that FGF inhibition works as part of a differentiation cocktail for peripheral neural differentiation (Chambers et al., 2012). This raises the hypothesis that the

exposure to FGF may provide the difference between neural and non-neural differentiation for neural crest cells. To test this hypothesis, culturing hPSC derived cells in media supplemented with FGF or FGF inhibitors and assessing fate for chondrogenic precursors (SOX9+) or neural precursors (PERIPHERIN+). In addition, knocking out or constitutive activation of the FGF pathway can be used to test this hypothesis.

Peripheral neurons that are derived from the neural crest include the sympathetic, parasympathetic, enteric and sensory nervous systems (Bhatt, Diaz and Trainor, 2013). We present the formation of BRN3A/ISL1 positive peripheral neurons from our putative neural crest cells. Whilst this in principle shows the ability of neural crest cells to form peripheral neurons in general, it does remain the signals and switches that are involved in the formation of different peripheral nervous systems as well as raising the question of anterior posterior identity in the formation of neural derivatives. We utilised a neural specification media for three days containing WNT activation (CHIR99021), NOTCH inhibition (DAPT) and FGF inhibition (SU5402) **(Figure 2.5a)**, which will have affected the specification of neural subtypes and propose that inhibition of NOTCH and FGF signalling specifies neural differentiation from neural crest. In the Chick, *Notch* plays a role in neural or glial fate through lateral inhibition (Wakamatsu, Maynard and Weston, 2000), specifically in cells where Notch is activated, they go on to form glia. As discussed before, FGF has been demonstrated to play a key role in the formation of non-neural derivatives both *in vivo* and *in vitro* and thus, the combination of these inhibitors may go onto promote peripheral neural differentiation. β-catenin has a key role in early sensory neurogenesis through canonical WNT from migrating neural crest cells (Hari et al., 2002) (Lee et al., 2004). This is also demonstrated through reports generating autonomic neurons from hPSCs not utilising CHIR99021 to specify neurons (Zeltner et al., 2016). We propose that by substituting the CHIR99021 in the differentiation protocol used here, we may be able to generate other types of peripheral neurons from Neural Crest cells *in vitro.* It may be possible that the presence of CHIR99021 in the neural crest differentiation media until day 5 may prime all the cells in being nuclear β-

catenin^{HIGH} and thus give an overestimate as to the potential of these cells to form sensory neurons. By optimising the protocol whereby growth factors are only present during neural crest differentiation for two of the five days of differentiation **(Figure 2.3Di)** may alleviate this and make it possible to generate more diverse neural subtypes *in vitro*.

2.4.5 Understanding the anterior posterior identity of cells *in vitro*

In vivo work has shown that the spatial identity on the downstream differentiation on neural crest cells. For example, enteric neurons are derived from the vagal (somites 1-7) and sacral (posterior to somite 28) populations of neural crest (Gershon, 2010). In addition, the ability to form mesectoderm *in vivo* is restricted to the cephalic neural crest in the chick (Le Lièvre and Le Douarin, 1975) and this raises the possibility that the gene expression profile, particularly the HOX gene expression, may influence the ability of these neural crest cells to further differentiate. This has been demonstrated by HOX gene expression being required for both enteric (Zhu et al., 2014) and sympathetic neural differentiation (Huber et al., 2012). This facet of differentiation has been investigated with the regard to the possibility of ectomesenchyme differentiation through a series of elegant quail-chick transplantation experiments (Le Lièvre and Le Douarin, 1975), where it was found that cells more posterior to the 5th somite were not able to form mesenchymal derivatives.

Our data are consistent with the idea that these neural crest cells are anterior in character through marker expression **(Figure 2.6).** In particular, the expression of OTX2, which specifies the anterior neural tube by negatively repressing GBX (a posterior neural tube specifier) (Kondoh, Takada and Takemoto, 2016) is a good indicator of anterior specification. The expression of the six genes postulated as anterior markers from whole transcriptome analysis in the chick neural crest is another indicator of these cells having an anterior identity (Simões-Costa and Bronner, 2016). In addition, these genes also demonstrated the ability to make

posterior neural crest cells (previously unable to form ectomesenchyme (Le Lièvre and Le Douarin, 1975)) form cartilage *in vivo*. This is consistent with the ability of our putative Neural Crest cells to form ectomesenchyme *in vitro* **(Figure 2.4 C,D)** and leads to the conclusion that these cells are cranial in nature. The expression of the ETS1 in day 5 of *in vitro* derived neural crest cells, gives further evidence to their cranial identity and coupled with its requirement for *Alx1* expression (Simões-Costa and Bronner, 2016), which is expressed high in neural crest from rhombomeres 1-2 (Lumb et al., 2017) and its role in correct craniofacial development (Uz et al., 2010).

The HOX clusters have long been associated with axial patterning and display co-linear acquisition in hPSC derived differentiations (Lippmann et al., 2015), whereby HOX genes are induced and the further along the cluster the gene is, the more posterior the cell is. Our data shows very low expression of only HOXB1 and HOXB2 which is present throughout all the time points with HOX genes indicative of either hindbrain or truncal identity are not amplified. The low expression of both *HOXB1* and *HOXB2* in the differentiation samples compared to the positive control may indicate that this is expression is very low and not having a major impact, technical issues with the primer/probe combination or may reflect the posteriorisation required for neural crest induction. In addition, our group has RNA-sequencing data from hPSCs showing that there is very low to negligible expression of some HOX genes which may show that the transcript detection from qPCR experiments here is very low and that induction of HOX genes is required.

The neural crest does not form at the anterior fold of the embryo, which is fated to form the forebrain, instead forming at the medial and posterior regions of the embryo. In *Xenopus Laevis,* integration of X*Wnt*, X*Retinoic Acid* and X*Fgf* signals working downstream of intermediate BMP that specifies mediolateral position of the developing ectoderm has been postulated to be the key mechanism behind this (Villanueva, Glavic, Ruiz and Mayor, 2002). WNT and BMP signalling are key to our protocol for deriving neural crest cells, but Retinoic Acid is not required for the formation of neural crest from our data. This may be because WNT is acting

as a posteriorising agent in this context, and thus retinoic acid may further pattern neural crest cells to a hindbrain/truncal identity. It should also be noted, that the AP identity of neural crest cells from hPSCs may vary depending on supplements to differentiation media. Leung et al report midbrain identity of their neural crest cells based on expression of *ENGRAILED1* and use B27 as a supplement to their media. There is Retinol, a precursor to retinoic acid, present the B27 used in this media, so it is possible that they are supplementing their differentiation media with a low level of Retinoic Acid signalling that is inducing this patterning effect. We use N2 supplement, and whilst we have not assayed for ENGRAILED expression, if any retinoic acid biosynthesis is occurring in culture, then we hypothesis it would induce a more posterior identity in cells from this protocol.

2.5 Summary

In conclusion, the data presented here goes some way to answering the aims at the outset of the chapter. We have been able to assess the character of cells from an adapted 5-day protocol to derive neural crest cells with both qPCR and FACs analysis. By monitoring gene and antigen expression throughout this differentiation, we can also generate hypotheses regarding the development of the neural crest in the human system and the key marker genes in this. In addition, we have presented data that shows that putative hPSC derived neural crest cells can generate neural and non-neural derivatives showing that these cells show functional properties of neural crest cells. We can further link the formation of derivatives to the anterior posterior identity of these cells.

We have presented data showing a differentiation protocol that gives rise to SOX10+ putative migratory neural crest cells after 5/6 days of differentiation. These cells co-express other neural crest specifiers TFAP2α, PAX3, SOX9, PAX7 as well as showing high expression of P75 by immunoreactivity of the antibody ME20.4. By cross examining the expression of a SOX10::GFP reporter line, we further demonstrate that it is possible to sort pure populations of neural crest cells in non-engineered cells by $P75^{++}$ expression. Previous work utilising the longer 7 day iteration and in the Menendez protocol(Menendez et al., 2011)

demonstrated that expression of SOX10 and the CNS specifier PAX6 are segregated by this expression consistent with our data. In addition, by interrogating the expression of antigens and genes associated with pluripotent cells, we can show data consistent with the hypothesis that neural crest cells are determined early from the epiblast (Basch, Bronner-Fraser and García-Castro, 2006) through retention of the pluripotency associated genes OCT4, SOX2 and NANOG, immunoreactivity to SSEA3 and little to no expression of the pro-neural gene SOX1.

We also demonstrated that putative neural crest cells not only expressed markers indicative of neural crest fate, but also formed ectomesenchyme *in vitro* and peripheral neurons after sorting for neural crest cells. This is a key functional proof of neural crest cells showing their ability to differentiate and when taken with the marker expression can give further weight to the conclusion that these are hPSC derived neural crest cells.

Combining the ability of these cells to form ectomesenchyme with expression of genes shown to mark cranial neural crest cells *in vivo,* we can also infer that these cells have a cranial identity. In addition, the lack of expression of HOX genes in these cells can lend further weight to this conclusion- this is consistent with the hypothesis that anterior is the default fate of cells from differentiation and that posteriorisation is an active process (Gouti et al., 2014).

Chapter 3: Retinoic Acid mediated patterning of hPSC derived Neural Crest Cells

3.1 Introduction

The first models of *in vitro* differentiation characterised the addition of retinoic acid to embryonal carcinoma (EC) cells (the malignant counterparts to pluripotent stem cells). Supplementing culture media with retinoic acid induced morphological and functional changes mouse F9 cells (Strickland and Mahdavi, 1978). Here it was found that following treatment with 10^{-7} M all-trans retinoic acid induced secretion of plasminogen activator indicative of the formation of parietal endoderm (Strickland and Mahdavi, 1978). Exposure of the human embryonal carcinoma cell line NTERA2 to all trans retinoic acid induced neuronal differentiation when 10^{-5} M all trans retinoic acid left over 7 days (Andrews, 1984). In addition to this, it was later found that different concentrations of retinoic acid induced *HOX* genes during neuronal differentiation of NTERA2 clonal lines (Simeone A, 1990). The highest concentration assayed during these differentiations (10^{-5} M) was able to induce 5' genes in the *HOXB* cluster, whilst low concentrations (10^{-9} M) was only able to induce 3' *HOX* genes. These early experiments demonstrated that retinoic acid playing a key role during *in vitro* differentiations, as well as showing that the positional identity of cells *in vitro* could be altered by retinoic acid exposure. As use of embryonic stem cells became more widespread, it more differentiation protocols demonstrated the role of retinoic acid patterning differentiated cell types *in vitro*. The induction of *HOX* genes being dependent on the concentration of retinoic acid was also shown during the neural differentiation of mouse embryonic stem cells, whereby a concentration of 2 molar retinoic acid into the media induced expression of *HOX* genes to a posterior limit of *Hoxc6* (consistent with anterior spinal cord identity) (Okada, Shimazaki, Sobue and Okano, 2004), whilst the lowest concentration assayed (10^{-9} M) only induced expression of *HoxB1* and *HoxA2* expression. Conversely, no *HOX* genes were expressed in cells not exposed to retinoic acid. In addition, Okada et al also did not see *Hoxc8* or *Hoxc10* which are found at the

thoracic spinal cord level at any level of retinoic acid addition. These data indicate that retinoic acid mediated patterning can only inform positional identity to a posterior limit of the cervical spinal cord. This hypothesis has been given further weight by analysis of the responsiveness of *HOX* genes to different signals. In the chick, the *HOXB* cluster can be split in two based on signals that induce their expression. The 3' end (at the anterior side of the embryo respond to retinoic acid, shown by the expression pattern of *Hoxb4* extending more anterior following exposure of chick embryos to RA (Bel-Vialar, Itasaki and Krumlauf, 2002). On the other hand, *Hoxb9* showed no change in expression following this treatment. They confirmed these findings after electroporation a dominant negative RARα1 construct that reduced the *Hoxb4* expression domain in the neural tube, whilst *Hoxb9* expression was not affected (Bel-Vialar, Itasaki and Krumlauf, 2002). This is also reinforced by the finding that mouse *HoxA1* and *HoxB1* genes have enhancers with Retinoic Acid Response Elements (RAREs) in (Langston, Thompson and Gudas, 1997).

Only recently has the addition of all-trans retinoic acid to neural crest differentiation protocols been reported, with one paper showing 10^{-6}M all trans retinoic acid results in induction of trunk neural crest cells following exposure to all-trans retinoic acid (Huang et al., 2016), by induction of *HOX* gene expression, including those that are found in the very posterior of the embryo, genes in combination with *PHOX2B* expression following treatment of patterned neural crest cells with BMPs, indicative of sympatho-adrenal precursors. These are a trunk neural crest specific derivative, so the combination of putative sympatho-adrenal differentiation with HOX gene transcript induction as their evidence. Meanwhile, another report concludes that retinoic acid works to pattern neural crest cells to a vagal identity (Fattahi et al 2016). Vagal neural crest cells arise from the neural tube that at the very anterior of the spinal cord, corresponding to somites 1-7. Fattahi et al showed that addition of all trans retinoic acid to neural crest differentiation induced expression of *HOXB2-5* and subsequently described the directed differentiation to enteric neurons (that arise from the vagal crest *in vivo*) (Fattahi et al., 2016) (Burns, Delalande and Le Douarin, 2002). Fattahi et al,

demonstrated hPSC derived enteric neurons formed neuromuscular junctions, and when transplanted *in vivo* into the mouse caecum, were able to rescue of a common enteric neuropathy Hirschsprung's disease (Fattahi et al., 2016). Exposure of hPSC derived vagal neural crest cells to GDNF signalling induced a wide range of enteric neural subtypes that, when transplanted into the caecum, could rescue the $EDNRB^{s-l/s-l}$ Hirschsprung's model mouse. This has been followed by reports showing hPSC derived enteric neurons were able to be transplanted onto hPSC derived intestinal organoids to innervate them (Workman et al., 2016). Moreover, Workman et al were able to show that the innervation of the gut was crucial to the maturation of both the neurons and gut itself (Workman et al., 2016). These findings have shown the promise for generation of enteric neurons for a cell replacement therapy to treat enteric neuropathies such as Hirschsprung's disease and their key role in studying the homeostasis of the gut as a whole (Workman et al., 2016). In addition, this protocol has also been used to show that CRISPR-CAS9 mediated gene repair is able to rescue RET mediated defecits in enteric neuronal differentiation (Lai et al 2017).

3.2 Aims

To address the issues regarding what axial level retinoic acid patterns hPSC derived neural crest cells *in vitro* and to assess how axial identity alters downstream differentiation, the experiments performed in this chapter were aimed at answering the following aims.

1. Determine how retinoic acid affects the specification and identity of hPSC derived neural crest cells
2. Determine the signals that specify the formation of enteric neural precursors
3. Assess the ability of hPSC derived enteric neural precursors be transplanted and engraft into the mouse gut

3.3 Results

3.3.1 All-Trans Retinoic Acid exposure patterns neural crest cells in a time dependent manner.

To test the effect of retinoic acid on the neural crest differentiation, we determined the optimal time to add retinoic acid so as not to perturb neural crest differentiation. It has previously been shown that the time of retinoic acid addition to had an effect on the efficiency of differentiation (Mica et al., 2013). This system utilises a serum based media, which has been found to affect the dosage of retinoic acid that can be used *in vitro*. For instance, in the presence of serum, cells can be subjected to 10-fold higher RA than those in a serum free media without toxicity (Peter Andrews, personal communication), thus the presence of serum in the Mica protocol may influence the dose response. We thus decided to repeat the experiment outlined by Mica et al (Mica et al., 2013) by adding in 1μM all trans retinoic acid at various time points during neural crest differentiation using FACS analysis to determine the proportion of SOX10::GFP positive cells after 5 days

of differentiation **(Figure 3.1A)**. We tested adding 1μM retinoic at day 0, day 3 and day 4 of differentiation and compared the efficiency to TDI alone **(Figure 3.1B)**. Addition of retinoic acid at day zero of the protocol completely abolished the formation of neural crest and resulted in 0% GFP positive cells being present. Addition of retinoic acid later during differentiation, resulted in more GFP+ cells. Exposure from day three to day five gave rise was average of 38% SOX10::GFP positive cells, whilst exposure from day four until day 5 gave rise to 56% SOX10::GFP positive cells. 59% of the cells assessed were GFP positive when no retinoic acid was added **(Figure 3.1C i)**. Between each repeat of this, we saw the same trend of early addition of retinoic acid perturbing neural crest formation.

We calculated the amount of GFP positive cells in relation to untreated in each biological to confirm this trend **(Figure 3.1C ii)**. Cells treated on day zero had 1% of cells GFP positive relative to the untreated, showing that early treatment abolished neural crest differentiation. Cells exposed from days three to five only gave rise to 70% GFP positive relative to untreated, whilst cells exposed at days four to five resulted in 95% GFP positive relative to untreated. Thus, exposure to 1μM all-trans retinoic acid between days four and five of differentiation resulted in the optimal level of neural crest cells.

Following this, we next wanted to test if retinoic acid treated neural crest cells were patterned by Hox gene expression. We performed qPCR analysis for transcripts for neural crest specifiers, to confirm the FACS data, and HOX genes to assess patterning. We saw similar levels of the neural crest markers *SOX10*, *PAX7* and *TFAP2*α and higher expression of *PAX3* and *SOX9* **(Figure 3.2A)**. In addition, we saw statistically significant increase in transcript for *HOXB1* and *HOXB2*. In addition, we also saw expression *HOXB4* and *HOXB5* **(Figure 3.2B)** indicative of patterning to vagal neural crest, which corresponds to the hindbrain.

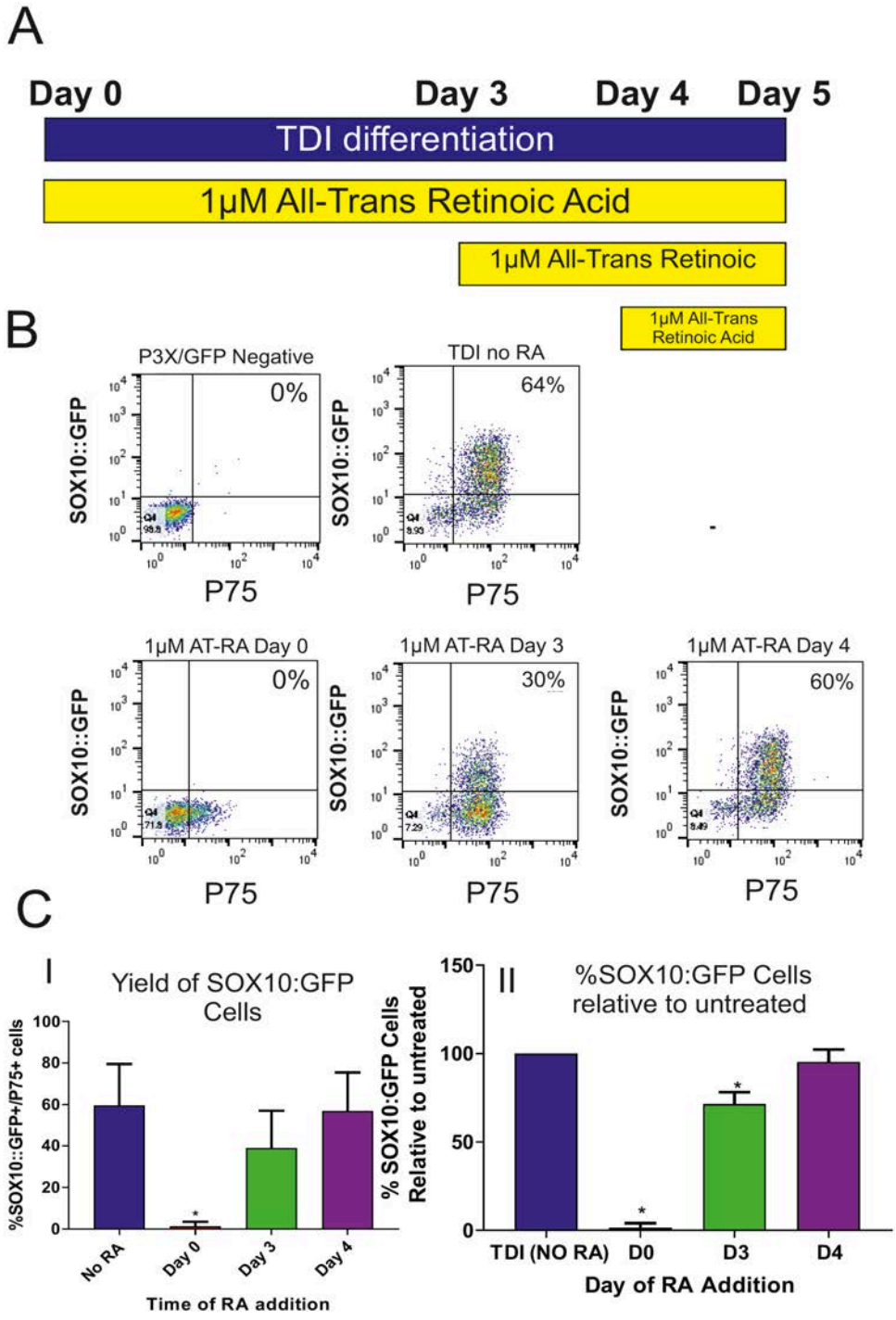

Figure 3.1 All trans Retinoic acid patterns neural crest in a time dependent manner. (A) Schematic showing addition of 1uM all trans Retinoic Acid at different time points in neural crest differentiation. **(B)** Representative FACs plots after 5 days of differentiation showing RA addition at day 0 and day 3 reduces the yield of SOX10:GFP+ cells from differentiation. Addition of RA at day 4 of differentiation gives a similar yield to no RA condition. **(C i)** Quantification of % SOX10::GFP+ cells from 3 independent experiments show significant difference when RA is added at day 0 of differentiation. **(C ii)** When each replicate is calculated as the proportion of the untreated, both treatment at day 0 and day 3 show a reduction in SOX10::GFP cells compared to untreated (Bars are Mean+SD; *P<0.01 One-Way ANOVA; Dunnett's multiple comparison).

A

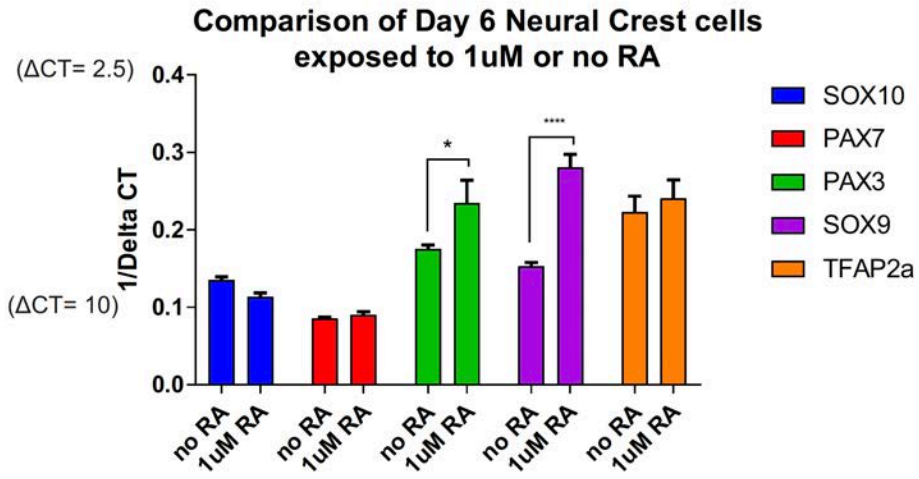

B

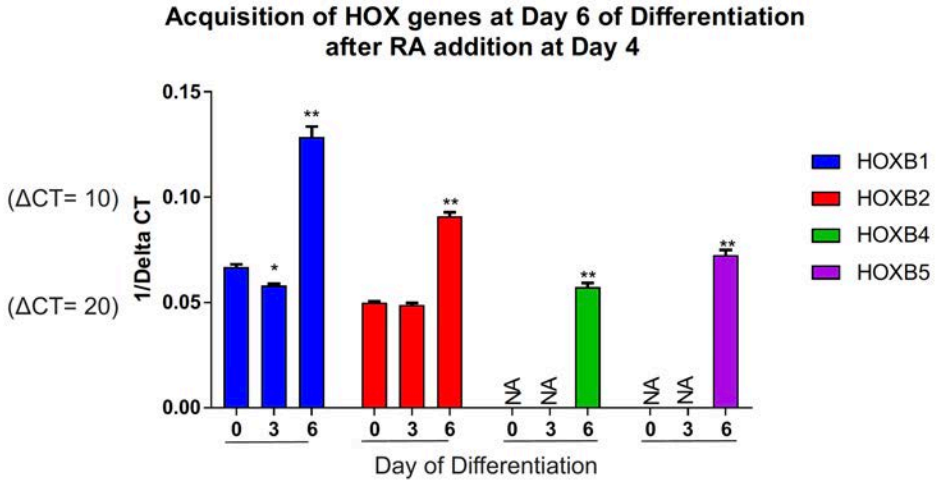

Figure 3.2 Retinoic Acid treated cells express neural crest markers and *HOX* genes. (A) qPCR analyses shows that crest markers such as *SOX10, PAX7* and *TFAP2α* are expressed at similar levels in both retinoic acid treated and non retinoic acid treated cultures, whilst *PAX3* and *SOX9* are significantly higher in retinoic acid treated. *HOX* genes are induced after retinoic acid treatment (Day 6 of differentiation) not before retinoic acid (day 0- hPSCs or day 3 differentiated cells). (Mean+SEM N=3 independent experiments Two-way ANOVA *P<0.05, **P<0.01 Dunnett's multiple comparison test relative to hPSC)

3.3.2 Retinoic Acid patterns neural crest in a dose dependent manner

We wanted to determine whether the patterning of all trans retinoic acid in neural crest differentiation worked in a dose dependent manner as well reported in other systems (Simeone et al., 1990). We exposed cells to different concentrations of retinoic acid from 10^{-6}M to 10^{-9}M between days four to six and assessed *HOX* gene induction **(Figure 3.3A)**. We saw *HOXB1* amplification in all samples, with low levels in the untreated (as seen previously in Figure 3.2B) and cultures treated with 10^{-9}M and 10^{-8}M. Cultures treated with 10^{-7}M retinoic acid showed an increase of *HOXB1* with 10^{-6}M showing the highest expression. This same trend is seen for *HOXB2* where low concentrations of retinoic acid give a similar amplification of *HOXB2.* These low concentrations of retinoic acid did not show amplification of *HOXB4* and *HOXB5*. We only see expression of *HOXB4* **(Figure 3.3iv)** and *HOXB5* **(Figure 3.3 iii)** at higher concentrations of retinoic acid (10^{-6}M and 10^{-7}M). In addition, 10^{-6}M retinoic acid showed the highest induction of both genes compared to 10^{-7}M retinoic acid **(Figure 3.3B iii; 3.3iv)**. We did not see expression of *HOXB8* and *HOXC9* by qPCR (data not shown) following retinoic acid treatment at any concentration suggesting an alternative signal is required to pattern to more posterior levels. These data consistent with a retinoic acid gradient that patterns the forebrain (Hox negative) to cervical spinal cord (*HOXB5* positive). This subset of retinoic acid responsive *HOX* genes has been demonstrated in the chicken embyros (Bel-Vialar, Itasaki and Krumlauf, 2002). We also tested expression of *SOX10*, *PAX3* and *PAX7* across all concentrations of retinoic acid to assess if different concentrations of retinoic acid affected neural crest differentiation. We saw induction of these genes, consistent with neural crest identity despite different Hox gene expression **(Figure 3.3C)**. *PAX3* transcript expression was more varied between the samples, which may be due to either early enteric neural differentiation or may be indicative of failed neural crest differentiation and increased neural plate differentiation in these samples. In this instance, we did not see the statistically significant increase in *PAX3* between untreated and 10^{-6}M RA treated cells, which may indicate that dose of *PAX3* is not playing a role in potential early enteric neurogenesis, but rather shows

a potential increase in neural ectoderm derived cells (Betters et al., 2010b) (Maczkowiak et al., 2010). From these data, we propose retinoic acid patterns hPSC derived neural crest cells in a dose dependent manner from the forebrain to cervical spinal cord.

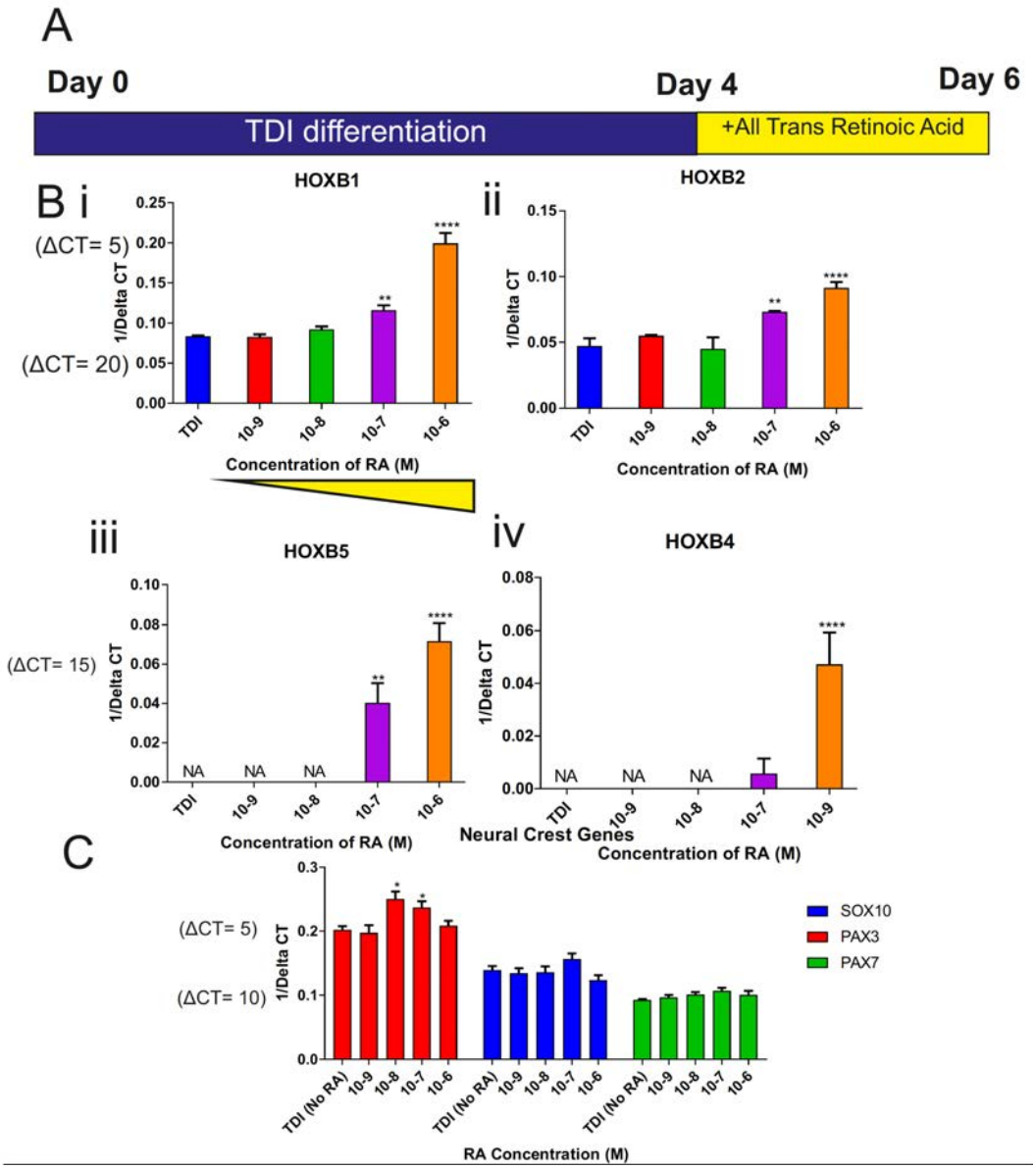

Figure 3.3 RA patterning is dose dependent. (A) Schematic of differentiation timeline showing addition of all trans retinoic acid to TDI media between days 4 and 6 based on findings from Figure 3.1. **(B)** qPCR analyses of *HOX* gene expression in Neural Crest differentiations with no retinoic acid (TDI) or with retinoic acid supplemented (units are M) . *HOXB1* **(B I)** and *B2* **(B ii)** expression are highest at 10^{-6}M retinoic acid exposure and decrease in expression down to 10^{-9} showing low to negligible induction similar to hPSCs. HOXB4 (Biii) and HOXB5 **(B iv)** (indicative of hindbrain/upper spinal cord identity) only show amplification in higher concentrations of all trans retinoic acid indicating cultures subjected to this concentration of retinoic acid are more posterior than those subjected to low concentrations of retinoic acid. **(C)** qPCR analyses shows similar induction of neural crest markers *SOX10* and *PAX7* in all concentrations of retinoic acid and those not subjected to retinoic acid exposure. There is a significantly higher induction of *PAX3* in cultures subjected to 10^{-8} and 10^{-7} M retinoic acid. (All qPCR graphs are N=3 biological repeats, bars are Mean+SEM; 2 way ANOVA with Dunnett's multiple comparison *P<0.05 ** P<0.001; *** P<0.0001)

3.3.3 Retinoic Acid patterned neural crest cells can be further differentiated to Enteric Neural Progenitors

Retinoic acid mediated patterning of neural crest differentiation can induce further neural crest differentiation into enteric neural derivatives (Fattahi et al., 2016; Workman et al., 2016). Early enteric neural specifiers PAX3, RET and EDNRB have been shown to be expressed in retinoic acid patterned neural crest alongside (Fattahi et al., 2016). Following on from these data, we wanted to determine if we could replicate the findings of Fattahi et al and induce enteric neural precursor differentiation. Fattahi et al showed that CD49d+/SOX10+ cells from their 11-day protocol (after five days of RA exposure) had marker expression consistent with enteric neural precursors *in vitro* and when transplanted, demonstrated function to rescue a Hirschsprung's model mouse (Fattahi et al., 2016). We wanted to test for these markers in our protocol and determine the signals and timings involved in enteric neural specification. 10^{-6} M retinoic acid treatment induces neural crest cells consistent with a vagal identity (*SOX10*+/*HOXB5*+), we wanted to test whether these putative vagal neural crest cells showed gene expression consistent with further differentiation to enteric neural precursors.

First, we assessed 10^{-6} M retinoic acid or untreated day 6 neural crest for early enteric neural specifier genes **(Figure 3.4A)**. We saw that both conditions had similar expression of *SOX10* consistent with multipotent migratory neural crest identity. In addition, we assessed the expression of genes that are consistent with early enteric neural differentiation including *PHOX2B* (Elworthy et al., 2005), *ASCL1* (Memic et al., 2016) and *HAND2* (D'Autreaux et al., 2011). We saw that these genes were expressed at similar, low levels in both conditions **(Figure 3.4A).** *SOX10* was expressed more highly in both conditions and is indicative of multipotent, migratory neural crest cells. We then tested for proteins levels of the GDNF receptor RET, a marker of early enteric neural development (Durbec et al., 1996). We performed immunostaining for RET and SOX10::GFP to confirm qPCR data. We detected SOX10::GFP expression but did not detect any signal after immunostaining against RET **(Figure 3.4B)**. These are consistent with the hypothesis that these cells are not yet specified enteric neural precursors. The

differentiation protocols previously published are longer than our protocol (11 days in Fattahi et al; 10 days in Workman et al). Thus we differentiated neural crest cells with 10^{-6}M RA exposure between days 4 and 6, and used FACs sorting SOX10::GFP **(Figure 3.5A)** or $P75^{++}$ **(Figure 3.5C)** to purify putative vagal neural crest cells. After sorting for SOX10::GFP, we plated cells down for 24 hours, then fixed and performed immunostaining for RET. We found homogenous expression for RET **(Figure 3.5B)** consistent with further RA exposure being required for enteric neural precursor specification.

In addition the Fattahi protocol utilises spheres before further plating to induce enteric neurons *in vitro* (Fattahi et al., 2016). We thus sorted out $P75^{++}$ cells **(Figure 3.5C)** after vagal neural crest differentiation, formed spheres following plating into non-adherent wells and continued growing these for two days. We then plated the spheres down in neural crest media containing 10^{-6}M RA and performed immunostaining for RET after 48 hours **(Figure 3.5D)** . These cells also expressed RET, showing that sorting for both P75++ and SOX10::GFP can purify neural crest cells that will go on to be specified to enteric neural progenitors. We can purify populations of these cells in transgenic and non-transgenic lines through use of SOX10::GFP reporter and an antibody to P75 respectively for downstream applications.

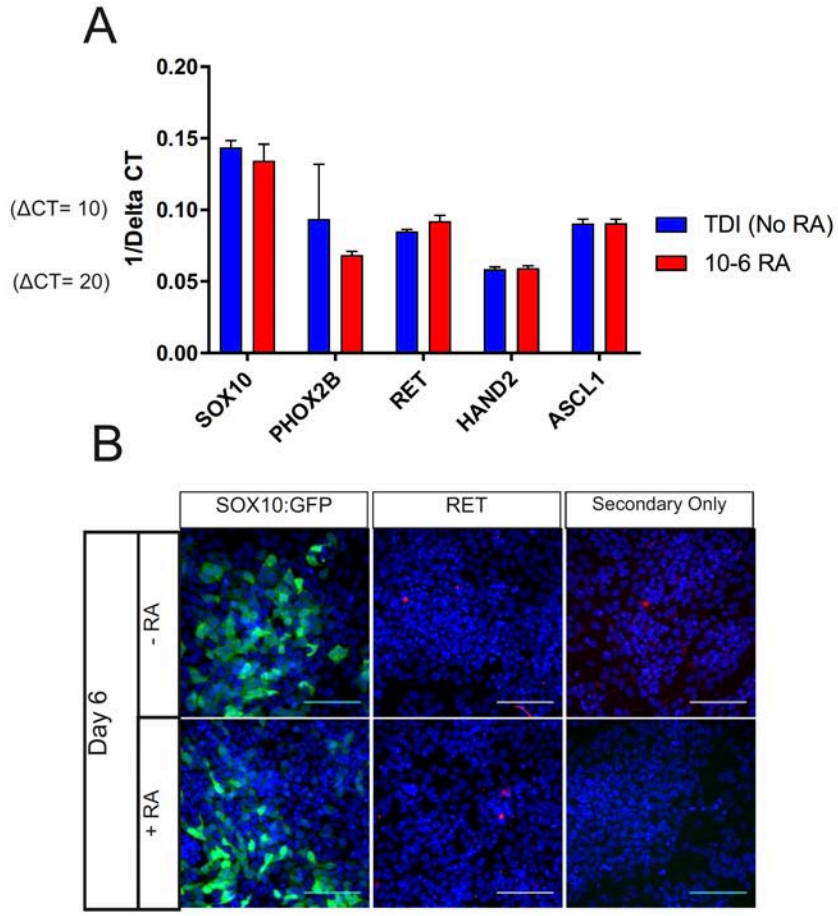

Figure 3.4 Retinoic Acid treated neural crest cells do not express early enteric neural markers after initial retinoic acid patterning. (A) qPCR analyses showing low expression of early peripheral neural genes after 6 days of differentiation in both TDI with and without all trans retinoic acid. In addition, cells still express SOX10, consistent with early migratory neural crest identity (N=3 biological repeats; bars are Mean +SEM; data not significant student's t-test). **(B)** Immunostaining for RET confirms that despite low level of transcript is detected in these cells, they are do not show immunoreactivity, whilst showing SOX10::GFP expression (N=3 Biological repeats. Scale Bar=100µm)

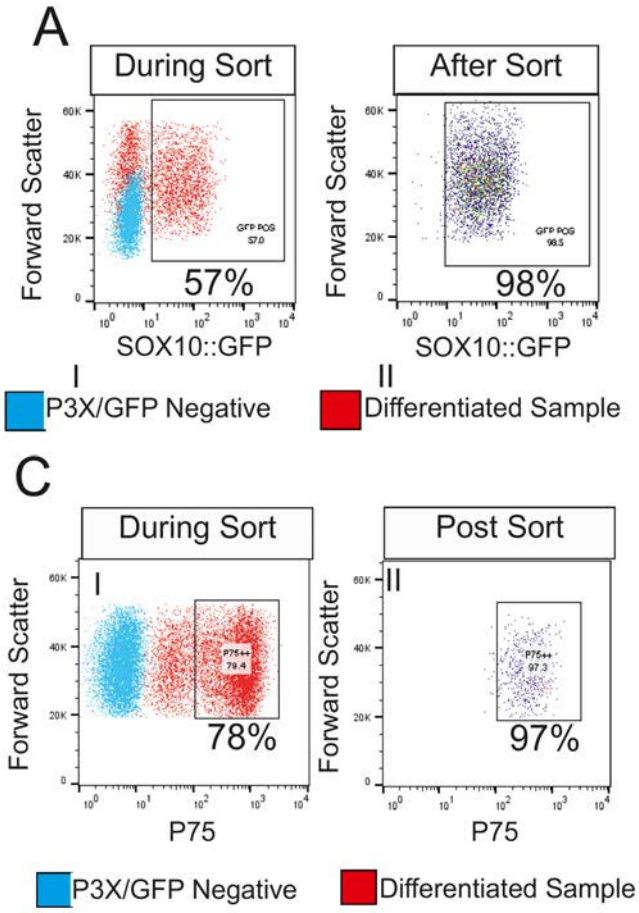

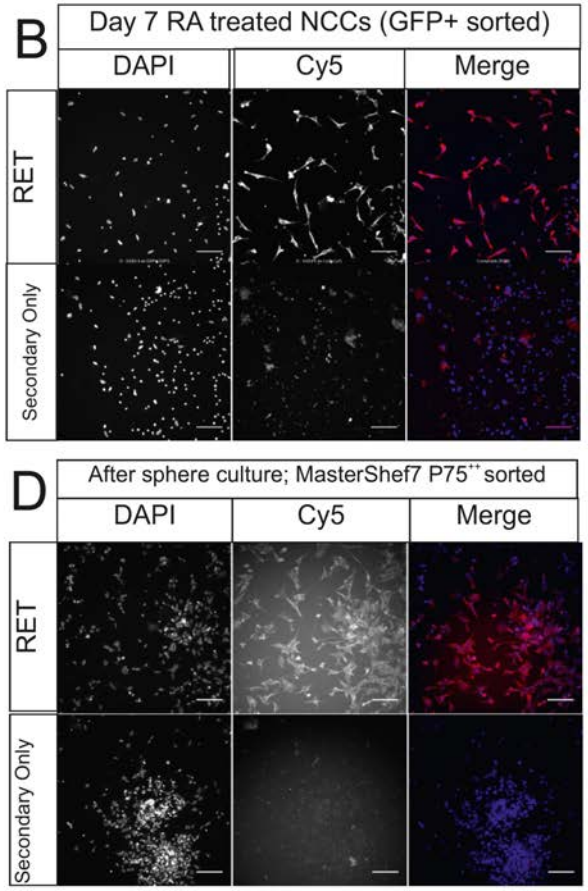

Figure 3.5 Sorting for putative neural crest and continued exposure to RA induces RET expression. (A) FACs strategy using H9:SOX10 showing representative FACs plots after 6 days of differentiation **(i)** and sort purity **(ii)** following sorting shows the fidelity of the sorting process. Replating these cells and using immunostaining at day 7 shows that RET is induced following more time exposed to all trans retinoic acid signalling. **(C)** Sorting for P75++ and placing cells in non-adherent conditions followed and replating (D) shows that RET+ cells are present following sphere culture consistent with enteric neural precursor identity (scale bar=100µm; n=2 biological repeats for each line).

3.3.4 Optimisation of Transplantation of Enteric Neural Precursors.

Having demonstrated the onset of some markers consistent with enteric neural precursors, we wanted to test the ability of these cells to engraft and differentiate *in vivo*. We performed neural crest differentiation and sent cells to Dr Conor McCann and Dr Julie Cooper in Dr Alan Burns' lab at the Institute of Child Health at UCL. They transplanted cells we differentiated into the caecum of immunosuppressed mice. The ability of similar cell types to engraft *in vivo* has been shown in putative hPSC (Fattahi et al., 2016) and mouse ES cell (Kawaguchi et al., 2010) derived enteric neural precursors as well as adult enteric neural precursors from both mouse (Natarajan et al., 2014) and human (Cooper et al., 2016).

We thus wanted to test the cells derived from our protocol to determine their ability to engraft into mouse gut and form enteric neurons. To optimise transplantation and find the best ways to assess the ability of these cells to engraft, we undertook a range of transplants working up to the most optimal conditions for transplant. Parameters included for optimisation were: differentiation protocol, cell labelling technique, FACs purification and whether cells are transplanted as a suspension or as aggregates.

Initial experiments were done using H9:SOX10 hPSCs that had been induced to neural crest (without exposure to retinoic acid). Following induction, we labelled with the lipophilic dye DiI (Life Technologies V22885) that is incorporated into the cell **(Figure 3.6A)**. We did not FACS purify for neural crest cells and we transported cells to London, where the team at the ICH transplanted differentiated cultures as a suspension. Following two weeks *in vivo* we assessed whether the cells had engrafted. We detected few cells in the gut and no evidence of these cells extending projections as would be expected from further neuronal differentiation. We also performed immunostaining for the neural markers P75 and TUJ1 and saw co-expression of these markers with DiI positive cells. Overall, from these first transplants, the DiI was difficult to find in the gut, due to loss of intensity and was potentially being lost from the cells by dilution potentially from

proliferation of the cells. We did have initial evidence of further neural differentiation of transplanted cells *in vivo* from P75 and TUJ1 expression upon assessment after transplantation.

We next wanted to assess lentiviral mediated delivery of GFP and TdTomato to label cells for transplantation (Natarajan et al., 2014). We then assessed the ability of these methods to label cells for transplantation **(Figure 3.6B)**. Due to the requirement to deliver the virus during the differentiation, following transfection, our collaborators first stained some cells *in vitro* for early enteric neural markers P75 and TUJ1. P75 was widely expressed, which is consistent with the differentiation success as well as some TUJ1 positive cells, that may be indicative of either neural plate cells or very early peripheral neural differentiation. In addition, we also assessed the expression of the glial marker GFAP and only found a few positive cells. These data are consistent with our *in vitro* data that cells from our differentiation are early putative neural crest and a low level of TUJ1 and GFAP immunoreactivity also indicate that these cells are beginning to further differentiate into derivatives.

The team in London subsequently to transplanted these cells *in vivo* and after two weeks, were not able to find many cells. The cells they did find showed a stellate cell morphology and showed early neuronal process formation **(Figure 3.6B).** In addition, they also found that these GFP positive cells also expressed P75 and were in close association with the host neural network (P75+/GFP-).

Previous reports from Alan Burns' lab had also found that TdTomato labelled adult enteric adult stem cells were able to be transplanted and engraft into mouse gut (Natarajan et al., 2014). We opted to use this lentiviral label and this would allow the observation of SOX10::GFP expression *in vitro* to assess neural crest differentiation in both putative cranial and RA treated neural crest cultures in Sheffield before transplantation as a quality control mechanism. In addition, it would allow the team in London to assess glial differentiation following transplantation **(Figure 3.6C)**. Following two weeks *in vivo*, the gut was removed in London and imaged. The TdTomato labelling was patchy, but was visible in cells

from both conditions. In addition, immunostaining for TUJ1 was seen in the labelled cells from both differentiation protocols, again showing that transplanted cells undergo further differentiation toward neurons *in vivo*. We did not observe SOX10::GFP co-expressing with the TdTomato expression after two weeks which is consistent with TUJ1 marker neural crest derived neurons. The absence of SOX10::GFP signal may be indicative of neural over glial fate in these cells.

Labelling the cells with either DiI or the lentiviral method was allowing us to visualise cells, but adding these in added an extra layer of complexity to the directed differentiation that may have interfered with the ability to form neural crest.

We next decided to utilise ZIPs, an iPS line that has constitutive expression of ZsGreen in the AAVS safe harbour locus (a kind gift from Professor Lesley Forrester's lab), which negated the need for transfection of lentiviral reporters. We decided to FACs purify labelled, $P75^{++}$ cells in Sheffield that express genes consistent with early enteric neural differentiation **(Figure 3.6D)** and form aggregates, then transport transplant them as small aggregates in London. We also decided to assess the fate of the cells after 4 weeks of transplantation *in vivo* as this was common time point used by the team in London to assess transplants. We again assessed for neural markers *in vivo* to determine if these cells had further differentiated. The endogenous GFP from these cells allowed us to find the cells in the gut more easily and we could find more cells *in vivo.* Like previous attempts, we saw co-expression of TUJ1 with the transplanted human cells. In addition, cells found after 4 weeks were found in groups consistent with the formation of ganglia and were in very close association with the host neural network. We also found cells co-expressing ZsGreen, P75 and GFAP consistent with neural and glial differentiation respectively.

Blank Page

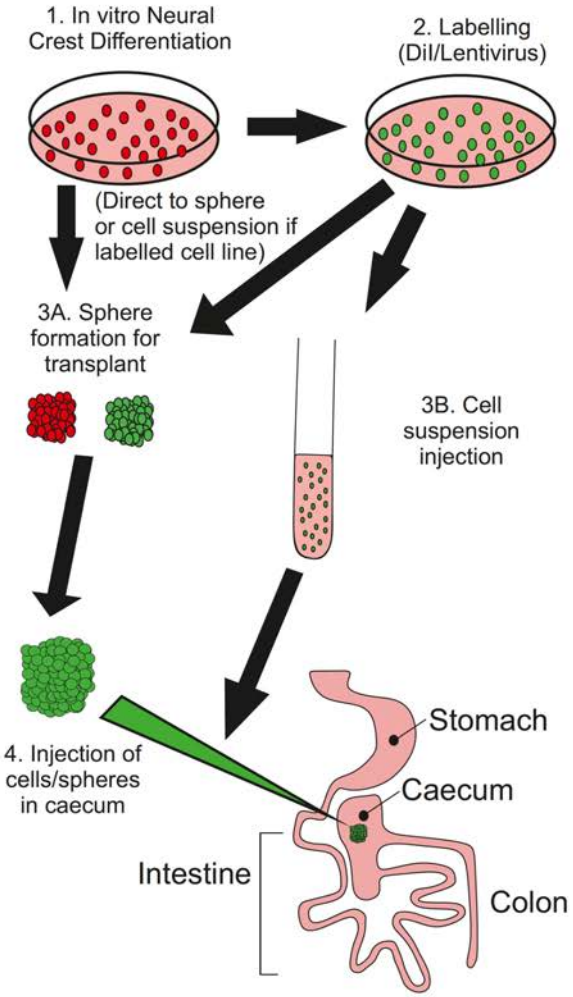

Transplant	Differentiation	Cell Line	Labelling	Outcome
1 (Figure 3.6A)	Cranial Neural Crest (NCN2- pre TDI media without BMP control) Unsorted	H9:SOX10 (Chambers et al 2012)	DiI (Life Tech #V22885)	Few cells found. Labelling not ideal Unknown quality of differentiation. DiI cells express P75 and TUJ1
2 (Figure 3.6B)	Cranial Neural Crest (NCN2) Unsorted	H9:SOX10 (Chambers et al 2012)	Lentiviral GFP (Natarajan et al 2014)	In vitro cells showed expression of Neural (P75, TUJ1) and Glial (GFAP) markers. In vivo,GFP+/P75+ cells found in caecum.
3 (Figure 3.6C)	1. Cranial NC (TDI) (Figure 3.6Ci) 2. Vagal NC (TDI+RA) (Figure 3.6Cii) Unsorted	H9:SOX10 (Chambers et al 2012)	Lentiviral TdTomato (Natarajan et al 2014)	Few cells found. No SOX10::GFP expression detected. TUJ1 expression seen in TdTomato+ cells
4. (Figure 3.6D)	Vagal Neural Crest. Sorted for $P75^{++}$	ZIPs (ZsGreen reporter in safe harbor in genome)	Consituitive ZsGreen expression	Better labelling. with more green cells found than other methods. Good integration into gut. Expression of Neural (P75, TUJ1) and Glial (GFAP) markers after 4 weeks *in vivo*

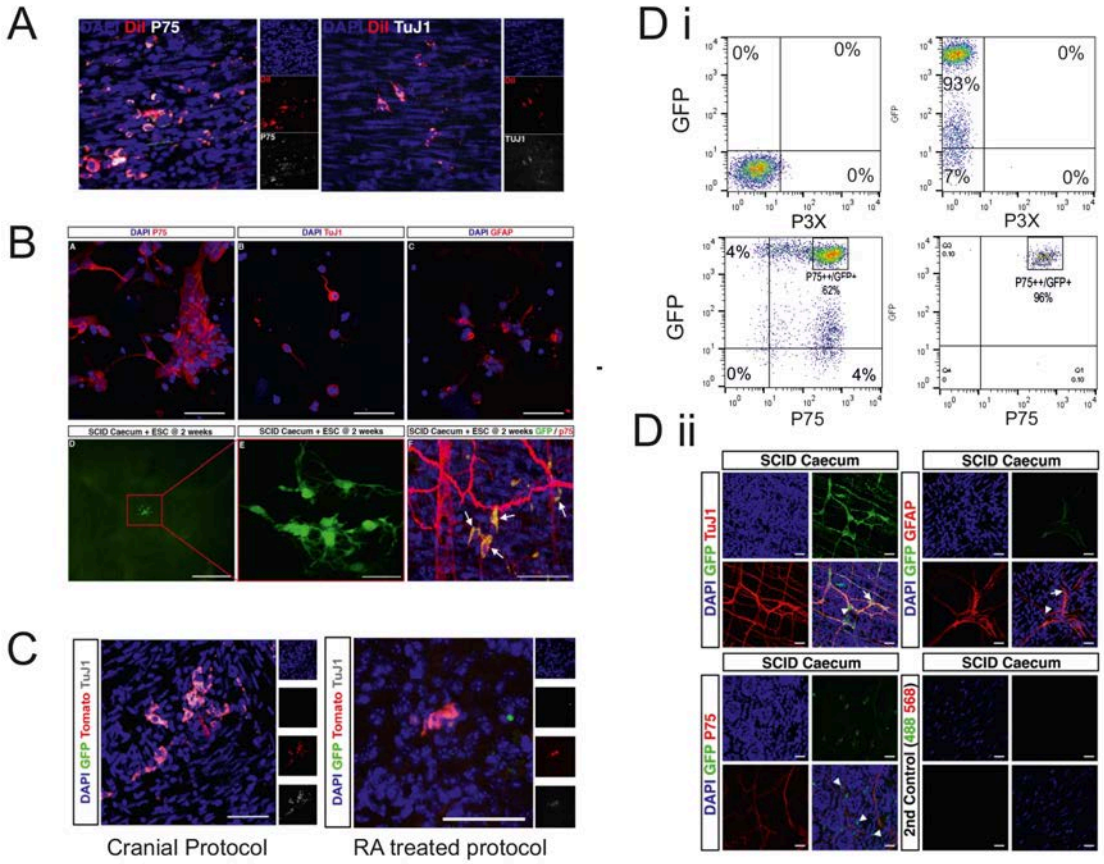

Figure 3.6 Outcome of neural crest transplants into caecum. (A). DiI labelling can be seen, but is patchy and seems to be incomplete. Cells that can be found are shown to express P75 and TUJ1 consistent with neural identity. B. In vitro analyses show expression of TUJ1, P75 and GFAP in cells further cultured **(Ba, Bb Bc).** After lentiviral labelling cells can be found, and this labelling shows morphology of cells **(Bd, Be)** in close association with host neural network and expression of P75 consistent with enteric neural identity (Bf). Using lentiviral TdTomato labelling before transplantation and comparison of cells from cranial and vagal differentiation protocols shows both sets of cells can give rise to TUJ1 expressing cells in the gut **(C).** Very little SOX10:GFP is seen indicative of further neural differentiation. **(Di)** Sorting strategy for ZIPs line constituitively expressing ZsGreen for P75++ cells. (**DiA)** shows doublenegative gates, (DiB) confirms the expression of GFP in the line, **(DiC)** shows gate for GFP expressing P75 cells only and confirmation of sort purity **(DiD).** These cells can be visualised in the gut (Dii), integrate well with the host neural network and give rise to cells express neural markers TUJ1 **(DiiA)** and P75 **(DiiC)** as well as G F A P **(Dii B)** . *All cellular transplantation and imaging of mouse gut was carried out by Julie Cooper & Conor McCann. Burns' group, Institute of Child Health, UCL.*

3.4 Discussion

3.4.1 RA exposure throughout differentiation affects cell fate.

Retinoic acid was one of the first signals to be robustly characterised as a modulator of cell fate *in vitro.* Early work using embryonal carcinoma cells showed that following addition of all-trans retinoic acid, cells underwent morphological and physiological changes that could be detected in culture (Strickland and Mahdavi, 1978; Andrews, 1984). The fate of cells exposed to retinoic acid varied based on the species of model, as mouse F9 embryonal carcinoma cells were shown to form parietal endoderm (Strickland and Mahdavi, 1978), whilst human cells formed differentiated cultures that included neural cells (Andrews, 1984). It should be noted that in retinoic acid mediated differentiation of NTERA2, the cultures were not composed entirely of neurons, but crudely, the cells could be split into neural and non-neural derivatives (Peter Andrews; personal communication). In addition, the use of retinoic acid to generate neural subtypes has been well characterised *in vitro* with many protocols utilising it to pattern neural differentiation cocktails (Okada et al., 2004; Lippmann et al., 2015). Utilising single cell transcriptomics Semrau and colleagues found that mouse ES cells treated to RA underwent differentiation into and split into two broad clusters, one showing evidence of ectoderm differentiation and the other showing extraembryonic endoderm formation (Semrau et al., 2016).

This may relate to inherent heterogeneity within the stem cell compartment as a determinant in lineage decisions. This has been demonstrated in hPSCs whereby separation of cells on the expression intensity of the stem cell associated antigen SSEA3, Tonge et al found the formation of both neural and non-neural colonies in clonogenic assays from these cells (Tonge, Shigeta, Schroeder and Andrews, 2011). They also showed that lower SSEA3 expression formed colonies that classified as both neural and non-neural, whilst SSEA3 high cells formed compact colonies indicative in retention of pluripotency. Whilst the sorting of these cells within the culture does show some initial variation in differentiation potency, the

resolution of heterogeneity within cultures has recently been investigated further to single cell levels with more complex analyses of cell fate.

The variation in cell fate shown from these data were a first indicator that the temporal addition of retinoic acid and thus how it is a key component to its function during neural crest development. Cells from our protocol subjected to RA formed a monolayer of fibroblast like cells *in vitro* with no discernible indicator of the fate of these cells (data not shown). In addition, we did not observe P75 immunoreactivity in these cells **(Figure 3.1B)**, whilst we have previously shown that neural cells do express P75 (Hackland et al., 2017).

These data may indicate that the formation of endodermal cultures based on the fate decision that has been shown from previous investigations into cell fate here. The first hypothesis to test is to confirm the expression of early endodermal markers, work from mouse cells has shown they form cells indicative of extra embryonic endoderm but this would seem unlikely as hPSCs have not been shown to form this cell type *in vitro*. If any form of endoderm has been form, it would most likely be Definitive Endoderm that is marked by *SOX17* and *FOXA2* co-expression (Loh et al., 2014). For a more comprehensive analysis, mRNA-sequencing at a single cell level would allow the changes in gene expression to be monitored and determine whether hPSCs showed the formation of both endoderm and ectoderm following retinoic acid treatment *in vitro* like Semrau et al's observations in mouse.

3.4.2 RA patterns hPSC derived neural crest cells in a dose dependent manner as far as the vagal neural crest

The importance of timing during retinoic mediated patterning of neural crest differentiation from hPSCs was previously demonstrated by Mica et al who showed that early exposure perturbed neural crest specification completely (Mica et al., 2013). Their findings match our results **(Figure 3.2)** and may indicate that the patterning process occurs after a specification of a cell type has passed a critical point. In addition, the timing of retinoic acid for patterning has been

implicated due to the length of time it takes for a threshold concentration to activate HOX genes (Maves and Kimmel, 2005). Following the identification of the optimal time for retinoic acid exposure to cells undergoing neural crest differentiation *in vitro,* we observed induction of HOX genes consistent with forebrain identity (*HOXB1*, *HOXB2*) as well as induction of hindbrain/spinal cord HOX genes (*HOXB4*, *HOXB5*). In addition, we utilised transcript data to corroborate our FACs analysis of the SOX10::GFP reporter to determine if retinoic acid perturbed the neural crest differentiation at all concentrations assessed. Having not seen a decrease in expression of any of the neural crest related transcripts is consistent with the hypothesis that retinoic acid added at the correct time point does not perturb, but rather patterns these cells **(Figure 3.2).** Our initial findings corroborate data from other groups by showing 10^{-6} M all trans retinoic acid patterns vagal neural crest cells by expression of *HOXB4/B5* **(Figure 3.2)**. In order to determine if the concentration of retinoic acid mediated the extent of posteriorisation of neural crest cells, we decided to mimic the approach taken in by Simeone et al in NTERA2 differentiation, where 10^{-6} M retinoic acid activated 5' HOX genes, whilst 10^{-9} M retinoic acid, the lowest concentration tested, only activated 3' genes (Simeone et al., 1990). We found the same trend whereby the highest concentration of retinoic acid (10^{-6}M) was required for induction of the5' HOX genes (*HOXB4*/*HOXB5*) of the vagal level and as the concentration reduced, we only saw 3' HOX genes (*HOXB1/HOXB2*) **(Figure 3.3)**. In addition, we also saw a reduction in the amount of the 3' HOX genes as the concentration of retinoic acid decreased, for instance *HOXB1* expression was highest after 10^{-6} M exposure. These data consistent with the dose effect of retinoic acid on HOX genes that has been postulated from many systems. To further the data from our findings and confirm the dose dependent patterning is acting on neural crest cells, performing transcript analysis on cells sorted for $P75^{++}$ or SOX10::GFP positive cells would confirm this effect on neural crest cells. This would also allow for the early interrogation into the effect on neural crest cells about their further differentiation which has been shown to have an impact on this. In addition, as a mixed culture of cells, it is possible that there is a heterogeneous mix of cells of many different identities within the culture. Within

cell culture dishes, there are micro-gradients created throughout the culture and the position of cells within cultures has an effect on the ability to respond to signals (Etoc et al., 2016). This may result cell plasticity being seen overall in the culture due to the high level of mixing, which has been demonstrated *in vivo* (Trainor and Krumlauf, 2000a). To determine the finely tuned patterning that is seen by these cells across a retinoic acid gradient, an engineered approach creating a fine gradient of retinoic acid across cultures can be used to expose cells to precise amounts of a morphogen to pattern them. To test the plasticity of these cells *in vitro*, these cells can subsequently mixed either as clumps of cells or single cells and their gene expression assessed to determine if a) these cells are plastic and b) if the plasticity has a threshold based on cell number. In addition, single cell transcriptomics/epigenomics could determine any change in gene expression or chromatin remodelling behind this. As aforementioned, the gold standard assay of this which would allow more directly comparable results to previous experiments, would be the grafting of these cells into different rhombomeres of the chicken embryo. From here we could analyse the HOX gene expression to determine any change in gene expression in our *in vitro* derived cells as has been seen in the mouse. In addition, by changing the axial level to which we transplant into, we can attempt to mimic the work by Nicole Le Douarin where the posterior limit to mesectoderm differentiation was identified (Le Lièvre and Le Douarin, 1975). This would complement the recent work carried out showing the poised state of many positional dependent enhancers which have shown the mechanism to explain how changing environments affect plasticity of cells (Minoux et al., 2017).

One of the key findings that we present here is the limit to which retinoic acid can pattern the neural crest to the vagal level corresponding to the hindbrain and upper spinal cord, anterior to the cervical thoracic boundary of the spinal cord. This is in contrast to recent findings where it has been claimed that retinoic acid patterning derive trunk neural crest cells, that are posterior to the cervical thoracic boundary (Huang et al., 2016). Whilst retinoic acid has played a key role in patterning that is held across many species and into hPSC models of neural

crest (from this work and others (Workman et al., 2016; Mica et al., 2013; Fattahi et al., 2016; Lippmann et al., 2015)) the extent of the patterning we find does not extend to truncal level. In the Huang protocol, there are some differences to other models utilising retinoic acid as a patterning molecule. First, whilst they do show HOX gene expression, they use *PHOX2B* as an indicator of truncal identity due to its role in sympathoadrenal differentiation which is typically trunk derivative (Huber et al., 2012). Whilst this is the case, *PHOX2B* is also present in the differentiation of neural crest cells into the enteric nervous system (Elworthy et al., 2005), which is derived primarily from the vagal neural crest (Burns, Champeval and Le Douarin, 2000). *PHOX2B* has also been shown to be a marker of hindbrain motor neurons, which arise from a similar region of the anterior posterior axis as the vagal neural crest (Pattyn, Hirsch, Goridis and Brunet, 2000). To fully confirm the case of *PHOX2B* being a marker of putative trunk neural crest cells, FACs purification of neural crest cells would enable a more robust conclusion of truncal identity.

3.4.3 Further specification of Neural Crest cells to enteric neural progenitors *in vitro*

Retinoic acid has been shown to play a role in the further differentiation of neural crest cells in addition to its key role in patterning. We thus wanted to test if putative vagal neural crest cells *in vitro* could be further specified to early enteric neural progenitors. Previous reports have shown the expression of early enteric neural specifiers expressed immediately at the end of vagal neural crest differentiations (Fattahi et al., 2016; Workman et al., 2016). We also wanted to test this and found to the contrary that we did not see robust induction of these genes by qPCR (Figure 3.4) and was confirmed by immunostaining (Figure 3.4B). Thus, we hypothesised that further exposure to retinoic acid would induce markers of enteric neural progenitors, particularly RET. This observation has been shown in cells taken from E12.5 mouse gut (Sato and Heuckeroth, 2008) and so we found that following FACs purification of retinoic acid treated neural crest cells, we found robust expression of RET. Our observations subsequently give rise to the hypothesis that time of retinoic acid exposure affects specification to we

had earlier less committed vagal neural crest rather than enteric committed progenitor cells.

To further specify enteric neural progenitors to enteric neurons, extended culture in conditions that promote further differentiation are required. GDNF has been used to promote enteric neurogenesis, as assessed by marker expression and innervation of target tissues (Fattahi et al., 2016). We have demonstrated the expression of the RET, the receptor tyrosine kinase, expressed on enteric neural progenitors, that is crucial for ENS development (Natarajan et al., 2002; Heanue and Pachnis, 2008) but additional characterisation of these cells is required. For example, the expression of the co-receptor GFRα1 is required for the activation of the RET receptor, thus demonstrating expression of this may allow for the prediction of this receptor to work functionally. To fully test this hypothesis, we would also be required to assess the phosphorylation status of RET after GDNF exposure. Looking to other pathways, the Endothelin B receptor (EDNRB) is also a crucial signalling pathway involved in Enteric Nervous System development, as shown by the Piebald model displaying aganglionosis (Bolande, 1975). Expression of this receptor has been shown in other hPSC derived enteric neural progenitors (Fattahi et al., 2016), but the role of endothelin signalling in these cells is yet to be explored. It has been shown that signalling through RET and EDNRB interplay to balance the self-renewal and differentiation of these progenitors for enteric neurons to stop and form ganglia along the gut, but also so that there are enough cells to innervate the entirety of the gut (Reviewed in Heanue and Pachnis, 2007).

Following characterisation of the gene expression profiles of these cells, we would also assess the role of Endothelin-3 signalling with regards to the possibility of expanding these cells. Through understanding the interplay between proliferation and differentiation, this may assist in future cell replacement therapies for Hirschsprung's disease, where large numbers of cells are required to rescue to the aganglionosis of the gut.

In addition to the marker expression of these cells, the migratory characteristics are a key determinant to the formation of the enteric nervous system and

migratory characteristics of neural crest cells vary based on their anterior posterior identities. Vagal neural crest cells move in a characteristic chain-like pattern (Young et al., 2004) that progressively moves towards the caudal end of the gut, this is a unique aspect of this cell population. It may be possible to establish an assay that allows us to study the directional migration of these cell *in vitro* in response to certain growth factors, such as GDNF. Comparing putative cranial and vagal neural crest in their responses to chemokines *in vitro* and assessing the patterns in which they migrate would be an easy and effective functional comparison of these cells *in vitro. In vivo* imaging cranial neural crest cells in the chick has shown subpopulations of cranial neural crest cells emerging that direct the migration of these cells into the branchial arches (McLennan et al., 2015b).

In vitro functional assessment of more mature enteric neurons and their ability to innervate smooth muscle *in vitro* and *in vivo* would also allow us to determine the efficacy of these cells in treating Hirschsprung's disease. These experiments have already been done in the context of hPSC derived smooth muscle (Fattahi et al., 2016) and hPSC derived gut organoids (Workman et al., 2016). In addition, we must can also assess how the neurons within ganglia communicate with each other and may assist to delinate further the mechanisms by which the enteric nervous system is built by a series clones that form the neurons and glia in the enteric nervous system in a co-ordinated manner (Lasrado et al., 2017).

Furthermore, the formation of less specified vagal neural crest or committed enteric neural progenitors will provide information of the genes and signals in formation of the cardiac neural crest. The cardiac neural crest forms the outflow tract and structural element of the heart are derived from the neural crest between somites one to three (Kirby, Gale and Stewart, 1983). Modulation of signals such as FGF, which is seen in low amounts by the cardiac neural crest (Trainor, Ariza-McNaughton and Krumlauf, 2002) are important in this, although many of the key signalling molecules that modulate cardiac fate are not well characterised. The ability for the vagal neural crest to form the cardiac neural crest may be an extension of the ability of more posterior neural crest cells to

form ectomesenchymal derivatives. Whilst the positioning of the cardiac neural crest is within the range shown to be competent for forming head mesenchyme (it arises from the crest emanating from somite 1-3 whilst somite 5 was the posterior limit implicated (Le Lièvre and Le Douarin, 1975), it does raise the possibility that the type of mesenchyme produced by the neural crest is dependent on its positioning, rather than the ability of neural crest to form mesenchymal derivatives.

3.4.4 Transplantation of hPSC derived enteric neural precursors as a potential cell therapy for Hirschsprung's disease

We present data showing the optimisation of transplanting hPSC derived neural crest cells modulating the way in which we differentiate, label and deliver the cells. Overall, the data show that upon transplantation, the cells transplanted undergo neuronal differentiation *in vivo* as marked by TUJ1 and P75 immunoreactivity **(Figure 3.6)**. Whilst these data are encouraging, they cannot be conclusively determined to be neural crest derived enteric neurons as these cells were not FACs purified and these markers are found on many other neuronal types. As mentioned before, the *in vitro* differentiation requires further characterisation about marker expression allowing us to determine whether the cells are consistent with enteric progenitors *in vitro.* The early transplants **(Figure 3.6 Transplants 1, 2 and 3)** do not utilise sorted cells and most likely have neural plate cells 'contaminating' the differentiation. These cells also undergo differentiation into neurons expressing TUJ1 and P75 and so the cells we have seen can arguably be non-neural crest derived. With the last set of transplants utilising cells sorted for neural crest and expressing markers of enteric neural progenitors *in vitro* **(Figure 3.5)**, this may add weight to the hypothesis that these cells are putative enteric neurons *in vitro*. These data are consistent with those presented by Lorenz Studer's group (Fattahi et al., 2016) who demonstrated engraftment, spread and function following transplantation. In addition to our preliminary data showing TUJ1 and P75 expression, assessing the expression of neural subtypes formed *in vivo* will also be advantageous, specifically formation of *nNOS* expressing neurons that work to relax the smooth muscle in the gut are

desirable to improve peristalsis and allow for defecation. Although our data show the presence of neuronal cell types *in vivo*, the function of these cells has not been assessed and by utilising genetically encoded calcium sensors (GCAMP vectors) the calcium waves throughout the ganglia can be visualised easily *in vivo* (Dana et al., 2016). Furthermore, utilising these would enable us to visualise whether the host enteric neurons are forming connections with the transplanted which is required due to the co-ordinated effort of enteric neurons for peristalsis being a crucial determinant in stool motility. On the other hand, recent work has shown a potential mechanism of rescue of enteric neuropathy as well as engraftment and direct restoration of function, but also indirect effects on the support cells found in the gut (McCann et al., 2017). Throughout the process of optimising transplants, we have faced significant difficulty with visualising the cells following transplantation and there are several factors that play a role in this. Firstly, by transplanting cells as a suspension, this would result in occurrences where there are only few cells together and any signal from these cells would be lost and not easily visualised. In addition, the use of chemical dyes, such as DiI **(Figure 3.6 Transplant 1/ 3.6A)** that have previously been used to follow up transplanted cells *in vivo* were ineffective in our hands and lost fluorescence intensity over time. Optimising this method would have been possible, for example by increasing the concentration of DiI that we label with to allow more to integrate into the cell membrane. We subsequently moved into the use of lentiviral mediated labelling that has been developed in our collaborating lab (Natarajan et al., 2014). They reported effective labelling and visibility following infection of adult enteric neural stem cells with the virus and whilst we also could visualise cells from this labelling, we had technical issues with cell density resulting in incomplete labelling of cultures as well as the background auto fluorescence from matrix proteins such as collagen (Reviewed in Croce and Bottiroli, 2014). We found some cells with virus mediated labelling, particularly efficiently with the GFP labelled cells **(Figure 3.6 transplant 2/3.6B)**, the incomplete labelling was a major hindrance. Furthermore, utilising the SOX10::GFP line, we wanted to utilise a red label using lentivirus and as a result we also found problems with the TdTomato labelling, which was dimmer and

harder to find *in vivo*. Many transplantation experiments had subsequently used constitutively labelled cell lines to trace cell that have been engrafted, for example GAPDH reporter cell lines have been developed (Kao et al., 2016) for constitutive labelling. Silencing of transgenic reporters was also an issue we were wary of throughout this, there have been reports of reporter silencing due to changes in epigenetic control of random integration sites (Stewart et al., 2008) and so the identification of the AAVS safe harbour site (the human equivalent of the mouse ROSA26 locus) to subsequently engineer in reporter proteins (Ogata, Kozuka and Kanda, 2003) is we think the most robust approach to this. This will allow for protection against any changes in epigenetic status of gene silencing allowing us to track cell fate over long periods of time. Our transplants using an induced Pluripotent Stem cell line with ZsGreen engineered into this locus (called ZIPs), gave the best results and allowed us greater control over the cells we could transplant in. We demonstrated the ability to sort out and purify ZsGreen+/P75^{++} cells **(Figure 3.6D i)** to transplant. Following this, we are now able to make more robust conclusions and determine that the TUJ1 and P75 expressing cells are derived from the vagal neural crest protocol which is consistent with putative enteric neuronal differentiation. We are also able to control cell number following transplantation of these cells, which is a major facet of the transplants to gain control of in the attempt to work up to a cell therapy. Transplantation studies to regenerate primate hearts following an induced heart attack required 1x10^{7} cells in order to see an optimal level of rescue (Chong et al., 2014). Thus, with the area of the gut that may be required to innervate, it is not out of the question for even more of these cells to be required in this context.

Our comparison of putative vagal and cranial neural crest cells transplanted into the gut showed that we saw neuronal differentiation in both cases **(Figure 3.6 Transplant 3/3.6C)**. This is consistent with reports of enteric neural progenitors engrafted onto hPSC derived gut organoids (Workman et al., 2016). They saw neuronal differentiation when cranial (non retinoic acid treated) were combined with gut organoids (an *in vitro* model of the intestine), which is consistent with our initial findings and demonstrates the plasticity of these cells with regard to

their cell fate. The major caveat to transplanting cranial cells as found by Workman and colleagues, was the observation of pigment cells in the gut. This observation gives rise to fears of unwanted cell types in gut, which may in turn form a melanoma if any serious mutations arise. In addition, the fundamental question of whether these cells are *bona fide* enteric neurons is also raised, as these cells would not come from vagal neural crest and possibly not arise in the same manner as endogenous enteric neurons.

Finally, we have not used a model of Hirschsprung's disease to determine if these cells can rescue the disease phenotype. This has been demonstrated to some extent by the Studer group, although there are issues surrounding the severity of the phenotype in the mouse model used in these studies. They used a less severe EDNRB mutant ($EDNRB^{s-l}$) (Huang et al., 2015), which may have resulted in greater survival of mice and is not a true reflection of the severity that can be seen in other models. In addition, it has been noted that large numbers of the $EDNRB^{s-l}$ heterozygote mice survive and successfully breed (https://www.jax.org/strain/000308) To our knowledge, there have been no successful attempts to rescue the phenotype of more severe models due to premature death of mice.

3.5 Summary

In summary, the data we have addressed the aims of the chapter to some extent. Firstly, we have determined that retinoic acid patterns hPSC derived neural crest to the vagal level that occurs in a temporal **(Figure 3.1)** and concentration **(Figure 3.3)** dependent fashion. This is consistent with other reports from hPSC models and *in vivo* models indicating the retinoic acid mediated patterning is conserved from Zebrafish to Chicks, mice and humans. Having determined the concentration gradient that patterns the neural crest along the hindbrain, we can now assess the mechanisms of how cell fate is controlled in these cells. Much of the work *in vivo* has determined the cell fate is plastic and mediated by *HOX* gene expression, differential expression of chemokine receptors in neural crest populations and signals emanating from neighbouring tissues, such as the underlying mesoderm.

In addition, we can now address the heterogeneity within these cells by developing cell sorting and single cell transcriptomics to determine gene expression patterns between cells along the gradient. Furthermore, combining these cells with *in vivo* models such as the chick will allow for the development of assays to determine how plastic these cells are in comparison to host neural crest cells and develop models to this respect.

We can also now determine the changes in gene expression and cell function along the AP axis and determine how gene expression changes can modulate the differentiation potential of these cells. We can assess if hPSC derived neural crest cells consistent with an identity posterior to somite 5 can form mesectoderm when placed in differentiation conditions (as per Chapter 2) or if transplanted into the chicken embryo.

We have determined that the time after retinoic acid addition is crucial with the respect to the specification of enteric committed neural crest cells from vagal neural crest cells **(Figures 3.4 & 3.5**). This has so far been overlooked in other hPSC models of neural crest patterning and overlooks the signals and fate decisions that separate the vagal neural crest that will go to the heart or the gut. We still require more characterisation to robustly determine the gene expression patterns and signals in putative enteric neural crest cells that are derived from retinoic acid patterned hPSC derived neural crest cells. Furthermore, we have also demonstrated the optimal labelling and cell format (suspension vs aggregate) for transplantation into the gut **(Figure 3.6)**. This will enable the development of these cells for a potential regenerative medicine treatment for enteric neuropathies. Whist much work is yet to be done on this including long term safety and functional follow ups, we have established a starting point from which to build upon this.

Chapter 4: Modulation WNT/FGF signalling identifies a novel ontogeny of hPSC derived trunk neural crest cells

4.1 Introduction

Recent work has shown that modulating WNT and FGF signalling in both mouse epiblast stem cells and hPSCs results in formation of axial stem cells, also known as Neuromesodermal progenitors (NMPs) (Gouti et al., 2014; Tsakiridis and Wilson, 2015; Lippmann et al., 2015). Following their differentiation from hPSCs to NMPs, these cells have been demonstrated to be able to derive posterior paraxial mesoderm and posterior motor neurons (Gouti et al., 2014). Gouti et al compared gene expression profiles of motor neuron differentiation from mouse epiblast stem cells patterned with WNT/FGF or retinoic acid. They found that retinoic acid patterned motor neurons expressed HoxB4 and Phox2b that mark hindbrain motor neurons, whilst WNT/FGF patterned cells gave rise to more caudal Hox genes (Hoxc6 and Hoxc9). In addition, the role of retinoic acid has been shown to be axial level dependent, whereby it induces caudal fates shown by HOX gene induction in the anterior neural tube. In the trunk, following WNT FGF patterning, Retinoic Acid has been shown to halt patterning effect of WNT and FGF and induces differentiation toward a neural identity (Lippmann et al., 2015).

Spinal cord motor neurons have so far been the main derivative to be compared between anterior, Retinoic Acid patterned and WNT/FGF patterned axial progenitors, with NMPs being exposed to Sonic Hedgehog (SHH) and retinoic acid signalling (Gouti et al., 2014; Lippmann et al., 2015). Whilst these are signals that are crucial for the development of this cell type, they have shown the ability of *in vitro* derived NMPs to form the floor plate, and yet there has not been a comprehensive assessment of whether *in vitro* derived NMPs may be differentiated to form the dorsal neural tube derivatives. In a mouse ES cell model of the developing Neurectoderm, the dorsal neural tube was the default identity and SHH treatment was required to induce a ventral fate (Meinhardt et al., 2014).

In addition, the addition of SHH to hPSC derived models of anterior Neurectoderm development has been shown to induce a ventral identity instead of a dorsal identity (Chambers et al., 2009). Only recently has a renewed attempt to investigate the formation of dorsal neural cell types from hPSC derived NMPs been carried out (Verrier, Davidson, Gierliński and Storey, 2017a). Verrier and colleagues use Dual-SMAD inhibition (a differentiation protocol utilising inhibitors of BMP and TGFβ signalling pathways) combined with retinoic acid exposure to hPSC derived NMPs and have seen expression of dorsal neural tube markers such as *PAX3, PAX7* and *SOX10* in these conditions. This reflects what is seen in anterior differentiations and is indicative that previous differentiation protocols haven't investigated the full range of cell type derivatives *in vitro*. In addition, the expression of neural crest markers from Dual-SMAD inhibition is also seen in anterior cultures, but this is often as a contaminant cell type and does not elucidate the mechanisms involved in trunk neural crest differentiation. In addition, through the generation of hPSC derived neural crest cells, a thorough comparison of differentiation potency can be done to assess if *in vitro* counterparts of neural crest cells also retain some aspects of fate restriction (Le Lièvre and Le Douarin, 1975).

In addition, the generation of cell types potentially useful for regenerative medicine and disease modelling can be generated if the correct signals and genes can be identified and studied. Sympathoadrenal precursors are a bi-potent derivative of trunk neural crest *in vivo* (Lumb and Schwarz, 2015) that form chromaffin cells in the adrenal gland or sympathetic neurons in the trunk. After trunk neural crest cells delaminate from the neural tube and migrate from the dorsal neural tube to the ventral aspect of the embryo, they are specified to differentiate into sympathoadrenal precursors by Sonic Hedgehog signalling from the floor plate and BMP signalling from the Dorsal Aorta (Reviewed in Huber, 2006). Sympathoadrenal precursors have been linked with the development of the paediatric cancer Neuroblastoma (Cheung and Dyer, 2013) and may be due to a reprogramming to a neural crest-like state as has been demonstrated in melanoma models (Kaufman et al., 2016). A recent report has described

generation of *in vitro* Sympathoadrenal precursors from hPSCs through a putative neural crest intermediate, but the efficacy of this protocol was not optimal (~4% of cells were putative sympathoadrenal precursors) (Oh et al., 2016). This leaves the possibility that proper patterning of neural crest cells derived from hPSCs is required to efficiently generate cell axial specific subtypes *in vitro*. This has previously been demonstrated in the generation of enteric neurons (Fattahi et al., 2016; Workman et al., 2016)

4.2 Aims

To address the issues raised above, the experiments presented in this chapter will have the following aims

1. Determine if hPSC derived NMPs can be further specified into trunk Neural Crest
2. Characterise the gene expression throughout trunk neural crest specification and compare it to hPSC derived cranial neural crest cells
3. Determine if axial patterning may determine prospective fate of neural crest derivatives *in vitro*

4.3 Results

4.3.1 In vitro generation of Neuromesodermal Progenitors from hPSCS.

We first wanted to test whether we could derive NMPs from hPSCs *in vitro* by replicating previously published protocols exposing hPSCs to WNT/FGF signalling. We plated down cells down in N2B27 media supplemented with the GSK3β inhibitor (CHIR99021) and recombinant FGF2 for 3 days as described by Gouti et al (Gouti et al., 2014) **(Figure 4.1A).** After three days, we saw expression of the key NMP markers T (BRACHYURY) and SOX2 and HOXC9**(Figure 4.1B)**. qPCR analysis for T/SOX2/HOXC9 and the NMP markers *NKX1*-2, *WNT3a*, *FGF8* and *CDX2* **(Figure 4.1C)** showed upregulation compared to hPSCs. Expression of *BRACHYURY* has been reported in undifferentiated cells (Gokhale, Giesberts and Andrews, 2000) and so to further assess the differentiated state of these cells, we wanted to determine the expression of the pluripotency associated gene *NANOG* which we found to be lower in these cells. These data are consistent with the findings from Gouti et al that WNT and FGF signalling can induce the formation of putative NMPs from hPSCs *in vitro*.

4.3.2 NMPs co-express early neural crest specifiers with BRACHYURY

Cranial neural crest differentiation is postulated to begin at gastrulation (Basch, Bronner-Fraser and García-Castro, 2006) so we wanted to test whether any early putative neural plate border specifiers are expressed NMP state. We performed qPCR for a panel of early neural crest specifiers including *PAX7*, *PAX3*, *SOX9* and *MSX1*. We saw increased expression in NMPs, indicative of a turning on of expression as postulated in *MSX1*, *SOX9* and *PAX3* or retention of expression (*ZIC3*). These data show that neural plate border specifiers are present in cell expression T/SOX2/HOXC9 and indicate that NMPs share some gene expression with neural crest cells. In addition, we postulate that any neural crest differentiation from NMPs may be specified early in the differentiation timeline. Furthermore, we also wanted to confirm that these early neural crest specifiers were co-expressed with the key NMP gene BRACHYURY. We performed

immunostaining for PAX3, SOX9 and SLUG in NMPs and showed co-expression of these early putative neural crest genes *in vitro*. Overall, these data show the expression early neural crest GRN in NMPs and we hypothesised that if NMPs can make neural plate cells, as has been robustly demonstrated *in vitro* (Gouti et al., 2014; Lippmann et al., 2015; Tsakiridis and Wilson, 2015) and *in vivo* (Wymeersch et al., 2016), then we may be able to influence these cells to derive posterior neural crest cells *in vitro*.

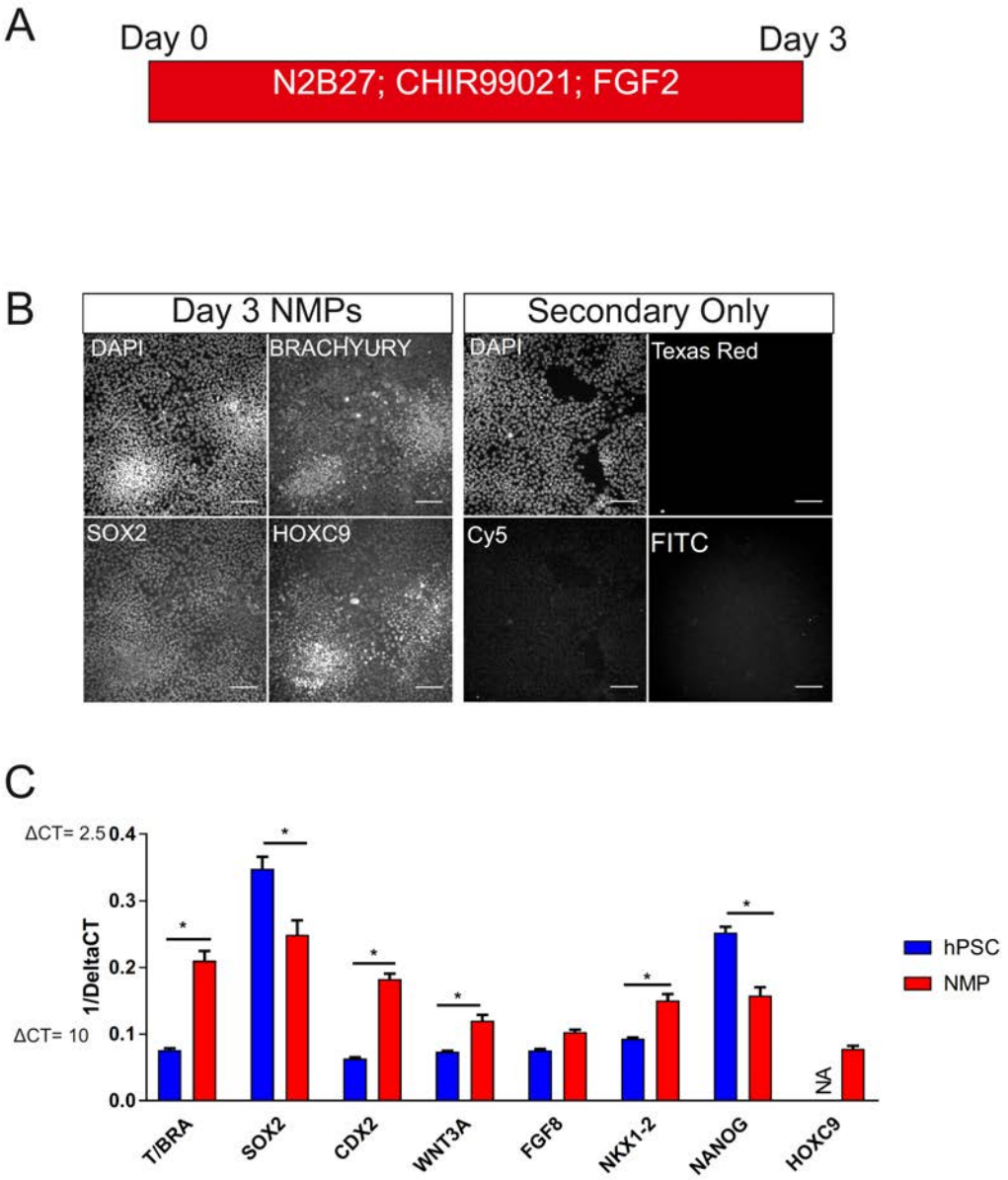

Figure 4.1 In vitro generation of Neuromesodermal Progenitors (NMPs). (A) Schematic of protocol from Gouti et al 2014 showing exposure of hPS cells to high levels of CHIR99021 and FGF2 and analysis point after 3 days of exposure. **(B)** Representative Immunofluoresnece images of MIFF1 iPS cells after 3 days exposure to CHIR+FGF2 shows populations of BRACHYURY+/SOX2+/HOXC9+ positive cells indicitive of NMPs (Scale bar= 100µm) (N=2 Biological repeats). **(C)** qPCR analyses also show induction of these genes, as well as other markers of NMPs such as CDX2, NKX1-2, WNT3a whilst the pluripotency associated marker *NANOG* is downregulated. (N=3 independent experiments, Bars are Mean+SEM; Student's T-test)

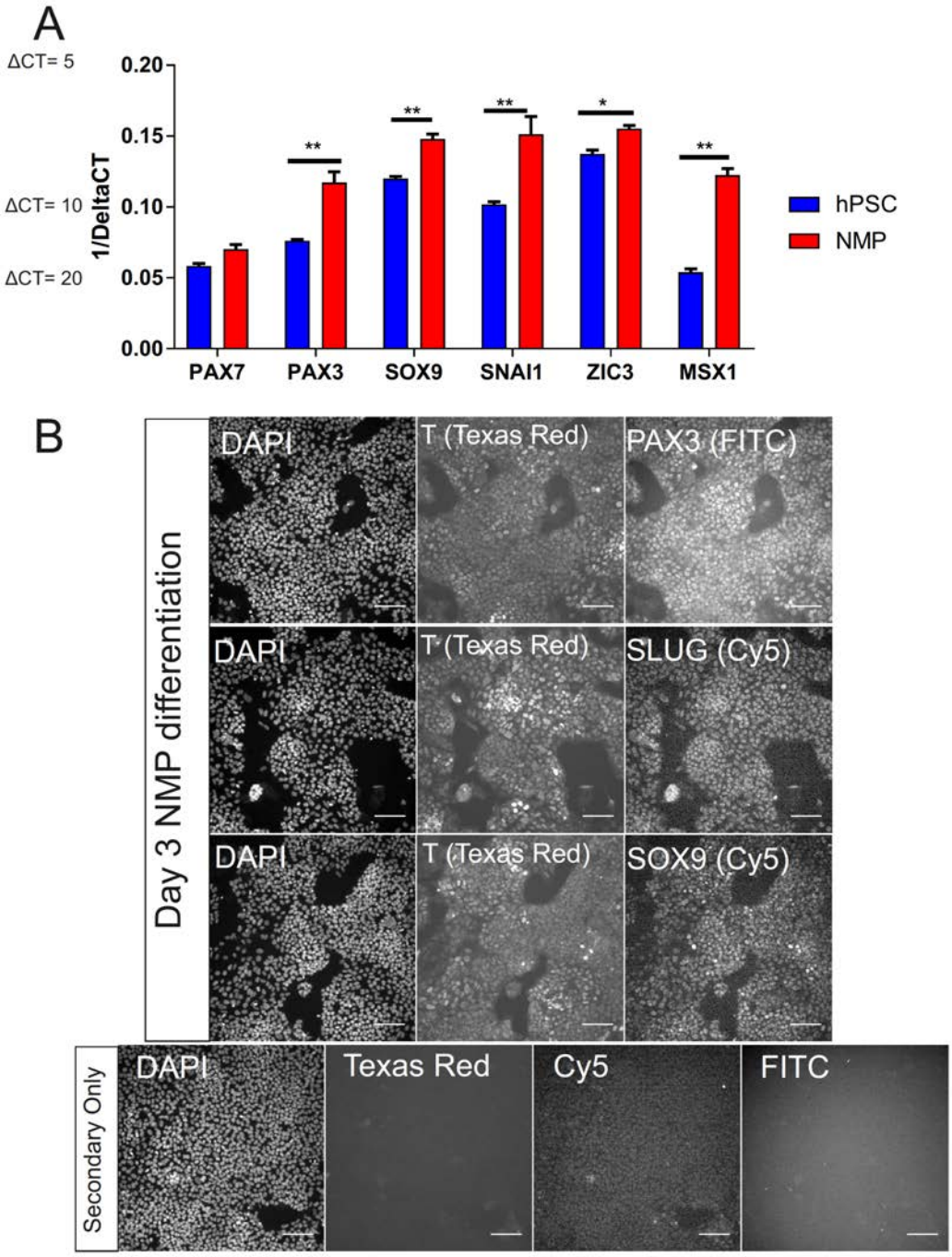

Figure 4.2 NMPs express early Neural Crest specifier genes. (A) qPCR analyses of day 3 NMP cultures showed a significant upregulation of early neural crest specifier genes including MSX1, ZIC3, SNAI1, SOX9 and PAX3 in NMPs over hPS cells. (Bars are mean +SEM of 3 independent experiments. (Student's T-Test *=P<0.05, **=P<0.001). **(B)** immunofluorescence analysis shows co-expression at the protein level of these genes with the key NMP gene T (BRACHYURY) (N=2 biological repeats, scale bar= 100μm).

4.3.3 hPSC derived NMPs can be replated and differentiate into putative trunk neural crest cells *in vitro*

Our data show the shared gene expression between early neural crest differentiation and NMPs. Whilst previous reports claim to derive neural crest cells by BMP exposure to a 'caudal neural progenitor' (Denham et al., 2015), we tested whether hPSC derived NMPs could be re-plated into neural crest differentiation conditions and form neural crest cells **(Figure 4.3A)**. We took RNA at days 0 (hPSCS); day three (NMPs); day six (3 days in Neural Crest conditions) and day nine (6 days in Neural crest conditions) and performed qPCR to assess the expression of neural crest specifiers **(Figure 4.3B)**. We saw increased expression of the dorsal neural tube markers *SOX9*, *PAX3* and *PAX7* **(Figure 4.3Bi)** in putative NMPS at day 3 of differentiation with highest expression at day 6 of differentiation before showing a decrease in expression from day 6 to day 8. *PAX7* peaks at day 6 of differentiation and is consistent with the role of *PAX7* early in neural crest differentiation *in vivo* (Basch, Bronner-Fraser and García-Castro, 2006) and *in vitro* (Leung et al., 2016) The neural crest specifiers *TFAP2*α and *SOX10* did not show upregulation until NMPs were re-plated into neural crest conditions (Day 6 and Day 9) **(Figure 4.3B i)**. *FOXD3*, a key neural crest specifier, is expressed in hPSCs, but was downregulated in NMPs **(Figure 4.3B ii)**. Expression increased following replating into neural crest conditions, this is the only case where a gene is potentially switched off in NMP conditions (day 3 of differentiation) and then reactivated in neural crest differentiation (days 6 and 9). In addition, consistent with our previous observations **(Figure 4.2A; Figure 4.2B)**, we saw expression of both *SNAI1* and *SLUG* in all cell populations, including hPSCs and neural crest cells which is consistent with previous reports. Upregulation of these markers following NMP differentiation is similar the patterns of induction in putative cranial neural crest differentiation.

We performed immunostaining for HOXC9 and SOX10 and saw co-expression of **(Figure 4.3C)** in many cells but did see instances of SOX10+/HOXC9- negative cells. This may indicate incomplete NMP differentiation and 'contamination' of cranial

neural crest cells in cultures, or HOXC9 may be downregulated through neural crest differentiation and thus some true trunk neural crest cells expressing other HOX genes but not HOXC9.

We used qPCR to determine the expression of other *HOX* genes and NMP markers in these cultures and saw co-linear activation of *HOX* genes **(Figure 4.4)**. NMP markers, *BRACHYURY, CDX1* and *NKX1-2* were all downregulated through neural crest differentiation, consistent with their role to alternate NMP fates, such as paraxial mesoderm (*BRACHYURY)* (Edwards et al., 1996) or neural fates (*NKX1*-2) (Verrier, Davidson, Gierliński and Storey, 2017b).

CDX2 and *SOX2* are the only two genes in this panel that we see retained through neural crest differentiation **(Figure 4.4A)**. These data are consistent with previous reports that demonstrate expression of *CDX2* (Sanchez-Ferras et al., 2016) and *SOX2* (Wakamatsu, Endo, Osumi and Weston, 2004) with trunk neural crest. In addition, we also tested the expression of a panel of HOX genes that span the anterior-posterior axis. We have previously seen expression of *HOXA1*, *B1*, *B4* and *B5* in cranial and putative vagal neural crest cells, but we have never seen induction of *HOXB8* and *C9* in these populations. In putative neural crest cells derived from NMPs, HOX genes were retained which corroborates immunofluorescence data showing SOX10/HOXC9 double positive cells **(Figure 4.3C)**.

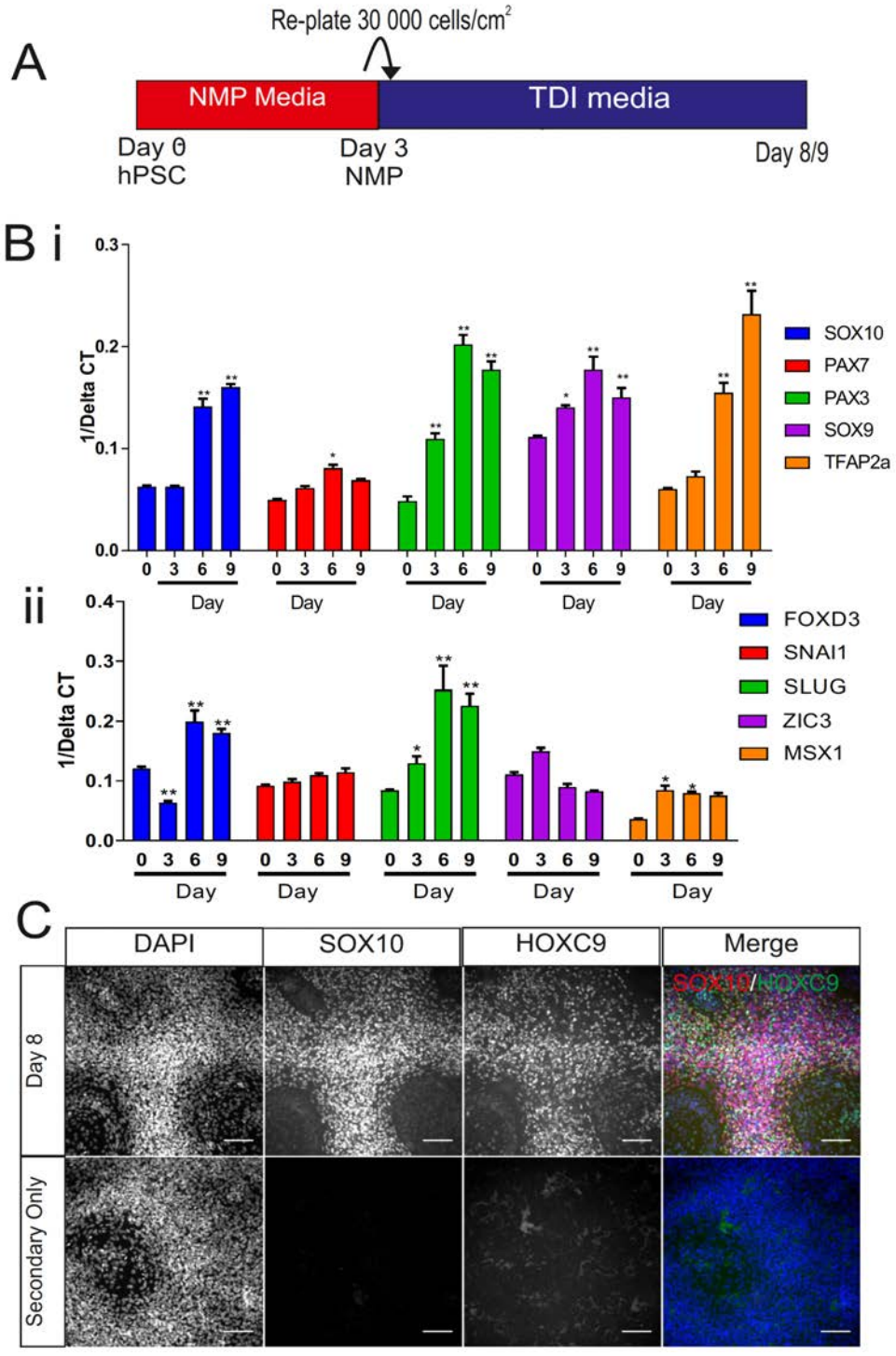

Figure 4.3 Putative Trunk Neural Crest cells can be induced from hPSCs through NMPs. (A) Schematic showing differentiation protocol to derive neural crest cells from NMPs. **(B)** qPCR analyses of neural crest genes that are upregulated throughout differentiation. Some Neural Crest specifiers show upregulation in NMPs, whilst other markers of neural crest (such as SOX10 and FOXD3) are upregulated after 6 and 9 days of differentiation. This is indicative of day 6 corresponding to neural crest precursors and day 9 being migratory neural crest cells (data shown as Mean+SEM; Two- Way ANOVA with Dunnett's Multiple comparison *P<0.05, ** P<0.01 compared to hPSCs (Day 0 differentiation)). (N=3 independent experiments in H9:SOX10 cells). **(C)** Immunofluorescent images showing co-expression of SOX10 with HOXC9 after 8 days of differentiation in MIFF1 iPSCs (N=2 biological repeats).

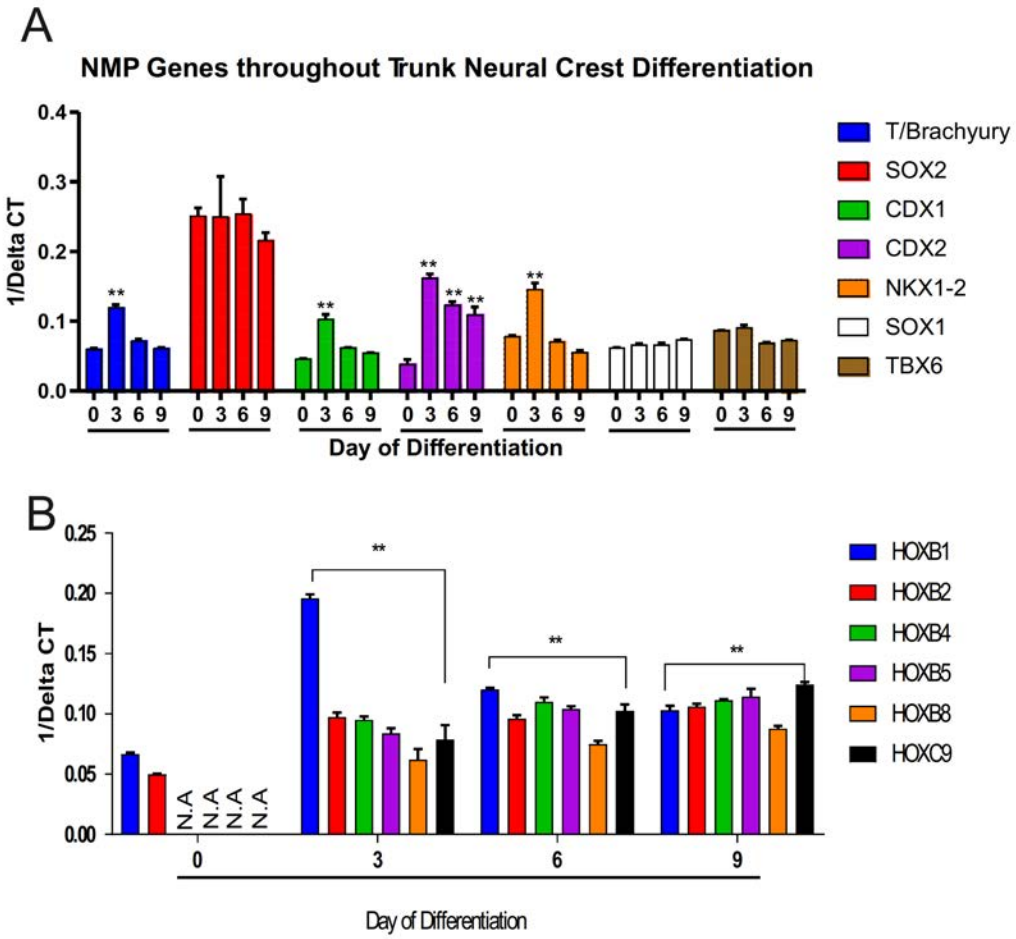

Figure 4.4 Putative Trunk neural crest cells show expression of caudal related genes (A) qPCR analysis of NMP marker genes throughout trunk neural crest differentiation including expression in hPSCs (day 0) showing retention of CDX2 throughout NMP to neural crest induction. **(B)** qPCR analysis showing expression of HOX gene expression consistent of a trunk identity in cultures from day 3 of differentiation (corresponding to NMPs). (N.A= No amplification in sample. data shown as Mean+SEM; Two-Way ANOVA- Dunnett Multiple comparison *P<0.05, ** P<0.01 compared to hPSCs). (N=3 independent experiments in H9:SOX10 cells).

4.3.4 Gene Expression comparisons between putative cranial and trunk neural crest cells

Based on the expression of core neural crest regulatory genes such as *SOX10*, *SOX9*, *PAX3* and *PAX7* and *TFAP2*α gene expression coinciding with trunk HOX gene and CDX2 expression, we believe these are consistent with trunk neural crest cells *in vitro.* We performed qPCR on day 6 differentiated cells from the cranial protocol and day 9 differentiated cells from the trunk protocol **(Figure 4.5A)** as these are the two time-points assessed consistent with migratory neural crest. We did not see significant difference in well characterised neural crest markers (*SOX10*, *SOX9*, *PAX3*, *PAX7* and *TFAP2*α) **(Figure 4.5B)**. Which is consistent with findings from model systems and the hypothesis that these genes are involved in neural crest differentiation generally. Neural crest cells have different differentiation potency *in vivo* with respect to their ability to form ectomesenchyme where neural crest cells of the cephalic region are the only cells that show competency to do this(Le Lièvre and Le Douarin, 1975). In addition, position dependent regulatory units have been identified for genes such as *FOXD3* (Simões-Costa et al., 2012) and *SOX10* (Betancur, Bronner-Fraser and Sauka-Spengler, 2010).

Recent work has shown the expression of 6 genes (*BRN3C, TFAP2*β*, SOX8, ETS1, LHX5, DMBX1*) in the cranial neural crest that are not expressed in the trunk in chick embryos (Simões-Costa and Bronner, 2016). We assessed their expression in putative hPSC derived trunk and cranial neural crest cells by qPCR **(Figure 4.5C).** We also tested *OTX2* (a specifier of the anterior neural plate) and HES6 (a marker of trunk neural crest as picked out by (Simões-Costa and Bronner, 2016)). *OTX2*, *LHX5* and *DMBX1* showed statistically significant higher expression in cranial neural crest over trunk, whilst *HES6* was higher in the trunk. We did not see a significant difference in any other genes, including *ETS1* which is a well-established cranial neural crest marker (Barembaum and Bronner, 2013).

Contrary to these observations, we saw the similar expression levels in both the cranial and the trunk populations. To test that the *ETS1* expressing cells were not

cranial contaminants, we did co-stained for ETS1 and HOXC9 in cells that were from both the cranial and trunk neural crest cell protocols. In the cranial cells, we saw ETS1 positive cells, but did not see HOXC9 expression in any cells, whilst in the trunk cells, we saw double positive cells confirming that ETS1 was expressed in the cells that also have HOXC9 expression **(Figure 4.5D)**.

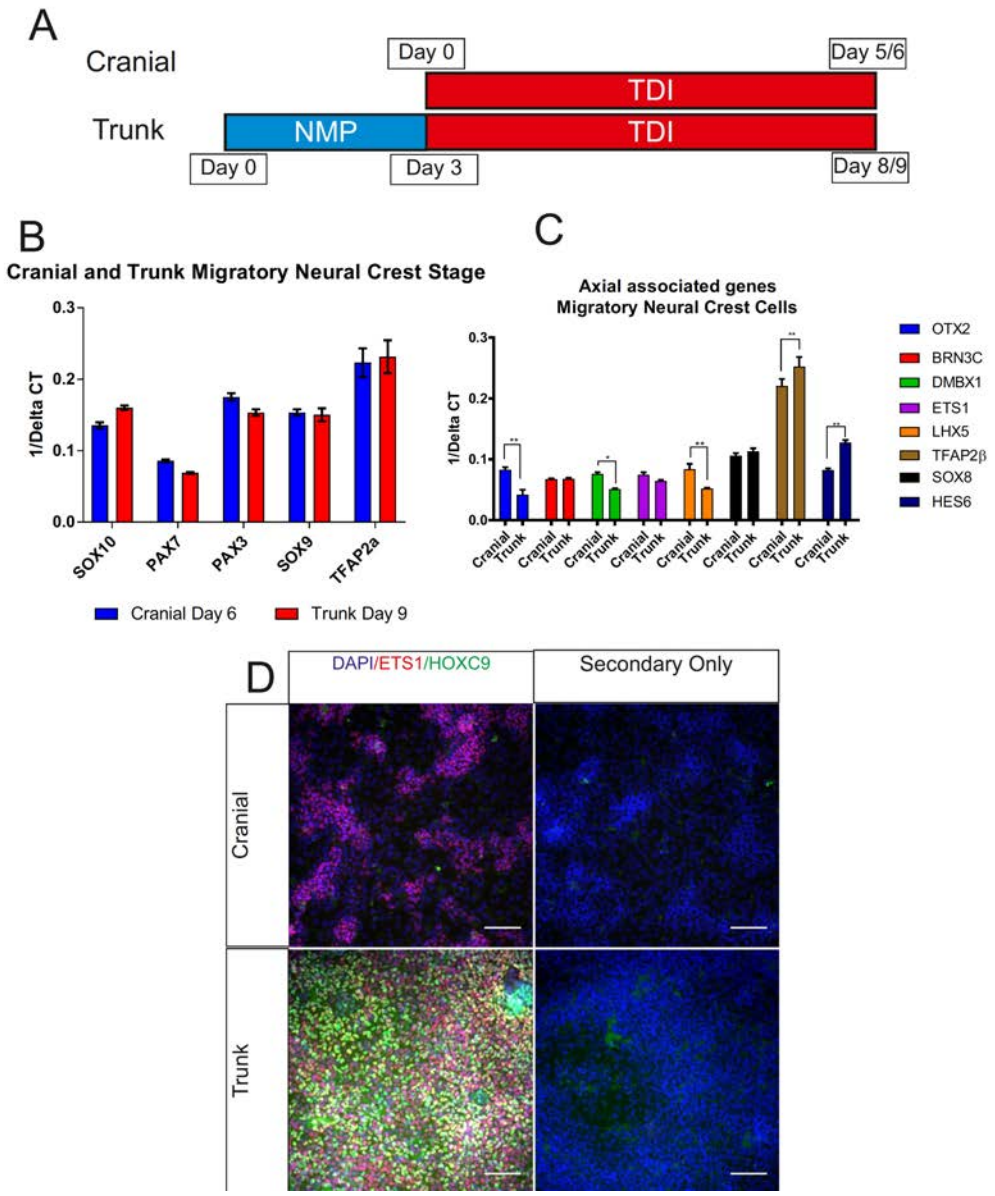

Figure 4.5 Comparison of gene expression between Cranial and Trunk Neural Crest cells. (A) Schematic showing protocols to derive cranial and trunk neural crest cells and time points. **(B)** qPCR plots showing expression of neural crest markers in both trunk and cranial neural crest cells **(C)** qPCR plots showing expression of cranial neural crest markers (Simoes Costa et al 2016), anterior neural plate specifier *OTX2* and trunk neural crest marker *HES6*. These genes similar expression in both cranial and trunk. Whilst *LHX5*, *DMBX1* and *OTX2* show higher expression in cranial, whilst *HES6* is higher in trunk neural crest. **(D)** Immunostaining to confirm the co-expression of ETS1 with HOXC9 in trunk neural crest cells, whilst cranial neural crest cells show ETS1 expression but not HOXC9 (N=2 Biological Repeats). *All qPCR graphs are Mean+SEM from 3 independent experiments, Student's T-Test *P<0.05, **P<0.01).*

4.3.5 Microarray analysis to find novel markers in cranial and trunk neural crest cells

We used whole genome microarray analysis determine if there were any markers that were differentially expressed in our model system **(Figure 4.6A/B)** We took RNA from cells in the cranial differentiation at day 3 and day 6 to correspond to neural plate border-like cells and neural crest cells respectively. In addition, we also assessed putative vagal neural crest cells after retinoic acid exposure **(as per Figure 3.2A)**. For trunk samples, we took RNA from NMPs and then day 6 and day 9 differentiated cells that correspond to putative trunk neural plate border cells and trunk migratory neural crest respectively **(Figure 4.3A/Figure 4.6A).**

Following microarray analysis, we utilised Principal Component Analysis to assess how the cells clustered based on the variance in the samples **(Figure 4.6C)**, principal component 1, that accounts for most the variance between the samples, seemed to split the cells based on their differentiation state, with hPSCs clustering at one side, migratory neural crest cells at the opposite side and progenitor time points between them. We see separation between the anterior and posterior samples with the initial separation appearing at cranial day 3 and NMP cultures and continuing through the subsequent differentiation samples. The retinoic acid treated neural crest clusters very closely with the cranial migratory neural crest indicating that these two samples are very similar in terms of their gene expression. This is consistent with the notion of these two neural crest populations differentiating through the same anterior precursor. Furthermore, we used venn diagrams to look at a whole population level the similarities and differences in gene expression between these samples **(Figure 4.6C).** We determined the genes that showed a two-fold change; $P<0.05$ between each terminal neural crest sample and hPSCs to generate all the genes that were upregulated in each neural crest sample. We have subsequently used these data to generate gene lists that are shared and separated between these samples and

assessing these lists for novel markers of cranial and trunk neural crest cells **(Figure 4.6C).**

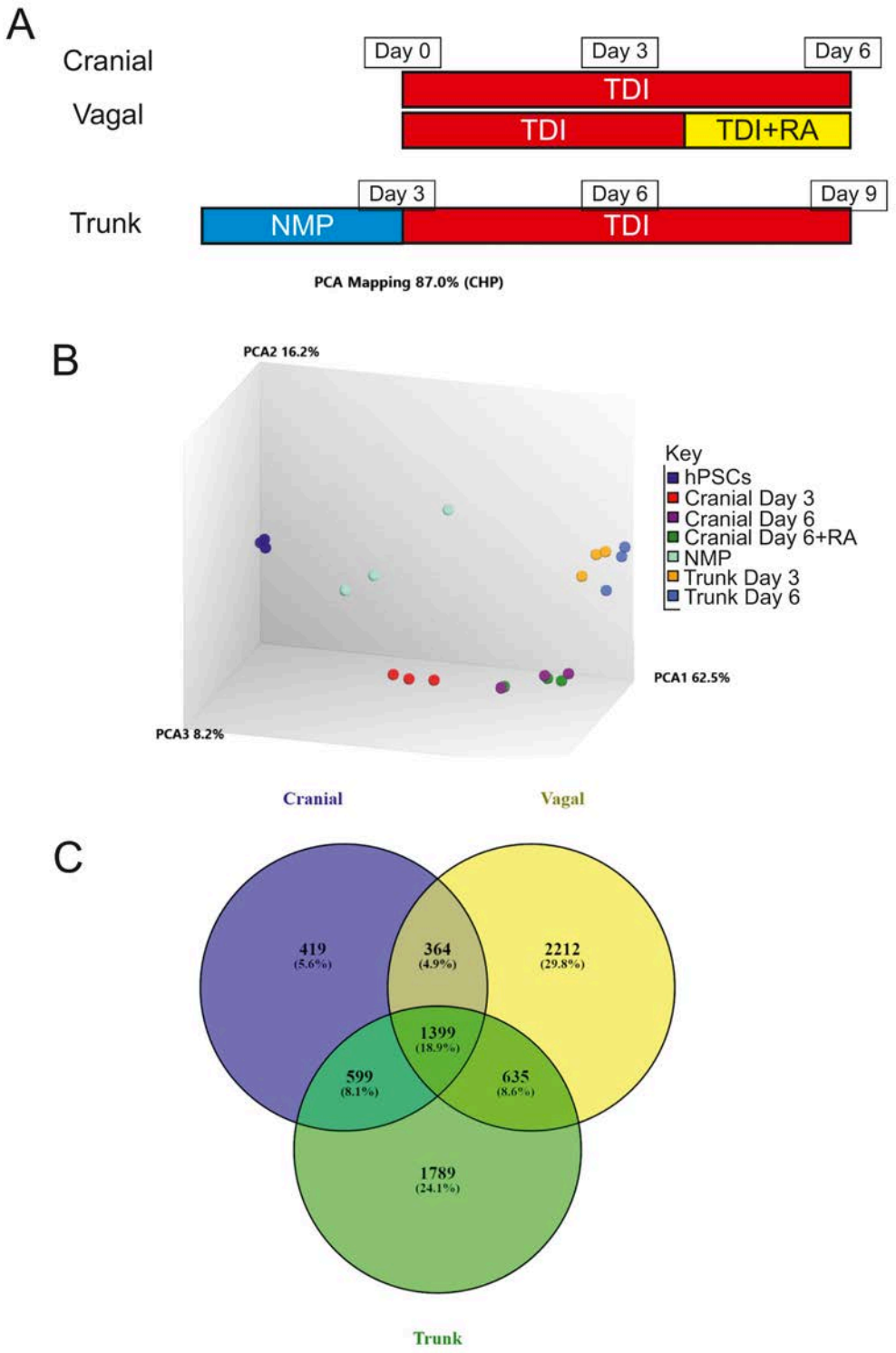

Figure 4.6 Microarray comparison of cranial, vagal and trunk neural crest cells. **(A)** Differentiation Schematic to show timepoints in cranial, vagal and trunk differentiations. **(B)** Code for microarray samples and PCA plot showing separation of trunk and cranial derived neural crest populations consistent with a different ontogeny of trunk neural crest. **(C)** Venn diagram showing shared and distinct gene expression in cranial (day 6), vagal (day 6) and trunk (day 9) migratory neural crest cell populations after normalisation to hPSCs.

4.3.6 Pairwise comparisons between trunk and cranial neural crest cells

To determine the key differences between similar stages of differentiation from hPSCs to cranial and trunk neural crest cells, we performed a pairwise comparison between cells from day 3 of the cranial protocol and day 6 of the trunk protocol. We filtered genes for 2-fold change and P<.05 **(Figure 4.7A)**. We found 1933 genes with 2-fold higher expression in cranial over trunk populations, and 2313 more highly expressed in the trunk cultures **(Figure 4.7B)**. In addition, in both cases, we see coding genes being differentially regulated between these two populations (16% found in the putative cranial genes and 8% in the trunk genes). When we looked at the top 20 differentially expressed genes in the cranial culture over trunk, we observed genes classically shown as anterior, such as *OTX2* which had over 1000-fold change between the samples **(Figure 4.7C)**. In addition, we also saw two genes proposed to mark cranial neural crest cells, *LHX5* and *DMBX1*, with greater expression in the cranial precursor population **(Figure 4.7C)**. Which indicates that the role of these genes being confined to an axial level may be conserved in our hPSC model of differentiation.

Signalling molecules show higher expression in cranial over trunk neural crest, for examples, *BMP2* and *DLK1* that are agonists of the BMP and *NOTCH* pathways respectively both show differential expression between cranial and trunk. The expression of *DLK1* in hPSC models of neural crest differentiation has also been seen in other work (Curchoe et al., 2010). The genes upregulated in trunk cultures shows enrichment of HOX genes, for example *HOXB9*, *HOXB3*, *HOXB4*, *HOXB7* and *HOXA* as well as the long non-coding RNA *HOXB*-AS3.

CDX2 is more highly expressed in trunk and not cranial neural crest to coincide with our qPCR data and to add to the list of genes that are associated with patterning to the list of differentially expressed genes. There are neural crest related genes also differentially expressed in these populations, with *PAX7* showing 74-fold higher expression in cranial, and *NR2F1* and *NR2F2* with 28 and 26-fold higher expression in trunk cultures respectively. Other genes upregulated in trunk cultures include *GFRA2* and *MOXD1* (involved in catecholamine

production) that are genes indicative of neural crest derivative differentiation. The expression of these genes coincides with the further progression of the trunk samples along the first component in the PCA analysis **(Figure 4.6C).**

We then used Gene ontology analysis (https://toppgene.cchmc.org/enrichment.jsp) to assess any link between the genes found differentially expressed in our microarray analysis with their molecular and biological functions. Molecular function analysis of the top 100 upregulated genes in trunk cultures **(Figure4.7D i)** showed that the molecular function was consistent with the top differentially expressed genes were coding. This can add clarity to Figure 4.7Bi where coding genes only accounted for 8% of the differentially expressed probes. In addition, we also see glial cell derived neurotropic receptor (GDNFr) activity showing greater prevalence in trunk cells. Consistent with the high expression of GFRA2 (a co-receptor for glial cell neurotrophic signalling). When we assessed the Gene Ontology terms with respect for biological process, that showed upregulation of genes in trunk cultures were involved with anterior posterior development, this is consistent with the presence of *HOX* genes showing differential regulation. are gene actively involved in patterning or in cellular compartmentalisation. In addition, to confirm the findings from our qPCR analysis **(Figure 4.5**), we also assessed the signal of known neural crest specifiers between the two samples, we saw similar signal level of many neural crest specifiers between the two samples

In addition, we also wanted to assess the expression differences in the anterior-posterior genes from (Simões-Costa and Bronner, 2016). We saw expression of many of these genes in both samples, including *ETS1* and *HES6* expression in both samples **(Figure 4.5C)**.

HOX gene expression between the two samples from our microarray samples were also consistent with previous immunostaining and qPCR analyses, where we see expression of HOX genes in the trunk samples across all clusters that correspond to a trunk identity. In addition, we also did not see induction of more

posterior genes consistent with tail bud identity (such as *HOXC13*), further consistent with the notion these are trunk-like neural crest cells and not tail bud.

Figure 4.7 Pairwise comparison of Cranial Day 3 and Trunk Day 6 cells.

A

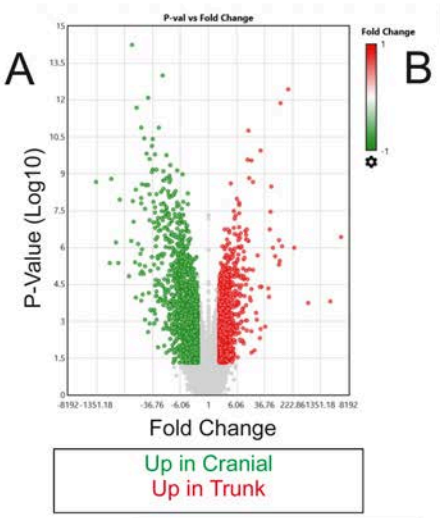

B

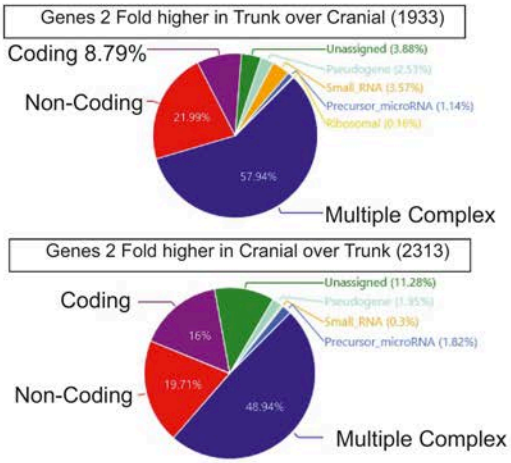

C

Top 20 genes upregulated in cranial over trunk

Gene Symbol	Fold Change	P-val
OTX2	1388.61	2.18E-09
JAKMIP2-AS1	583.22	4.29E-06
LMO1	508.17	1.63E-09
CLU	378.32	6.33E-07
LHX5	301.72	1.10E-08
BMP2	167.74	1.49E-05
DLK1	145.44	5.35E-07
CDH9	136.03	5.64E-15
PAX2	133.35	1.31E-08
LHX5-AS1	126.81	9.22E-08
VAT1L	108.89	0.0001
DMBX1	103.4	2.01E-12
ESRG	92.86	7.08E-07
PAMR1	82.16	4.84E-06
ANXA3	78.54	1.82E-06
CDH23	78.08	1.15E-05
LRRTM1	75.69	0.0001
VSNL1	75.48	1.64E-08
PAX7	74.67	1.34E-11
CAPN6	71.19	1.20E-06

Top 20 genes upregulated in trunk over cranial

Gene Symbol	Fold Change	P-val
HOXB9	5085.5	3.74E-07
HOXB-AS3	2494.12	0.0002
COL11A2	245.57	1.00E-06
HOXA2	164.29	3.72E-13
HOXB3	113.9	9.15E-07
HOXB4	113.9	9.15E-07
HOTAIRM1	103.6	1.35E-12
MOXD1	97.29	3.60E-06
HOXB7	94.86	5.15E-06
NPR3	94.69	5.13E-07
HHIP	73.65	2.22E-06
ADAM12	62.29	1.01E-06
ASXL3	57.82	3.39E-09
CDX2	48.23	0.0001
HOXA7	38.9	0.0017
GFRA2	29.71	4.05E-05
NR2F1	28.41	0.0022
MGLL	27.78	1.13E-10
HAGLR	27.26	0.005
NR2F2	26.88	4.08E-05

D

GO Terms in Genes upregulated in Trunk

	GO TERMS: Molecular Function	
	Name	pValue
1	sequence-specific DNA binding	6.02E-13
2	transcription factor activity, sequence-specific DNA binding	5.82E-10
3	nucleic acid binding transcription factor activity	5.82E-10
4	glial cell-derived neurotrophic factor receptor activity	6.73E-05
5	transcription regulatory region DNA binding	2.12E-04
	GO TERMS: Biological Process	
	Name	**pValue**
1	regionalization	1.34E-24
2	anterior/posterior pattern specification	2.29E-24
3	pattern specification process	9.64E-24
4	skeletal system development	1.09E-21
5	embryonic skeletal system development	3.30E-21

(Continued on next page)

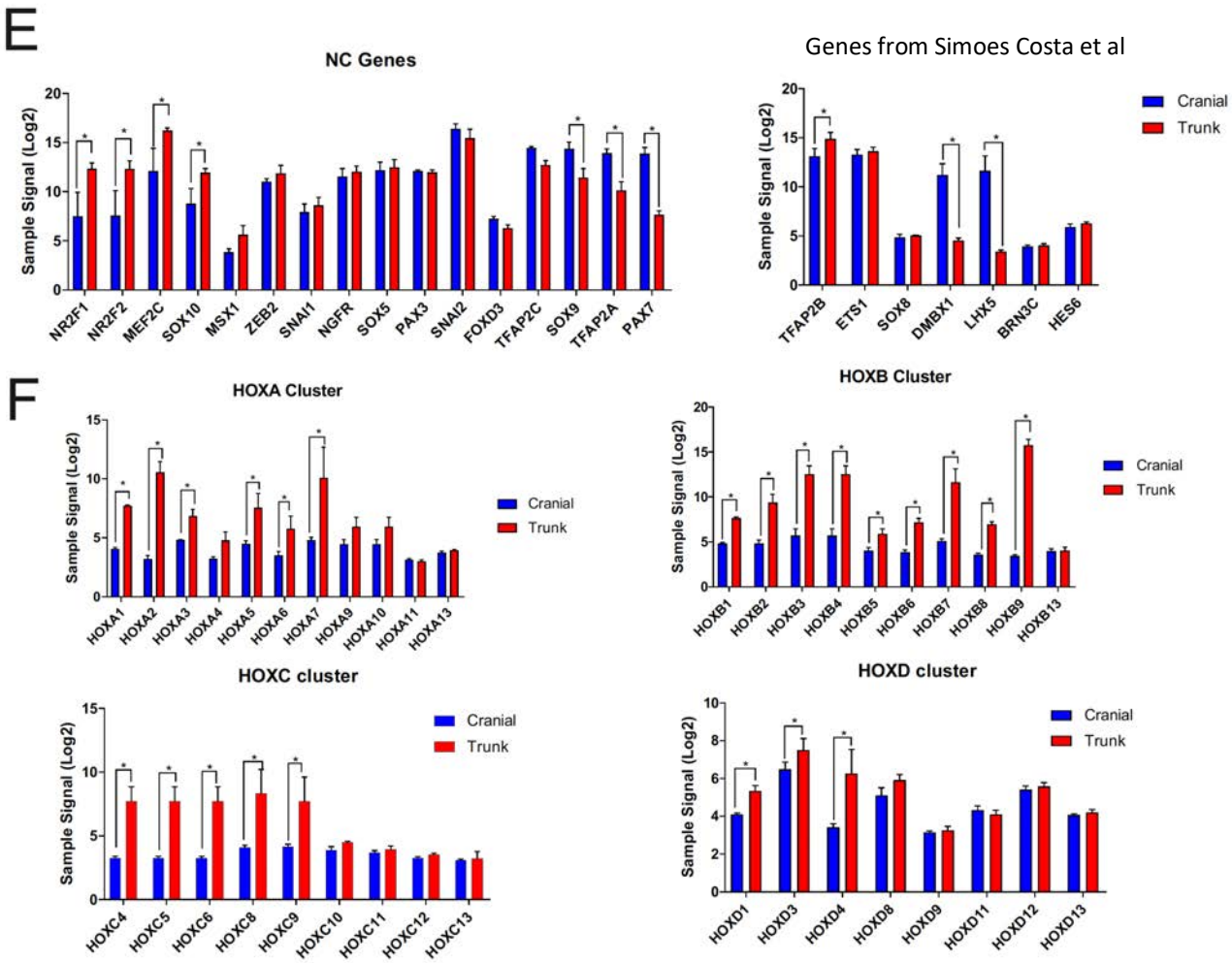

Figure 4.7 Pairwise comparison of Cranial Day 3 and Trunk Day 6 cells. (A) Volcano plot showing genes two fold upregulated and P<0.05 in cranial cultures (Green) and trunk (Red). (B) Pie chart showing the gene description of the differentially regulated genes. (Ci) Top 20 genes expressed in cranial cultures over trunk (ii) and trunk cultures over cranial. (D) GO terms of molecular function of Top 100 differentially expressed genes in trunk encompassing molecular function (I) consistent with transcription factor binding and (ii) biological function consistent with genes associated with anterior posterior development. (E) Comparison of neural crest related transcripts including the genes from Simoes Costa et al 2017 (NC AP genes) shows similar expression in most genes cranial (blue bars) neural crest cultures trunk (red). (F) Comparison of the HOX gene expression in both cultures shows robust induction of HOX genes in the trunk neural crest. (Bars are Mean+SD of 3 independent experiments- Student's T-Test (*P<0.01).

Figure 4.8 Pairwise comparison of Cranial Day 6 and Trunk Day 9 cells.

A

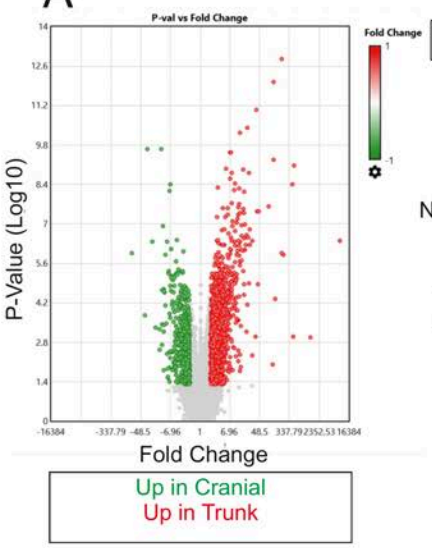

B

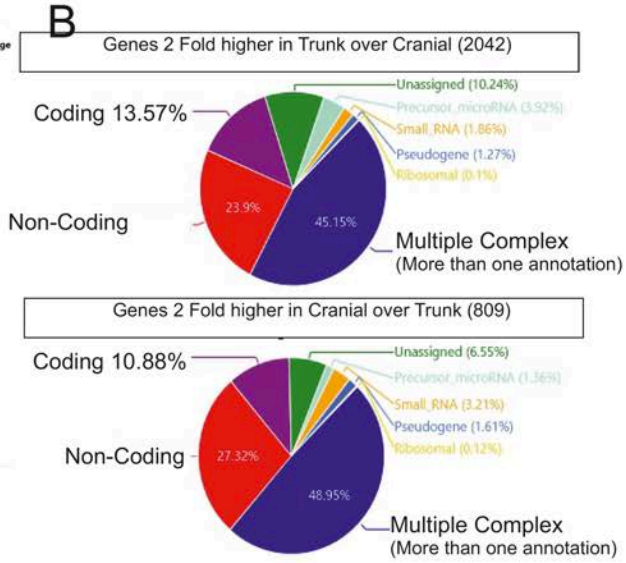

C

Top 20 genes upregulated in cranial over trunk

Gene Symbol	Fold Change	P-val
OTX2	88.45	1.07E-06
SPRY4	36.29	2.00E-04
ZFP42	32.02	2.22E-10
CYP2S1	22.76	4.27E-07
DMKN	18.27	5.00E-04
CLU	14.1	5.00E-04
TGFBI	13.81	2.90E-03
FGD5	12.5	2.23E-10
IER3	12.07	4.00E-04
ETV5	11.81	0.002
SMAGP	11.7	2.26E-05
TUNAR	11.45	1.16E-07
ESRP1	11.02	4.00E-04
PROCR	10.83	2.47E-05
BST2	10.71	0.0007
SEL1L3	10.61	2.13E-05
JAKMIP2-AS1	10.58	1.53E-02
ADAMTS19	10.48	2.77E-05
PRKCB	9.75	8.01E-05
ADAMTS4	9.64	1.25E-06

Top 20 genes upregulated in trunk over cranial

Gene Symbol	Fold Change	P-val
HOXB9	9293.97	3.98E-07
HOXB-AS3	1334.18	0.0011
MOXD1	448.95	8.46E-10
HOXB3	233.05	1.26E-06
HOXB4	233.05	1.26E-06
HOXB7	207.64	1.08E-06
HOXA2	204.16	1.33E-13
HOTAIRM1	119.7	8.88E-13
NEUROG1	119.05	5.13E-10
HOXC8	113.89	9.80E-03
TSHZ2	85.32	2.34E-08
HOXB2	44.84	3.64E-08
SUSD2	43.6	1.34E-05
DCT	40.88	3.63E-08
MGLL	39.19	8.68E-12
HOXA7	37.35	0.001
CDX2	29.85	4.60E-03
RNASE1	29.26	3.89E-07
ASXL3	25.69	1.53E-07
CDH19	25.6	5.52E-07

D

GO Terms in Genes upregulated in Trunk

	Upregulated Trunk Genes: GO Terms Molecular Function	
	Name	pValue
1	sequence-specific DNA binding	4.86E-11
2	transcription factor activity, sequence-specific DNA binding	1.75E-10
3	nucleic acid binding transcription factor activity	1.75E-10
4	HMG box domain binding	1.85E-04
5	transcriptional activator activity, RNA polymerase II transcription regulatory region sequence-specific binding	3.55E-04

	Upregulated Trunk Genes: GO Terms Biological Process	
	Name	pValue
1	anterior/posterior pattern specification	7.09E-26
2	regionalization	1.34E-24
3	embryonic skeletal system development	1.85E-24
4	skeletal system development	3.77E-24
5	pattern specification process	2.92E-21

(Caption on next page)

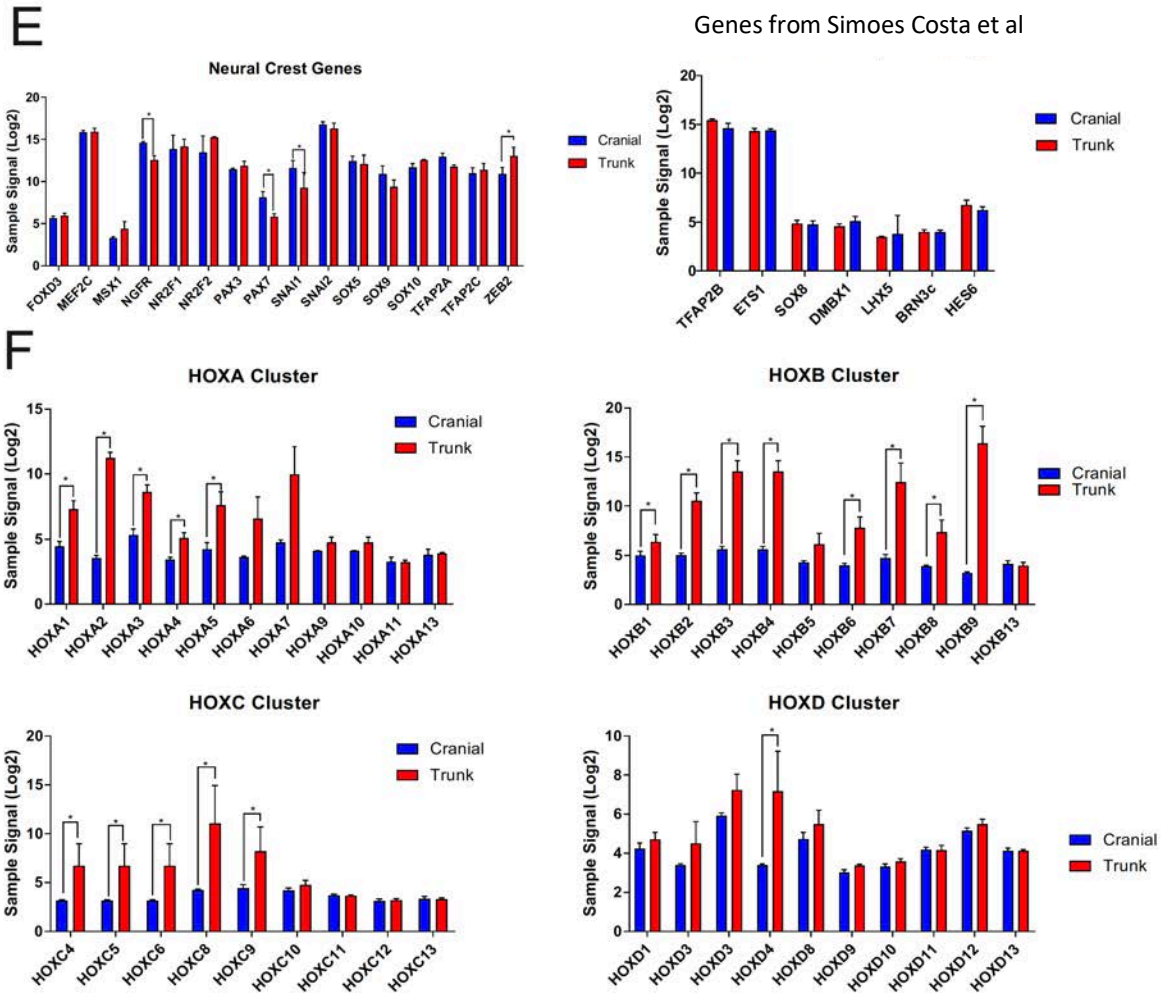

Figure 4.8 Pairwise comparison of Cranial Day 6 and Trunk Day 9 cells. (A) Volcano plot showing genes two-fold upregulated and P<0.05 in cranial cultures (Green) and trunk (Red). **(B)** Pie chart showing the gene description of the differentially regulated genes. **(Ci)** Top 20 genes expressed in cranial cultures over trunk **(ii)** and trunk cultures over cranial. **(D)** GO terms of molecular function of Top 100 differentially expressed genes in trunk encompassing molecular function **(I)** consistent with transcription factor binding and biological function **(ii)** consistent with genes associated with anterior posterior development. **(E)** Comparison of neural crest related transcripts shows similar expression in most genes consistent with neural crest identity and neural crest AP genes identitifed in Simoes-Costa et al 2016. Like Figure 4.7, *OTX2* is shows greater expression in cranial over trunk and CDX2 along with truncal *HOX* genes are expressed more in trunk cultures. **(F)** Comparison of the *HOX* gene expression in both cultures shows robust induction of *HOX* genes consistent with trunk identity in the trunk neural crest. We also note that tail bud HOX genes are not induced in trunk neural crest cultures (Bars are Mean+SD of 3 independent experiments- Student's T-Test (*P<0.01).

We also performed a pairwise comparison between the time-points consistent with migratory neural crest, (Cranial day six and trunk day nine). We used a volcano plot and assessed all genes that showed 2-fold change in gene expression and P<0.05 **(Figure 4.8A)**. We saw 809 genes upregulated in cranial cultures after 6 days of differentiation over trunk neural crest cells, whilst we did see 2042 genes upregulated in trunk over cranial cultures. Of the 800 genes significantly higher in cranial neural crest, 10% of these were coding genes, whilst 13.5% of the 2042 genes in 2 fold higher in trunk neural crest were coding **(Figure 4.8B)**. Furthermore, when we collate the top 20 differentially expressed genes in cranial **(Figure 4.6C i)** and trunk **(Figure 4.6C ii)**, we see a similar pattern as was seen in the day 3 cranial and day 6 trunk differentiated samples. *OTX2* shows 88-fold difference in expression between cranial and trunk, which is the same as was seen for the previous sample.

In addition, we have seen an upregulation of one of the RA oxidation genes, CYP2S1 consistent with their expression at the very anterior and posterior of the embryo to create an RA sink. In the trunk sample, we see expression of HOX and caudal related genes (*HOXB9*, *HOXB3*, *HOXB4 HOXB7 HOXA2 HOXC8, HOXB2* and *CDX2*), which is consistent with the pairwise comparison of the preceding samples. In addition, we also see expression of genes consistent with neural crest derivative differentiation, again seeing *MOXD1*, *NEUROG1* showing higher expression as well as DCT (which is expressed in melanoblasts).

Furthermore, when we assessed Gene Ontology of the 100 genes showing higher expression in trunk samples over cranial, we saw the molecular function consistent with transcription factor binding indicative that coding genes were a key feature to the differences between these samples. Furthermore, the biological process showed genes associated with anterior posterior identity, which is consistent with analysis of the previous time point and induction of patterning genes with trunk neural crest **(Figure 4.8D)**.

Genes consistent with neural crest differentiation are conserved across the anterior posterior axis. We saw statistically significant difference in expression of

PAX7 between cranial and trunk samples again, which is consistent with our previous time point **(Figure 4.7E)**, but we see similar expression of almost all other neural crest related transcripts between the two samples. Furthermore, analysis of the four HOX clusters again shows the expression of HOX genes consistent with trunk identity in the NMP derived neural crest, with absence of tailbud associated HOX genes **(Figure 4.8F).**

4.3.7 Optimising Trunk neural crest differentiation into putative sympathoadrenal precursors

Trunk identity has been shown to influence sympathoadrenal identity *in vivo* (Huber et al., 2012) and we wanted to assess differentiation of sympathoadrenal precursors from trunk neural crest cells *in vitro*. A recent report shown that BMP and SHH signalling in a neural crest differentiation model is able to induce putative sympathoadrenal precursors that express the key specifier PHOX2B (Oh et al., 2016). We used the same PHOX2B:GFP reporter line and optimised conditions from this protocol to match our protocol to generate trunk neural crest cells. We replated trunk neural crest cells into one of three conditions: BMP4 alone, BMP4+recombinant SHH or BMP4+recomibinant SHH+ Purmorphamine and assess PHOX2B:GFP after 4 days of exposure.

In the BMP4 alone conditions, we did not see any GFP induction after one day in these conditions but saw 2% of cells expressing GFP after 2 days. This level did not increase over the time course and through all repeats, we saw similar low levels of GFP induction. When we added recombinant SHH to this, we saw a similar trend, whereby only after 2 days in culture did we see PHOX2B:GFP induction at a low level, but this did not show much of an increase over the subsequent days in culture. The addition of Purmorphamine, a SMOOTHEND agonist, was shown by Oh et al to be the key addition to the differentiation cocktail. We tested this and saw a similar induction of GFP over 2 days, but on the third day, we saw an increase to 9% GFP+ cells. This higher level of GFP was also

seen at day 4 of the differentiation and indicated that the addition of Purmorphamine was a key ingredient to the media.

We quantified the amount of GFP positive cells after 4 days in all conditions and found that the average yield was highest in the conditions containing Purmorphamine. Furthermore, our mean yield from our differentiation is like the yield shown by Oh et al, who report a representative FACs plot with 4% GFP positive cells in their conditions (Oh et al., 2016). It must also be noted that the large standard deviation in these differentiations reflects the changes we have seen throughout this protocol. We have also seen up to 60% GFP cells after 4 days of differentiation (data not shown), but the source of this variability has not yet been identified.

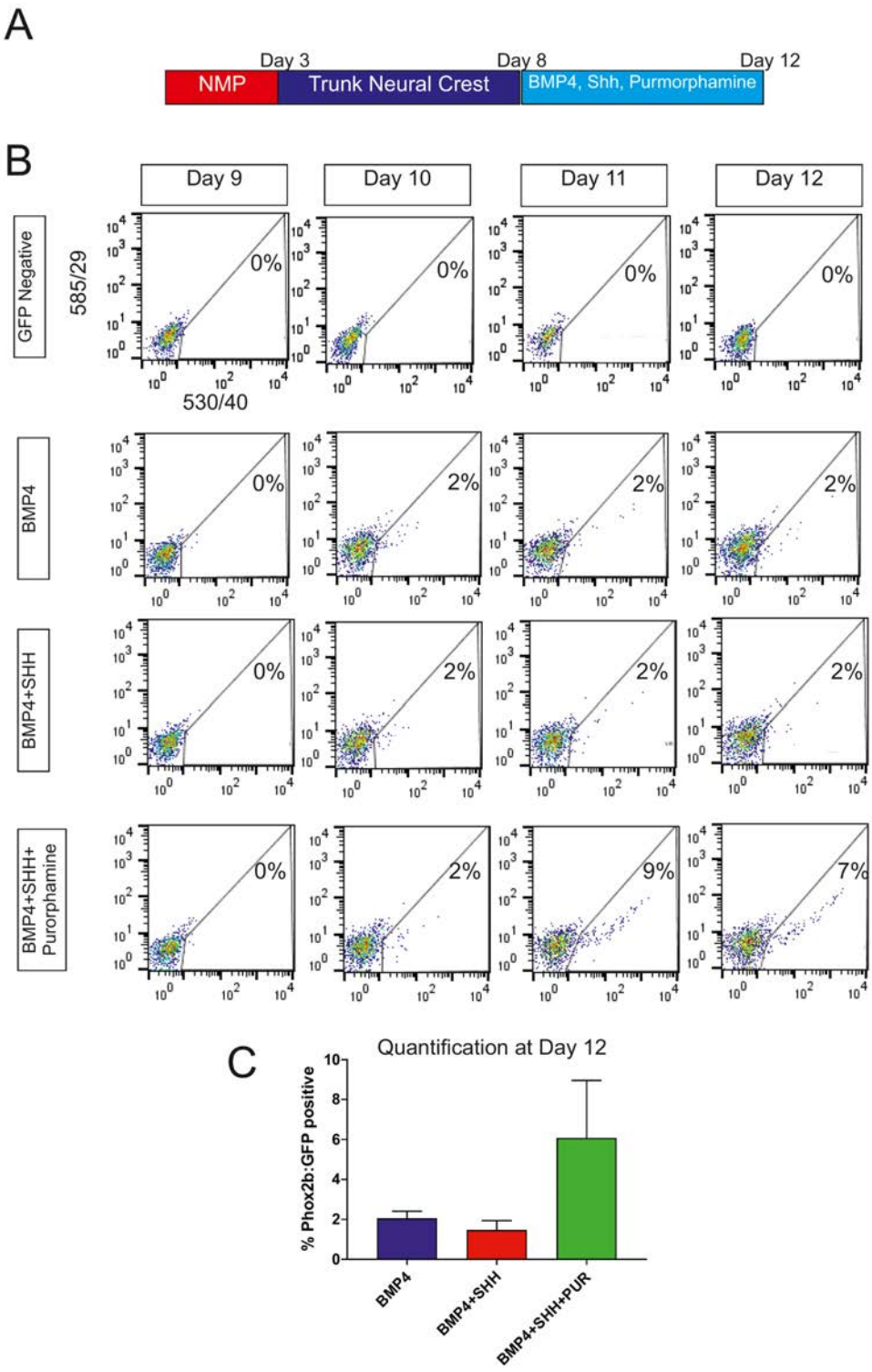

Figure 4.9 Preliminary identification of conditions to specify sympathoadrenal precursors (SAPs) from trunk neural crest. (A) Schematic of differentiation from Trunk Neural Crest cells to sympathoadrenal lineage and timings of analysis. **(B)** Representative FACs plots comparing induction of PHOX2b:GFP in different conditions. In all conditions, GFP expression is induced over 4 days of exposure to growth factors. Both BMP4 and BMP4+SHH conditions show the lowest induction, whilst addition of the small molecule agonist Purmorphamine induces highest levels of Phox2b induction. Quantification of GFP positive cells by Flow cytometry analysis derived from these conditions after 4 days of exposure are quanitified in (**C)** (N=2-4 biological repeats) (Data Not statistically significant, One-Way ANOVA (Turkey multiple comparison)).

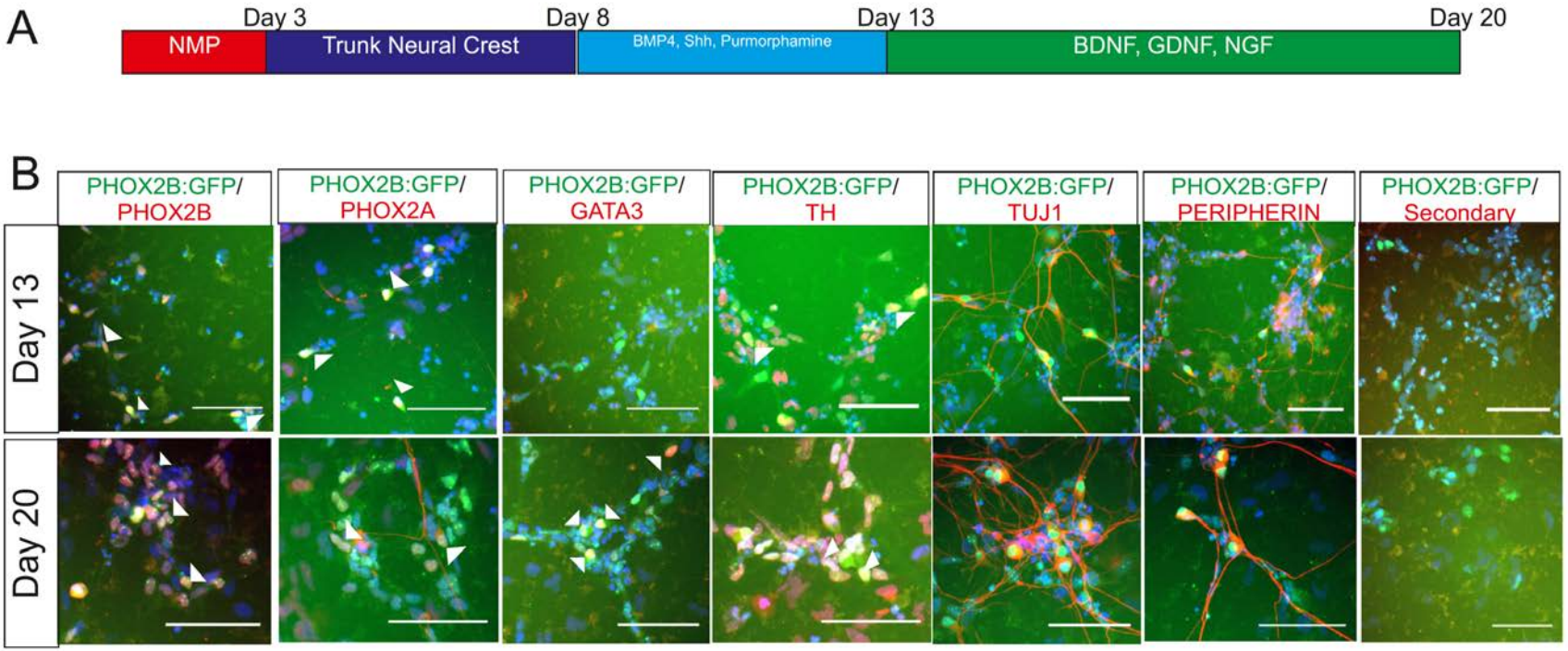

Figure 4.10 PHOX2B::GFP co-expresses with sympathetic neural differentiation genes. (A) Schematic of differentiation, with day 13 cells having been exposed to BMP, SHH and Purmorphamine followed by culturing in neurotrophin media. **(B)** Images showing co-expression of GFP (endogenous GFP- which appears in punctate fashion as shown in Oh et al 2016) with other sympathoadrenal markers (including PHOX2b for reporter fidelity), PHOX2a. Markers for further differentiated sympathetic neuronal subtypes (TH and GATA3) are only found after 7 days additional exposure to neurotrophins in the case of GATA3, whilst TH shows low expression after exposure to BMP, SHH and PUR that increases with subsequent neurotrophin (BDNF, GDNF, NGF) exposure.

We wanted to assess if the cells from the BMP4, SHH and Purmorphamine conditions expressed markers consistent with sympathoadrenal precursors. We used immunostaining for sympathoadrenal precursor markers (PHOX2B, PHOX2A), sympathetic neurons (TH, GATA3) and peripheral neurons (TUJ1, PERIPHERIN). We fixed cells at two time points at day 13 (Figure 4.10A) which corresponds to 8 days of trunk neural crest differentiation and 5 days BMP4, SHH, Purmorphamine exposure) and day 20 (Further week of exposure to BDNF, GDNF, and NGF). We performed immunostaining for PHOX2B using a monoclonal antibody against PHOX2B to assess reporter fidelity **(Figure 4.10B white arrowheads).** We then tested for other sympathoadrenal markers co-expressed with PHOX2B:GFP.

Preliminary analysis at day 13, in addition to PHOX2B expression, PHOX2a was expressed in GFP positive cells as well as TH, TUJ1 and PERIPHERIN. There was no expression of GATA3 (a marker of mature sympathetic neurons). These data are consistent with cells from being exposed to these signalling molecules are putative sympathetic neuronal precursors and indicate that these cells are forming the cell type of interest.

We also wanted to test if putative sympathoadrenal precursors would further induce genes consistent with downstream sympathetic neural differentiation. We exposed BMP, SHH and Purmorphamine specified cells to neurotrophins and performed immunostaining for the same panel of markers as above. GFP and PHOX2B monoclonal antibody both were co-expressed as well as PHOX2A, TH, TUJ1, PERIPHERIN matching observation of day 13. GATA3 was induced following more neuronal differentiation and is indicative of catacholeminergic neural subtypes that are found in the sympathetic nervous system.

4.4 Discussion

5.4.1 Neuromesodermal progenitors (NMPs) and the formation of the trunk

We have presented data initially to replicate the ability to differentiate hPSCS into NMPs. Exposure of hPSCs to high levels of CHIR99021 and FGF2 give rise to cells co-expressing BRACHYURY/SOX2/HOXC9 after 3 days' differentiation **(Figure 4.1B)**. Our data vary from the protocols shown whereby we have used 4µM CHIR99021 which is higher than the conditions used in previous protocols (Gouti et al., 2014; Lippmann et al., 2015). We have found that higher CHIR99021 in our differentiation gave rise to greater expression of BRACHYURY and SOX2 by immunofluorescence (data not shown). This facet may be due to the difference in cell lines used between this study and the published protocols. RNA-sequencing data from our lab comparing two human embryonic stem cell lines showed that one line had expression of early mesendoderm genes whilst still in an undifferentiated state and has also been demonstrated in a study comparing iPSC lines (Kilpinen et al., 2017). This may result in these cells being able to differentiate into mesodermal cell types more readily than other lines for example. The presence of SOX2 in undifferentiated cells and within the pluripotency network is well established and BRACHYURY can be seen in cultures of undifferentiated embryonal carcinoma cells (Gokhale, Giesberts and Andrews, 2000). Furthermore, our lab also seen expression of the primitive streak markers MIXL1 and BRACHYURY in undifferentiated cells *in vitro*. Overall, these data indicate that the presence of BRACHYURY and SOX2 alone cannot confirm the formation of NMPs *in vitro.* Thus, it may be the more conclusive to use expression BRACHYURY and SOX2 with HOXC9 to confirm their axial identity and give greater weight to the presence of the differentiated cell type. In addition, a good strategy to enable purification of NMPs and assess the signals in differentiation would be to perform mRNA-sequencing and assess the expression of known surface molecules in differentiation and to use these as a marker to separate cells by flow cytometry. In some cases, negative selection of hPSCs, by purifying SSEA3-

negative (SSEA3 being the most sensitive antigen on hPSCS (Draper, Pigott, Thomson and Andrews, 2002)) may be used to remove undifferentiated cells, but we have observed SSEA3 immunoreactivity in day 3 differentiated NMP cultures (data not shown).

There is a retention of genes that are associated in pluripotency throughout axial elongation. OCT4 has been shown to be a crucial determinant in trunk length (Aires et al., 2016) and so in this sense, using it strictly as a marker of undifferentiated cell is not accurate and conclusions as to its function is context dependent. Thus, this leaves NANOG expression as one of the last remaining current opportunities to discriminate between differentiated NMPs and undifferentiated cells, but without a cell line containing a fluorescent reporter, immunostaining would have to be performed as an indicator of NMP differentiation. Overall, whilst this is an issue that may surround future work, we have demonstrated the expression of other markers of NMP identity, such as *WNT3a*, *CDX2*, *FGF8* and *NKX1*-2 **(Figure 4.1C)** consistent with the culture on a whole being consistent with an NMP identity being further evidence that we have generated cultures consistent with NMP identity.

4.4.2 Early Neural Crest specifiers are expressed in NMPs

It is currently thought that both BRACHYURY and SOX2 function both in the self-renewal of NMPs, but they can also interact with other in further differentiation to either mesodermal or neural fate *in vitro* (Tsakiridis and Wilson, 2015; Koch et al., 2017). Our finding of the dorsal neural tube/neural crest markers SLUG, SOX9 and PAX3 **(Figure 4.2B)** co-expressed with BRACHYURY may indicate the early potency to form neural crest cells *in vitro*. This is like the recent finding in the developing ectoderm, whereby early ectoderm cells in the chick can co-express Sox2, Pax7 and Six1 consistent with neural, neural crest and placodal fates. It was subsequently proposed that these cells make their fate decisions by reaching a threshold of expression of one specifier leading to repression of alternate fates (Roellig et al., 2017).

Thus, the time and mechanism by which NMPs are committed to a downstream fate is yet to be fully elucidated and is currently only descriptive. The expression of PAX3, SLUG and SOX9 may be indicative of neural crest competence, but these genes are involved in the development of mesodermal cell types including NMP derived somites (Betters et al., 2010a). To confirm NMP identity, that are not yet committed or differentiated, in *PAX3/T* co-expressing cells, determining expression of downstream differentiation genes such as MESOGENIN and TBX6 with PAX3 would be consistent with mesodermal differentiation. PAX3, T and *SOX2* co-expression on the other hand would be consistent with NMP identity. Functional assays, such as serial grafting, or clonogenic assays demonstrating single NMPs forming colonies composed of many derivatives would confirm these cells as self-renewing stem cells and not committed.

Our lab has performed single cell RNA-sequencing data on day three differentiated NMPs that show cells with *PAX3* expression without *MESOGENIN* or *TBX6,* that are consistent with mesoderm fate. This is consistent with some cells exhibiting the early differentiation into dorsal neural tube like cells. These findings give rise to the complexity within NMPs in governing how these cells self-renew to allow for axial elongation or differentiate to form the derivatives along the formation of the trunk. To further elucidate the heterogeneity within NMPs, single cell transcriptomics would allow for the further sub division subsets within these cells. In addition, single cell clonogenic assays *in vitro* and grafting into the chicken embryo would allow us to determine the fate of these cells.

4.4.3 SOX10 HOXC9 co-expressing cells show consistencies with neural crest identity

Plating hPSC derived NMPs into conditions that can specify neural crest cells from hPSCs also shows the ability of putative NMPs to be further specified into neural crest cells. These data are indicative of the novel ontogeny of trunk neural crest cells from NMPs. Our data is also consistent with data indicating that two distinct mechanisms derive the anterior and posterior neural axes (Kondoh, Takada and

Takemoto, 2016) rather than the transformation hypothesis that governs retinoic acid mediated patterning (Durston et al., 1989).

In addition, these data indicate that the GRN governing the formation of trunk neural crest cells may involve similar signals (such as WNT and intermediate BMP signalling), but has a different input of genes at the beginning. Assessing functional roles of NMP markers, such as SOX2 and CDX2 during neural crest formation by initial knockout experiments would assess how early trunk and cranial neural crest cells segregate in GRN. This raises the hypothesis that different inputs to these regulatory units are crucial for specifying identity. *Cdx2* is a key patterning gene that has been implicated as to the driver of WNT and FGF mediated HOX gene expression in the trunk by removal of inhibitory histone mark from HOX clusters to allow transcription (Mazzoni et al., 2013).

A *Cdx2* and *Sox2* binding site has been identified in the *Pax3* (Sanchez-Ferras, Bernas, Laberge-Perrault and Pilon, 2014) and is a putative link between the NMP state and neural crest induction. Thus, the conserved neural crest genes such as *SOX10*, *PAX7* and *FOXD3* **(Figure 4.3B)**, may also have undescribed regulatory units that are regulated by genes present in NMPs. ChIP-sequencing to determine binding sites for CDX2, SOX2, BRACHYURY in NMPs and early stages of neural, mesodermal and neural crest differentiation would allow for a comprehensive overview of how these genes influence downstream differentiation *in vitro*. There is already evidence for different axial specific enhancers for genes in the chicken such as *Sox2* (Uchikawa et al., 2003), *Foxd3* (Simões-Costa et al., 2012) and *Sox10* (Betancur, Bronner-Fraser and Sauka-Spengler, 2010). Identifying specific inputs to these enhancers would be a good starting point for any insight into epigenetic regulation of trunk neural crest differentiation.

Marker expression analysis of putative trunk neural crest cells reveals that there is not full overlap SOX10 and HOXC9 expression **(Figure 4.3C)**. This may result from several reasons. First, as discussed early, we do not have ways of purifying NMPs at an early stage, and thus in the trunk differentiation protocol, we may have contaminating cranial neural crest cells that account for the SOX10+ HOXC9-

cells. Only by means of purifying NMP cultures can we fully test this hypothesis. There may be a temporal aspect to HOXC9 expression throughout neural crest differentiation. Live cell imaging with a transgenic reporter of GFP for HOXC9 would allow for tracking of cells by live cell imaging. In addition, it would also allow for purification of *HOXC9* positive cells and comparison of *HOXC9* positive and negative cells. It may also be possible that HOXC9 is turned off at some point of neural crest differentiation, dynamic HOX gene expression has been well characterised in many cell types. Live cell imaging of a HOXC9 transgenic reporter cell line would allow us to determine what time point HOXC9 stopped expression and to correlate this to time during differentiation.

Single cell transcriptomics on these cells and comparison of the markers expressed in SOX10+/HOXC9- cells compared to SOX10+/HOXC9+ cells may show us the gene expression differences with regards to developmental time or potentially with subsequent fate where HOXB8 has been implicated in noradrenergic neuronal development (Huber et al., 2012). Performing clonogenic assays on HOXC9+ and HOXC9- cells and assessing the rate at which they may form different cell types show how the HOX genes influence subsequent fate. Moreover, this may also indicate heterogeneity within the trunk neural crest cluster. Retinoic acid mediated patterning can induce cells down to the anterior spinal cord, whilst WNT/FGF patterning can pattern the entirety of the spinal cord below the cervical spinal cord. We may have neural crest cells in the trunk of the embryo, but that are more anterior than the *HOXC9* expression domain.

We have demonstrated marker expression that is consistent with neural crest fate, to make more conclusions as to the identity of these cells, functional analysis is required. Neural crest cells show two functions in further differentiation and migration. Further differentiation is once facet that offers the ability to assess some of the long-lasting questions in neural crest biology. In putative cranial neural crest cells, we have demonstrated the ability of these cells to form both neural and non-neural cell types *in vitro* which gives further evidence to neural crest identity. In addition, from this, we can now attempt to compare the perspective fate and prospective potency of these cells *in* vitro. In particular,

assessing the ability of putative *in vitro* trunk neural crest cells to form ectomesenchyme to test the hypothesis proposed that cells posterior to somite 5 do not form ectomesenchyme (Le Lièvre and Le Douarin, 1975). Although this experiment is important, our current method demonstrating the formation ectomesenchyme may not be fully reflective of the cells found *in vivo* nor may it be a good test of cell potency.

Marker expression is not sufficient to determine these cells as true trunk neural crest cells. First, we need to test the function of these neural crest cells, particularly with differentiation into derivatives. For cranial neural crest cells, we demonstrated formation of peripheral neurons as well as bone and cartilage reflecting *in vivo* differentiation. We need to determine whether trunk neural crest cells can form the correct derivatives, particularly peripheral neurons.

We can now also assess the prospective potency and fate of hPSC derived cranial and trunk neural crest cells *in vitro*. In particular, trunk neural crest cells cannot form ectomesenchyme when transplanted into the head *in vivo* (Le Lièvre and Le Douarin, 1975). In contrast, trunk neural crest cells have been demonstrated to contribute to mesenchymal cell types *in vivo* in the mouse such as in the mesenchymal cells the bone marrow (Isern et al., 2014). Both cranial and trunk neural crest cells may form non-neural derivatives, but they form diverse non-neural derivatives. For example, trunk neural crest cells to form craniofacial mesenchyme has always been the assay that has been used, and may be looking at a different differentiation of mesenchyme.

To test the prospective fate and potency of neural crest cells *in vitro,* clonogenic assays performed on different axial levels of neural crest cells. We can then determine whether trunk and cranial neural crest form neural or non-neural derivatives at different rates and may indicate the potency of trunk neural crest to form non-neural derivatives. This has been demonstrated in chicken trunk neural crest cells *in vitro* where they formed myofibroblasts in clonogenic assays (Trentin, Glavieux-Pardanaud, Le Douarin and Dupin, 2004). In addition, grafting of hPSC derived neural crest cells with putative cranial and trunk identity into

different regions of the chicken neural tube and assessing how they migrate and behave would allow us to understand how they react within different niches. Grafting experiments would allow for the effect of the niche on cell types to be controlled and test the hypothesis of whether any differences in the cranial and trunk GRN may alter cell fate by changing how cells respond to the niche.

In addition, the function of neural crest differs along the anterior posterior axis, trunk neural crest cells show a different migratory pattern to cranial neural crest cells. Cranial neural crest cells have been shown to migrate as a collective (McLennan et al., 2015a), but trunk neural crest cells migrate in a chain like formation (Richardson et al., 2016). In cranial neural crest migratory leader cells with higher levels of *TFAP2*α and *HAND2* (McLennan et al., 2015a) and no mixing, whilst in the zebrafish showed mixing was present between the leader and trailer cells in the cranial neural crest that was not found in the trunk (Richardson et al., 2016). Cranial and trunk neural crest cells exhibit drastic differences in their migratory behaviour and a key characterisation of putative *in vitro* derived neural crest cells would be to perform migratory assays and assess the speed and pattern of migration. By performing migration experiments *in vitro*, we can subsequently determine if the difference in migratory characteristics may be due to environment or a cell-autonomous effect. In addition to this, it has been demonstrated that neural crest cells show differences in responsiveness to chemokines to prevent unwanted mixing of populations *in vivo* (Zuhdi et al., 2014). Determining signals that cranial and trunk neural crest cells respond to may provide insight as to why neural crest cells exhibit different behaviours and can be further used to assess how this may alter cell fate.

4.4.4 Assessing gene expression differences between putative hPSC derived cranial and trunk neural crest cells

We have demonstrated the shared gene expression of a core neural crest gene regulatory network including genes such as *PAX3*, *FOXD3*, *PAX7*, *SOX9* and *SOX10*

(Figure 4.3B), but we wanted to determine what other genes may be expressed in a spatial pattern in the neural crest. Recent work from the chicken embryo comparing RNA-seq profiles from cranial and trunk neural crest cells has demonstrated gene expression differences between these two populations (Simões-Costa and Bronner, 2016). In assessing gene expression differences between putative cranial and trunk neural crest cells *in vitro, BRN3C, TFAP2β, SOX8, LHX5, DMBX1* and *ETS1* outlined from this study were good candidates to first screen for differences between our *in vitro* model and *in vivo* neural crest cells. We did not see differential expression with regards to presence or absence in all the genes tested here, only *DMBX1*, *LHX5* and *HES6* showed differential expression between the two populations **(Figure 4.5)**. ETS1 co-expression with HOXC9 in NMP derived neural crest cells, does not reflect what is seen in the chick embryo by in situ hybridisation (Barembaum and Bronner, 2013) or sequencing (Simões-Costa and Bronner, 2016).

There are drawbacks to our work which may come into consideration though, for example we have worked on qPCR of whole cultures that contain non-neural crest derivatives, such as posterior neural plate as well as potential cranial contaminants. Immunostaining showing that ETS1 and HOXC9 are found co-expressed is required to confirm that we do not have two mutually exclusive populations *in vitro* **(Figure 4.5D)** although it does not rule out the possibility of cranial contaminants contributing the qPCR data. Further techniques to determine the protein levels and single cell level of expression of these genes is also required to confirm the expression of genes proposed as cranial specific in our system. Though, we see more genes carried across from cranial to trunk, than genes present in trunk in cranial. For example, we have shown the absence of HOXC9 staining in cranial cultures **(Figure 4.5D)** and we do not see *CDX2* expression in cranial cultures from microarray analysis.

The anterior specific genes proposed by Simoes-Costa et al to be part of a cranial specific putative ectomesenchyme differentiation network may not fully reflect the roles of these genes. For example, *Sox8* is in the SOXE family of genes with

Sox9 and *Sox10* that are well established in forming both cranial and trunk neural crest (Betters et al., 2010a; Cheung et al., 2005). In addition, they have also been shown to function redundantly with SOX10 in the context of oligodendrocyte differentiation (Stolt, Lommes, Friedrich and Wegner, 2004b). TFAP2β has shown redundancy and co-expression with TFAP2α (Schmidt et al., 2011), which is expressed in all neural crest cells. These genes play similar, essential, roles in neural crest formation and differentiation and that such dramatic changes in gene expression may perturb trunk neural crest formation and function.

The difference in findings we have from *in vitro* derived putative neural crest cells and *in vivo* neural crest cells may also be a species difference as a comprehensive analysis of human *in vivo* neural crest cells has not been done due to the rarity of appropriately aged tissues. To assess whether our findings are due to difference in species or differences in model, assessing expression of ETS1 in human embryos would be required as well as confirmation of restriction of HOXC9.

Unbiased whole genome approaches have also been widely used to assess novel markers in populations and to compare similarly expressed genes. Our data shows a similar expression of the core neural crest GRN (including genes such as *FOXD3, SOX10, SOX9, PAX3, PAX7*) in equivalent time stages of differentiation (i.e neural crest precursors at day 3 for cranial and day 6 for trunk). These data are another method to validate our findings from other methods that we are producing putative neural crest cells in cultures subjected to our differentiation conditions. To further assess our claims that initial differentiation to NMPs is required for trunk neural crest differentiation, we are then able to compare our microarray data to that of previously published protocols and map our data to their data. For instance, Kreitzer et al have reported subpopulations of cranial, cardiac and trunk neural crest cells all from one differentiation protocol similar to Dual-SMAD inhibition (Kreitzer et al., 2013). This is in disagreement with other protocols and our data that have established patterning molecules (Fattahi et al., 2016; Workman et al., 2016; Huang et al., 2016). Thus, we can map our microarray data with that or Kreitzer et al and determine based on our work which it clusters

to more closely using principal component analysis. Our data shows cranial and trunk clustering away from each other and thus we would easily be able to see the differential clustering of these cells with our putative protocols.

The separate clustering of cranial and trunk neural crest cells indicates that these cells differ early on their differentiation protocol and adds to our hypothesis that cranial and trunk neural crest cells are induced through different gene regulatory networks. This notion has been proposed recently for the development of the anterior and posterior neural plates (Kondoh, Takada and Takemoto, 2016). The mechanism has further evidence with different tissue specific *Sox2* enhancers in anterior and posterior neural plate (Uchikawa et al., 2003) as well as differential expression of *Otx2* and *Gbx2* (Iwafuchi-Doi et al., 2012) that act to cross repress each other for anterior and posterior development respectively. Knocking out OTX2 and GBX2 in the context of cranial and trunk differentiation and assessing the expression of SOX10 and HOXC9 in neural crest cells differentiated cells this would confirm this hypothesis being conserved in hPSC *in vitro* differentiations. In addition, testing *Sox2* axial enhancer expression *in vitro* would be a similar method to determine the different origin of neural crest cells from anterior and posterior neural plate.

Identifications of novel markers in different populations of cells can offer a wide range of opportunities to unravel mechanisms in differentiations and allow for a thorough comparison of cell types both *in vivo* and *in vitro.* We used microarrays to assess for any novel markers in trunk neural crest that had not been described in the literature. We can also consider differential expression of cell surface antigens to tease apart small populations to characterise.

There are drawbacks to our approach using whole cultures rather than sorted populations. For instance, we have contaminating cell types that although we tried to minimise, will still show up in the microarrays. Our preliminary approach to find novel genes expressed in these populations has shown differences and similarities in gene expression by Venn diagram analysis. Gene Ontology analysis of genes upregulated in trunk all showed enrichment of genes involved in anterior

posterior patterning **(Figure 4.7D & Figure 4.8D)** and is shown by HOX genes being in the most differentially expressed between cranial and trunk in a pairwise comparison.

The middle part of the Venn diagram shows shared genes between these sample, we saw this contained well described neural crest genes, such as *SOX10, SOX9, PAX7* and *PAX3*, which reflects the hypothesis that these genes form a core neural crest GRN. This would need to be confirmed by assessing the formation of neural crest upon knockout of these genes *in vitro*.

4.4.5 Optimisation of sympathoadrenal precursor differentiation from hPSCs via Trunk neural crest cells

Sympathoadrenal precursors are a bipotent progenitor derived from the trunk neural crest cell that can form either chromaffin cells in the adrenal gland, or sympathetic neurons (Anderson and Axel, 1986). These cells have been demonstrated to only be formed by trunk neural crest cells *in vivo* (Reviewed in Le Douarin, Creuzet, Couly and Dupin, 2004) and thus derivation of these cells *in vitro* is a key candidate to test if anterior posterior identity affects cell fate *in vitro*.

One recent report has derived these cells *in vitro* from a protocol that where the anterior posterior identity is not clear (Oh et al., 2016). They mimicked conditions found *in vivo* utilising Sonic Hegdehog and BMP signalling whose role has been well characterised (Reviewed in Huber, 2006). They then assessed the expression of both the sympathoadrenal markers *ASCL1* and *PHOX2B* by generating knock in reporter lines and from their protocol, seeing 46% and 4% induction of these markers respectively (Oh et al., 2016). The yields of 4% indicate that this protocol is not particularly efficient in yielding sympathetic neuronal precursors. Reasons for this may include low SOX10 induction (approximately 20%) (Oh et al., 2016) or lack of correct patterning. If correct patterning is important in correct specification of these cells, we would expect to see higher yields when trunk cells go through this protocol than cranial neural crest cells. To first test this, we need to adapt the protocol in Oh et al and optimise it for our conditions. We tested the

same signalling pathways, albeit with one key difference. We used recombinant Sonic Hedgehog with no modifications, whilst Oh et al use Sonic C25II (R&D systems 464-SH) which has two Isoleucine residues added to the N-terminus and has 10 fold higher activity (Fasano et al., 2010) than regular recombinant Sonic Hedgehog (that we have used). Inactive SHH may explain why we see the same efficiency of GFP+ positive cells by flow cytometry in conditions with BMP4 only and BMP4+Sonic Hedgehog **(Figure 4.9B)**. The addition of the small molecule Purmorphamine, a SMOOTHENED agonist (Sinha and Chen, 2006), increases the yield of PHOX2B::GFP positive cells to 7% after 4 days of exposure. Thus, future optimisation steps for this would be to use the N-terminal modified C25II SHH to further activate this pathway. Combining the small molecule agonist Purmorphamine with SAG, another SMOOTHENED agonist, has also increased efficiency in motor neuron differentiation of hPSCs (Amoroso et al., 2013) is another addition to the differentiation cocktail to test. We have seen yields of up to 60% PHOX2B:GFP (data not shown) in cells put through this differentiation from trunk neural crest cells, but this has so far not been robustly repeated. This indicates that we have potential sources of variation through this differentiation, for example, we have not purified progenitor cell types at any stage of differentiation, i.e NMPs or trunk neural crest. We may be carrying through cell types that will not form sympathoadrenal precursors such as cranial contaminants from incomplete NMP differentiation and posterior neural plate cells from the neural crest differentiation. Purifying trunk neural crest cells (SOX10+/HOXC9+) and then assessing the number of PHOX2B+ positive cells would give the best idea and would allow for a direct comparison with cranial neural crest cells (SOX10+HOXC9-).

Despite the variable yield, we wanted to assess if we were making the correct cell type *in vitro* to assess the cells we were deriving were putative sympathoadrenal precursors. We carried this protocol forward to and utilised immunostaining to assess the markers of Sympathoadrenal fate *in vitro*. Whilst the immunofluorescence data are very preliminary analyses, they do correlate with

the findings from Oh et al that this differentiation cocktail does give rise to PHOX2B positive cells that can give rise to catecholamine synthesising neurons.

As sympathetic neurons are found along the anterior posterior axis, whilst the formation of these bipotent cells that form chromaffin cells that go to the adrenal gland are restricted to the trunk. Testing for expression of chromaffin cell markers such as *Chromogranin A* and also Phenylethanolamine N-methyltransferase (PNMT) that are genes involved in epinephrine biosynthesis (Huber, 2015) would allow for us to confirm the formation of sympathoadrenal precursors, that are axial specific, rather than just sympathetic neurons. Testing the bipotency of PHOX2B positive cells at the single cell level would also be another way to assess the *in vitro* differentiation potential of cranial and trunk neural crest cells as any difference in potency would be seen in the ability of these cells to differentially form neuroendocrine cells. Transplant putative cranial and trunk neural crest cells into the chick or mouse and assess their migratory routes and subsequent function would be the gold standard to describe these cells. We would expect to see sympathoadrenal precursors undergo a dorsal-ventral migration and see cells present in the spinal ganglia and adrenal medulla (Lumb and Schwarz, 2015).

Comprehensive transcript analysis and comparison with the genes shown to be expressed in Oh et al would allow us to understand more of the gene expression status of these cells. We aim to find the stages of differentiation and when the cells express *ASCL1,* a precursor marker, and the time points we see induction of more mature neuronal markers to assess neuroendocrine function. Downstream applications for these cells include studying the effect of neural crest derived cells neurons on target tissues. Oh et al showed that hPSC derived sympathetic neurons induced functional maturation when co-cultured with mouse neonatal cardiac tissue (Oh et al., 2016). Sympathetic neurons have also been implicated in haematopoiesis whereby GATA3 expressing sympathetic neurons have been shown regulate the formation of hematopoietic stem cells (Fitch et al., 2012). To assess the function of sympathoadrenal precursor cells *in vitro,* first we would assess the secretion of catecholamines from PHOX2B::GFP/GATA3+ expressing cells *in vitro* such as dopamine and norepinephrine as demonstrated previously

(Oh et al., 2016). Combining the function of these neurons, with assessing an effect on target tissues would demonstrate that these cells function correctly *in vitro* and assessing if hPSC derived sympathoadrenal precursors can recapitulate this effect on a dissected aortic-gonads-mesonephros (AGM) region from mice would mimic endogenous neurons. In addition, producing hematopoietic stem cells from hPSCs has so far been elusive, with the most promising report coming recently, but did not show full function compared to endogenous hematopoietic stem cells (Sugimura et al., 2017). This adds to the hypothesis that for full hematopoietic function, then additional tissues and signals play this role, which is critical for regulation.

In addition, the paediatric cancer neuroblastoma shows risk genes that are key to early sympathoadrenal precursors. There are recent reports of melanoma recapitulating the phenotype of the developing neural crest in zebrafish models (Kaufman et al., 2016). Thus, a once sympathoadrenal precursors can be efficiently derived *in vitro,* making iPSC lines from familial cases and assessing any changes in proliferation, differentiation and cell death may show the early onset of neuroblastoma. In addition, further assessments of gene expression and epigenomic regulation in any potential tumorigenic outgrowths from these may show an increase in neural crest proliferation genes such as *SOX10.* This would further the findings of Kaufman et al who showed expression of the early neural crest gene *crestin* in melanoma tissues (Kaufman et al., 2016) and showed this was due to changes in chromatin structure allowing for re-expression of these genes in ectopic locations.

4.5 Summary

In summary, the experiments from this chapter have allowed us to answer to some extent the aims for the chapter. We have determined that hPSC derived Neuromesodermal progenitors can be further differentiated into neural crest cells. We can derive cultures with homogeneous amounts of

BRACHYURY/SOX2/HOXC9 expressing cells that when exposed to conditions known to derive neural crest cells from hPSCs, also give rise to neural crest cells that retain HOXC9 expression. These data are consistent with the cells being of a truncal identity, as NMPs are found in the posterior of the embryo *in vivo* and the expression of the segmentation gene HOXC9, that is consistent with trunk identity also informs this. Whilst we have begun to show the greater potency of these cells when derived from hPSCs, we still need to demonstrate tri-potency (neural, mesodermal and neural crest fates) can be generated from a single NMP or whether there is a population of posterior neural crest progenitors within the culture. To add complexity to this, we have demonstrated expression of putative neural crest genes in NMPs, such as *PAX3* and *SOX9* whose expression may add complexity to the current model that *BRACHYURY* and *SOX2* drive either mesodermal or neural differentiation respectively and opening the possibility that these genes may regulate the early neural crest specifiers in respect to their differentiation. Furthermore, this data adds weight to the hypothesis that the mechanism of induction of the posterior neural plate is a separate distinct pathway rather than a signal inducing a posterior transformation of an anterior cell. In addition, we have begun to assess the gene expression differences between these cells, initial analysis showed that genes shown to be differentially expressed *in vivo* do not fully carry over *in vitro*, which may signify either species or model difference that can only be resolved through analysis of human embryo gene expression. Utilising microarrays, we have seen that cranial and trunk hPSC derived neural crest cells do show differences as they cluster apart in PCA analysis and work is ongoing to determine novel markers that are differentially expressed between the two. From our preliminary analysis, we have seen well described patterning genes differentially expressed, such as *CDX2* that has been demonstrated to bind to promoter regions of neural crest related transcripts such as *PAX3*. In addition to assessing the gene expression differences of hPSC derived trunk and cranial neural crest cells, cis regulatory units of these genes are also prime candidates to be compared with the inputs to these genes potentially driving the differences between these populations of neural crest cells. We have also begun to assess the ability of hPSC derived trunk neural crest cells to form a

derivative that is restricted to the trunk neural crest *in vivo*. Sympathoadrenal precursor differentiation has been demonstrated *in vitro* but is as of yet very inefficient, we have preliminary data showing a greater differentiation efficiency, bt without a direct comparison with our putative cranial hPSC differentiation to sympathoadrenal precursors, we cannot conclude as to the different differentiation potential between these genes across the anterior posterior axis.

Chapter 5: Final Discussion

5.1 Differentiation of Neural crest cells and their derivatives.

The data presented in this body of work describe the efficient generation and methods of purification of putative neural crest cells from hPSCs. In addition, the model we have presented has allowed for the dissection of the mechanisms of neural crest differentiation from hPSCs. This model can be used to infer the ontogeny of neural crest cells from hPSCs and corroborate data from model organisms such as the chicken where neural crest cells are seen to be determined at gastrulation and independent of other ectodermal tissues (Basch, Bronner-Fraser and García-Castro, 2006). In addition, we can now further build on this work to assess the differentiation potential of neural crest cells and assess the extent to which they are multipotent. We have demonstrated that cultures of purified neural crest cells are able to form derivatives that are typically ectodermal **(Figure 2.5)** and mesodermal **(Figure 2.4)**- and this ability to differentiate into cells spanning germ layers is a key characteristic of these cells that sets them apart from most tissues in the developing embryo (Hall, 2000). Whilst the potential of these cells in bulk has been demonstrated here, the ability of a single neural crest cell to form these derivatives is the true test of differentiation potency and is a clear next step to investigate the potency of these cells.

hPSCs models of embryonic cell types can also be harnessed for translational effects with the neural crest being the source of a diverse range of diseases termed neurocristopathies. With mutations present in these diseases affecting many aspects of neural crest biology, it is not uncommon to see more than one disease appearing in the same patient. As of yet, the extent of the recapitulation of neural crest biology in some diseases has yet to be elucidated, with potential reprogramming to a multipotent neural crest state being a key driver of cancers that have a poor prognosis (Kaufman et al., 2016).

In developing these models, the extent to which different anterior-posterior populations of neural crest cells differ to one another will play a key role in the ability of these cells to be studied for the benefitting human health are still a long way off. In addition, the basic biology of whether all neural crest cells are the same or whether they are similar, but distinct cell populations, is something that has not been determined.

5.2 Retinoic Acid changes identity and fate of neural crest cells

The transformation theory proposed by Nieuwkoop (Durston et al., 1989) has long been seen as the key mechanism to which embryonic tissues are patterned and Retinoic Acid has long been seen as the one of the key mediators in this process. Our work has shown that this is the case through neural crest differentiation, but only to an extent. Our data show that this hypothesis can explain neural crest patterning hindbrain and rostral aspect of the spinal cord and does not pattern more posterior tissues- including the entire trunk of the embryo **(Figures 3.2 & 3.3)**. The extent to which identity alters fate as not been fully elucidated, but we have recapitulated findings from others that we can now derive putative enteric neural progenitors (Fattahi et al., 2016; Workman et al., 2016). In addition to cells expressing genes consistent with this identity, function is the gold standard for hPSC differentiation protocols and we have worked in conjunction with Dr Alan Burns' group in assessing the ability of these cells to function *in vivo* **(Figure 3.6)**. Furthermore, we are taking one of the overarching advantages of hPSC differentiation and working this into a method to derive enteric neural progenitors for preclinical studies to determine these as a cell therapy for Hirschsprung's disease. This line of investigation can then be carried across into other peripheral neuropathies, although cell replacement therapies are not always possible, hPSCs derived cell types can also be developed for drug screening.

5.3 A novel source of trunk neural crest cells

The source of neural crest cells in the trunk has been elusive in *in vitro* investigations of neural crest cells with only one report claiming to be able to derive them from hPSCs (Huang et al., 2016). Our data investigating the role of Retinoic acid has shown that utilising this to transform anterior cells to a posterior identity only works to an extent. We have demonstrated that a posterior progenitor cell type, called Neuromesodermal progenitors, present in the tail bud of the developing embryo is able to form trunk neural crest *in vitro* **(Figure 4.4)**. These data are consistent with the hypothesis that the anterior and posterior neural plates come from distinct populations with different gene regulatory networks. The effect of this on the gene regulatory network underlying neural crest differentiation is now something that needs investigation and our preliminary analysis have shown differences, particularly with the expression of genes corresponding with the posterior of the embryo **(Figure 4.5, 4.6, 4.7, 4.8)**. Continuing along this line of investigation will allow for greater insight into the gene regulatory network underlying the induction of trunk neural crest cells and in addition allow for purification and further study of hPSC derived neural crest cells. Furthermore, we are beginning on the putative analysis of how the axial identity of neural crest affects cell fate. We are beginning to optimise the protocol to differentiate sympathoadrenal precursors from trunk neural crest cells and this will open an assay to compare differentiation potential. Furthermore, to correspond with Retinoic acid patterned neural crest, we can use this to assess the mechanisms behind the paediatric cancer, neuroblastoma.

5.4 Concluding Remarks

Overall, the data here have opened the field of neural crest biology with a new model system to explore the formation, patterning and subsequent fate of neural crest cells. This model system can give rise to new hypotheses that can be used to infer what happens in the human system. From this, we can now work begin work on all aspects of neural crest biology. Whilst this system will open new avenues of research, it cannot be done without further studies from the classical

developmental models. Embracing the two together by combining hPSC derived cells and transplanting these *in vivo* can result in powerful studies to enhance the understanding of neural crest biology.

Chapter 6: Methods

6.1 Cell culture

6.1.1 Pluripotent Cell culture

6.1.1.1 Cell Lines

All lines used are specified below in table 6.1

Table 6.1

Cell Line	Source/Information
H9 (WA09)	Gift from Professor James Thompson (Thomson, 1998)
H9::SOX10 (Subclone 20.9.12)	Gift from Professor Lorenz Studer (Chambers et al., 2012) Re-cloned in Sheffield for optimal GFP expression (Hackland et al., 2017).
H9:Phox2b (Clone 14)	Gift from Dr Gabsang Lee (Oh et al., 2016)
MIFF1	reprogrammed in house by mRNA
ZIPs	Gift from Professor Lesley Forrester
MasterShef7	Derived by Professor Harry Moore

6.1.1.2 Culture Conditions

Cells were cultured in mTESR1 (Stem Cell Technologies #05850) on Geltrex (Life Technologies #A1413202) 1:50 in DMEM/F12 or Laminin 521 (2.5μg/ml in PBS with Ca^{2+}/Mg^{2+}) (BioLamina LN521-02). Media was changed every day and cells were passaged when at 60-70% confluence using ReLeSR (following manufacturer's instructions) (Stem Cell Technologies #05872). In brief, media was aspirated from cells and washed once with PBS (without Ca^{2+}/Mg^{2+}) and further

washed once with ReLeSR. Cells were left at RT for 5 minutes and subsequently washed off with media as small clumps (<50-100 cells).

Cells were plated at densities between 1:3-1:6. Cells were kept at 37°C in a humidified environment with 5% CO_2.

6.1.1.3 Plate Preparation

6.1.1.3.1 Geltrex

Geltrex (Life Technologies A1413202) was kept at -20°C in 0.5ml aliquots. When needed, it was thawed on ice until liquid and quickly resuspended in cold DMEM/F12 (Sigma D6421) at a 1:50 ratio. Plates were coated with the solution and left to set either overnight at 4°C or for 1 hour at 37°C.

6.1.1.3.2 Vitronectin

Vitronectin (VTN-N) (Life Technologies A14700) was kept at 500μg/ml at -80°C. It was thawed at room temperature and diluted in PBS (without Ca^{2+}/Mg^{2+}) (Sigma D1408) to a final concentration of 5μg/ml. Plates were left to set for one hour at room temperature or stored at 4°C for a maximum of one week.

6.1.1.3.3 Laminin

Laminin-521 (Biolamina LN521-02) and Laminin 111 (BioLamina LN111-02) stock at 1mg/ml was kept at -20°C until use. It was subsequently resuspended at 2.5μg/ml in PBS (with Ca^{2+}/Mg^{2+}) (ThermoFisher 14040133). Plates were set either overnight at 4°C or for 2 hours at 37°C.

6.1.1.4 Cell Stock Maintenance

6.1.1.4.1 Cell Freezing

Cells at 60% confluency and still in Log phase of growth had media removed and were washed once with 1x PBS (without Ca^{2+}/Mg^{2+}) and subsequently washed with ReLeSR briefly (less than 30 seconds). After 4 minutes, cells were washed off in Stem Cell Banker (Clontech CB045) and were aliquoted into cryovials (Corning #430488). These were placed in a Mr Frosty and frozen at -80°C overnight and placed in liquid nitrogen the next day for long term storage.

6.1.1.4.2 Cell Thawing

Cells were thawed by quick resuspension in media and centrifugation (1100rpm/4min) at Room temperature. The pellet was then re-suspended in mTESR1 media supplemented with 10μM Y27632-dihydrochloride (Tocris 1254) and plated down on previously prepared Laminin521or geltrex coated plates.

6.1.2 Directed Differentiation

6.1.2.1 Neural Crest Differentiation

Neural Crest differentiation was modified from previous protocol from(Hackland et al., 2017). For full composition of media, including final concentrations and volumes, see **Table 6.2**. When hPSCs were at 60-70% confluency, cells were dissociated to single cells using Accutase (Thermo Fisher A1110501) for 10 minutes at 37°C. Single cells were confirmed by observing down an inverted microscope. Single cells were then counted manually and then re-seeded on at 25-30000 cells/cm^2 on 1:50 Geltrex coated plates or 30000/cm^2 on 2.5μg/ml Laminin521 coated plates in TDI differentiation media (Hackland et al., 2017) this is day zero of the differentiation. For full recipe, see **Table 6.2**. All-trans Retinoic Acid (Sigma R2625) was diluted in DMSO (Sigma) at a stock concentration of 10mM and was added to TDI media at times and concentrations specified in the text. During differentiation, media was changed on day two to remove Y-27631-dihydrochloride and again on Day 4 to replenish media. Cells were harvested for analysis/further differentiation based on timings from (Leung et al., 2016). Any deviations from this protocol are stated in the figures.

Table 6.2 TDI media recipe

Component	**Stock Concentration**	**Volume**	**Final Concentration**
DMEM/F12	N/A	48.5ml	N/A
N2 supplement (ThermoFisher 17502048)	100x	0.5ml	1x
Non-Essential Amino Acids (ThermoFisher 11140035)	100x	0.5ml	1x
Glutamax (ThermoFisher 35050061)	100x	0.5ml	1x
BMP4 (ThermoFisher PHC9533)	50ug/ml	20µl	20ng/ml
DMH1 (Tocris 4126)	10mM	5□l	1□M
CHIR99021 (Tocris 4432)	10mM	5□l	1□M
SB431542 (Tocris 1614)	10mM	10□l	2□M

6.1.2.2 Neural Crest Derivative differentiation

6.1.2.2.1 Ectomesoenchyme Differentiation

Sorted neural crest cells (see **Figure 2.4**) were plated down at 50 000/cm^2 in Mesencult-ACF supplemented with 10μM Y-27632-dihydrochloride (Tocris 1254). The next day, media was changed to Mesencult-ACF (Stem Cell Technologies 05449) with media changes every two days for ten days.

For chondrocyte differentiation, day 10 ectomesenchymal cells were dissociated with Accutase for 10 minutes and counted using a haemocytometer. Cells were resuspended at 1x10^6 cells/ml in Mesentult™-ACF Chondrogenic Differentiation Medium (Stem Cell Technologies 05455) or kept in Mesencult-ACF medium as basal condition and 0.5x10^6 cells were pipetted into a 15ml propylene tube and spun in a centrifuge at 300xg for 10 minutes. The cap was loosened and the tube placed into the incubator. Media was changed twice a week and to prevent full attachment of cells to the plastic, the pellet was flicked gently. After 21 days, the cell pellet was fixed by replacing the media with 4% paraformaldehyde for 10 minutes at room temperature and then subsequently wash three times with 1x PBS (without Ca^{2+} or Mg^{2+}). Cells were then mounted in OCT and then cryosectioned with 10μm thick sections onto slides for Toluidine blue staining (Acros Organics 384600050).

For osteocyte differentiation, day 10 ectomesenchymal cells were plated down onto plastic at 6x10^3 cells/cm^2 in Mesencult-ACF media. Cells were grown in this until 80% confluency and media replaced with Osteogenic stimulatory kit (Stem Cell Technologies 05404) or Mesencult ACF as basal condition for 14 days. Cells were subsequently fixed with 4% paraformaldehyde for 10 minutes at room temperature and subsequently stained used Alizarin Red (Sigma A5533)

6.1.2.2.2 Peripheral Neural Differentiation

Day 5 neural crest cells were lifted using Accutase (Thermo Fisher A1110501) and counted manually. Cells were then resuspended at 1x10^6 cells/ml and plated down onto Geltrex (1:50) or pre-coated Poly-L-Ornithine (Sigma P4957-50ML) (pre-coating of Poly-L-Ornithine was done by putting solution onto the plate and incubating at 37°C for 30 minutes and washed three times in 1x $PBS^{-/-}$) and Laminin111 (BioLamina LN111) at 2.5μg/ml in Neural Crest differentiation media **(Table 6.2)** supplemented with 10μM Y-27631-dihydrochloride (Tocris 1254) overnight. Media was subsequently changed to BrainPhys (StemCell Technologies #05790) supplemented with 1x N2 supplement (Life Technologies 17502001), 1x B27 supplement (Life Technologies 17504044), 1 x NEAA (Life Technologies 11140035), 1 x Glutamax (Life Technologies 35050061) supplemented with 10ng/ml of each BDNF (Peprotech 450-02), GDNF (Peprotech 450-10) and NGF (Peprotech 450-01).

6.1.2.2.3 Neuromesodermal progenitor differentiation

Neuromesodermal progenitor differentiation was based on (Gouti et al. 2014), with a few modifications. In brief, hPSCs were treated with accutase to give a single cell suspension (as above). 60-80000 cells/cm^2 were plated on plates coated on Day 0 with 5μg/ml recombinant truncated Vitronectin (VTN-N; Life Tech A14700) in differentiation media comprised of N2B27 (for composition see **Table 6.3**) supplemented with CHIR99021 (4μM), FGF2 (20ng/ml) (R&D systems 233-FB), Y-27631-dihydrochloride (10μM) was added for the first day to assist in plating. Media was changed the next day (Day 1) and cells left until day 3 for analysis/further differentiation.

Table 6.3 N2B27 Recipe

Component	**Stock Concentration**	**Volume**	**Final Concentration**
DMEM/F12 (Sigma D6421)	N.A	100ml	N/A
Neurobasal (ThermoFisher 21103049)	N.A	100ml	N/A
N2 Supplement (ThermoFisher 17502001)	100x	2ml	1x
B27 Supplement (ThermoFisher 17504044)	50x	4ml	1x
Non Essential Amino Acids (ThermoFisher 11140035)	100x	2ml	1x
Glutamax (ThermoFisher 35050061)	100x	2ml	1x
B-mercaptoethanol (ThermoFisher 31350010)	50mM	200ul	.05mM

6.1.2.2.4 Sympathoadrenal precursor differentiation

Day 8 trunk neural crest cells were lifted using accutase (Thermo Fisher A1110501) counted and resuspended at $1x10^6$ cells/ml. Cells were subsequently plated down on Geltrex (1:50 dilution) coated plates in BrainPhys (StemCell Technologies #05790) supplemented with 1x N2 supplement (Life Technologies 17502001), 1x B27 supplement (Life Technologies 17504044), 1 x NEAA (Life Technologies 11140035), 1 x Glutamax (Life Technologies 35050061) supplemented with combinations of BMP4 50ng/ml (ThermoFisher PHC9533); Sonic Hedgehog 50ng/ml (Peprotech 100-45); 1μM Purmorphamine (Sigma SML0868). For maturation, media was changed to BrainPhys supplemented with 1x N2 supplement, 1x B27 supplement, 1x NEAA, 1x Glutamax, 10ng/ml BDNF (Peprotech 450-02), 10ng/ml GDNF (Peprotech 450-10) and 10ng/ml NGF (Peprotech 450-01)

6.1.2.2.5 *In vivo* hPSC derived neural crest transplants.

Neural Crest cells were generated in Sheffield as per methods 6.1.2.1. For sphere induction, cells post sort were plated into cell culture plates at 150 000 cells/cm^2. Plates were coated with 1% agarose that had set to create a non-adherent surface in TDI media. Cells as a monolayer or as spheres were transported to London and all transplants carried out by Julie Cooper and Conor McCann (Burns Lab, Institute of Child Health, UCL). Methods are the similar to those described in (McCann et al., 2017). In short, cells were transplanted into the caecum of Rag2-/γc-/C5- mice aged between four to six weeks by laparotomy. An incision was made in the *tunica muscularis* with a 30G needle. Cell suspensions or spheres were injected through the bevel of a 30G needle. Mice were maintained for 2-4 weeks after transplantation in a clean room and then killed and removal of the gut for analysis. Transplants were performed under home office license of Conor McCann and Julie Cooper and in accordance with UCL ethics guidelines.

6.1.3 In Situ analysis

6.1.3.1 Immunofluoresence

6.1.3.1.1 Immunostaining

Cells were fixed with 4% PFA at room temperature for 10 minutes and then washed 3 times with 1x PBS (without Ca^{2+} or Mg^{2+}). Plates were either stained immediately or stored at 4°C until stained. Following fixing and washing, cells were permeabilised and blocked in with 1x PBS (without Ca^{2+} or Mg^{2+}) containing 1% BSA (Millipore 821001) and 0.3% Triton-X (see solutions for recipe) for one hour at room temperature. Primary antibodies were suspended in this buffer and allowed to stain at 4°C overnight with agitation. Cells were subsequently washed 3 times with 1x PBS (without Ca^{2+} or Mg^{2+}) before secondary antibody staining. Secondary antibodies were also suspended in permeabilisation buffer and incubated with Hoechst 33342 (1:1000) (Life Tech H3570) for one hour at 4°C in the dark. Cells were again washed 3 times with 1x PBS (without Ca^{2+} or Mg^{2+}) before imaging on InCell 2200 (GE Healthcare).

Images were processed on ImageJ at the same time and in the same manner as negative controls by using the same values for brightness in each field.

6.1.3.1.2 Flow Cytometry

Cells were lifted into a single cell suspension using Accutase (as previously described) and resuspended in FACs buffer (DMEM with 10% v/v FCS) to neutralise Accutase before centrifugation at 1100rpm/4min. Cells were then resuspended in FACs buffer at $1x10^6$ cells/ml and 100,000 cells were placed in FACs tubes (Falcon 352053) with primary antibody (see table 6.4 for dilution of primary antibodies) for 15 minutes at 4°C Cells were washed with 4ml FACS buffer and spun down (1100rpm/4min) before being resuspended in 100µl FACs buffer containing secondary antibody. Cells were stained with secondary antibody for 15 minutes at 4°C in the dark before being washed three times. Stained cells were

resuspended in 0.3ml FACs buffer before analysis on BD FACSJazz (BD Bioscience). Negative control for FACs analysis was set using the primary antibody P3X (a control monoclonal antibody secreted from the P3X63Ag8 myeloma and does not show expression on human cells) showing a max of 5% expression in the first decade. When analysing cells carrying a GFP reporter, negative was set using parental line not carrying reporter.

6.1.3.1.3 FACS

For cell sorting, cells were lifted and stained as above, except that a cell suspension concentration of $2x10^6$ cells/ml was made with appropriate antibodies in was used **(see Table 6.4)**.

Cell were sorted into FACs buffer containing 10μM Y27632-dihydrochloride and Gentamicin (50μg/ml) (Sigma G1397). All sorted populations were re-analysed for minimum 95% purity.

6.1.3.1.4 Antibodies

6.1.3.1.4.1 Primary Antibodies for Flow Cytometry

Table 6.4 Antibodies for Flow Cytometry

Antibody	Details	Dilution	Reference/Catalogue number
P3X	Monoclonal Mouse IgG(in house hybridoma concentrate)	1:10	(KOHLER and MILSTEIN, 1975)
P75 (Clone ME20.4)	Monoclonal Mouse IgG (in house hybridoma concentrate)	1:10	(Ross et al., 1984b)
SSEA3	Monoclonal Rat IgM (in house hybridoma concentrate)	1:10	(Shevinsky, Knowles, Damjanov and Solter, 1982)
Tra-1-85	Mouse IgG1 (in house hybridoma concentrate)	1:10	(Williams et al., 1988)
CD49d	Mouse Monoclonal IgG1 Clone 9F10	1:100	BioLegend 304301
CD90	Mouse Monoclonal IgG1	1:100	Abcam ab23894
CD73	Monoclonal Mouse IgG1 Clone AD2 PE conjugate	1:100	BD 550257
CD105	Mouse Monoclonal IgG	1:100	Abcam ab11414

6.1.3.1.4.2 Primary Antibodies for Immunostaining

Antibody	Details	Format	Dilution

SOX10	Cell Signalling Technology #89356 (D5V9L) Monoclonal Rabbit IgG	Purified Antibody	1:300
SOX9	Cell Signalling Technology #82630 (D8G8H) Monoclonal Rabbit IgG	Purified Antibody	1:200
PAX3	Developmental Studies Hybridoma Bank. Monoclonal Mouse IgG2a	Hybridoma concentrate	1:200
T(Brachyury)	R&D Systems: AF2085-SP Polyclonal Goat IgG	Purified Antibody	1:200
SOX2	Cell Signalling Technology # 3579 (D6D9) Monoclonal Rabbit IgG	Purified Antibody	1:200
HOXC9	Abcam: ab50839. Mouse Monclonal IgG2b	Purified Antibody	1:10
SLUG	Cell Signalling Technology #9585 (C19G7) Monoclonal Rabbit IgG	Purified Antibody	1:200
PERIPHERIN	Millipore AB1530 Rabbit Polyclonal	Purified Antibody	1:100
TUJ1 (β-Tubulin III)	Sigma T8660 Mouse Monoclonal IgG2b Clone SDL.3D10	Purified Antibody	1:500
RET	R&D Systems MAB718: Mouse Monoclonal IgG	Purified Antibody	1:50
LHX5	R&D systems AF6290 Polyclonal Goat IgG	Purified Antibody	1:50
ETS1	Cell Signalling Technology #14069 (D8O8A) Monoclonal Rabbit IgG	Purified Antibody	1:200
Brn3a	Millipore AB5945 Rabbit Polyclonal	Purified Antibody	1:100
Islet1/2	39.4D5 Developmental Studies Hybridoma Bank Mouse Monoclonal IgG2b	Hybridoma concentrate	1:200

Table 6.5

6.1.3.1.4.3 Secondary Antibodies

Table 6.6

Antibody	Details	Assay	Dilution
Goat anti Mouse Affinipure IgG+IgM (H+L) AF647 conjugate	Stratech 115-605-044-JIR	FACs; Immunofluorescence	1:200
Donkey Anti Mouse IgG (H+L) AF488 conjugate	Life Technologies A-21202	Immunofluorescence	1:500
Donkey anti- Mouse IgG (H+L) AF647 conjugate	Life Technologies A-31571	Immunofluorescence	1:500
Donkey Anti Goat IgG (H+L) AF594	Life Technologies A-11058	Immunofluorescence	1:500
Donkey Anti Rabbit IgG (H+L) AF488	Life Technologies A-21206	Immunofluorescence	1:500
Donkey Anti Rabbit IgG (H+L) 647	Life Technologies A-31573	Immunofluorescence	1:500

6.1.3 Repeats

Repeats in the figure legends are classed as: technical repeats, biological repeats or independent experiments.

Technical repeats are findings from different iterations of the experiment from the same starting population of cells.

Biological repeats are iterations of the same experiment from different starting groups of cells (i.e different flasks) each with technical repeats for each biological set of cells.

Independent experiments are different starting populations of cells that are at least one passage apart.

6.1.4 Transcriptome Analysis

6.1.4.1 RNA extraction

Cell pellets were lifted using accutase and neutralised DMEM/F12 (Sigma D6421) to create a cell suspension. This was then centrifuged at 1100rpm/4min at room temperature and the supernatant aspirated off to create a cell pellet which was either frozen at -80°C or extracted immediately using the Qiagen RNeasy Mini Kit (Qiagen 74134) and eluted in ddH_2O. The concentration of RNA eluted was determined by Nanodrop and stored at -80°C. RNA with 260/280 values between 1.8 and 2.0 was considered pure and used cDNA conversion.

6.4.1.2 cDNA synthesis

2μg of RNA was calculated and n combined with reagents from High Capacity cDNA Reverse Transcription Kit (Life Technologies 4368814). ddH_2O was added to make a final volume of 20μl in PCR tubes (See table 6.7 for composition). Reverse Transcription was then performed as per manufacturer's instructions by placing in a Thermocycler (Applied Biosystems 2720). Cycle conditions are as follows: 25°C-10 mins; 37°C- 120 mins; 85°C- 5 mins. cDNA was diluted to a 5ng/μl stock and stored at -20°C until use.

Component	**Volume for 1 reaction (μL)**
Reverse Transcriptase	1
10x Random Primers	2
dNTPS (100nM)	0.8
10x RT Buffer	2
RNA	Volume for 2ug
Water	14.2-volume of RNA
TOTAL	**20**

6.1.4.3 qPCR

Quantitative Real Time PCR was performed using the Roche Universal Probe library system, whereby small oligonucleotides bound to probes are incorporated into PCR products to read out amplification of a specific amplicon. Reactions were set up as per **Table 6.7**. All reactions were set up in 384 well plates. All PCR reactions were run on QuantStudio 12K Flex Real-Time PCR system (Life Technologies 4471087). Cycling conditions were as followed: 95°C- 10 min (Initial denaturation); 95°C (10 seconds) 60°C (1 minute) for 45 cycles followed by 4°C storage.

Table 6.7

Component	Volume per reaction
2x Taq (ThermoFisher 4352042)	5µl
Water	2.7µl
Primer (containing 5µM F/R)	0.2µl
Probe	0.1µl
cDNA (5ng/µl)	2µl

GAPDH was used as housekeeping gene for normalisation of gene expression for 1/Delta CT values using the following formula:

Delta CT= CT Gene of Interest- CT GAPDH

TBP was run as a second housekeeping gene for internal quality control for the PCR run and no template controls were included in all qPCR runs. Primers were designed using the Roche UPL primer design assay (https://lifescience.roche.com/en_gb/brands/universal-probe-library.html) and checked on NCBI primer design tool for specificity. All primer sequences used are found in **Table 6.8.**

Primers

Table 6.8

Gene	Forward	Reverse	Roche Probe
SOX10	ggctcccccatgtcagat	ctgtcttcggggtggttg	21
FOXD3	gaagccgccttactcgtaca	cgctcagggtcagcttctt	9
ETS1	gcagaatgagctactttgtgga	ttgctaggtccttgcctca	3
TFAP2a	acatgctcctggctacaaaac	aggggagatcggtcctga	62
SOX8	cttggagatgggcaccac	ctgctgcagctccgtctt	77
SOX9	gtacccgcacttgcacaac	tctcgctctcgttcagaagtc	61
PAX3	aggaggccgacttggaga	cttcatctgattggggtgct	13
PAX7	gaaaacccaggcatgttcag	gcggctaatcgaactcactaa	66
TFAP2b	cctgcactcccgaaagaata	gcgccagtagatccgtaaat	49
BRN3c	ccaaattctccagtctgcact	catcaaagcttccaaatatattaccc	14
DMBX1	ccccaaagctgagaagagc	gccacaggagtgatggtca	23
SNAI1	gctgcaggactctaatccaga	atctccggaggtgggatg	11
SNAI2 (Slug)	tggttgcttcaaggacacat	gcaaatgctctgttgcagtg	7
LHX5	cgtgtgcaaagacgactacc	acaaactgcggtccgtaca	42
OTX2	gggtatggacttgctgcac	ccgagtgaacgtcgtcct	81
HES6	agcccctggtggagaaga	cagcacttcggcgttctc	17
DBX1	gacgacgtttctgaagtttgg	caaggctggggatgtttct	55
ZIC3	tgcgcaaacacatgaagg	tatagcgggtggagtggaag	74
MSX1	ctcgtcaaagccgagagc	cggttcgtcttgtgtttgc	7
HOXA1	actccttgtcccctctcca	ccaggtagccgtactctcca	83
HOXB1	ccagctagggggcttgtc	atgctgcggaggatatgg	39
HOXB2	aatccgccacgtctcctt	gctgcgtgttggtgtaagc	70
HOXB4	ctggatgcgcaaagttcac	agcggttgtagtgaaattcctt	62
HOXB5	aagcttcacatcagccatga	cggttgaagtggaactccttt	1

HOXB8	agctcttcccctggatgc	atagggattaaataggaactccttctc	1
HOXC8	tcccagcctcatgtttcc	tgataccggctgtaagtttgc	86
HOXC9	gcagcaagcacaaagagga	cgtctggtacttggtgtaggg	85
PHOX2B	ctaccccgacatctacactcg	ctcctgcttgcgaaacttg	17
ASCL1	cgacttcaccaactggttctg	atgcaggttgtgcgatca	38
HAND2	tcaagaagaccgacgtgaaa	gttgctgctcactgtgcttt	35
FGF8	agctcgcttccctgttcc	attaggtgaggactgaacagttacc	45
WNT3a	ctgagggtgggcttttcc	gaggagtactgccccgttta	15
CDX2	atcaccatccggaggaaag	tgcggttctgaaaccagatt	34
NKX1-2	gtcgaagcggggaaagat	gatcctccgcatcctcct	78
TBP	gaacatcatggatcagaacaaca	atagggattccgggagtcat	87
GAPDH	agccacatcgctcagacac	gcccaatacgaccaaatcc	60
OCT4	gtggagagcaactccgatg	tgcagagctttgatgtcctg	78
NANOG	agatgcctcacacggagact	ggactggtggaagaatcagg	69
SOX1	gaagcccagatggaaatacg	ggacaaggaagggtgttgag	66

6.1.4.4Microarray Analysis

Neural Crest differentiation was carried out as specified in the methods/text using H9::SOX10:GFP reporter line on three separate occasions with at least one passage between replicates. Total RNA was taken from the cells and homogenised in 300ul Trizol (Life Technologies 15596018). RNA was extracted using the Zymospin Mini Kit (R0205) following manufacturer's instructions. RNA quantity and quality was assessed using a Nanodrop Lite Spectrophotometer (Life Technologies). RNA with 260/280 values of 1.8-2.00 was then used for microarray analysis using Clariom D chips (Life Tech 902922).

Samples were prepared according to the Affymetrix WT Plus protocol for Gene Chip ® Whole Transcript Expression Arrays. Briefly 200ng of high quality total RNA, (RNA integrity number (RIN) greater than 9), was converted to double stranded cDNA with the introduction of a T7 polymerase binding site. This allowed the synthesis of an antisense RNA molecule against which a sense DNA strand was prepared. The RNA strand was digested and the resulting single stranded DNA fragmented and biotin labelled. Along with appropriate controls the labelled fragmented DNA was hybridised to Affymetrix Clariom D arrays overnight using the Affymetrix 640 hybridisation oven; 16 hours with rotation at 60 rpm at 450C. The arrays were washed and stained according to standard protocols which allowed the introduction of streptavidin-phycoerythrin in order to generate a fluorescent signal from the hybridised biotinylated fragments. The washed and stained arrays were scanned using the Affymetrix 3000 7G scanner with autoloader. The generated CEL files were taken forward for analysis.CEL files from microarrays were then analysed using Life Technologies Transcriptome Analysis Console. Venn diagrams were created by exporting gene lists and utilising Venny (http://bioinfogp.cnb.csic.es/tools/venny/). Gene ontology (GO) terms were assessed by placing genes into ToppGene Suite (https://toppgene.cchmc.org/enrichment.jsp)

6.1.5 Solutions

FACs buffer: DMEM (Sigma D5796) v/v 20% FBS (HyClone SV30160.03)

For 100ml: 80ml DMEM and 20ml FBS.

Permeablisation/Blocking Buffer: 1x PBS (without Ca^{2+} or Mg^{2+}) (Sigma D1408) containing 1% BSA (Millipore) and 0.3% Triton-X 100 (Acros Organics 215682500)

For 100ml of buffer- 99.7ml PBS; 1 gram BSA; 0.3ml Triton-X 100 (Acros Organics 215682500).

1% Agarose Solution for Crestospheres:

For 100ml of solution: 100ml double distilled H_2O and 1 gram Agarose (Sigma A9539).

1x PBS (Without $Ca2^+$ or $Mg2^+$)

A commercial 10x stock was purchased from Sigma Aldrich (Sigma D1408) and diluted in double distilled H_2O and autoclaved before use.

For 500ml. 50ml of 10x PBS added to 450ml double distilled H_2O

4% PFA

Paraformaldehyde powder (Sigma 158127) was purchased and a 4% w/v solution was prepared by dissolving in 1x PBS as prepared above. Solution was heated until paraformaldehyde was in solution. 4% solution was filter sterilised using a 0.2μm Steritop filter (Millipore SCGPS02RE). 50ml aliquots were made and stored at -20°C and once thawed for use were stored at 4°C.

For 1000ml: 40 grams of paraformaldehyde powder added to 1000ml of PBS.

Chapter 7: References

Aires, R., Jurberg, A.D., Leal, F., Novoa, A., Cohn, M.J. and Mallo, M., 2016. Oct4 Is a Key Regulator of Vertebrate Trunk Length Diversity. *Dev Cell*, 38(3), pp.262–274.

Alberga, A., Boulay, J.L., Kempe, E., Dennefeld, C. and Haenlin, M., 1991. The snail gene required for mesoderm formation in Drosophila is expressed dynamically in derivatives of all three germ layers. *Development*, 111(4), p.983.

Amiel, J., Sproat-Emison, E., Garcia-Barcelo, M., Lantieri, F., Burzynski, G., Borrego, S., Pelet, A., Arnold, S., Miao, X., Griseri, P., Brooks, A.S., Antinolo, G., de Pontual, L., Clement-Ziza, M., Munnich, A., Kashuk, C., West, K., Wong, K.K.-Y., Lyonnet, S., Chakravarti, A., Tam, P.K.H., Ceccherini, I., Hofstra, R.M.W., Fernandez, R. and Hirschsprung Disease, C., 2008. Hirschsprung disease, associated syndromes and genetics: a review. *J Med Genet*, 45(1), pp.1–14.

Amin, S., Neijts, R., Simmini, S., van Rooijen, C., Tan, S.C., Kester, L., van Oudenaarden, A., Creyghton, M.P. and Deschamps, J., 2016. Cdx and T Brachyury Co-activate Growth Signaling in the Embryonic Axial Progenitor Niche. *Cell Rep*, 17(12), pp.3165–3177.

Amoroso, M.W., Croft, G.F., Williams, D.J., O'Keeffe, S., Carrasco, M.A., Davis, A.R., Roybon, L., Oakley, D.H., Maniatis, T., Henderson, C.E. and Wichterle, H., 2013. Accelerated high-yield generation of limb-innervating motor neurons from human stem cells. *J Neurosci*, 33(2), pp.574–586.

Anderson, D.J. and Axel, R., 1986. A bipotential neuroendocrine precursor whose choice of cell fate is determined by NGF and glucocorticoids. *Cell*, 47(6), pp.1079–1090.

Anderson, R.B., Stewart, A.L. and Young, H.M., 2006. Phenotypes of neural-crest-derived cells in vagal and sacral pathways. *Cell Tissue Res*, 323(1), pp.11–25.

Andrews, P.W., 1984. Retinoic acid induces neuronal differentiation of a cloned human embryonal carcinoma cell line in vitro. *Developmental Biology*, 103(2), pp.285–293.

Arduini, B.L. and Brivanlou, A.H., 2012. Modulation of FOXD3 activity in human embryonic stem cells directs pluripotency and paraxial mesoderm fates. *STEM CELLS*, 30(10), pp.2188–2198.

Arnold, S.J. and Robertson, E.J., 2009. Making a commitment: cell lineage allocation and axis patterning in the early mouse embryo. *Nature reviews. Molecular cell biology*, 10(2), pp.91–103.

Aulehla, A., Wehrle, C., Brand-Saberi, B., Kemler, R., Gossler, A., Kanzler, B. and Herrmann, B.G., 2003. Wnt3a plays a major role in the segmentation clock

controlling somitogenesis. *Dev Cell*, 4(3), pp.395–406.

Aulehla, A., Wiegraebe, W., Baubet, V., Wahl, M.B., Deng, C., Taketo, M., Lewandoski, M. and Pourquie, O., 2008. A beta-catenin gradient links the clock and wavefront systems in mouse embryo segmentation. *Nat Cell Biol*, 10(2), pp.186–193.

Aybar, M.J., Nieto, M.A. and Mayor, R., 2003. Snail precedes slug in the genetic cascade required for the specification and migration of the Xenopus neural crest. *Development*, 130(3), pp.483–494.

Baggiolini, A., Varum, S., Mateos, J.M., Bettosini, D., John, N., Bonalli, M., Ziegler, U., Dimou, L., Clevers, H., Furrer, R. and Sommer, L., 2015. Premigratory and migratory neural crest cells are multipotent in vivo. *Cell Stem Cell*, 16(3), pp.314–322.

Bajpai, R., Chen, D.A., Rada-Iglesias, A., Zhang, J., Xiong, Y., Helms, J., Chang, C.-P., Zhao, Y., Swigut, T. and Wysocka, J., 2010. CHD7 cooperates with PBAF to control multipotent neural crest formation. *Nature*, 463(7283), pp.958–962.

Balmer, J.E. and Blomhoff, R., 2005. A robust characterization of retinoic acid response elements based on a comparison of sites in three species. *The Journal of steroid biochemistry and molecular biology*, 96(5), pp.347–354.

Barembaum, M. and Bronner, M.E., 2013. Identification and dissection of a key enhancer mediating cranial neural crest specific expression of transcription factor, Ets-1. *Dev Biol*, 382(2), pp.567–575.

Barlow, A., de Graaff, E. and Pachnis, V., 2003. Enteric nervous system progenitors are coordinately controlled by the G protein-coupled receptor EDNRB and the receptor tyrosine kinase RET. *Neuron*, 40(5), pp.905–916.

Baroffio, A., Dupin, E. and Le Douarin, N.M., 1991. Common precursors for neural and mesectodermal derivatives in the cephalic neural crest. *Development*, 112(1), pp.301–305.

Basch, M.L., Bronner-Fraser, M. and García-Castro, M.I., 2006. Specification of the neural crest occurs during gastrulation and requires Pax7. *Nature*, 441(7090), pp.218–222.

Baynash, A.G., Hosoda, K., Giaid, A., Richardson, J.A., Emoto, N., Hammer, R.E. and Yanagisawa, M., 1994. Interaction of endothelin-3 with endothelin-B receptor is essential for development of epidermal melanocytes and enteric neurons. *Cell*, 79(7), pp.1277–1285.

Beddington, R.S., 1994 Induction of a second neural axis by the mouse node. *Development*, 120(3): 613-620

Beddington, R.S., Rashbass, P. and Wilson, V., 1992. Brachyury--a gene affecting

mouse gastrulation and early organogenesis. *Dev Suppl*, pp.157–165.

Bel-Vialar, S., Itasaki, N. and Krumlauf, R., 2002. Initiating Hox gene expression: in the early chick neural tube differential sensitivity to FGF and RA signaling subdivides the HoxB genes in two distinct groups. *Development*, 129(22), pp.5103–5115.

Betancur, P., Bronner-Fraser, M. and Sauka-Spengler, T., 2010. Genomic code for Sox10 activation reveals a key regulatory enhancer for cranial neural crest. *Proc Natl Acad Sci U S A*, 107(8), pp.3570–3575.

Betters, E., Liu, Y., Kjaeldgaard, A., Sundström, E. and García-Castro, M.I., 2010a. Analysis of early human neural crest development. *Developmental Biology*, 344(2), pp.578–592.

Betters, E., Liu, Y., Kjaeldgaard, A., Sundström, E. and García-Castro, M.I., 2010b. Analysis of early human neural crest development. *Developmental Biology*, 344(2), pp.578–592.

Bhatt, S., Diaz, R. and Trainor, P.A., 2013. Signals and switches in Mammalian neural crest cell differentiation. *Cold Spring Harb Perspect Biol*, 5(2), pp.a008326–a008326.

Bixby, S., Kruger, G.M., Mosher, J.T., Joseph, N.M. and Morrison, S.J., 2002. Cell-intrinsic differences between stem cells from different regions of the peripheral nervous system regulate the generation of neural diversity. *Neuron*, 35(4), pp.643–656.

Bolande, R.P., 1974. The neurocristopathies: A unifying concept of disease arising in neural crest maldevelopment. *Human Pathology*, 5(4), pp.409–429.

Bolande, R.P., 1975. Hirschsprung's disease, aganglionic or hypoganglionic megacolon. Animal model: aganglionic megacolon in piebald and spotted mutant mouse strains. *Am J Pathol*, 79(1), pp.189–192.

Bondurand, N., 2003. Neuron and glia generating progenitors of the mammalian enteric nervous system isolated from foetal and postnatal gut cultures. *Development*, 130(25), pp.6387–6400.

Bondurand, N., Natarajan, D., Barlow, A., Thapar, N. and Pachnis, V., 2006. Maintenance of mammalian enteric nervous system progenitors by SOX10 and endothelin 3 signalling. *Development*, 133(10), pp.2075–2086.

Bondurand, N., Pingault, V., Goerich, D.E., Lemort, N., Sock, E., Le Caignec, C., Wegner, M. and Goossens, M., 2000. Interaction among SOX10, PAX3 and MITF, three genes altered in Waardenburg syndrome. *Hum Mol Genet*, 9(13), pp.1907–1917.

Bonstein, L., Elias, S. and Frank, D., 1998. Paraxial-Fated Mesoderm Is Required

for Neural Crest Induction inXenopusEmbryos. *Developmental Biology*, 193(2), pp.156–168.

Bowles, J., Schepers, G. and Koopman, P., 2000. Phylogeny of the SOX family of developmental transcription factors based on sequence and structural indicators. *Developmental Biology*, 227(2), pp.239–255.

Burns, A.J. and Douarin, N.M., 1998. The sacral neural crest contributes neurons and glia to the post-umbilical gut: spatiotemporal analysis of the development of the enteric nervous system. *Development*, 125(21), pp.4335–4347.

Burns, A.J., Champeval, D. and Le Douarin, N.M., 2000. Sacral Neural Crest Cells Colonise Aganglionic Hindgut in Vivo but Fail to Compensate for Lack of Enteric Ganglia. *Developmental Biology*, 219(1), pp.30–43.

Burns, A.J., Delalande, J.-M.M. and Le Douarin, N.M., 2002. In ovo transplantation of enteric nervous system precursors from vagal to sacral neural crest results in extensive hindgut colonisation. *Development*, 129(12), pp.2785–2796.

Cai, D.H. and Brauer, P.R., 2002. Synthetic matrix metalloproteinase inhibitor decreases early cardiac neural crest migration in chicken embryos. *Dev Dyn*, 224(4), pp.441–449.

Cai, D.H., Vollberg, T.M.S., Hahn-Dantona, E., Quigley, J.P. and Brauer, P.R., 2000. MMP-2 expression during early avian cardiac and neural crest morphogenesis. *Anat Rec*, 259(2), pp.168–179.

Cambray, N. and Wilson, V., 2002. Axial progenitors with extensive potency are localised to the mouse chordoneural hinge. *Development*, 129(20), pp.4855–4866.

Catala M, Teillet MA, Le Douarin NM., 1995. Organization and development of the tail bud analyzed with the quail-chick chimaera system. Mech Dev. 51(1):51-65.

Chalazonitis, A., Rothman, T.P., Chen, J. and Gershon, M.D., 1998. Age-dependent differences in the effects of GDNF and NT-3 on the development of neurons and glia from neural crest-derived precursors immunoselected from the fetal rat gut: expression of GFRalpha-1 in vitro and in vivo. *Developmental Biology*, 204(2), pp.385–406.

Chambers, S.M., Fasano, C.A., Papapetrou, E.P., Tomishima, M., Sadelain, M. and Studer, L., 2009. Highly efficient neural conversion of human ES and iPS cells by dual inhibition of SMAD signaling. *Nat Biotechnol*, 27(3), pp.275–280.

Chambers, S.M., Qi, Y., Mica, Y., Lee, G., Zhang, X.-J., Niu, L., Bilsland, J., Cao, L., Stevens, E., Whiting, P., Shi, S.-H. and Studer, L., 2012. Combined small-molecule inhibition accelerates developmental timing and converts human pluripotent stem cells into nociceptors. *Nat Biotechnol*, [online] 30(7), pp.715–720. Available

at: <http://www.ncbi.nlm.nih.gov/pubmed/22750882>.

Chawengsaksophak, K., James, R., Hammond, V.E., Kontgen, F. and Beck, F., 1997. Homeosis and intestinal tumours in Cdx2 mutant mice. *Nature*, 386(6620), pp.84–87.

Cheung, M. and Briscoe, J., 2003a. Neural crest development is regulated by the transcription factor Sox9. *Development*, 130(23), pp.5681–5693.

Cheung, M. and Briscoe, J., 2003b. Neural crest development is regulated by the transcription factor Sox9. *Development*, 130(23), pp.5681–5693.

Cheung, M., Chaboissier, M.-C., Mynett, A., Hirst, E., Schedl, A. and Briscoe, J., 2005. The transcriptional control of trunk neural crest induction, survival, and delamination. *Dev Cell*, 8(2), pp.179–192.

Cheung, N.-K.V. and Dyer, M.A., 2013. Neuroblastoma: developmental biology, cancer genomics and immunotherapy. *Nat Rev Cancer*, 13(6), pp.397–411.

Chithalen, J.V., Luu, L., Petkovich, M. and Jones, G., 2002. HPLC-MS/MS analysis of the products generated from all-trans-retinoic acid using recombinant human CYP26A. *Journal of lipid research*, 43(7), pp.1133–1142.

Chong, J.J.H., Yang, X., Don, C.W., Minami, E., Liu, Y.-W., Weyers, J.J., Mahoney, W.M., Van Biber, B., Cook, S.M., Palpant, N.J., Gantz, J.A., Fugate, J.A., Muskheli, V., Gough, G.M., Vogel, K.W., Astley, C.A., Hotchkiss, C.E., Baldessari, A., Pabon, L., Reinecke, H., Gill, E.A., Nelson, V., Kiem, H.-P., Laflamme, M.A. and Murry, C.E., 2014. Human embryonic-stem-cell-derived cardiomyocytes regenerate non-human primate hearts. *Nature*, 510(7504), pp.273–277.

Cohen, M.E., Yin, M., Paznekas, W.A., Schertzer, M., Wood, S. and Jabs, E.W., 1998. Human SLUG gene organization, expression, and chromosome map location on 8q. *Genomics*, 51(3), pp.468–471.

Cooper, J.E., McCann, C.J., Natarajan, D., Choudhury, S., Boesmans, W., Delalande, J.-M., Vanden Berghe, P., Burns, A.J. and Thapar, N., 2016. In Vivo Transplantation of Enteric Neural Crest Cells into Mouse Gut; Engraftment, Functional Integration and Long-Term Safety. *PLoS One*, 11(1), p.e0147989.

Croce, A.C. and Bottiroli, G., 2014. Autofluorescence Spectroscopy and Imaging: A Tool for Biomedical Research and Diagnosis. *European Journal of Histochemistry : EJH*, 58(4), p.2461.

Cunningham, T.J., Brade, T., Sandell, L.L., Lewandoski, M., Trainor, P.A., Colas, A., Mercola, M. and Duester, G., 2015a. Retinoic Acid Activity in Undifferentiated Neural Progenitors Is Sufficient to Fulfill Its Role in Restricting Fgf8 Expression for Somitogenesis. *PLoS One*, 10(9), p.e0137894.

Cunningham, T.J., Kumar, S., Yamaguchi, T.P. and Duester, G., 2015b. Wnt8a and

Wnt3a cooperate in the axial stem cell niche to promote mammalian body axis extension. *Dev Dyn*, 244(6), pp.797–807.

Curchoe, C.L., Maurer, J., McKeown, S.J., Cattarossi, G., Cimadamore, F., Nilbratt, M., Snyder, E.Y., Bronner-Fraser, M. and Terskikh, A.V., 2010. Early Acquisition of Neural Crest Competence During hESCs Neuralization. *PLoS One*, 5(11), p.e13890.

D'Autreaux, F., Margolis, K.G., Roberts, J., Stevanovic, K., Mawe, G., Li, Z., Karamooz, N., Ahuja, A., Morikawa, Y., Cserjesi, P., Setlick, W. and Gershon, M.D., 2011. Expression level of Hand2 affects specification of enteric neurons and gastrointestinal function in mice. *Gastroenterology*, 141(2), pp.576–87– 587.e1–6.

Dana, H., Mohar, B., Sun, Y., Narayan, S., Gordus, A., Hasseman, J.P., Tsegaye, G., Holt, G.T., Hu, A., Walpita, D., Patel, R., Macklin, J.J., Bargmann, C.I., Ahrens, M.B., Schreiter, E.R., Jayaraman, V., Looger, L.L., Svoboda, K. and Kim, D.S., 2016. Sensitive red protein calcium indicators for imaging neural activity. *Elife*, 5, p.413.

Das, B.C., Thapa, P., Karki, R., Das, S., Mahapatra, S., Liu, T.-C., Torregroza, I., Wallace, D.P., Kambhampati, S., Van Veldhuizen, P., Verma, A., Ray, S.K. and Evans, T., 2014. Retinoic acid signaling pathways in development and diseases. *Bioorganic & medicinal chemistry*, 22(2), pp.673–683.

del Barrio, M.G. and Nieto, M.A., 2002. Overexpression of Snail family members highlights their ability to promote chick neural crest formation. *Development*, 129(7), pp.1583–1593.

Denans, N., Iimura, T. and Pourquie, O., 2015. Hox genes control vertebrate body elongation by collinear Wnt repression. *Elife*, 4, p.226.

Denham, M., Hasegawa, K., Menheniott, T., Rollo, B., Zhang, D., Hough, S., Alshawaf, A., Febbraro, F., Ighaniyan, S., Leung, J., Elliott, D.A., Newgreen, D.F., Pera, M.F. and Dottori, M., 2015. Multipotent caudal neural progenitors derived from human pluripotent stem cells that give rise to lineages of the central and peripheral nervous system. *STEM CELLS*, 33(6), pp.1759–1770.

Draper, J.S., Pigott, C., Thomson, J.A. and Andrews, P.W., 2002. Surface antigens of human embryonic stem cells: changes upon differentiation in culture. *Journal of Anatomy*, 200(3), pp.249–258.

Dubrulle, J. and Pourquie, O., 2004. fgf8 mRNA decay establishes a gradient that couples axial elongation to patterning in the vertebrate embryo. *Nature*, 427(6973), pp.419–422.

Durbec, P., Marcos-Gutierrez, C.V., Kilkenny, C., Grigoriou, M., Wartiowaara, K., Suvanto, P., Smith, D., Ponder, B., Costantini, F., Saarma, M., Sariola, H. and Pachnis, V., 1996. GDNF signalling through the Ret receptor tyrosine kinase. *Nature*, 381(6585), pp.789–793.

Durston, A.J., Timmermans, J.P., Hage, W.J., Hendriks, H.F., de Vries, N.J., Heideveld, M. and Nieuwkoop, P.D., 1989. Retinoic acid causes an anteroposterior transformation in the developing central nervous system. *Nature*, 340(6229), pp.140–144.

Edery, P., Lyonnet, S., Mulligan, L.M., Pelet, A., Dow, E., Abel, L., Holder, S., Nihoul-Fekete, C., Ponder, B.A. and Munnich, A., 1994. Mutations of the RET proto-oncogene in Hirschsprung's disease. *Nature*, 367(6461), pp.378–380.

Edwards, Y.H., Putt, W., Lekoape, K.M., Stott, D., Fox, M., Hopkinson, D.A. and Sowden, J., 1996. The human homolog T of the mouse T(Brachyury) gene; gene structure, cDNA sequence, and assignment to chromosome 6q27. *Genome Res*, 6(3), pp.226–233.

Elworthy, S., Pinto, J.P., Pettifer, A., Cancela, M.L. and Kelsh, R.N., 2005. Phox2b function in the enteric nervous system is conserved in zebrafish and is sox10-dependent. *Mech Dev*, 122(5), pp.659–669.

Etoc, F., Metzger, J., Ruzo, A., Kirst, C., Yoney, A., Ozair, M.Z., Brivanlou, A.H. and Siggia, E.D., 2016. A Balance between Secreted Inhibitors and Edge Sensing Controls Gastruloid Self-Organization. *Dev Cell*, 39(3), pp.302–315.

Fasano, C.A., Chambers, S.M., Lee, G., Tomishima, M.J. and Studer, L., 2010. Efficient derivation of functional floor plate tissue from human embryonic stem cells. *Cell Stem Cell*, 6(4), pp.336–347.

Fattahi, F., Steinbeck, J.A., Kriks, S., Tchieu, J., Zimmer, B., Kishinevsky, S., Zeltner, N., Mica, Y., El-Nachef, W., Zhao, H., de Stanchina, E., Gershon, M.D., Grikscheit, T.C., Chen, S. and Studer, L., 2016. Deriving human ENS lineages for cell therapy and drug discovery in Hirschsprung disease. *Nature*, 531(7592), pp.105–109.

Faure, S., de Santa Barbara, P., Roberts, D.J. and Whitman, M., 2002. Endogenous patterns of BMP signaling during early chick development. *Developmental Biology*, 244(1), pp.44–65.

Findlay, Q., Yap, K.K., Bergner, A.J., Young, H.M. and Stamp, L.A., 2014. Enteric neural progenitors are more efficient than brain-derived progenitors at generating neurons in the colon. *Am J Physiol Gastrointest Liver Physiol*, 307(7), pp.G741–8.

Finotto, S., Krieglstein, K., Schober, A., Deimling, F., Lindner, K., Bruhl, B., Beier, K., Metz, J., Garcia-Arraras, J.E., Roig-Lopez, J.L., Monaghan, P., Schmid, W., Cole, T.J., Kellendonk, C., Tronche, F., Schutz, G. and Unsicker, K., 1999. Analysis of mice carrying targeted mutations of the glucocorticoid receptor gene argues against an essential role of glucocorticoid signalling for generating adrenal chromaffin cells. *Development*, 126(13), pp.2935–2944.

Fitch, S.R., Kimber, G.M., Wilson, N.K., Parker, A., Mirshekar-Syahkal, B., Göttgens, B., Medvinsky, A., Dzierzak, E. and Ottersbach, K., 2012. Signaling from

the Sympathetic Nervous System Regulates Hematopoietic Stem Cell Emergence during Embryogenesis. *Cell Stem Cell*, 11(4), pp.554–566.

Fuentealba, L.C., Eivers, E., Ikeda, A., Hurtado, C., Kuroda, H., Pera, E.M. and De Robertis, E.M., 2007. Integrating Patterning Signals: Wnt/GSK3 Regulates the Duration of the BMP/Smad1 Signal. *Cell*, 131(5), pp.980–993.

Fukuta, M., Nakai, Y., Kirino, K., Nakagawa, M., Sekiguchi, K., Nagata, S., Matsumoto, Y., Yamamoto, T., Umeda, K., Heike, T., Okumura, N., Koizumi, N., Sato, T., Nakahata, T., Saito, M., Otsuka, T., Kinoshita, S., Ueno, M., Ikeya, M. and Toguchida, J., 2014. Derivation of mesenchymal stromal cells from pluripotent stem cells through a neural crest lineage using small molecule compounds with defined media. *PLoS One*, 9(12), p.e112291.

Funa, N.S., Schachter, K.A., Lerdrup, M., Ekberg, J., Hess, K., Dietrich, N., Honoré, C., Hansen, K. and Semb, H., 2015. β-Catenin Regulates Primitive Streak Induction through Collaborative Interactions with SMAD2/SMAD3 and OCT4. *Cell Stem Cell*, 16(6), pp.639–652.

Furness, J.B., 2012. The enteric nervous system and neurogastroenterology. *Nat Rev Gastroenterol Hepatol*, 9(5), pp.286–294.

Gans, C. and Northcutt, R.G., 1983. Neural crest and the origin of vertebrates: a new head. *Science*, 220(4594), pp.268–273.

García-Castro, M.I., Marcelle, C. and Bronner-Fraser, M., 2002. Ectodermal Wnt function as a neural crest inducer. *Science*, 297(5582), pp.848–851.

Garnett, A.T., Square, T.A. and Medeiros, D.M., 2012. BMP, Wnt and FGF signals are integrated through evolutionarily conserved enhancers to achieve robust expression of Pax3 and Zic genes at the zebrafish neural plate border. *Development*, 139(22), pp.4220–4231.

Garriock, R.J., Chalamalasetty, R.B., Kennedy, M.W., Canizales, L.C., Lewandoski, M. and Yamaguchi, T.P., 2015. Lineage tracing of neuromesodermal progenitors reveals novel Wnt-dependent roles in trunk progenitor cell maintenance and differentiation. *Development*, 142(9), pp.1628–1638.

Gaunt, S.J., Krumlauf, R. and Duboule, D., 1989. Mouse homeo-genes within a subfamily, Hox-1.4, -2.6 and -5.1, display similar anteroposterior domains of expression in the embryo, but show stage- and tissue-dependent differences in their regulation. *Development*, 107(1), pp.131–141.

Gavriouchkina, D., Williams, R.M., Lukoseviciute, M., Hochgreb-Hägele, T., Senanayake, U., Chong-Morrison, V., Thongjuea, S., Repapi, E., Mead, A. and Sauka-Spengler, T., 2017. From pioneer to repressor: Bimodal foxd3 activity dynamically remodels neural crest regulatory landscape in vivo. *bioRxiv*, p.213611.

Gershon, M.D., 2010. Developmental determinants of the independence and complexity of the enteric nervous system. *Trends Neurosci*, 33(10), pp.446–456.

Gokhale, P.J., Giesberts, A.M. and Andrews, P.W., 2000. Brachyury is expressed by human teratocarcinoma cells in the absence of mesodermal differentiation. *Cell growth & differentiation : the molecular biology journal of the American Association for Cancer Research*, 11(3), pp.157–162.

Goldberg, E.L., 1984. An epidemiological study of Hirschsprung's disease. *International journal of epidemiology*, 13(4), pp.479–485.

Gouti, M., Tsakiridis, A., Wymeersch, F.J., Huang, Y., Kleinjung, J., Wilson, V. and Briscoe, J., 2014. In vitro generation of neuromesodermal progenitors reveals distinct roles for wnt signalling in the specification of spinal cord and paraxial mesoderm identity. *PLoS Biol*, 12(8), p.e1001937.

Guillemot, F., Lo, L.C., Johnson, J.E., Auerbach, A., Anderson, D.J. and Joyner, A.L., 1993. Mammalian achaete-scute homolog 1 is required for the early development of olfactory and autonomic neurons. *Cell*, 75(3), pp.463–476.

Gurdon, J.B., 1988. A community effect in animal development. *Nature*, 336(6201), pp.772–774.

Hackland, J.O.S., Frith, T.J.R., Thompson, O., Marin Navarro, A., García-Castro, M.I., Unger, C. and Andrews, P.W., 2017. Top-Down Inhibition of BMP Signaling Enables Robust Induction of hPSCs Into Neural Crest in Fully Defined, Xeno-free Conditions. *Stem Cell Reports*.

Hall, B.K., 2000. The neural crest as a fourth germ layer and vertebrates as quadroblastic not triploblastic. *Evolution & Development*, 2(1), pp.3–5.

Hammerschmidt, M. and Nusslein-Volhard, C., 1993. The expression of a zebrafish gene homologous to Drosophila snail suggests a conserved function in invertebrate and vertebrate gastrulation. *Development*, 119(4), p.1107.

Hao, J., Ho, J.N., Lewis, J.A., Karim, K.A., Daniels, R.N., Gentry, P.R., Hopkins, C.R., Lindsley, C.W. and Hong, C.C., 2010. In Vivo Structure Activity Relationship Study of Dorsomorphin Analogs Identifies Selective VEGF and BMP Inhibitors. *ACS chemical biology*, 5(2), pp.245–253.

Hari, L., Brault, V., Kléber, M., Lee, H.-Y., Ille, F., Leimeroth, R., Paratore, C., Suter, U., Kemler, R. and Sommer, L., 2002. Lineage-specific requirements of beta-catenin in neural crest development. *J Cell Biol*, 159(5), pp.867–880.

Heanue, T.A. and Pachnis, V., 2007. Enteric nervous system development and Hirschsprung's disease: advances in genetic and stem cell studies. *Nat Rev Neurosci*, 8(6), pp.466–479.

Heanue, T.A. and Pachnis, V., 2008. Ret isoform function and marker gene

expression in the enteric nervous system is conserved across diverse vertebrate species. *Mech Dev*, 125(8), pp.687–699.

Hirsch, M.R., Tiveron, M.C., Guillemot, F., Brunet, J.F. and Goridis, C., 1998. Control of noradrenergic differentiation and Phox2a expression by MASH1 in the central and peripheral nervous system. *Development*, 125(4), pp.599–608.

Hirst, C.S., Foong, J.P.P., Stamp, L.A., Fegan, E., Dent, S., Cooper, E.C., Lomax, A.E., Anderson, C.R., Bornstein, J.C., Young, H.M. and McKeown, S.J., 2015. Ion channel expression in the developing enteric nervous system. *PLoS One*, 10(3), p.e0123436.

His, W., 1868. *Untersuchungen über die erste Anlage des Wirbelthierleibes*.

Hofstra, R.M., Osinga, J., Tan-Sindhunata, G., Wu, Y., Kamsteeg, E.J., Stulp, R.P., van Ravenswaaij-Arts, C., Majoor-Krakauer, D., Angrist, M., Chakravarti, A., Meijers, C. and Buys, C.H., 1996. A homozygous mutation in the endothelin-3 gene associated with a combined Waardenburg type 2 and Hirschsprung phenotype (Shah-Waardenburg syndrome). *Nature Genetics*, 12(4), pp.445–447.

Hore, T.A., Meyenn, von, F., Ravichandran, M., Bachman, M., Ficz, G., Oxley, D., Santos, F., Balasubramanian, S., Jurkowski, T.P. and Reik, W., 2016. Retinol and ascorbate drive erasure of epigenetic memory and enhance reprogramming to naive pluripotency by complementary mechanisms. *Proc Natl Acad Sci U S A*, 113(43), pp.12202–12207.

Hosoda, K., Hammer, R.E., Richardson, J.A., Baynash, A.G., Cheung, J.C., Giaid, A. and Yanagisawa, M., 1994. Targeted and natural (piebald-lethal) mutations of endothelin-B receptor gene produce megacolon associated with spotted coat color in mice. *Cell*, 79(7), pp.1267–1276.

Howard, M.J., 2005. Mechanisms and perspectives on differentiation of autonomic neurons. *Developmental Biology*, 277(2), pp.271–286.

Huang, J., Dang, R., Torigoe, D., Lei, C., Lan, X., Chen, H., Sasaki, N., Wang, J. and Agui, T., 2015. Identification of Genetic Loci Affecting the Severity of Symptoms of Hirschsprung Disease in Rats Carrying Ednrbsl Mutations by Quantitative Trait Locus Analysis. *PLoS One*, 10(3), p.e0122068.

Huang, M., Miller, M.L., McHenry, L.K., Zheng, T., Zhen, Q., Ilkhanizadeh, S., Conklin, B.R., Bronner, M.E. and Weiss, W.A., 2016. Generating trunk neural crest from human pluripotent stem cells. *Sci Rep*, 6, p.19727.

Huber, K., 2006. The sympathoadrenal cell lineage: specification, diversification, and new perspectives. *Developmental Biology*, 298(2), pp.335–343.

Huber, K., 2015. Segregation of neuronal and neuroendocrine differentiation in the sympathoadrenal lineage. *Cell Tissue Res*, 359(1), pp.333–341.

Huber, K., Franke, A., Bruhl, B., Krispin, S., Ernsberger, U., Schober, A., Bohlen und Halbach, von, O., Rohrer, H., Kalcheim, C. and Unsicker, K., 2008. Persistent expression of BMP-4 in embryonic chick adrenal cortical cells and its role in chromaffin cell development. *Neural Dev*, 3, p.28.

Huber, K., Kalcheim, C. and Unsicker, K., 2009. The development of the chromaffin cell lineage from the neural crest. *Autonomic neuroscience : basic & clinical*, 151(1), pp.10–16.

Huber, L., Ferdin, M., Holzmann, J., Stubbusch, J. and Rohrer, H., 2012. HoxB8 in noradrenergic specification and differentiation of the autonomic nervous system. *Dev Biol*, 363(1), pp.219–233.

Ikenouchi, J., Matsuda, M., Furuse, M. and Tsukita, S., 2003. Regulation of tight junctions during the epithelium-mesenchyme transition: direct repression of the gene expression of claudins/occludin by Snail. *J Cell Sci*, 116(Pt 10), pp.1959–1967.

Ikeya, M. and Takada, S., 2001. Wnt-3a is required for somite specification along the anteroposterior axis of the mouse embryo and for regulation of cdx-1 expression. *Mech Dev*, 103(1-2), pp.27–33.

Isern, J., Garcia-Garcia, A., Martin, A.M., Arranz, L., Martin-Perez, D., Torroja, C., Sanchez-Cabo, F. and Mendez-Ferrer, S., 2014. The neural crest is a source of mesenchymal stem cells with specialized hematopoietic stem cell niche function. *Elife*, 3, p.e03696.

Itasaki, N., Sharpe, J., Morrison, A. and Krumlauf, R., 1996. Reprogramming Hox Expression in the Vertebrate Hindbrain: Influence of Paraxial Mesoderm and Rhombomere Transposition. *Neuron*, 16(3), pp.487–500.

Iwafuchi-Doi, M., Matsuda, K., Murakami, K., Niwa, H., Tesar, P.J., Aruga, J., Matsuo, I. and Kondoh, H., 2012. Transcriptional regulatory networks in epiblast cells and during anterior neural plate development as modeled in epiblast stem cells. *Development*, 139(21), pp.3926–3937.

Izpisua Belmonte, J.C., Falkenstein, H., Dolle, P., Renucci, A. and Duboule, D., 1991. Murine genes related to the Drosophila AbdB homeotic genes are sequentially expressed during development of the posterior part of the body. *EMBO J*, 10(8), pp.2279–2289.

Jiang, X., Gwye, Y., McKeown, S.J., Bronner-Fraser, M., Lutzko, C. and Lawlor, E.R., 2009. Isolation and characterization of neural crest stem cells derived from in vitro-differentiated human embryonic stem cells. *Stem Cells Dev*, 18(7), pp.1059–1070.

John, N., Cinelli, P., Wegner, M. and Sommer, L., 2011. Transforming growth factor beta-mediated Sox10 suppression controls mesenchymal progenitor generation in neural crest stem cells. *STEM CELLS*, 29(4), pp.689–699.

Kao, T., Labonne, T., Niclis, J.C., Chaurasia, R., Lokmic, Z., Qian, E., Bruveris, F.F., Howden, S.E., Motazedian, A., Schiesser, J.V., Costa, M., Sourris, K., Ng, E., Anderson, D., Giudice, A., Farlie, P., Cheung, M., Lamande, S.R., Penington, A.J., Parish, C.L., Thomson, L.H., Rafii, A., Elliott, D.A., Elefanty, A.G. and Stanley, E.G., 2016. GAPTrap: A Simple Expression System for Pluripotent Stem Cells and Their Derivatives. *Stem Cell Reports*, 7(3), pp.518–526.

Kappen, C., Schughart, K. and Ruddle, F.H., 1989. Two steps in the evolution of Antennapedia-class vertebrate homeobox genes. *Proc Natl Acad Sci U S A*, 86(14), pp.5459–5463.

Kaufman, C.K., Mosimann, C., Fan, Z.P., Yang, S., Thomas, A.J., Ablain, J., Tan, J.L., Fogley, R.D., van Rooijen, E., Hagedorn, E.J., Ciarlo, C., White, R.M., Matos, D.A., Puller, A.-C., Santoriello, C., Liao, E.C., Young, R.A. and Zon, L.I., 2016. A zebrafish melanoma model reveals emergence of neural crest identity during melanoma initiation. *Science*, 351(6272).

Kawaguchi, J., Nichols, J., Gierl, M.S., Faial, T. and Smith, A., 2010. Isolation and propagation of enteric neural crest progenitor cells from mouse embryonic stem cells and embryos. *Development*, 137(5), pp.693–704.

Kellerer, S., 2006. Replacement of the Sox10 transcription factor by Sox8 reveals incomplete functional equivalence. *Development*, 133(15), pp.2875–2886.

Khudyakov, J. and Bronner-Fraser, M., 2009. Comprehensive spatiotemporal analysis of early chick neural crest network genes. *Developmental Dynamics*, 238(3), pp.716–723.

Kilpinen, H., Goncalves, A., Leha, A., Afzal, V., Alasoo, K., Ashford, S., Bala, S., Bensaddek, D., Casale, F.P., Culley, O.J., Danecek, P., Faulconbridge, A., Harrison, P.W., Kathuria, A., McCarthy, D., McCarthy, S.A., Meleckyte, R., Memari, Y., Moens, N., Soares, F., Mann, A., Streeter, I., Agu, C.A., Alderton, A., Nelson, R., Harper, S., Patel, M., White, A., Patel, S.R., Clarke, L., Halai, R., Kirton, C.M., Kolb-Kokocinski, A., Beales, P., Birney, E., Danovi, D., Lamond, A.I., Ouwehand, W.H., Vallier, L., Watt, F.M., Durbin, R., Stegle, O. and Gaffney, D.J., 2017. Common genetic variation drives molecular heterogeneity in human iPSCs. *Nature*.

Kim, J., Lo, L., Dormand, E. and Anderson, D.J., 2003. SOX10 Maintains Multipotency and Inhibits Neuronal Differentiation of Neural Crest Stem Cells. *Neuron*, 38(1), pp.17–31.

Kim, Y.J., Lim, H., Li, Z., Oh, Y., Kovlyagina, I., Choi, I.Y., Dong, X. and Lee, G., 2014. Generation of multipotent induced neural crest by direct reprogramming of human postnatal fibroblasts with a single transcription factor. *Cell Stem Cell*, 15(4), pp.497–506.

Kirby, M.L., Gale, T.F. and Stewart, D.E., 1983. Neural crest cells contribute to normal aorticopulmonary septation. *Science*, 220(4601), pp.1059–1061.

Kispert, A. and Herrmann, B.G., 1994. Immunohistochemical analysis of the Brachyury protein in wild-type and mutant mouse embryos. *Developmental Biology*, 161(1), pp.179–193.

Knight, R.D., Nair, S., Nelson, S.S., Afshar, A., Javidan, Y., Geisler, R., Rauch, G.-J. and Schilling, T.F., 2003. lockjaw encodes a zebrafish tfap2a required for early neural crest development. *Development*, 130(23), pp.5755–5768.

Koch, F., Scholze, M., Wittler, L., Schifferl, D., Sudheer, S., Grote, P., Timmermann, B., Macura, K. and Herrmann, B.G., 2017. Antagonistic Activities of Sox2 and Brachyury Control the Fate Choice of Neuro-Mesodermal Progenitors. *Dev Cell*.

KOHLER, G. and MILSTEIN, C., 1975. Continuous cultures of fused cells secreting antibody of predefined specificity. *Nature*, 256(5517), pp.495–497.

Kondoh, H., Takada, S. and Takemoto, T., 2016. Axial level-dependent molecular and cellular mechanisms underlying the genesis of the embryonic neural plate. *Dev Growth Differ*, 58(5), pp.427–436.

Kreitzer, F.R., Salomonis, N., Sheehan, A., Huang, M., Park, J.S., Spindler, M.J., Lizarraga, P., Weiss, W.A., So, P.-L. and Conklin, B.R., 2013. A robust method to derive functional neural crest cells from human pluripotent stem cells. *American journal of stem cells*, 2(2), pp.119–131.

Krishnakumar, R., Chen, A.F., Pantovich, M.G., Danial, M., Parchem, R.J., Labosky, P.A. and Blelloch, R., 2016. FOXD3 Regulates Pluripotent Stem Cell Potential by Simultaneously Initiating and Repressing Enhancer Activity. *Cell Stem Cell*, 18(1), pp.104–117.

Krumlauf, R., 1994. Hox genes in vertebrate development. *Cell*, 78(2), pp.191–201.

Kulesa, P.M. and Fraser, S.E., 1998. Neural crest cell dynamics revealed by time-lapse video microscopy of whole embryo chick explant cultures. *Developmental Biology*, 204(2), pp.327–344.

Kumar, S. and Duester, G., 2014. Retinoic acid controls body axis extension by directly repressing Fgf8 transcription. *Development*, 141(15), pp.2972–2977.

LaBonne, C. and Bronner-Fraser, M., 1998. Neural crest induction in Xenopus: evidence for a two-signal model. *Development*, 125(13), pp.2403–2414.

LaBonne, C. and Bronner-Fraser, M., 2000. Snail-Related Transcriptional Repressors Are Required in Xenopus for both the Induction of the Neural Crest and Its Subsequent Migration. *Developmental Biology*, 221(1), pp.195–205.

Lai, F.P.-L., Lau, S.-T., Wong, J.K.-L., Gui, H., Wang, R.X., Zhou, T., Lai, W.H., Tse, H.-F., Tam, P.K.H., Garcia-Barcelo, M.M. and Ngan, E.S.-W., 2017. Correction of Hirschsprung-Associated Mutations in Human Induced Pluripotent Stem Cells Via

Clustered Regularly Interspaced Short Palindromic Repeats/Cas9, Restores Neural Crest Cell Function. *Gastroenterology*.

Lamb, T.M., Knecht, A.K., Smith, W.C., Stachel, S.E., Economides, A.N., Stahl, N., Yancopolous, G.D. and Harland, R.M., 1993. Neural induction by the secreted polypeptide noggin. *Science*, 262(5134), pp.713–718.

Lang, D. and Epstein, J.A., 2003. Sox10 and Pax3 physically interact to mediate activation of a conserved c-RET enhancer. *Hum Mol Genet*, 12(8), pp.937–945.

Langston, A.W., Thompson, J.R. and Gudas, L.J., 1997. Retinoic acid-responsive enhancers located 3' of the Hox A and Hox B homeobox gene clusters. Functional analysis. *Journal of Biological Chemistry*, 272(4), pp.2167–2175.

Lasrado, R., Boesmans, W., Kleinjung, J., Pin, C., Bell, D., Bhaw, L., McCallum, S., Zong, H., Luo, L., Clevers, H., Vanden Berghe, P. and Pachnis, V., 2017. Lineage-dependent spatial and functional organization of the mammalian enteric nervous system. *Science*, 356(6339), pp.722–726.

Le Douarin, N.M. and Dupin, E., 2003. Multipotentiality of the neural crest. *Curr Opin Genet Dev*, 13(5), pp.529–536.

Le Douarin, N.M. and Teillet, M.A., 1973. The migration of neural crest cells to the wall of the digestive tract in avian embryo. *J Embryol Exp Morphol*, 30(1), pp.31–48.

Le Douarin, N.M. and Teillet, M.A., 1974. Experimental analysis of the migration and differentiation of neuroblasts of the autonomic nervous system and of neurectodermal mesenchymal derivatives, using a biological cell marking technique. *Developmental Biology*, 41(1), pp.162–184.

Le Douarin, N.M., 2004. The avian embryo as a model to study the development of the neural crest: a long and still ongoing story. *Mech Dev*, 121(9), pp.1089–1102.

Le Douarin, N.M., Creuzet, S., Couly, G. and Dupin, E., 2004. Neural crest cell plasticity and its limits. *Development*, 131(19), pp.4637–4650.

Le Lièvre, C.S. and Le Douarin, N.M., 1975. Mesenchymal derivatives of the neural crest: analysis of chimaeric quail and chick embryos. *J Embryol Exp Morphol*, 34(1), pp.125–154.

Le-Douarin, N., 1973. A biological cell labeling technique and its use in experimental embryology. *Developmental Biology*, 30(1), pp.217–222.

Lee, G., Kim, H., Elkabetz, Y., Shamy, Al, G., Panagiotakos, G., Barberi, T., Tabar, V. and Studer, L., 2007. Isolation and directed differentiation of neural crest stem cells derived from human embryonic stem cells. *Nat Biotechnol*, 25(12), pp.1468–1475.

Lee, G., Papapetrou, E.P., Kim, H., Chambers, S.M., Tomishima, M.J., Fasano, C.A., Ganat, Y.M., Menon, J., Shimizu, F., Viale, A., Tabar, V., Sadelain, M. and Studer, L., 2009. Modelling pathogenesis and treatment of familial dysautonomia using patient-specific iPSCs. *Nature*, 461(7262), pp.402–406.

Lee, H.-Y., Kléber, M., Hari, L., Brault, V., Suter, U., Taketo, M.M., Kemler, R. and Sommer, L., 2004. Instructive role of Wnt/beta-catenin in sensory fate specification in neural crest stem cells. *Science*, 303(5660), pp.1020–1023.

Leung, A.W., Kent Morest, D. and Li, J.Y.H., 2013. Differential BMP signaling controls formation and differentiation of multipotent preplacodal ectoderm progenitors from human embryonic stem cells. *Dev Biol*, 379(2), pp.208–220.

Leung, A.W., Murdoch, B., Salem, A.F., Prasad, M.S., Gomez, G.A. and García-Castro, M.I., 2016. WNT/β-catenin signaling mediates human neural crest induction via a pre-neural border intermediate. *Development*, 143(3), pp.398–410.

Levin, A.A., Sturzenbecker, L.J., Kazmer, S., Bosakowski, T., Huselton, C., Allenby, G., Speck, J., Kratzeisen, C., Rosenberger, M. and Lovey, A., 1992. 9-cis retinoic acid stereoisomer binds and activates the nuclear receptor RXR alpha. *Nature*, 355(6358), pp.359–361.

Lewis, A.E., Vasudevan, H.N., O'Neill, A.K., Soriano, P. and Bush, J.O., 2013. The widely used Wnt1-Cre transgene causes developmental phenotypes by ectopic activation of Wnt signaling. *Dev Biol*, 379(2), pp.229–234.

Lewis, E.B., 1978. A gene complex controlling segmentation in Drosophila. *Nature*, 276(5688), pp.565–570.

Lewis, J.L., Bonner, J., Modrell, M., Ragland, J.W., Moon, R.T., Dorsky, R.I. and Raible, D.W., 2004. Reiterated Wnt signaling during zebrafish neural crest development. *Development*, 131(6), pp.1299–1308.

Li, W., Huang, L., Zeng, J., Lin, W., Li, K., Sun, J., Huang, W., Chen, J., Wang, G., Ke, Q., Duan, J., Lai, X., Chen, R., Liu, M., Liu, Y., Wang, T., Yang, X., Chen, Y., Xia, H. and Xiang, A.P., 2016. Characterization and transplantation of enteric neural crest cells from human induced pluripotent stem cells.

Liem, K.F., Jr., Tremml, G., Roelink, H. and Jessell, T.M., 1995. Dorsal differentiation of neural plate cells induced by BMP-mediated signals from epidermal ectoderm. *Cell*, 82(6), pp.969–979.

Liem, K.F.J., Jessell, T.M. and Briscoe, J., 2000. Regulation of the neural patterning activity of sonic hedgehog by secreted BMP inhibitors expressed by notochord and somites. *Development*, 127(22), pp.4855–4866.

Lindley, R.M., Hawcutt, D.B., Connell, M.G., Almond, S.N., Vannucchi, M.G., Faussone-Pellegrini, M.S., Edgar, D.H. and Kenny, S.E., 2008. Human and Mouse

Enteric Nervous System Neurosphere Transplants Regulate the Function of Aganglionic Embryonic Distal Colon. *Gastroenterology*, 135(1), pp.205–216.e6.

Linker, C., Bronner-Fraser, M. and Mayor, R., 2000. Relationship between gene expression domains of Xsnail, Xslug, and Xtwist and cell movement in the prospective neural crest of Xenopus. *Developmental Biology*, 224(2), pp.215–225.

Lippmann, E.S., Williams, C.E., Ruhl, D.A., Estevez-Silva, M.C., Chapman, E.R., Coon, J.J. and Ashton, R.S., 2015. Deterministic HOX patterning in human pluripotent stem cell-derived neuroectoderm. *Stem Cell Reports*, 4(4), pp.632–644.

Liu, J.P., Laufer, E. and Jessell, T.M., 2001. Assigning the positional identity of spinal motor neurons: rostrocaudal patterning of Hox-c expression by FGFs, Gdf11, and retinoids. *Neuron*, 32(6), pp.997–1012.

Lobb, R.R. and Hemler, M.E., 1994. The pathophysiologic role of alpha 4 integrins in vivo. *J Clin Invest*, 94(5), pp.1722–1728.

Loh, K.M., Ang, L.T., Zhang, J., Kumar, V., Ang, J., Auyeong, J.Q., Lee, K.L., Choo, S.H., Lim, C.Y.Y., Nichane, M., Tan, J., Noghabi, M.S., Azzola, L., Ng, E.S., Durruthy-Durruthy, J., Sebastiano, V., Poellinger, L., Elefanty, A.G., Stanley, E.G., Chen, Q., Prabhakar, S., Weissman, I.L. and Lim, B., 2014. Efficient Endoderm Induction from Human Pluripotent Stem Cells by Logically Directing Signals Controlling Lineage Bifurcations. *Cell Stem Cell*, 14(2), pp.237–252.

Loh, K.M., Chen, A., Koh, P.W., Deng, T.Z., Sinha, R., Tsai, J.M., Barkal, A.A., Shen, K.Y., Jain, R., Morganti, R.M., Shyh-Chang, N., Fernhoff, N.B., George, B.M., Wernig, G., Salomon, R.E.A., Chen, Z., Vogel, H., Epstein, J.A., Kundaje, A., Talbot, W.S., Beachy, P.A., Ang, L.T. and Weissman, I.L., 2016. Mapping the Pairwise Choices Leading from Pluripotency to Human Bone, Heart, and Other Mesoderm Cell Types. *Cell*, 166(2), pp.451–467.

Lumb, R. and Schwarz, Q., 2015. Sympathoadrenal neural crest cells: the known, unknown and forgotten? *Dev Growth Differ*, 57(2), pp.146–157.

Lumb, R., Buckberry, S., Secker, G., Lawrence, D. and Schwarz, Q., 2017. Transcriptome profiling reveals expression signatures of cranial neural crest cells arising from different axial levels. *BMC Dev Biol*, 17(1), p.5.

Luo, T., Lee, Y.-H., Saint-Jeannet, J.-P. and Sargent, T.D., 2003. Induction of neural crest in Xenopus by transcription factor AP2α. *Proc Natl Acad Sci U S A*, 100(2), pp.532–537.

MacDonald, B.T., Tamai, K. and He, X., 2009. Wnt/β-catenin signaling: components, mechanisms, and diseases. *Dev Cell*, 17(1), pp.9–26.

Maczkowiak, F., Matéos, S., Wang, E., Roche, D., Harland, R. and Monsoro-Burq, A.H., 2010. The Pax3 and Pax7 paralogs cooperate in neural and neural crest

patterning using distinct molecular mechanisms, in Xenopus laevis embryos. *Developmental Biology*, 340(2), pp.381–396.

Mallo, M. and Alonso, C.R., 2013. The regulation of Hox gene expression during animal development. *Development*, 140(19), pp.3951–3963.

Mangelsdorf, D.J., Ong, E.S., Dyck, J.A. and Evans, R.M., 1990. Nuclear receptor that identifies a novel retinoic acid response pathway. *Nature*, 345(6272), pp.224–229.

Martin, B.L. and Kimelman, D., 2012. Canonical Wnt Signaling Dynamically Controls Multiple Stem Cell Fate Decisions during Vertebrate Body Formation. *Dev Cell*, 22(1), pp.223–232.

Maves, L. and Kimmel, C.B., 2005. Dynamic and sequential patterning of the zebrafish posterior hindbrain by retinoic acid. *Developmental Biology*, 285(2), pp.593–605.

Mazzoni, E.O., Mahony, S., Peljto, M., Patel, T., Thornton, S.R., McCuine, S., Reeder, C., Boyer, L.A., Young, R.A., Gifford, D.K. and Wichterle, H., 2013. Saltatory remodeling of Hox chromatin in response to rostrocaudal patterning signals. *Nat Neurosci*, 16(9), pp.1191–1198.

McCann, C.J., Cooper, J.E., Natarajan, D., Jevans, B., Burnett, L.E., Burns, A.J. and Thapar, N., 2017. Transplantation of enteric nervous system stem cells rescues nitric oxide synthase deficient mouse colon. *Nat Commun*, 8, p.15937.

McCusker, C., Cousin, H., Neuner, R. and Alfandari, D., 2009. Extracellular Cleavage of Cadherin-11 by ADAM Metalloproteases Is Essential for Xenopus Cranial Neural Crest Cell Migration. *Molecular Biology of the Cell*, 20(1), pp.78–89.

McKeown, S.J., Lee, V.M., Bronner-Fraser, M., Newgreen, D.F. and Farlie, P.G., 2005a. Sox10 overexpression induces neural crest-like cells from all dorsoventral levels of the neural tube but inhibits differentiation. *Dev Dyn*, 233(2), pp.430–444.

McKeown, S.J., Lee, V.M., Bronner-Fraser, M., Newgreen, D.F. and Farlie, P.G., 2005b. Sox10 overexpression induces neural crest-like cells from all dorsoventral levels of the neural tube but inhibits differentiation. *Developmental Dynamics*, 233(2), pp.430–444.

McKeown, S.J., Stamp, L., Hao, M.M. and Young, H.M., 2013. Hirschsprung disease: a developmental disorder of the enteric nervous system. *Wiley Interdiscip Rev Dev Biol*, 2(1), pp.113–129.

McLennan, R., Schumacher, L.J., Morrison, J.A., Teddy, J.M., Ridenour, D.A., Box, A.C., Semerad, C.L., Li, H., McDowell, W., Kay, D., Maini, P.K., Baker, R.E. and Kulesa, P.M., 2015a. Neural crest migration is driven by a few trailblazer cells with a unique molecular signature narrowly confined to the invasive front.

Development, 142(11), pp.2014–2025.

McLennan, R., Schumacher, L.J., Morrison, J.A., Teddy, J.M., Ridenour, D.A., Box, A.C., Semerad, C.L., Li, H., McDowell, W., Kay, D., Maini, P.K., Baker, R.E. and Kulesa, P.M., 2015b. VEGF signals induce trailblazer cell identity that drives neural crest migration. *Dev Biol*, 407(1), pp.12–25.

McPherron, A.C., Lawler, A.M. and Lee, S.J., 1999. Regulation of anterior/posterior patterning of the axial skeleton by growth/differentiation factor 11. *Nature Genetics*, 22(3), pp.260–264.

Meinhardt, A., Eberle, D., Tazaki, A., Ranga, A., Niesche, M., Wilsch-Bräuninger, M., Stec, A., Schackert, G., Lutolf, M. and Tanaka, E.M., 2014. 3D Reconstitution of the Patterned Neural Tube from Embryonic Stem Cells. *Stem Cell Reports*, 3(6), pp.987–999.

Memic, F., Knoflach, V., Sadler, R., Tegerstedt, G., Sundström, E., Guillemot, F., Pachnis, V. and Marklund, U., 2016. Ascl1 Is Required for the Development of Specific Neuronal Subtypes in the Enteric Nervous System. *J Neurosci*, 36(15), pp.4339–4350.

Mendjan, S., Mascetti, V.L., Ortmann, D., Ortiz, M., Karjosukarso, D.W., Ng, Y., Moreau, T. and Pedersen, R.A., 2014. NANOG and CDX2 Pattern Distinct Subtypes of Human Mesoderm during Exit from Pluripotency. *Cell Stem Cell*, 15(3), pp.310–325.

Menendez, L., Yatskievych, T.A., Antin, P.B. and Dalton, S., 2011. Wnt signaling and a Smad pathway blockade direct the differentiation of human pluripotent stem cells to multipotent neural crest cells. *Proc Natl Acad Sci U S A*, 108(48), pp.19240–19245.

Mica, Y., Lee, G., Chambers, S.M., Tomishima, M.J. and Studer, L., 2013. Modeling neural crest induction, melanocyte specification, and disease-related pigmentation defects in hESCs and patient-specific iPSCs. *Cell Rep*, 3(4), pp.1140–1152.

Milunsky, J.M., Maher, T.A., Zhao, G., Roberts, A.E., Stalker, H.J., Zori, R.T., Burch, M.N., Clemens, M., Mulliken, J.B., Smith, R. and Lin, A.E., 2008. TFAP2A Mutations Result in Branchio-Oculo-Facial Syndrome. *Am J Hum Genet*, 82(5), pp.1171–1177.

Minoux, M., Holwerda, S., Vitobello, A., Kitazawa, T., Kohler, H., Stadler, M.B. and Rijli, F.M., 2017. Gene bivalency at Polycomb domains regulates cranial neural crest positional identity. *Science*, 355(6332), p.eaal2913.

Monsoro-Burq, A.-H., Fletcher, R.B. and Harland, R.M., 2003. Neural crest induction by paraxial mesoderm in Xenopus embryos requires FGF signals. *Development*, 130(14), pp.3111–3124.

Monsoro-Burq, A.-H., Wang, E. and Harland, R., 2005. Msx1 and Pax3 cooperate to mediate FGF8 and WNT signals during Xenopus neural crest induction. *Dev Cell*, 8(2), pp.167–178.

Mori-Akiyama, Y., Akiyama, H., Rowitch, D.H. and de Crombrugghe, B., 2003. Sox9 is required for determination of the chondrogenic cell lineage in the cranial neural crest. *Proc Natl Acad Sci U S A*, 100(16), pp.9360–9365.

Morikawa, Y., Maska, E., Brody, H. and Cserjesi, P., 2009. Sonic hedgehog signaling is required for sympathetic nervous system development. *Neuroreport*, 20(7), pp.684–688.

Motohashi, T., Watanabe, N., Nishioka, M., Nakatake, Y., Yulan, P., Mochizuki, H., Kawamura, Y., Ko, M.S.H., Goshima, N. and Kunisada, T., 2016. Gene array analysis of neural crest cells identifies transcription factors necessary for direct conversion of embryonic fibroblasts into neural crest cells. *Biol Open*, 5(3), pp.311–322.

Murdoch, B., DelConte, C. and García-Castro, M.I., 2012. Pax7 Lineage Contributions to the Mammalian Neural Crest. *PLoS One*, 7(7), p.e41089.

Nakagawa, S. and Takeichi, M., 1995. Neural crest cell-cell adhesion controlled by sequential and subpopulation-specific expression of novel cadherins. *Development*, 121(5), pp.1321–1332.

Nataf, V., Amemiya, A., Yanagisawa, M. and Le Douarin, N.M., 1998. The expression pattern of endothelin 3 in the avian embryo. *Mech Dev*, 73(2), pp.217–220.

Natarajan, D., Cooper, J., Choudhury, S., Delalande, J.-M., McCann, C., Howe, S.J., Thapar, N. and Burns, A.J., 2014. Lentiviral labeling of mouse and human enteric nervous system stem cells for regenerative medicine studies. *Neurogastroenterol Motil*, 26(10), pp.1513–1518.

Natarajan, D., Marcos-Gutierrez, C., Pachnis, V. and de Graaff, E., 2002. Requirement of signalling by receptor tyrosine kinase RET for the directed migration of enteric nervous system progenitor cells during mammalian embryogenesis. *Development*, 129(22), pp.5151–5160.

Neuner, R., Cousin, H., McCusker, C., Coyne, M. and Alfandari, D., 2008. Xenopus ADAM19 is involved in neural, neural crest and muscle development. *Mech Dev*, 126(3-4), pp.240–255.

Niederreither, K., McCaffery, P., Drager, U.C., Chambon, P. and Dolle, P., 1997. Restricted expression and retinoic acid-induced downregulation of the retinaldehyde dehydrogenase type 2 (RALDH-2) gene during mouse development. *Mech Dev*, 62(1), pp.67–78.

Niederreither, K., Subbarayan, V., Dolle, P. and Chambon, P., 1999. Embryonic retinoic acid synthesis is essential for early mouse post-implantation

development. *Nature Genetics*, 21(4), pp.444–448.

Nieto, M.A., Bennett, M.F., Sargent, M.G. and Wilkinson, D.G., 1992. Cloning and developmental expression of Sna, a murine homologue of the Drosophila snail gene. *Development*, 116(1), pp.227–237.

Nieto, M.A., Sargent, M.G., Wilkinson, D.G. and Cooke, J., 1994. Control of cell behavior during vertebrate development by Slug, a zinc finger gene. *Science*, 264(5160), pp.835–839.

Nikitina, N., Sauka-Spengler, T. and Bronner-Fraser, M., 2008. Dissecting early regulatory relationships in the lamprey neural crest gene network. *Proc Natl Acad Sci U S A*, 105(51), pp.20083–20088.

Nishiyama, C., Uesaka, T., Manabe, T., Yonekura, Y., Nagasawa, T., Newgreen, D.F., Young, H.M. and Enomoto, H., 2012. Trans-mesenteric neural crest cells are the principal source of the colonic enteric nervous system. *Nat Neurosci*, 15(9), pp.1211–1218.

Noden, D.M., 1983. The role of the neural crest in patterning of avian cranial skeletal, connective, and muscle tissues. *Developmental Biology*, 96(1), pp.144–165.

Noy, N., Slosberg, E. and Scarlata, S., 1992. Interactions of retinol with binding proteins: studies with retinol-binding protein and with transthyretin. *Biochemistry*, 31(45), pp.11118–11124.

O Rahilly, R. and Müller, F., 2007. The development of the neural crest in the human. *J Anat*, 211(3), pp.335–351.

O'Donnell, M., Hong, C.-S., Huang, X., Delnicki, R.J. and Saint-Jeannet, J.-P., 2006. Functional analysis of Sox8 during neural crest development in Xenopus. *Development*, 133(19), pp.3817–3826.

Ogata, T., Kozuka, T. and Kanda, T., 2003. Identification of an insulator in AAVS1, a preferred region for integration of adeno-associated virus DNA. *Journal of virology*, 77(16), pp.9000–9007.

Oh, Y., Cho, G.-S., Li, Z., Hong, I., Zhu, R., Kim, M.-J., Kim, Y.J., Tampakakis, E., Tung, L., Huganir, R., Dong, X., Kwon, C. and Lee, G., 2016. Functional Coupling with Cardiac Muscle Promotes Maturation of hPSC-Derived Sympathetic Neurons. *Cell Stem Cell*, 19(1), pp.95–106.

Okada, Y., Shimazaki, T., Sobue, G. and Okano, H., 2004. Retinoic-acid-concentration-dependent acquisition of neural cell identity during in vitro differentiation of mouse embryonic stem cells. *Developmental Biology*, 275(1), pp.124–142.

Olivera-Martínez, I., Harada, H., Halley, P.A. and Storey, K.G., 2012. Loss of FGF-

Dependent Mesoderm Identity and Rise of Endogenous Retinoid Signalling Determine Cessation of Body Axis Elongation. *PLoS Biol*, 10(10), p.e1001415.

Osorio, L., Teillet, M.-A., Palmeirim, I. and Catala, M., 2009. Neural crest ontogeny during secondary neurulation: a gene expression pattern study in the chick embryo. *The International journal of developmental biology*, 53(4), pp.641–648.

Papalopulu, N. and Kintner, C., 1996. A posteriorising factor, retinoic acid, reveals that anteroposterior patterning controls the timing of neuronal differentiation in Xenopus neuroectoderm. *Development*, 122(11), pp.3409–3418.

Papalopulu, N., Clarke, J.D., Bradley, L., Wilkinson, D., Krumlauf, R. and Holder, N., 1991. Retinoic acid causes abnormal development and segmental patterning of the anterior hindbrain in Xenopus embryos. *Development*, 113(4), pp.1145–1158.

Pattyn, A., Hirsch, M., Goridis, C. and Brunet, J.F., 2000. Control of hindbrain motor neuron differentiation by the homeobox gene Phox2b. *Development*, 127(7), pp.1349–1358.

Pattyn, A., Morin, X., Cremer, H., Goridis, C. and Brunet, J.F., 1999. The homeobox gene Phox2b is essential for the development of autonomic neural crest derivatives. *Nature*, 399(6734), pp.366–370.

Paznekas, W.A., Okajima, K., Schertzer, M., Wood, S. and Jabs, E.W., 1999. Genomic organization, expression, and chromosome location of the human SNAIL gene (SNAI1) and a related processed pseudogene (SNAI1P). *Genomics*, 62(1), pp.42–49.

Pearce, J.J. and Evans, M.J., 1999. Mml, a mouse Mix-like gene expressed in the primitive streak. *Mech Dev*, 87(1-2), pp.189–192.

Piccolo, S., Sasai, Y., Lu, B. and De Robertis, E.M., 1996. Dorsoventral patterning in Xenopus: inhibition of ventral signals by direct binding of chordin to BMP-4. *Cell*, 86(4), pp.589–598.

Portier, M.M., de Nechaud, B. and Gros, F., 1983. Peripherin, a new member of the intermediate filament protein family. *Developmental neuroscience*, 6(6), pp.335–344.

Rada-Iglesias, A., Bajpai, R., Prescott, S., Brugmann, S.A., Swigut, T. and Wysocka, J., 2012. Epigenomic Annotation of Enhancers Predicts Transcriptional Regulators of Human Neural Crest. *Cell Stem Cell*, 11(5), pp.633–648.

Reijntjes, S., Gale, E. and Maden, M., 2004. Generating gradients of retinoic acid in the chick embryo: Cyp26C1 expression and a comparative analysis of the Cyp26 enzymes. *Dev Dyn*, 230(3), pp.509–517.

Respuela, P., Nikolić, M., Tan, M., Frommolt, P., Zhao, Y., Wysocka, J. and Rada-Iglesias, A., 2016. Foxd3 Promotes Exit from Naive Pluripotency through Enhancer

Decommissioning and Inhibits Germline Specification. *Cell Stem Cell*, 18(1), pp.118–133.

Rhinn, M. and Dollé, P., 2012. Retinoic acid signalling during development. *Development*, 139(5), pp.843–858.

Richardson, J., Gauert, A., Briones Montecinos, L., Fanlo, L., Alhashem, Z.M., Assar, R., Marti, E., Kabla, A., Hartel, S. and Linker, C., 2016. Leader Cells Define Directionality of Trunk, but Not Cranial, Neural Crest Cell Migration. *Cell Rep*, 15(9), pp.2076–2088.

Riddle, R.D., Johnson, R.L., Laufer, E. and Tabin, C., 1993. Sonic hedgehog mediates the polarizing activity of the ZPA. *Cell*, 75(7), pp.1401–1416.

Roellig, D., Tan-Cabugao, J., Esaian, S. and Bronner, M.E., 2017. Dynamic transcriptional signature and cell fate analysis reveals plasticity of individual neural plate border cells. *Elife*, 6, p.169.

Ross, A.H., Grob, P., Bothwell, M., Elder, D.E., Ernst, C.S., Marano, N., Ghrist, B.F., Slemp, C.C., Herlyn, M. and Atkinson, B., 1984a. Characterization of nerve growth factor receptor in neural crest tumors using monoclonal antibodies. *Proc Natl Acad Sci U S A*, 81(21), pp.6681–6685.

Ross, A.H., Grob, P., Bothwell, M., Elder, D.E., Ernst, C.S., Marano, N., Ghrist, B.F., Slemp, C.C., Herlyn, M. and Atkinson, B., 1984b. Characterization of nerve growth factor receptor in neural crest tumors using monoclonal antibodies. *Proc Natl Acad Sci U S A*, 81(21), pp.6681–6685.

Sakai, D., Tanaka, Y., Endo, Y., Osumi, N., Okamoto, H. and Wakamatsu, Y., 2005. Regulation of Slug transcription in embryonic ectoderm by beta-catenin-Lef/Tcf and BMP-Smad signaling. *Dev Growth Differ*, 47(7), pp.471–482.

Sancandi, M., Ceccherini, I., Costa, M., Fava, M., Chen, B., Wu, Y., Hofstra, R., Laurie, T., Griffths, M., Burge, D. and Tam, P.K., 2000. Incidence of RET mutations in patients with Hirschsprung's disease. *J Pediatr Surg*, 35(1), pp.139–42– discussion 142–3.

Sanchez-Ferras, O., Bernas, G., Farnos, O., Touré, A.M., Souchkova, O. and Pilon, N., 2016. A direct role for murine Cdx proteins in the trunk neural crest gene regulatory network. *Development*, 143(8), pp.1363–1374.

Sanchez-Ferras, O., Bernas, G., Laberge-Perrault, E. and Pilon, N., 2014. Induction and dorsal restriction of Paired-box 3 (Pax3) gene expression in the caudal neuroectoderm is mediated by integration of multiple pathways on a short neural crest enhancer. *Biochimica et biophysica acta*, 1839(7), pp.546–558.

Sasselli, V., Pachnis, V. and Burns, A.J., 2012. The enteric nervous system. *Dev Biol*, 366(1), pp.64–73.

Sato, T., Sasai, N. and Sasai, Y., 2005. Neural crest determination by co-activation of Pax3 and Zic1 genes in Xenopus ectoderm. *Development*, 132(10), pp.2355–2363.

Sato, Y. and Heuckeroth, R.O., 2008. Retinoic acid regulates murine enteric nervous system precursor proliferation, enhances neuronal precursor differentiation, and reduces neurite growth in vitro. *Developmental Biology*, 320(1), pp.185–198.

Sauka-Spengler, T. and Bronner-Fraser, M., 2008. A gene regulatory network orchestrates neural crest formation. *Nature reviews. Molecular cell biology*, [online] 9(7), pp.557–568. Available at: <http://www.ncbi.nlm.nih.gov/pubmed/18523435>.

Sauka-Spengler, T., Meulemans, D., Jones, M. and Bronner-Fraser, M., 2007. Ancient Evolutionary Origin of the Neural Crest Gene Regulatory Network. *Dev Cell*, 13(3), pp.405–420.

Schmidt, M., Huber, L., Majdazari, A., Schutz, G., Williams, T. and Rohrer, H., 2011. The transcription factors AP-2beta and AP-2alpha are required for survival of sympathetic progenitors and differentiated sympathetic neurons. *Developmental Biology*, 355(1), pp.89–100.

Schoenwolf, G.C., Chandler, N.B. and Smith, J.L., 1985a. Analysis of the origins and early fates of neural crest cells in caudal regions of avian embryos. *Developmental Biology*, 110(2), pp.467–479.

Schoenwolf, G.C., Chandler, N.B. and Smith, J.L., 1985b. Analysis of the origins and early fates of neural crest cells in caudal regions of avian embryos. *Developmental Biology*, 110(2), pp.467–479.

Schorle, H., Meier, P., Buchert, M., Jaenisch, R. and Mitchell, P.J., 1996. Transcription factor AP-2 essential for cranial closure and craniofacial development. *Nature*, 381(6579), pp.235–238.

Schulte-Merker, S., van Eeden, F.J., Halpern, M.E., Kimmel, C.B. and Nusslein-Volhard, C., 1994. no tail (ntl) is the zebrafish homologue of the mouse T (Brachyury) gene. *Development*, 120(4), pp.1009–1015.

Sefton, M., Sanchez, S. and Nieto, M.A., 1998. Conserved and divergent roles for members of the Snail family of transcription factors in the chick and mouse embryo. *Development*, 125(16), pp.3111–3121.

Selleck, M.A. and Stern, C.D., 1991. Fate mapping and cell lineage analysis of Hensen's node in the chick embryo. *Development*, 112(2), pp.615–626.

Semrau, S., Goldmann, J., Soumillon, M., Mikkelsen, T.S., Jaenisch, R. and van Oudenaarden, A., 2016. Dynamics of lineage commitment revealed by single-cell transcriptomics of differentiating embryonic stem cells. *bioRxiv*, p.068288.

Sheng, G. and Stern, C.D., 1999. Gata2 and Gata3: novel markers for early embryonic polarity and for non-neural ectoderm in the chick embryo. *Mech Dev*, 87(1–2), pp.213–216.

Shevinsky, L.H., Knowles, B.B., Damjanov, I. and Solter, D., 1982. Monoclonal antibody to murine embryos defines a stage-specific embryonic antigen expressed on mouse embryos and human teratocarcinoma cells. *Cell*, 30(3), pp.697–705.

Shimozono, S., Iimura, T., Kitaguchi, T., Higashijima, S.-I. and Miyawaki, A., 2013. Visualization of an endogenous retinoic acid gradient across embryonic development. *Nature*, 496(7445), pp.363–366.

Simeone A, A.D.A.L.A.P.B.E.M.F., 1990. Sequential activation of HOX2 homeobox genes by retinoic acid in human embryonal carcinoma cells. *Nature*, 346(6286), pp.763–766.

Simeone, A., Acampora, D., Arcioni, L., Andrews, P.W., Boncinelli, E. and Mavilio, F., 1990. Sequential activation of HOX2 homeobox genes by retinoic acid in human embryonal carcinoma cells. *Nature*, 346(6286), pp.763–766.

Simões-Costa, M. and Bronner, M.E., 2015. Establishing neural crest identity: a gene regulatory recipe. *Development*, 142(2), pp.242–257.

Simões-Costa, M. and Bronner, M.E., 2016. Reprogramming of avian neural crest axial identity and cell fate. *Science*, 352(6293), pp.1570–1573.

Simões-Costa, M., Stone, M. and Bronner, M.E., 2015. Axud1 Integrates Wnt Signaling and Transcriptional Inputs to Drive Neural Crest Formation. *Dev Cell*, 34(5), pp.544–554.

Simões-Costa, M.S., McKeown, S.J., Tan-Cabugao, J., Sauka-Spengler, T. and Bronner, M.E., 2012. Dynamic and Differential Regulation of Stem Cell Factor FoxD3 in the Neural Crest Is Encrypted in the Genome. *PLoS Genet*, 8(12), p.e1003142.

Sinha, S. and Chen, J.K., 2006. Purmorphamine activates the Hedgehog pathway by targeting Smoothened. *Nature chemical biology*, 2(1), pp.29–30.

Southard-Smith EM, K.L.P.W., 1998. Sox10 mutation disrupts neural crest development in Dom Hirschsprung mouse model. *Nature Genetics*, 18(1), pp.60–64.

Spokony, R.F., Aoki, Y., Saint-Germain, N., Magner-Fink, E. and Saint-Jeannet, J.-P., 2002. The transcription factor Sox9 is required for cranial neural crest development in Xenopus. *Development*, 129(2), pp.421–432.

Stemple, D.L. and Anderson, D.J., 1992. Isolation of a stem cell for neurons and glia from the mammalian neural crest. *Cell*, 71(6), pp.973–985.

Stern, C.D., Charite, J., Deschamps, J., Duboule, D., Durston, A.J., Kmita, M., Nicolas, J.-F., Palmeirim, I., Smith, J.C. and Wolpert, L., 2006. Head-tail patterning of the vertebrate embryo: one, two or many unresolved problems? *The International journal of developmental biology*, 50(1), pp.3–15.

Steventon, B., Araya, C., Linker, C., Kuriyama, S. and Mayor, R., 2009. Differential requirements of BMP and Wnt signalling during gastrulation and neurulation define two steps in neural crest induction. *Development*, 136(5), pp.771–779.

Stewart, R., Yang, C., Anyfantis, G., Przyborski, S., Hole, N., Strachan, T., Stojkovic, M., Keith, W.N., Armstrong, L. and Lako, M., 2008. Silencing of the expression of pluripotent driven-reporter genes stably transfected into human pluripotent cells. *Regenerative medicine*, 3(4), pp.505–522.

Stolt, C.C., Lommes, P., Friedrich, R.P. and Wegner, M., 2004a. Transcription factors Sox8 and Sox10 perform non-equivalent roles during oligodendrocyte development despite functional redundancy. *Development*, 131(10), pp.2349–2358.

Stolt, C.C., Lommes, P., Friedrich, R.P. and Wegner, M., 2004b. Transcription factors Sox8 and Sox10 perform non-equivalent roles during oligodendrocyte development despite functional redundancy. *Development*, 131(10), pp.2349–2358.

Strickland, S. and Mahdavi, V., 1978. The induction of differentiation in teratocarcinoma stem cells by retinoic acid. *Cell*, 15(2), pp.393–403.

Sugimura, R., Jha, D.K., Han, A., Soria-Valles, C., da Rocha, E.L., Lu, Y.-F., Goettel, J.A., Serrao, E., Rowe, R.G., Malleshaiah, M., Wong, I., Sousa, P., Zhu, T.N., Ditadi, A., Keller, G., Engelman, A.N., Snapper, S.B., Doulatov, S. and Daley, G.Q., 2017. Haematopoietic stem and progenitor cells from human pluripotent stem cells. *Nature*, 545(7655), pp.432–438.

Takahashi, K. and Yamanaka, S., 2006. Induction of pluripotent stem cells from mouse embryonic and adult fibroblast cultures by defined factors. *Cell*, 126(4), pp.663–676.

Takemoto, T., Uchikawa, M., Kamachi, Y. and Kondoh, H., 2006. Convergence of Wnt and FGF signals in the genesis of posterior neural plate through activation of the Sox2 enhancer N-1. *Development*, 133(2), pp.297–306.

Takemoto, T., Uchikawa, M., Yoshida, M., Bell, D.M., Lovell-Badge, R., Papaioannou, V.E. and Kondoh, H., 2011. Tbx6-dependent Sox2 regulation determines neural or mesodermal fate in axial stem cells. *Nature*, 470(7334), pp.394–398.

Taneyhill, L.A., Coles, E.G. and Bronner-Fraser, M., 2007. Snail2 directly represses cadherin6B during epithelial-to-mesenchymal transitions of the neural crest. *Development*, 134(8), pp.1481–1490.

Tchieu, J., Zimmer, B., Fattahi, F., Amin, S., Zeltner, N., Chen, S. and Studer, L., 2017. A Modular Platform for Differentiation of Human PSCs into All Major Ectodermal Lineages. *Cell Stem Cell*, 21(3), pp.399–410.e7.

Tickle, C., Alberts, B., Wolpert, L. and Lee, J., 1982. Local application of retinoic acid to the limb bond mimics the action of the polarizing region. *Nature*, 296(5857), pp.564–566.

Timmer, J.R., Wang, C. and Niswander, L., 2002. BMP signaling patterns the dorsal and intermediate neural tube via regulation of homeobox and helix-loop-helix transcription factors. *Development*, 129(10), pp.2459–2472.

Tonge, P.D., Shigeta, M., Schroeder, T. and Andrews, P.W., 2011. Functionally defined substates within the human embryonic stem cell compartment. *Stem Cell Res*, 7(2), pp.145–153.

Trainor, P. and Krumlauf, R., 2000a. Plasticity in mouse neural crest cells reveals a new patterning role for cranial mesoderm. *Nat Cell Biol*, 2(2), pp.96–102.

Trainor, P.A. and Krumlauf, R., 2000b. Patterning the cranial neural crest: hindbrain segmentation and Hox gene plasticity. *Nat Rev Neurosci*, 1(2), pp.116–124.

Trainor, P.A., 2010. Craniofacial birth defects: The role of neural crest cells in the etiology and pathogenesis of Treacher Collins syndrome and the potential for prevention. *American Journal of Medical Genetics Part A*, 152A(12), pp.2984–2994.

Trainor, P.A., Ariza-McNaughton, L. and Krumlauf, R., 2002. Role of the isthmus and FGFs in resolving the paradox of neural crest plasticity and prepatterning. *Science*, 295(5558), pp.1288–1291.

Trentin, A., Glavieux-Pardanaud, C., Le Douarin, N.M. and Dupin, E., 2004. Self-renewal capacity is a widespread property of various types of neural crest precursor cells. *Proc Natl Acad Sci U S A*, 101(13), pp.4495–4500.

Tribulo, C., Aybar, M.J., Nguyen, V.H., Mullins, M.C. and Mayor, R., 2003. Regulation of Msx genes by a Bmp gradient is essential for neural crest specification. *Development*, 130(26), pp.6441–6452.

Tsakiridis, A. and Wilson, V., 2015. Assessing the bipotency of in vitro-derived neuromesodermal progenitors. *F1000Res*, 4, p.100.

Tsakiridis, A., Huang, Y., Blin, G., Skylaki, S., Wymeersch, F., Osorno, R., Economou, C., Karagianni, E., Zhao, S., Lowell, S. and Wilson, V., 2015. Distinct Wnt-driven primitive streak-like populations reflect in vivo lineage precursors. *Development*, 142(4), pp.809–809.

Tsuji, H., Spitz, L., Kiely, E.M., Drake, D.P. and Pierro, A., 1999. Management and

long-term follow-up of infants with total colonic aganglionosis. *J Pediatr Surg*, 34(1), pp.158–61– discussion 162.

Tzouanacou, E., Wegener, A., Wymeersch, F.J., Wilson, V. and Nicolas, J.-F., 2009a. Redefining the progression of lineage segregations during mammalian embryogenesis by clonal analysis. *Dev Cell*, 17(3), pp.365–376.

Tzouanacou, E., Wegener, A., Wymeersch, F.J., Wilson, V. and Nicolas, J.-F., 2009b. Redefining the Progression of Lineage Segregations during Mammalian Embryogenesis by Clonal Analysis. *Dev Cell*, 17(3), pp.365–376.

Uchikawa, M., Ishida, Y., Takemoto, T., Kamachi, Y. and Kondoh, H., 2003. Functional analysis of chicken Sox2 enhancers highlights an array of diverse regulatory elements that are conserved in mammals. *Dev Cell*, 4(4), pp.509–519.

Umeda, K., Oda, H., Yan, Q., Matthias, N., Zhao, J., Davis, B.R. and Nakayama, N., 2015. Long-term expandable SOX9+ chondrogenic ectomesenchymal cells from human pluripotent stem cells. *Stem Cell Reports*, 4(4), pp.712–726.

Unsicker, K., Finotto, S. and Krieglstein, K., 1997. Generation of cell diversity in the peripheral autonomic nervous system: the sympathoadrenal cell lineage revisited. *Annals of anatomy = Anatomischer Anzeiger : official organ of the Anatomische Gesellschaft*, 179(6), pp.495–500.

Uz, E., Alanay, Y., Aktas, D., Vargel, I., Gucer, S., Tuncbilek, G., Eggeling, von, F., Yilmaz, E., Deren, O., Posorski, N., Ozdag, H., Liehr, T., Balci, S., Alikasifoglu, M., Wollnik, B. and Akarsu, N.A., 2010. Disruption of ALX1 causes extreme microphthalmia and severe facial clefting: expanding the spectrum of autosomal-recessive ALX-related frontonasal dysplasia. *Am J Hum Genet*, 86(5), pp.789–796.

Verrier, L., Davidson, L., Gierliński, M. and Storey, K.G., 2017a. Generation, selection and transcriptomic profiling of human neuromesodermal and spinal cord progenitors in vitro. *bioRxiv*, p.182279.

Verrier, L., Davidson, L., Gierliński, M. and Storey, K.G., 2017b. Generation, selection and transcriptomic profiling of human neuromesodermal and spinal cord progenitors in vitro. *bioRxiv*, p.182279.

Villanueva, S., Glavic, A., Ruiz, P. and Mayor, R., 2002. Posteriorization by FGF, Wnt, and retinoic acid is required for neural crest induction. *Developmental Biology*, [online] 241(2), pp.289–301. Available at: <http://www.ncbi.nlm.nih.gov/pubmed/11784112>.

Waardenburg, P.J., 1951. A new syndrome combining developmental anomalies of the eyelids, eyebrows and noseroot with pigmentary anomalies of the iris and head hair and with congenital deafness; Dystopia canthi medialis et punctorum lacrimalium lateroversa, hyperplasia supercilii medialis et radicis nasi, heterochromia iridum totaliis sive partialis, albinismus circumscriptus (leucismus, polioss) et surditas congenita (surdimutitas). *American Journal of Human*

Genetics, 3(3), pp.195–253.

Wakamatsu, Y., Endo, Y., Osumi, N. and Weston, J.A., 2004. Multiple roles of Sox2, an HMG-box transcription factor in avian neural crest development. *Dev Dyn*, 229(1), pp.74–86.

Wakamatsu, Y., Maynard, T.M. and Weston, J.A., 2000. Fate determination of neural crest cells by NOTCH-mediated lateral inhibition and asymmetrical cell division during gangliogenesis. *Development*, 127(13), pp.2811–2821.

Wang, W.-D., Melville, D.B., Montero-Balaguer, M., Hatzopoulos, A.K. and Knapik, E.W., 2011. Tfap2a and Foxd3 regulate early steps in the development of the neural crest progenitor population. *Dev Biol*, 360(1), pp.173–185.

Williams, B.P., Daniels, G.L., Pym, B., Sheer, D., Povey, S., Okubo, Y., Andrews, P.W. and Goodfellow, P.N., 1988. Biochemical and genetic analysis of the OKa blood group antigen. *Immunogenetics*, 27(5), pp.322–329.

Wilson, Y.M., Richards, K.L., Ford-Perriss, M.L., Panthier, J.-J. and Murphy, M., 2004. Neural crest cell lineage segregation in the mouse neural tube. *Development*, 131(24), pp.6153–6162.

Winnier, G., Blessing, M., Labosky, P.A. and Hogan, B.L., 1995. Bone morphogenetic protein-4 is required for mesoderm formation and patterning in the mouse. *Genes & Development*, 9(17), pp.2105–2116.

Wolpert, L., 1969. Positional information and the spatial pattern of cellular differentiation. *Journal of Theoretical Biology*, 25(1), pp.1–47.

Workman, M.J., Mahe, M.M., Trisno, S., Poling, H.M., Watson, C.L., Sundaram, N., Chang, C.-F., Schiesser, J., Aubert, P., Stanley, E.G., Elefanty, A.G., Miyaoka, Y., Mandegar, M.A., Conklin, B.R., Neunlist, M., Brugmann, S.A., Helmrath, M.A. and Wells, J.M., 2016. Engineered human pluripotent-stem-cell-derived intestinal tissues with a functional enteric nervous system. *Nature Medicine*.

Wurtman, R.J. and Axelrod, J., 1966. **Control of Enzymatic Synthesis of Adrenaline in the Adrenal Medulla by Adrenal Cortical Steroids**. *Journal of Biological Chemistry*, 241(10), pp.2301–2305.

Wymeersch, F.J., Huang, Y., Blin, G., Cambray, N., Wilkie, R., Wong, F.C. and Wilson, V., 2016. Position-dependent plasticity of distinct progenitor types in the primitive streak. *Elife*, 5, p.841.

Yamada, T., 1994. Caudalization by the amphibian organizer: brachyury, convergent extension and retinoic acid. *Development*, 120(11), pp.3051–3062.

Yntema, C.L. and Hammond, W.S., 1954. The origin of intrinsic ganglia of trunk viscera from vagal neural crest in the chick embryo. *J Comp Neurol*, 101(2), pp.515–541.

Young, H.M., Bergner, A.J., Anderson, R.B., Enomoto, H., Milbrandt, J., Newgreen, D.F. and Whitington, P.M., 2004. Dynamics of neural crest-derived cell migration in the embryonic mouse gut. [online] 270(2), pp.455–473. Available at: <http://linkinghub.elsevier.com/retrieve/pii/S0012160604002027>.

Zeltner, N., Fattahi, F., Dubois, N.C., Saurat, N., Lafaille, F., Shang, L., Zimmer, B., Tchieu, J., Soliman, M.A., Lee, G., Casanova, J.-L. and Studer, L., 2016. Capturing the biology of disease severity in a PSC-based model of familial dysautonomia. *Nature Medicine*, 22(12), pp.1421–1427.

Zhu, J.J., Kam, M.K., Garcia-Barceló, M.-M., Tam, P.K.H. and Lui, V.C.H., 2014. HOXB5 binds to multi-species conserved sequence (MCS+9.7) of RET gene and regulates RET expression. *Int J Biochem Cell Biol*, 51, pp.142–149.

Zuhdi, N., Ortega, B., Giovannone, D., Ra, H., Reyes, M., Asención, V., McNicoll, I., Ma, L. and de Bellard, M.E., 2014. Slit molecules prevent entrance of trunk neural crest cells in developing gut. *Int J Dev Neurosci*, 41C, pp.8–16.